

The role of nicotianamine in the metal homeostasis of
Arabidopsis thaliana

Dissertation
Zur Erlangung des Grades
des Doktors der Naturwissenschaften
der Naturwissenschaftlich-Technischen Fakultät III
Chemie, Pharmazie, Bio- und Werkstoffwissenschaften
der Universität des Saarlandes

von

Mara Schuler

Saarbrücken

Mai 2011

Tag des Kolloquiums:

Dekan:

Berichterstatter:

.....

.....

Vorsitz:

Akad. Mitarbeiter:

ROMANES EUNT DOMUS

(Brian Cohen, 33AD)

Table of contents

Table of contents	0
Summary	3
Zusammenfassung	4
Abbreviations	5
1. Introduction	6
1.1 Physiological importance of iron and copper for all living organisms	6
1.1.1 Consequences of Fe malnutrition	7
1.1.2 Consequences of Cu malnutrition.....	7
1.2 Metal homeostasis of higher plants	8
1.2.1 Mobilization and uptake of Fe and Cu from the soil.....	9
1.2.2 Metal chelators.....	13
1.2.3 Nicotianamine (NA).....	18
1.2.4 Long-distance transport of Fe and Cu.....	26
1.2.5 Intracellular transport and storage of Fe	33
1.3 Improving Fe bioavailability in crop plants	39
1.3.1 Approaches for Fe biofortification of plants	40
1.3.3 Manipulation of the <i>NAS</i> genes as biotechnological approach	43
1.4 The use of <i>A.thaliana</i> as a model plant to investigate NA function.....	44
1.4.1 Functional genomics in Arabidopsis.....	45
1.4.2 High throughput transcriptome analysis	46
1.5 Prerequisites for this work.....	47
1.5.1 Predicted roles of NA in Fe and Cu homeostasis	47
1.5.2 The Arabidopsis <i>NAS</i> gene family.....	48
2. Aims of this project.....	52
3. Material and Methods	55
3.1 Material	55
3.1.1 Plant material:.....	55
3.1.2 Bacterial strains for molecular cloning	55
3.1.3 Plasmids.....	55
3.1.4 Oligonucleotides	56

Table of contents

3.1.5 Enzymes and Kits	60
3.2 Methods	61
3.2.1 Plant Methods	61
3.2.3 Protein techniques.....	71
3.2.4 Determination of NA contents.....	72
4. Results	73
4.1. Verification and further physiological characterization of <i>nas4x-1</i> mutants (published in Klatte, Schuler et al., 2009)	73
4.1.1 Supportive physiological investigation of <i>nas4x-1</i> mutants	73
4.1.2 Investigation of Fe, Zn and Cu deficiency effects on <i>nas4x-1</i> mutants	76
4.2 Genome wide expression study of <i>nas4x-1</i> mutants compared to wild type plants in a comparative gene chip experiment.....	78
4.2.1 Transcriptome analysis using the web-based tool GeneTrail	79
(published in Schuler et al., 2011).....	79
4.2.2 Analysis of differentially regulated genes on single gene level.....	88
(unpublished data)	88
4.3 Analysis of individual and overlapping functions of the four <i>NAS</i> genes.....	94
4.3.1 Determination of NA contents in single and triple <i>nas</i> mutants	94
4.3.2 Differential expression of <i>NAS</i> genes in multiple <i>nas</i> mutants compared to wild type plants.....	95
4.3.2 Effects of Fe deficiency to <i>nas</i> multiple mutants	97
4.3.3 Generation of <i>NAS3</i> and <i>NAS4</i> reporter constructs.....	99
4.4 Verification and detailed characterization of the second quadruple <i>nas</i> mutant <i>nas4x-2</i>	102
4.4.1 Verification of <i>nas4x-2</i> mutants	102
4.4.2 Detailed physiological characterization of <i>nas4x-2</i> plants	105
4.4.3 Investigation of the crosstalk of citrate and NA	116
4.4.4 Investigation of the influence of the loss of NA on reproduction	124
5. Discussion	134
5.1 Investigation of the NA-free mutant <i>nas4x-2</i> revealed distinct functions of NA in metal homeostasis	134

Table of contents

5.1.1 NA is needed for the phloem-dependent root-to-leaf Fe transport in young leaves, while its loss can be partially compensated by citrate	134
5.1.2 NA is required for phloem unloading in young leaves and for proper phloem loading in mature leaves.....	136
5.1.3 Successful reproduction requires NA for pollen production and cell death in female pistil tissue	140
5.1.4 NA has an essential function in root-to-shoot translocation of Cu	143
5.1.5 NA is needed for subcellular distribution of Fe	144
5.2 Supportive analysis of <i>nas4x-1</i> mutants combined with previous findings demonstrate the requirement of NA for seed Fe loading.....	145
5.3 NAS4 has an individual function upon Fe deficiency	147
5.4 Transcriptome analysis by GeneTrail revealed regulation of functional categories in response to alterations of iron homeostasis in <i>Arabidopsis thaliana</i>	147
6. Conclusion and Perspectives	152
Appendix	154
References	191
Danksagung	212
Curriculum vitae	213
Publication list.....	214

Summary

The non-proteinogenic amino acid *nicotianamine* (NA) chelates and transports essential metal ions in plants. The enhancing effect of NA on the bioavailability of metals makes it appealing for biofortification approaches. The goal of this project was the localization of NA activity and the elucidation of a concrete function of NA in Fe and Cu translocation throughout the plant using the model plant *Arabidopsis thaliana*.

Arabidopsis has four *NICOTIANAMINE SYNTHASE (NAS)* genes. To investigate NA function two quadruple *nas* mutants, named *nas4x-1* and *nas4x-2* were analyzed to study NA function in *Arabidopsis*: *nas4x-2* had a full loss of NAS function, was sterile, and suffered from severe chlorosis in young leaves. *nas4x-1* had residual NA contents, was still fertile and developed a interveinal leaf chlorosis upon transition from vegetative to reproductive stage. The obtained results indicate that NA participates in the phloem-dependent Fe transport and in the phloem- and xylem-dependent Cu transport in plants. Thereby NA has a distinct function in the phloem unloading process of metals in young growing tissues, reproductive floral organs and seeds. Moreover, NA is required for the remobilization of metals from old leaves to the inflorescence. These findings are fundamental for plant manipulation approaches to increase the amount of bioavailable Fe in seeds through the genetic modification of the *NAS* genes.

Zusammenfassung

Die nicht-proteinogene Aminosäure Nikotianamin (NA) chelatiert und transportiert essentielle Metallionen in Pflanzen. NA hat einen positiven Effekt auf die Bioverfügbarkeit von Metallen und ist deshalb ein attraktives Ziel zur genetischen Modifikation in der Herstellung von verbesserten Kulturpflanzen. Hauptziel dieser Arbeit war die genaue Lokalisierung der NA Aktivität und die Entdeckung ihrer konkreten Funktionen im Fe und Cu Haushalt der Pflanze.

Arabidopsis hat vier *NICOTIANAMINE SYNTHASE (NAS)* Gene. Die Funktion von NA wurde anhand von zwei vierfach *nas* Mutanten, *nas4x-1* und *nas4x-2*, untersucht. Die fertile *nas4x-1* Mutante hatte detektierbare, jedoch stark reduzierte NA Gehalte, was sich in der Entwicklung einer intervenalen Blattchlorose beim Wechsel vom vegetativen zum reproduktiven Wachstumsstadium äußerte. Die NA-freie *nas4x-2* Mutante dagegen war steril und entwickelte eine starke intervenale Blattchlorose in jungen Blättern.

Die Ergebnisse dieser Arbeit haben gezeigt, dass NA eine wichtige Rolle im Phloem-Fe-Transport und im Phloem- und Xylem-Cu-Transport spielt. Dabei hat NA eine konkrete Funktion in der Phloementladung von Metallen in jungen, wachsenden Geweben, in reproduktiven Blütenorganen und in Samen. Darüber hinaus wird NA in der Remobilisierung von Metallen aus Blättern zur Fe und Cu Versorgung der Infloreszenz gebraucht. Diese Erkenntnisse sind fundamental für die Verbesserung der Fe Bioverfügbarkeit in Samen durch die genetische Modifikation der *NAS* Gene.

Abbreviations

NA.....	Nicotianamine
NAS.....	Nicotianamine synthase
<i>A. thaliana</i>	<i>Arabidopsis thaliana</i>
Col-0.....	Columbia
GFP.....	Green fluorescent protein
GUS.....	β -Glucuronidase
<i>A. tumefaciens</i>	<i>Agrobacterium tumefaciens</i>
RT-qPCR.....	Reverse transcription real time quantitative PCR
IRT1.....	Iron regulated transporter1
FER1.....	Ferritin1
YSL.....	Yellow stripe-like transporter
OPT3.....	Oligopeptide transporter 3
FRO2.....	Ferric reduction oxidase 2
FIT.....	Fer-like iron deficiency induced transcription factor
FRD3.....	Ferric chelate reductase defective 3
ZIP.....	ZRT, IRT-like proteins

1. Introduction

1.1 Physiological importance of iron and copper for all living organisms

Iron (Fe) and copper (Cu) are essential elements for all living organisms because of their unique property of being able to catalyze oxidation/reduction reactions. Therefore, both metal ions serve as critical cofactors for components of the electron transfer chains in the mitochondria and the chloroplasts (Marschner 1995). Fe serves as a prosthetic group in proteins to which it is associated either directly or through a heme or an iron-sulfur cluster. It exists in two redox states, the reduced ferric Fe(III) and the oxidized Fe(II) form and is able to gain or lose an electron, respectively, within metalloproteins (e.g. ferrous ferredoxin and superoxide dismutase (SOD)). It functions as a component of many important enzymes and proteins involved in fundamental biochemical processes like the electron transfer chains of respiration and photosynthesis (cytochromes), the biosynthesis of DNA (ribonucleotide reductase), lipids (lipoxygenase) and hormones (1-aminocyclopropane 1-carboxylic acid (ACC)), the detoxification of reactive oxygen species (ROS) (peroxidase, catalase) and the nitrogen assimilation (nitrite and nitrate reductase) (Balk & Lobréaux, 2005; Marschner, 1995). The most abundant Cu protein in plants is plastocyanin, a protein that transfers electrons from the cytochrom b6f complex to photosystem I (PSI). Cu is used as a cofactor by proteins involved in protection from reactive oxygen species (CuZn-superoxide dismutase), lignification of the cell wall, pollen formation, proper carbohydrate metabolism, and formation of phenolics in response to pathogen attack. Cu is also required by the ethylene receptor for proper signaling (Pilon et al. 2006; Rengel and Marschner 2005; Rodríguez 1999; Puig et al. 2007). These cellular processes take place in distinct intracellular compartments, which therefore need to be provided with an adequate amount of Fe and Cu. Since both metals are involved in a wide range of essential processes, the undersupply with Fe and Cu can lead to severe deficiency symptoms in the affected organism.

1. Introduction

1.1.1 Consequences of Fe malnutrition

Fe deficiency is one of the most prevalent and most serious nutrient deficiencies threatening human health in the world, affecting approximately two billion people (WHO:http://www.who.int/nutrition/publications/micronutrients/anaemia_iron_deficiency/9789241596657/en/index.html). Various physiological diseases, such as anaemia, Wilson's, Parkinson's, and Menken's disease, are triggered by Fe deficiency (Yuan 1995). Especially countries, where people have little meat intake and the diets are based mostly on staple foods are affected. Young children, pregnant and postpartum women are the most commonly and severely affected population groups, because of the high Fe demands of infant growth and pregnancy. To enrich plant food products with bioavailable Fe may be the most effective and economic method to fight human health problems caused by Fe deficiency.

In plants, Fe is also one of the most common elements limiting plant growth because it exists predominantly in an oxidized ferric form Fe(III) in aerobic environments which have an extremely low solubility at neutral or basic pH and is not readily available to plants. Fe deficiency in plants causes a characteristic interveinal leaf chlorosis, which is appearing initially on the younger leaves, since Fe cannot be readily mobilized from older leaves. Under extreme or prolonged deficiency, leaf veins may also become chlorotic, causing the whole leaf to turn white. Fighting Fe deficiency is very important, since it limits plant growth and leads to decreased yield and food quality of crop plants. Conversely, an excess of Fe, especially Fe(II), is toxic and can be detrimental since it catalyzes the production of reactive oxigene species (ROS) in the Fenton reaction including the formation of the hydroxyl radical $\text{OH}\cdot$ (Hell and Stephan 2003; Fenton 1894). Since those radicals can react with many cell components by for example, peroxidase reactions with membrane lipids and oxidation of disulfide bonds, their formation results in oxidative stress and can finally lead to dramatic cell damages (Himmelblau and Amasino 2000; Valko et al., 2005).

1.1.2 Consequences of Cu malnutrition

Although Cu abundance is very low in the environment, Cu deficiency in humans is rare. Nevertheless, Cu deficiency does present a concern in specific situations. The symptoms are mainly related to decreased activity of Cu-requiring enzymes. Abnormalities associated with Cu deficiency include anemia, neurological damage,

1. Introduction

hypercholesterolemia, cardiomyopathy, osteoporosis and impaired immune function (Cordano 1998). Cu deficiency has been observed in individuals with restricted diets and in premature infants fed cow's milk products (Danks 1988, Naveh et al. 1981). Severe deficiency is often seen in Menken's disease, a genetic disorder characterized by a defect in copper efflux from various tissues (Danks, 1988). Also a chronic ingestion of large quantities of zinc reduces the efficiency of copper absorption and has been reported to cause deficiency (Fischer et al., 1984). Also individuals suffering from malnutrition and severe malabsorption syndromes as well as patients undergoing certain chelation therapies are at increased risk of Cu deficiency.

In plants, the initial symptom of Cu deficiency is the production of dark green leaves, which may contain necrotic spots. These necrotic spots appear first at the tips of the young leaves and then extend towards the leaf base along the margins. The leaves may also be twisted or malformed. Under extreme Cu deficiency, leaves may abscise prematurely.

Since both plants and humans are much more affected by Fe deficiency problems, genetical Fe homeostasis components are in general better characterized in comparison to factors involved in Cu homeostasis. The focus of this project is on Fe homeostasis, but nevertheless components of Cu homeostasis known thus far are also presented in context.

1.2 Metal homeostasis of higher plants

To meet Fe demand for growth and development and to avoid Fe excess with its potential toxicity, plant Fe homeostasis has to be tightly controlled. Plants contain a complex regulation network of genes which provide uptake, chelation, transport, sub-cellular distribution and the storage of Fe. This complex network of Fe homeostasis can be separated in 4 sub-processes and will be explained in the following order:

1. Mobilization and uptake of metals from soil
 - 1.1 Reduction-based uptake strategy
 - 1.2 Chelation-based uptake strategy
2. Metal chelation
 - 2.1 Nicotianamine
 - 2.2 Other metal chelators
3. Long-distance transport of Fe and Cu

1. Introduction

3.1 Root-to-shoot transport

3.2 Leaf-to-seed transport

4. Intracellular transport and storage of Fe

4.1 Sub-cellular distribution of Fe in plastids

4.2 Storage and loading of Fe into the vacuole

It is not possible to consider Fe homeostasis isolated from the homeostasis of other essential metal ions like Cu, zinc (Zn) and manganese (Mn) since changes in the content of one metal ion can influence the homeostasis of other metal ions. Therefore, components of metal homeostasis mostly address the regulation of several metal ions mentioned, if relevant, in the following sections.

1.2.1 Mobilization and uptake of Fe and Cu from the soil

Fe is highly abundant in soils, but it exists predominantly in an oxidized ferric form Fe(III) in aerobic environments. This ferric Fe, mostly existing as Fe hydroxides (FeOOH), has an extremely low solubility at neutral or basic pH and is not readily available to plants (Marschner 1995). Cu is primarily insoluble in soils because of its absorption to clay, CaCO₃ or organic matter. Plants and microbes need a Fe concentration of 10⁻⁶ M for optimal growth, but the concentration of free Fe(III) in aerobic, aqueous environment of the soil with a pH of 7 is about 10⁻¹⁷ M. The lower the pH, the more the solubility of Fe(III) increases, but to reach a Fe(III) concentration of 10⁻⁶ M, the pH has to be lowered to 3,3 (Hell and Stephan 2003). Unfortunately, 30% of the world's cropland is too alkaline for optimal plant growth. Moreover, it appears that some staple crops, like rice, are especially susceptible to Fe deficiency (Takahashi et al. 2001), which makes the situation difficult for farmers. Therefore much research has focused on plants strategies to cope with Fe limitation. To deal with the inaccessibility of some metals, two effective Fe acquisition systems known as strategy I and strategy II have evolved in higher plants (Roemheld and Marschner 1986). Strategy I plants mainly use a reduction-based Fe uptake strategy, while strategy II plants use a chelation-based strategy for Fe uptake (Roemheld and Marschner 1986) which are described below (see also Fig.1.1). In addition to the upregulation of their uptake machineries (Colangelo and Gueriot 2006; Dinneny et al. 2008) plants show morphological changes of roots, such as thickening of the subapical root zone and an increased formation of root hairs in order to increase their root surface (Marschner 1995). This allows plants as sessile organisms to adapt to changing environmental nutritional status.

1. Introduction

1.2.1.1 Reduction-based Strategy of Fe uptake

The group of strategy I plants includes all dicotyledonous (dicots) and all non-grass monocotyledonous plants (monocots). Arabidopsis, tomato (*Solanum lycopersicum*) and tobacco (*Nicotiana tabacum*) for example are known to utilize a reduction-based strategy, which is preceded by an acidification of the root environment (Fig. 1.1A). This acidification of the rhizosphere helps the plant to overcome the challenges of insolubility of metals in alkaline soils.

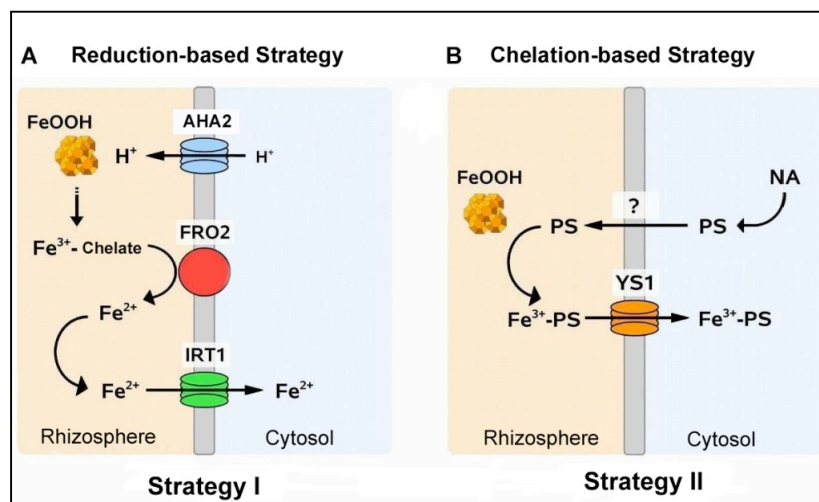


Fig. 1.1: Fe uptake strategies of higher plants

A) Reduction-based strategy, also named strategy I, is used by dicots and non-grass monocots. It starts with acidification by extruding protons by AHA2 into the rhizosphere to solubilize insoluble Fe-complexes in soil. The freed Fe(III) is reduced to Fe(II) by FRO2 and is taken up by IRT1 into the root Epidermis. **B)** Chelation-based strategy, also named strategy II, is utilized by grasses. Grasses extrude phytosiderophores (PSs) into the rhizosphere which chelate Fe from insoluble soil particles. This Fe(III)-PS is taken up by the YS1 transporter into the root epidermis.

Plants can use ATPase activity to extrude protons into the rhizosphere to lower the pH. Acidification can have a major impact since a unit drop in pH increases the solubility of Fe by 1,000-fold (Guerinot and Yi 1994). The ATPases responsible for proton extrusion and soil acidification under Fe deficiency are likely to be members of the AHA (Arabidopsis H⁺ ATPase) family (Palmgren 2001). Of the 12 family members in Arabidopsis, AHA1, AHA2 and AHA7 are the most likely candidates, as they are all expressed in the roots and are upregulated under Fe deficiency (Dinneny et al. 2008). A recent study from Santi and Schmidt (2009) suggests that the rhizosphere acidification in response to Fe deficiency is mainly mediated by AHA2, while AHA1 functions as a housekeeping isoform. The *aha7* knock-out mutant plants showed a reduced frequency of root hairs, suggesting an involvement of AHA7 in the differentiation of rhizodermic

1. Introduction

cells. The acidification capacity varied among *Arabidopsis* accessions and was associated with a high induction of *AHA2* and *IRT1* (Santi and Schmidt 2009). This acidification also results in an increased solubility of other divalent metal ions like Cu and Zn, since it promotes cation exchange and entails the release from insoluble chelates with soil particles. ATPase activity also allows for the establishment of a negative membrane potential, along the order of -100 to -250 mV, which serves to drive cation uptake (Palmgren 2001).

Once Fe and Cu are freed from insoluble chelates, they need to be reduced for uptake. The ferric-chelate reductase FRO2 (Connolly et al. 2003; Robinson et al. 1999) reduces Fe(III) to Fe(II) on root surface in the subapical region to make it accessible for its respective transporter. Fe is transported into the root epidermal cell in the divalent Fe(II) form in its reduced state primarily through the high affinity ferrous Fe transporter IRT1 (Henriques et al. 2002; Eide et al. 1996; Varotto et al. 2002; G Vert et al. 2002; Vacchina et al. 2003) (Fig.1.1A). IRT1 is an essential member of the ZIP (ZRT, IRT-like proteins) metal transporter family and localized to the plasma membrane of the root epidermis, it was shown to be the main iron transporter. The lethal phenotype of *irt1* mutants can be rescued by addition of exogenous Fe, which indicates that its primary role is in uptake of Fe (Varotto et al. 2002; G Vert et al. 2002). Although IRT1 has an essential role in Fe uptake, it can also transport other divalent metals (Korshunova et al. 1999), and *irt1* plants have reduced levels of Zn as well as other cations (Henriques et al. 2002; G Vert et al. 2002). Because *irt1* plants are able to survive without the addition of excess Zn, it is likely that Zn is primarily taken up into the plant via other transporters.

Unlike Fe and Zn, Cu is not taken up primarily as Cu(II), but instead transported as Cu^+ by COPT1 (Sancenón et al. 2004). COPT proteins are the *Arabidopsis* orthologs of the yeast transporter CTR1. COPT1 is able to complement yeast *ctr1* mutants and is upregulated under Cu deficiency in plants, and mutant plants show decreased Cu accumulation as well as upregulation of genes that respond to Cu limitation (Sancenón et al. 2004). Though Cu(II) is more common in the soil than Cu^+ (Puig et al. 2007), it is possible that Cu(II) is also reduced by FRO2, as reduction of Cu(II) is lost in *frd1-1* mutants and can be restored when FRO2 expression is restored (Robinson et al. 1999), although FRO2 seems not to be mainly responsible for the reduction of Cu for its uptake since it is not induced under Cu deficiency (Robinson et al. 1999; E L Connolly

1. Introduction

et al. 2003). In addition to uptake of Cu^+ through COPT1, plants may also take up Cu as the more abundant Cu(II) via a member of the ZIP family, a transporter family known to preferentially transport divalent cations. Both ZIP2 and ZIP4 are known to be upregulated by Cu deficiency and can complement *ctr1* yeast mutants for Cu uptake (Wintz et al. 2003), but further research with loss-of-function mutants is needed to test the involvement of these transporters in Cu uptake.

1.2.1.2 Chelation-based Strategy of Fe uptake

All monocotyledonous grasses are Strategy II plants, including all major crop plants like rice (*Oryza sativa*), barley (*Hordum vulgare*), wheat (*Triticum aestivum*) and maize (*Zea mays*). To increase soil Fe solubility under Fe limitation, they rely on a chelating mechanism by synthesis and secretion of small metabolites termed Phytosiderophores (PS). These PS are synthesized from methionine and are usually belonging to the mugineic acid family (MAs) (Fig.1.2.) and bind ferric Fe from the soil with a high binding affinity. The synthesis of mugineic acid (MA) is well understood and the components of the participating enzymes have been already cloned and described (Bashir et al. 2006; Nakanishi et al. 2000; Mori 1999). The precursor molecule of all MAs is *nicotianamine* (NA), which is a central player in Fe homeostasis. Genes involved in MA biosynthesis are upregulated under Fe deficiency (Nagasaka et al., 2009), but there is no suggested role for PS in Cu uptake. Once Fe is bound by PS, the whole Fe(III)-PS complex is taken up by Fe(III)-MAs transporters, termed Yellow Stripe 1 (YS1) (Fig. 1.1B). This transporter was originally identified in maize by analyzing the mutant *ys1* defective for PS uptake (Curie et al. 2001). This mutant showed a decreased Fe uptake and a constitutive Fe deficiency response. The decrease of Fe-containing proteins in leaves impairs chlorophyll biosynthesis resulting finally in a yellowing between the veins (Bell, Bogorad, and McIlrath 1958; N. von Wiren et al. 1994). This characteristic interveinal leaf chlorosis was eponymous for the Yellow Stripe transporter (YS1).

The chelation-based strategy is less sensitive to pH of the root environment than the reduction-based strategy I (Morrissey and Gueriot 2009) and there is a strong correlation between the volume of released PSs and resistance to Fe limiting soils. For instance, barley, which is adapted to alkaline soils, releases a much greater volume of PS than most rice species which are adapted for growing on anaerobic soils where Fe is more soluble (Nagasaka et al. 2009).

1. Introduction

The strict classification of plants in two distinct uptake strategies has been disarranged by the findings of the recent years. Ishimaru et al. found 2006 that rice, as Strategy II plants, induces both Fe(II) uptake by OsIRT1 and Fe(III)-MA uptake in response to Fe deficiency. Furthermore, Cheng et al. has demonstrated (2007) that rice is able to take up Fe(II) when NA synthesis is disrupted and PS cannot get produced. In aerated soils Fe already exists in the oxidized Fe(II) form and thus is available for the uptake through IRT1 (L Cheng et al. 2007). These findings suggest a greater flexibility of plants in their strategies in metal uptake that the long thought categorization of in two uptake strategies.

1.2.2 Metal chelators

Although it is not exactly known in which oxidation status metal ions are existing in the different cell compartments and tissues, very little metal ion content is expected to exist as free ions. Fe indeed exists mainly as highly stable complexes with organic ligands or inorganic phosphates (Haydon and Cobbett 2007). This is caused by the fact that the same qualities that make metals like Fe and Cu such essential as cofactors can also make them highly toxic within the cell. The deleterious effect of Fe toxicity is observed as blackening of the root tips, inhibition of root growth and necrotic spots on the leaves ('bronzing') (Snowden and Wheeler 1995; W. Schmidt and Fühner 1998). Several strategies to minimize oxidative stress induced by essential and non-essential heavy metals have been described in higher plants (Howden 1995; Salt and Rauser 1995; Murphy 1997; van der Zaal et al. 1999). The main strategy in the detoxification process is metal binding by ligands followed by the sequestration into the vacuole.

Plants, specially adapted to high metal amounts in the soil, are the so called hyperaccumulators which serve as important model plants to investigate the phenomenon of detoxification processes in plants. Examples for such hyperaccumulating plant species are the Zn hyperaccumulator *Arabidopsis halleri*, a Cd/Zn/Ni hyperaccumulator, *Thlaspi caerulescens*, a Cd/Zn hyperaccumulator and the Ni hyperaccumulator *Alyssum lesbiacum*. These plant species have naturally evolved the ability to translocate massive amounts of heavy metals from the roots to the shoots where they are stored in non-toxic forms (Stephan Clemens, Palmgren, and Ute Krämer 2002; Ute Krämer 2010). As mentioned above plants use the chelation and storage as

1. Introduction

very suitable mechanism against toxification with heavy metals. Organic acids like citrate and malate, the amino acid histidine (His) and NA are mainly involved in this process (Verbruggen et al., 2009).

Even under normal concentrations of essential heavy metals, like Fe, Zn and Cu, the metal ions need to be bound by chelator molecules. The binding through chelators enhances the availability of essential metals by keeping them soluble. Chelation also avoids toxicity by scavenging toxic metals in a non-reactive form. The solubilization and long-distance allocation of Fe and other metal ions between organs and tissues, as well as its subcellular compartmentalization and remobilization, involve various chelation and oxidation/reduction steps, transport activities and association with soluble proteins that store and buffer certain metals. Therefore, chelation is a central process in metal homeostasis. Chelators for heavy metals are low molecular weight organic molecules like NA and MA, amino acids, organic acids, polypeptides such as phytochelatins (PCs) and metallothioneins (MTs) which are involved in the tolerance to potentially toxic free heavy metal ions (Rausser 1999; Briat and Lebrun 1999; Robinson et al. 1993). NA, PCs and MTs are in particular needed to keep essential heavy-metal ions soluble, also under normal concentrations of these metals (Cobbett and Goldsbrough 2002a; Haydon and Cobbett 2007).

1.2.2.1 Nicotianamine (NA)

NA is one of the most investigated chelator molecules in plants within the last two decades, since it is supposed to play a central role in metal homeostasis. As mentioned in section 1.2, NA is a direct precursor of the PSs acting in the Fe uptake of grasses, the so called Strategy II plants (Fig. 1.1B). Strategy I plants, such as Arabidopsis, tomato and tobacco, do not synthesize MA but do synthesize NA, which is the precursor of MA (Fig. 1.2). NA is a nonproteinogenic amino acid and it results from the enzymatic condensation of three amino-carboxylpropyl groups of three S-adenosylmethionine molecules (SAM). The reaction is catalyzed by Nicotianamine synthases (NAS). NA is present in all higher plant species tested thus far and it is believed to function within the plant to maintain the solubility of Fe (Catherine Curie and Jean-François Briat 2003; Becker, Fritz, and Manteuffel 1995) and acts in the detoxification process of Ni (Ouerdane et al. 2006; Douchkov et al. 2005; Kim et al. 2005; Klatter et al. 2009; Mari et al. 2006; Pianelli et al. 2005; Callahan et al. 2007; Vacchina et al. 2003) and Zn (van de Mortel et al. 2006; Weber et al. 2004; Talke et al., 2006; Becher et al. 2004). There is

1. Introduction

also increasing evidence for a role for NA in Zn and Cu homeostasis, since *NICOTIANAMINE SYNTHASE* (*NAS*) genes are upregulated in roots and shoots of plants grown under Zn or Cu deficiency, as well as under Fe deficiency (Wintz et al. 2003). This project concentrates on the contribution of NA to metal homeostasis. Therefore, NA synthesis, chemical properties and transport are presented in detail in the next.

Similar to NA, Metallothionines (MTs) and Phytochelatines (PCs) are supposed to act in the maintaining of the homeostasis of essential heavy metals under normal growth. Additionally, a wide range of small, organic molecules as metal binding ligands for essential and non-essential heavy-metals exist in the plant kingdom.

In this section recent advances in elucidating the role of such ligands are shortly introduced (for detailed review see Cobbett and Goldsbrough, 2002; Haydon and Cobett, 2007).

1.2.2.2 Phytochelatins

The phytochelatins (PCs) are a family of metal-complexing peptides that have a general structure $(\gamma\text{-Glu Cys})_n\text{-Gly}$ where $n=2-11$, and are rapidly induced in plants by heavy metal treatments (Rauser, 1995; Cobbett and Goldsbrough, 2000). A clear role in Cd detoxification has been supported by a range of biochemical and genetic evidence (Howden 1995; Haag-Kerwer et al. 1999). Other PC could be detected in a complex with silver (Ag), Cu and arsenic acid (As) in later studies. Although evidence for the role for PCs in detoxification is strong, especially for Cd, these peptides may play other important roles in the cell, including essential heavy-metal homeostasis, sulphur metabolism or perhaps, as antioxidants (Dietz et al., 1999; Cobbett 2000; Rauser 1995).

1.2.2.3 Metallothionins

Metallothionein proteins are characterized as low molecular weight, cysteine-rich, metal-binding proteins (Kaegi and Schaeffer 1988). Higher plants contain two major types MT proteins which are classified based on the arrangement of Cys residues (Cherian and Chan 1993). Class I MTs contain 20 highly conserved Cys residues based on mammalian MTs and are widespread in vertebrates. MTs without this strict arrangement of cysteines are referred to as Class II MTs and include all those from plants and fungi as well as non-vertebrate animals. In this MT classification system,

1. Introduction

PCs are, somewhat confusingly, described as Class III MTs. Shortly after the discovery of PCs as an important metal ligand required for tolerance of plants to Cd, a MT protein was identified in wheat (Lane et al., 1987), the function of MTs in plants remain elusive. In animals MTs protect against Cd toxicity (Klaassen et al., 1999), but this function is clearly provided by PCs in plants. Mammalian MTs have a highly conserved sequence, are expressed in many tissues and respond to a wide variety of regulatory factors. Although these observations hint at an important function for MTs in mammals, the only role that has been established unequivocally is in protection against cadmium and zinc toxicity (Palmiter 1998). Therefore, although MTs are expressed ubiquitously and conserved in plants, since there is no mutant model plant available, determining their function remains a future challenge.

With regard to Fe, a specific role in protecting the cell against toxic concentrations of Fe has not yet been demonstrated for organic acid or amino acids. By means of N-terminal amino acid analysis of proteins, Becker et al. (1998) found also no evidence for induction of PC and MT synthesis in root tips and leaves of Fe over-accumulating pea mutants. Since they are not reacting to toxic concentrations of Fe, they seem to act exclusively in maintaining metal homeostasis under normal concentrations of essential metals. More details about the ferritin function are presented in section 1.2.4 and 1.3.

1.2.2.4 Ferritins

A specific role in the detoxification of Fe has been found for ferritin. Ferritins, a class of multimeric proteins with a high storage capacity for Fe are present in plants, animals, fungi and bacteria (Briat and Lobraux 1997; Briat 1996). Fe has been shown to be stored in plastids in ferritin, a protein nanocage that can store up to 4,500 atoms of Fe(III) in its interior as a Fe oxide mineral (Hintze and Theil 2006) and since in animals, ferritin is the primary storage form for Fe, it was long thought to be the main storage form of Fe in plants. Recent work refutes the thesis by suggesting that in *Arabidopsis* the role of ferritin is solely to deal with excess Fe and prevent oxidative damage (Ravet et al. 2009), much like the detoxifying role of ferritin in bacteria (Carrondo 2003) and *Chlamydomonas* (Long et al. 2008; Busch et al. 2008). Unlike in animals most plants use ferritin primarily to detoxify Fe rather than as a major storage unit.

1. Introduction

1.2.2.5 Organic acids

Organic acids have been linked to metal hyperaccumulation and tolerance in a range of plant species and were found to be associated with a range of metals like cadmium (Cd), Cu, Ni, and Zn. Analysis of tissues from metalhyperaccumulator species using X-ray absorption techniques has identified organic acids as the predominant ligands. By X-ray absorption spectrometry (XAS) and extended X-ray absorption fine structure (EXAFS) analysis, citrate was identified as the predominant ligand for Zn in leaves of *T.caerulescens* (Salt et al. 1999; Kuepper et al. 2004) while Zn-malate was the major Zn species in aerial tissues of *A.halleri* (Sarret et al. 2002). Similarly, Ni-citrate accounted for one quarter of the Ni species in leaves of the Ni-hyperaccumulator *Thlaspi goesingense* and in the related nonaccumulator *Thlaspi arvense* (Kramer et al., 2000). The identification of the vacuole as the major subcellular compartment for Zn, Cd and Ni (Krämer et al. 2000; Ma et al. 2005) and favouring of the formation of metal–organic acid complexes in the acidic environment of the vacuolar lumen suggest that citrate and malate are probably relevant only as ligands for these metals within vacuoles. In addition, secretion of malate or citrate from root apices is a well established mechanism for tolerance to Aluminium (Al) in a range of plant species (Delhaize and Ryan 1995), at which citrate is believed to be the predominant ligand for Fe in xylem (von Wiren et al., 1999). Although organic acids have been identified as metal ligands in vacuoles, it is not clear how these ligands are sequestered.

1.2.2.6 Histidine

Histidine (His) existing as free amino acid and in metal-coordination residues with proteins has a high affinity for binding metals. In particular, free His has been implicated as an important ligand in Ni hyperaccumulation. An increase of His content could be detected in xylem exudate of the Ni hyperaccumulator *Alyssum lesbiacum*, which shows a 36-fold higher Ni content in the xylem sap compared to nonaccumulator *Alyssum montanum*. XAS indicated coordination of His to Ni, and foliar application of His to *A. montanum* conferred enhanced Ni tolerance (Kraemer et al., 1996). Although organic acid complexes have been suggested to account for the majority of Zn in aerial tissues, X-ray absorption studies of *T.caerulescens*, the Cd/Zn/Ni hyperaccumulator, indicated that Zn–His was the second most abundant ligand in mature leaves. They also found that 70% of Zn complexed to His is in roots (Salt et al., 1999). In addition, studies of the Zn species in a range of aerial tissues of *T.caerulescens* at various

1. Introduction

developmental stages indicated that the speciation of Zn is dynamic, and suggested that His may be more important in chelating Zn in developing and older tissues. This may be related to a shift in the cellular or subcellular distribution of Zn at different developmental stages. All together, His plays an important role in the detoxification of Ni and in the chelation and sequestration of Zn depending on the developmental stage of the plant.

1.2.2.7 Phytic acid

Phytic acid (known as inositol hexaphosphate (IP₆) or phytate (when in salt form) is the primarily storage molecule for phosphorus (P) in many plant tissues, especially in the bran and seeds. It has also been implicated in binding and storage of metals, particularly Zn, in roots of a number of Zn-tolerant species (Rauser 1999). Protein bodies in mature seeds are special vacuoles in which P., Mg, K, Ca and other mineral nutrients are stored (Lott 1995). The chief storage form is phytin or phytate, a mixed salt of myoinositol hexaphoric acid or phytic acid. Phytate has a special relevance in agriculture and food bioscience, since it is not digestible to humans or non-ruminant animals, so it is not a source of either inositol or phosphate if eaten directly. Moreover, it chelates essential minerals such as zinc and iron and thus makes them unabsorbable. In addition, but to a lesser extent, it chelates macro minerals such as calcium and magnesium too. Therefore, biofortification approaches concentrate on the reduction of phytate in seeds of crop plants (see section 1.3).

1.2.3 Nicotianamine (NA)

1.2.3.1 Plants with altered NA contents

Much of the information of the role of NA *in planta* has been obtained with the NA-free tomato mutant *chloronerva*, which bears a single base change in the apparently single *NAS* gene (Ling et al. 1999). *chloronerva* has been first described by Böhme and Scholz (1960) as a spontaneous recessive, monogenic mutant of the tomato cultivar Bonner Beste which shows a severe growth and developmental inhibition, as well as a chlorophyll defect in the intercostal areas of young leaves. Flower buds are very rarely developed but do not unfold and die off. The phenotype could be completely restored to the original tomato wild type by grafting the mutated shoot upon wild type rootstock or by application of extracts of wild type plants to the leaves (Böhme and Günter Scholz

1. Introduction

1960; Guenter Scholz and Böhme 1961). However, the restoring effect of grafting reduces when the plant entered the reproductive stage, since the young leaves became again chlorotic. This formely called `normalization factor` was finally isolated in a crystalline state from alfalfa (*Medicago sativa*) (Scholz and Rudolph 1968; Buděšínský et al. 1980) and identified as water-soluble, ninhydrin positive substance. During studies of the nitrogen metabolism of *Nicotiana tabacum* (tobacco) in 1971 the substance *nicotianamine* (NA) has been isolated and already got its name (Noma, Noguchi, and Tamaki 1971).

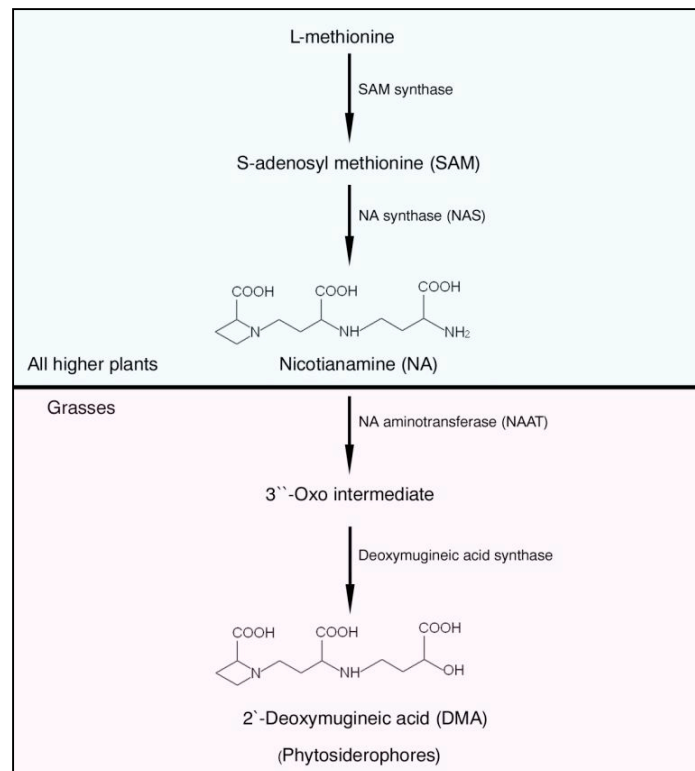


Fig. 1.2: Pathway of *nicotianamine* (NA) and *Deoxymugineic acid* (DMA) biosynthesis in higher plants

NA biosynthesis (upper part of the pathway) occurs in all tested higher plant species. DMA synthesis (lower part of the pathway) only proceeds in grasses. All enzymes and substrates participating in the pathway are shown.

Further evidence for the role of NA *in planta* derives from investigations of transgenic tobacco plants, named *naat* that constitutively expressed the gene encoding the nicotianamine aminotransferase (NAAT) from barley which led to the increased DMA synthesis consuming the NA pool of the plant (Takahashi et al. 2003). This NA shortage led to disorders in internal metal transport, sterility, reminiscent to the *chloronerva* phenotype. Furthermore, *naat* plants exhibited abnormal flower phenotypes (Takahashi et al. 2003).

1. Introduction

Consequences of the loss of NA in mutant plants led in general to alterations in the homeostasis of metals, in particular Fe and Cu, sterility and a characteristic interveinal leaf chlorosis in young leaves, reminiscent of Fe deficiency, reduced growth and complete sterility giving supportive evidence that NA plays a central role in the homeostasis of Fe and Cu.

An increase of NA content could be observed in the hyperaccumulating species *Thlaspi caerulescens* which showed elevated NA contents in roots upon Ni treatment which correlated with metal abundance in roots (Mari et al. 2006). The Zn hyperaccumulator *Arabidopsis hallerii* also showed an increased abundance of root NA (M Weber et al. 2004). These studies demonstrated that increased levels of NA confer tolerance to toxic amounts of heavy metals.

Specific predictions about NA function in Fe and Cu homeostasis deriving from results obtained with *chloronerva* and *naat* plants are presented in detail in the context of the next four sub-processes of plant metal homeostasis and in section 1.3.

1.2.3.2 Chemical properties of NA

During the synthesis of NA, three covalent bonds are broken to release three amino-carboxylpropyl groups from *S*-adenosylmethionine and three new covalent bonds are formed, including an internal cyclization, leading to the formation of an azetidin ring (Fig.1.3). The presence of three amino and three carboxyl groups in the molecule allows the formation of a hexadentate co-ordination that drives the formation of very stable octahedral chelates with a central metal ion (Buděšínský et al. 1980) (Fig.1.3).

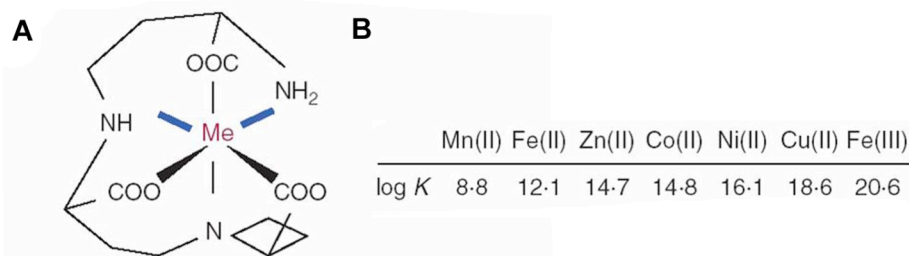


Fig. 1.3: Biochemical properties of nicotianamine (NA)

A) Proposed chemical structure of the NA-metal complex (Budesinsky et al, 1980) **B)** Summary of *in vitro* affinity constants log *K* of complexes of NA with various metals (von Benes et al., 1983, Anderegg and Ripperger, 1989; Wiren et al., 1999). Me= Metal (Fig. modified from Curie et al., 2009)

NA is able to form stable complexes with Mn, Fe(II), cobalt (Co), Zn, nickel (Ni) and Cu. It is able to bind these metals in an increasing order of affinity (Fig.1.3B) (Benes et

1. Introduction

al. 1983; Anderegg and Ripperger 1989). Moreover, NA has a high capacity to chelate Fe(III) which has been reported and demonstrated with different methods (Rellán-Álvarez, Abadia, and Álvarez-Fernández 2008; von Wiren et al. 1999; Weber et al., 2006). In the study of von Wiren et al. (1999) potentiometric and spectrophotometric measurements of the chelation capabilities of NA together with computer simulations investigating the pH-dependent stability of different NA-metal complexes were performed. From the results, the authors were able to draw the following conclusions about NA functions:

- a) For all the metals considered, the stability of the NA-metal complexes had its maximum at pH values above 6.5, suggesting that NA would be more likely a symplastic chelator of metal and is therefore binding metals predominately within cells and the phloem.
- b) Cu is an exception among the essential metals, since the Cu-NA complex is very stable in mild acidic conditions, which is a strong argument in favour of the possible occurrence of Cu-NA complexes in the apoplastic environment as prevailing in the xylem sap.
- c) NA is able to chelate Fe(III) *in vitro* with a high affinity, although the kinetic stability of this complex is much lower than Fe(II)-NA.
- d) In conditions of neutrality NA would be the main chelator. For pH values around 5.5 organic acids like citrate would be the predominant chelators of metal ions.
- e) In an experiment mixing NA and deoxymugineic acid (DMA; a PS derived from NA see figure 2A) with Fe(III), DMA would complex Fe in the pH range 3.5–5.5 whereas above this value NA would prevail, which illustrates that ligand exchanges can occur when switching from an apoplastic to a symplastic environment.

In contrast to computer-based simulations, Rellán-Álvarez et al. (2008) studied the formation of different metal-NA complexes by measuring free NA and metal-NA complexes at different pH conditions. For this purpose they used mass spectrometry techniques, namely electrospray ionization time-of-flight mass spectrometry and could indeed biochemically confirm previous predictions about NA, suggested under point a), b) and d). Taken together, NA has, through the ability to form hexadentate octahedral complexes, ideal structural features to be a stable metal chelator. The different complexes studied either through computational prediction and/or *in vitro* are more stable in neutral conditions, which implies that NA is likely to be a symplastic (phloem and intracellular) metal chelator.

1. Introduction

1.2.3.3 Role of NA in metal detoxification

The ability of NA to chelate divalent metal ions makes this molecule suitable to function in the detoxification process of heavy metals. Indeed NA was found to be important in the detoxification of Ni in *Thlaspi caerulescens* (*T. caerulescens*) (Vacchina et al. 2003). *T. caerulescens*, as Cd/Zn/Ni hyperaccumulator, has been used as a model to study the speciation of Ni in the xylem sap by mass spectrometry approaches. With the use of high-performance liquid chromatography coupled to inductively coupled plasma mass spectrometry (HPLC–ICPMS) and electrospray MS/MS, Ni–NA complexes have been detected in Ni-exposed roots of *T. caerulescens* (Vacchina et al., 2003; Ouerdane et al., 2006). Thus, *in vivo*, NA was able to form a stable complex with Ni that could represent up to 25% of the total Ni (Mari et al., 2006; Ouerdane et al., 2006). These results clearly showed a role of NA in the chelation and long-distance transport of a metal and established a new role of NA in the transport of Ni in a hyperaccumulator plant. Furthermore, a number of studies showing that transgenic overexpression of *NAS* in Arabidopsis or tobacco confers increased tolerance to Ni (Douchkov et al., 2005; Kim et al., 2005; Pianelli et al., 2005) supporting the role of NA in providing Ni tolerance. Ni hyperaccumulating plants were shown to have increased NA levels (Callahan et al., 2007), while Arabidopsis plants with reduced NA levels showed an increased sensitivity to Ni treatment (Klatte et al. 2009). In addition, *NAS* transcripts were more highly expressed in roots and shoots of the Zn-hyperaccumulating species *Arabidopsis halleri* (*A. halleri*) compared with *Arabidopsis thaliana* (*A. thaliana*), and heterologous expression of *AhNAS2* or *AhNAS3* in *Schizosaccharomyces pombe* and *Saccharomyces cerevisiae*, respectively, conferred increased tolerance to Zn, suggesting a direct role for NA in Zn tolerance *in vivo* (Becher et al., 2004; Weber et al., 2004). Comparative microarray experiments between *A. thaliana* and *A. halleri* also identified S-adenosyl methionine synthase (SAM) as being more highly expressed in *A. halleri*, further suggesting upregulation of NA biosynthesis in the Zn hyperaccumulator (Talke et al., 2006; van de Mortel et al., 2006).

1.2.3.4 Role of NA in the subcellular distribution of metals

The distribution of metals between cell organelles is an essential process of metal homeostasis and is described in detail in section 1.2.5. The symplastic compartment includes the cytoplasm and the cell compartments. Most of the cellular Fe is presumably

1. Introduction

bound to proteins or chelators like ferritin, phytic acid or NA. But, whether NA is involved in the delivery and distribution of Fe between cytoplasm and organelles remains elusive. Unfortunately the measurement of Fe in fractions enriched in any organelles has never been reported. Pich et al. (1997) performed immuno-histochemical approaches with anti-NA antibodies in root tips of the tomato cultivar Bonner Beste. The authors reported a staining in the vacuole lumen and, to a lesser extent, a staining in the cytosol whereas the other compartments of the cells were not labeled under control conditions. However, Pich et al., investigated (2001) the NA labelling in response to the Fe nutritional status and showed that in leaves and roots of Bonner Beste grown in control conditions (10 μM Fe) most of the labelling was cytosolic, whereas in Fe-loaded plants (100 μM) a strong labelling could be observed in the vacuole in electron-dense protein-rich structures (Pich et al. 2001). These results demonstrated that NA could act in the subcellular sequestration of Fe into the vacuole in times of Fe overload. This hypothesis was further corroborated using two pea mutants, *bronze (brz)* and *degenerated leaves (dgl)* that over-accumulate Fe in the leaves. In leaves and roots of both mutants the labelling of the vacuole was much stronger than in the corresponding wild-type genotypes accompanied with a 10–20 times increase of NA levels in leaves and roots. These observations, together with the finding that the Fe(II)–NA complex is a poor Fenton reagent (von Wiren et al., 1999), suggest an important role of NA in the detoxification of excess Fe by chelation and sequestration in the vacuole. The study of NA-free *chloronerva* leaves using energy dispersive X-ray micro analysis (EDXMA) indicated strongly altered Fe distribution at the cellular level. Fe accumulates in electron-dense deposits in the stroma of chloroplasts and in the phloem attributed to Fe-phosphate depositions (Becker et al., 1995). In *chloronerva* root cells, Fe accumulates in the cytosol and vacuole, whereas, in Bonner Beste, Fe was mainly detected in the cell walls. Thus, the main role of NA in standard conditions would be to keep Fe in a soluble form, enabling its correct distribution within the different compartments of the cell, since the absence of NA leads to Fe precipitations in chloroplasts and in the phloem sap, lowering its availability and mobility. Upon Fe excess conditions, NA presumably participates in the detoxification mechanisms by chelation and further sequestration in the vacuole (Fig. 1.6).

1. Introduction

1.2.3.5 Transport of metal-NA complexes throughout the plant

The circulation of Fe throughout the plant and the distribution to tissues and organelles relies on transmembrane transporters whose nature depends on the type of Fe substrate. Contrary to the transporters responsible for the entry of Fe from the soil solution into the root, candidate transporters that mediate long-distance transport within the plant have only been discovered in recent years. A family of proteins called Yellow Stripe-Like (YSL) was suggested to transport metals bound to NA (Curie et al., 2001). This suggestion was based on the sequence similarity between the YSL genes deduced from the *Arabidopsis thaliana* genome sequence and the recently cloned Yellow Stripe1 gene from maize (ZmYS1). YS1 is a proton coupled symporter (Schaaf et al., 2003) that transports iron complexed by specific plant-derived Fe(III) chelators known as phytosiderophores (PS) that form stable Fe(III) chelates (Curie et al. 2001; Louis A Roberts et al. 2004; Schaaf et al. 2004). NA is the direct biochemical precursor to PS, and as such, is structurally similar. Recently, ZmYS1 was shown to transport Fe from Fe(II)–NA complexes (Roberts et al., 2004; Schaaf et al., 2004), and was observed to transport metals other than Fe (Schaaf et al., 2004). Because PS are neither made nor used by non-grass species like Arabidopsis, the role of the YSL proteins in Arabidopsis is likely in the transport of metals complexed by the PS-related compound NA. Although final proof is still missing, experimental evidence points to a role of the YSL proteins in the long-distance and intracellular transport of metals, especially Fe, complexed to NA. Eight *YSL* genes could be identified in the Arabidopsis genome. Clustal analysis of YSL protein sequences indicated the existence of three distinct YSL sub-groups (Fig. 1.4), at which AtYSL1, AtYSL2 and AtYSL3 are the most closely related to ZmYS1 (DiDonato et al. 2004). Therefore, these three *YSL* genes are the best characterized genes. DiDonato et al. investigated the YSL genes using YSL2 as example, which is the closest relative of ZMYS1. When Fe is abundantly available, YSL2 expression was induced, while being repressed under Fe-limiting conditions in roots and shoots (DiDonato et al., 2004). As shown by DiDonato et al. 2004, Fe-NA complexes may not be the only substrates of YSLs. In this study the authors showed that, unlike ZmYS1, YSL2 was able to transport both Fe and Cu when these metals are complexed with NA. Consistent with this function, YSL2 transcription is regulated by the levels of these metals in the growth medium (Didonato et al., 2004). Furthermore,

1. Introduction

the rice ortholog OsYSL2, also localizes to the vasculature and has been shown to transport Fe-NA when expressed in *Xenopus laevis* oocytes (Koike et al. 2004).

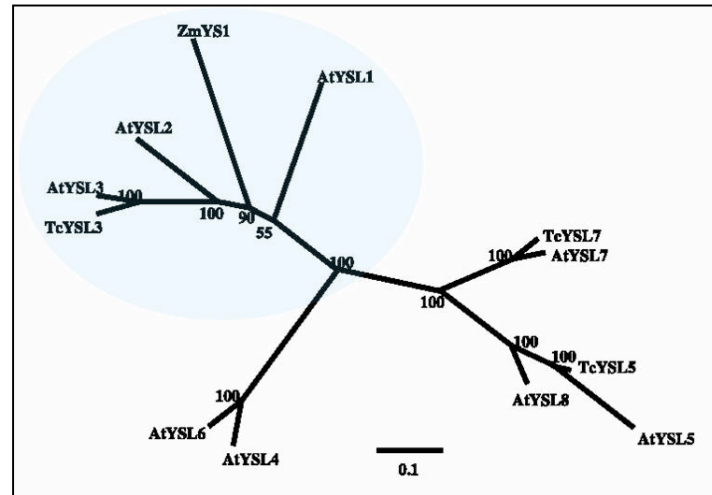


Fig. 1.4: Phylogenetic tree of TcYSL, AtYSL and ZmYS1 proteins

The phylogenetic analysis of YSL protein sequences indicated the existence of three distinct YSL subgroups, at which AtYSL1, AtYSL2 and AtYSL3 are the most closely related to ZmYS1 (highlighted in blue). 18 members of the Rice YSL family were not included in the analysis. (Figure: Modified from Gendre et al., 2006, calculations were performed by Gendre et al, 2006 using CLUSTAL W neighbor-joining method, the tree was visualized with phylodendron). Zm= *Zea mays*; At= *Arabidopsis thaliana*; Tc= *Thlaspi caerulescens*

By using transgenic *Arabidopsis* promoter-GUS constructs of the three YSL genes, several groups found their expression localized to the parenchyma of the vasculature throughout all plant tissues (DiDonato et al. 2004; Le Jean et al. 2005; Schaaf et al. 2005; Waters et al. 2006). This localization of YSL expression to the parenchyma of the vasculature suggests a role in the lateral movement of metals bound to NA. The repression under Fe limiting conditions points to a role in the restriction of xylem unloading in older tissues to guide metals to young developing tissues or seeds in times of Fe deficiency.

Waters et al. (2006) reported the ability of ATYSL1 and ATYSL3 to complement the yeast mutant *fet3fet4* (defective in Fe uptake) by supplementation of Fe(II)-NA to the growth medium. DiDonato et al., 2004 postulated the complementation of the yeast strains *fet3fet4* and the complementation of *ctr1* (defective in Cu uptake) by the transformation with AtYSL2 and supplementation of Fe(II)-NA and Cu(II) into the growth media. Schaaf et al., 2005 criticized the work of DiDonato et al., since they were not able to repeat the yeast complementation experiments of *fet3fet4* with the same YSL constructs in other expression vectors. Recently, Chen et al., 2010 did the same

1. Introduction

functional complementation studies. Although Fe(II)-NA transporter activity was expected for AtYSL1 and AtYSL3, it was surprising to find that only Fe(III)-PS could be used as substrate for transport by AtYSL3, since PS, including DMA used in the assay, are not produced by Arabidopsis. Only grass species (e.g. rice, maize, wheat, etc.) produce PS, so only these species would be expected to have YSLs that transport PS. Conclusively, a direct proof for the ability of the YSLs to transport NA-metal complexes *in planta* is still missing, but nevertheless findings about the YSL transporter pointing to their associated role with NA are presented in the context of the 4 sub-processes of metal homeostasis in the next sections.

1.2.4 Long-distance transport of Fe and Cu

After entering the root from soil most of the Fe is needed in the photosynthetic shoot tissue. Therefore, Fe has to be transported throughout the plant from root epidermal cells to the shoot tissue where it is needed (Fig. 1.5). It moves symplastically through the interconnected cytoplasm, perhaps diffusing along the concentration gradient (Marschner, 1995). At the endodermis, all metal ions have to be actively loaded into the xylem and transported by the transpiration stream to the shoot tissue. Not all tissues can be supplied with minerals by the transpiration stream. Seeds for example rely on the nutrient feed by the phloem. Very young tissues, like the developing leaves, must receive essential metals from the faster differentiating phloem in the provascular tissue, while the formation of the xylem is not yet completed (Curie et al. 2009). The loading and unloading of the vasculature is an essential process in plant metal transport, but the detailed interaction between transporters, ligands and metals in xylem and phloem remains elusive (Fig.1.5). Metals enter the xylem in the root and reach mature leaves and the inflorescence via the xylem. Metals and other important nutrients can be mobilized out of the photosynthetically active or senescing leaves and brought to the inflorescence and young developing leaves via the phloem in both directions.

1.2.4.1 Root-to-shoot xylem dependent transport of Fe

How exactly Fe enters the xylem is not known so far, but it is most likely chelated to molecules. Putative candidates are citrate and NA. As mentioned above, NA is ubiquitous in all higher plants studied until now. The mild acidic pH of the xylem favors the chelation of Fe to citrate rather than NA, whereby Cu has also a very stable binding to NA in the xylem (von Wiren et al., 1999). In the work of Durrett et al. (2007)

1. Introduction

it has been described that Fe exists in Fe(III)-citrate chelates in xylem and Alvarez et al., 2010 just recently identified tri-Fe(III)-tri-citrate complexes in the xylem sap of iron deficient tomato plants resupplied with Fe. The citrate transporter FRD3 (ferric reductase defective), which is localized to the plasma membrane of the pericycle (Green and Rogers 2004) mediates the efflux of citrate into the xylem and is required for the transport of Fe to the shoot (Durrett, W Gassmann, and E E Rogers 2007). *frd3* plants suffer from Fe deficiency in the shoot and show 40% reduced citrate levels in the xylem as well as an accumulation of Fe in the root (Durrett et al., 2007; Green and Rogers 2004; Rogers and Guerinot 2002). This suggests the necessity of FRD3 for the long-distance transport of Fe. Rice also relies on a *FRD3*-like gene, *OsFRDL1*, for efficient translocation of Fe to the shoot (Yokosho et al. 2009). Fe is thought to be unloaded from the vasculature into developed tissue through yet-unknown mechanisms. One possible candidate to transport Fe into the vasculature is IRON REGULATE1/ Ferroportin1 (IREG1/FPN1). It is localized to the plasma membrane and is expressed in the stele (Morrissey et al. 2009).

Although the FPN1 seem to mainly function in the Cobalt root-to-shoot transport, the loss of FPN1 results in chlorosis in *fpn1* mutants, suggesting that FPN1 loads iron into the vasculature. Yet, *fpn1* plants show no change in the iron deficiency response. The loss of the closely related IRON REGULATE2/ Ferroportin2 (IREG2/FPN2), however, results in a greatly increased iron deficiency response. This could be caused by changes in metal concentration and localization within the root, at both the subcellular and root layer level, altering the kinetics of Fe movement to the shoot (Morrissey et al., 2009). While the loss of FPN1 alone is not enough to alter iron sensing, it may play an important, but not essential role as Fe effluxer and might act redundantly with other Fe transporter in the stele.

All factors involved in uptake, xylem loading, long distance transport, remobilization and seed loading are illustrated in Fig. 1.5.

1.2.4.2 Root-to-shoot transport of Cu

Efflux of Cu into the vasculature is thought to occur through an HMA family transporter. A recent study has implicated HMA5 in Cu efflux by showing that HMA5 is predominantly expressed in the root and is strongly and specifically induced by Cu excess. *hma5* mutants overaccumulate Cu in the root, which suggests a compromised efflux system when HMA5 is absent (Andres-Colas et al. 2006). Further evidence in

1. Introduction

support of the role of HMA5 in Cu translocation from the roots to the shoots arises from a study of natural variation in Cu tolerance among *Arabidopsis* accessions, which identified HMA5 as a major QTL associated with Cu translocation capacity and sensitivity (Kobayashi et al. 2008). Based on the biochemical properties of NA, which have been mentioned above (von Wiren et al., 1999) and studies of the NA-free tomato mutant *chloronerva*, Cu is likely chelated to NA for translocation from the root to the shoot via the xylem. Surprisingly, measurements of Fe, Zn, Mn and Cu contents of different plant organs of *chloronerva* have revealed that this mutant contained significantly more Fe than wild type plants, irrespective of the Fe nutritional status (Pich et al., 1994). This finding indicates that the long-distance transport of Fe is not disrupted in this mutant. The main disorder in metal distribution in *chloronerva* concerns Cu. In a time course experiment it has been shown that Cu accumulates in the roots during growth, whereas leaves suffer from severe Cu deficiency, which increases for each leaf produced (Pich et al., 1994; Pich and Scholz 1996). Hence, the Cu-containing enzymes superoxide dismutases and plastocyanin were nearly absent in *chloronerva* leaves (Herbik et al. 1996). Finally, the measurement of Cu concentration and translocation rates in the xylem sap were three to five times lower than in the wild-type genotype and the addition of NA could restore part of the normal Cu concentration (Pich and Scholz, 1996). These examples of experimental evidence are largely in favour of a direct role of NA in the root-to-shoot translocation of Cu, via the xylem sap, which is strengthened by the demonstration of von Wiren et al., 1999 that the Cu–NA complex is completely stable at the pH of the mild acidic xylem sap, that ranges between 5 and 6 as explained in section 1.2.2.

1. Introduction

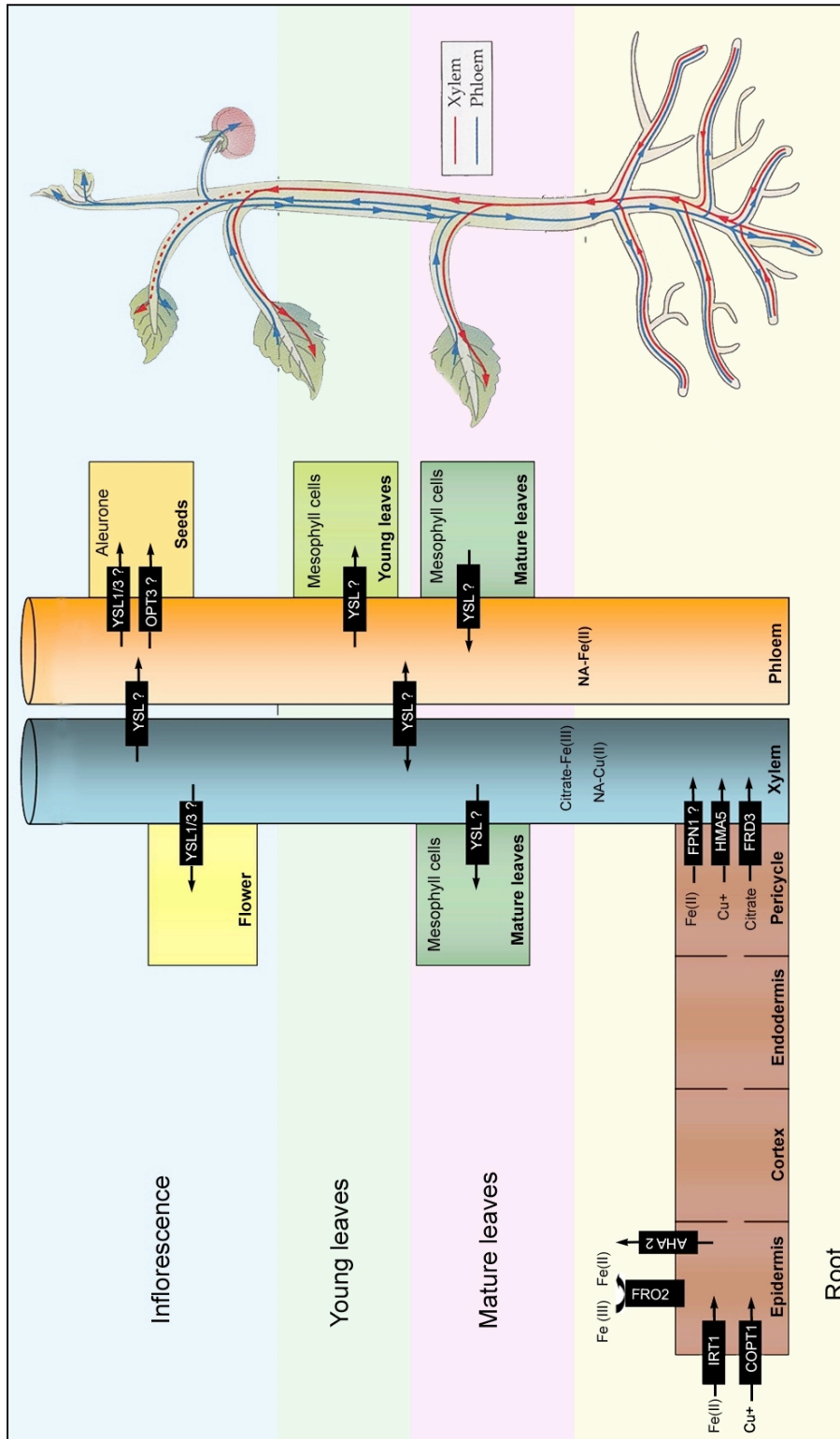


Fig. 1.5: Intercellular transport of Fe in dicotyledonous plants

Fe and Cu are taken up into the symplast by transporters located in the Epidermis. Reduction of Fe and possibly Cu by FRO2 and acidification of the soil by AHA2 contribute to increased metal uptake. Metals can then travel through the symplastic space to the vasculature, bypassing the Casparian strip on the endodermis. Metals have to get actively loaded into the vasculature but this transport into the xylem is still not fully characterized. It is thought to involve members of the HMA family and the citrate effluxer FRD3. FPN1 is also a putative candidate to load Fe into the xylem. In the shoot, metals are carried to the shoot through the transpiration stream bound to chelators like citrate and *nicotianamine* (NA). In the shoot they are unloaded into the tissue cells, most likely by members of the YSL family. YSLs may also translocate metals to the phloem, where they can then be delivered to the seed. YSL transporter and OPT3 are predicted to transport metal complexes bound to NA. The illustration of a dicotyledonous plant on the right shows the connection and transport direction of xylem and phloem. Xylem is represented by the red stream and brings nutrients with the transpiration stream from root to the shoot. The phloem is represented by the blue stream and transports sugar and minerals from the photosynthetic active plant parts to all other plant organs. References are cited in the text. NA = Nicotianamine

1. Introduction

1.2.4.3 Shoot-to-seed phloem dependent transport

Xylem transport is driven by the transpiration stream and since seeds do not transpire, Fe is most likely reaching the seed via the phloem (Grusak 1994). Seeds represent the major sink for Fe during their development, which they receive from roots and senescent leaves. The level of remobilization from shoot to seed varies from species to species: rice transports only 4 % of shoot Fe to the seeds, while wheat transports 77 % of shoot Fe to the seed (Garnett and Graham 2005). The timing and regulation of senescence have been shown to have a significant effect on Fe accumulation in seeds. In wheat, the knockdown of multiple NAM transcription factors involved in timing and regulation of metal seed loading, which is connected with senescing time of the plant, was found to delay senescence for three weeks, and to decrease seed Fe by over 30 % (Uauy et al. 2006). It is not clear how developmental changes influence Fe remobilization, but the correlation between flowering time, seed maturation and seed nutrient content has been disregarded in crop breeding in the past. Crop breeding has often been selected for improved grain maturation time but ignored nutrient accumulation in the grain as a desirable trait. In consequence, many staple crops are agronomically productive but have low levels of nutrients like Fe in the seed.

1.2.4.3.1 Fe movement in the phloem sap

Since Fe(II) is supposed to be transported in the phloem, it is likely, that it moves as NA chelate as mentioned above in section 1.2.1 (von Wiren et al., 1999, Curie et al., 2009). Because of its chelation properties, which are the highest at neutral and mild basic pH and its affinity and stability against other ligands like organic acids, NA is a predestinated phloem transporter (Stephan et al. 1996). Because of the extremely problematic collection of accurate amounts of phloem sap the detection of NA in the phloem sap has been achieved only in specific species like *Ricinus communis* seedlings, cucurbits and oilseed rape (*Brassica napus*) by wounding of fruits and exudation (Kehr and Rep 2007). NA could have been detected in the phloem sap of *Ricinus* hypocotyls (Stephan and Scholz 1993; Schmidke et al. 1999) and rape (Mendoza-Cózatl et al. 2008). The concentration in the phloem sap of *Ricinus* was estimated to be 200 μM (which is 10 times higher than the usual concentration in the xylem) and this concentration coincided with the aggregate concentration of Fe, Mn, Zn and Cu (Stephan and Scholz, 1993).

1. Introduction

The findings about NA dependent transport of Fe via the phloem has to be connected with studies of the members of the YSL transporter family, which are putative candidates involved in phloem loading and unloading with metal-NA complexes (Curie et al., 2009). The recently published work of Chu et al. (2010) emphasizes a role of YSL1 and YSL3 in phloem loading and unloading with NA-metal complexes in leaves and inflorescences. The authors showed by inflorescence grafting experiments of *ysl1ysl3* double mutants on wild type plants and vice versa that on one hand the activity of AtYSL1 and AtYSL3 in leaves is required for normal fertility and normal seed development, while on the other hand their activity in the inflorescences themselves is required for proper loading of metals into the seeds. These findings point to the role of YSL1 and YSL3 in loading of metals into the phloem in senescing leaves and phloem unloading in developing seeds. In further support of a role in transporting complexes into the vasculature, DiDonato et al. (2004) and Schaaf et al. (2005) found that YSL2 localizes to the lateral plasma membrane, which has been also demonstrated by Chu et al. (2010) for YSL1 and YSL3 and was elaborated in detail in section 1.2.2. If the YSL proteins indeed transport NA-metal complexes, these findings emphasize a role of NA in loading and unloading of the vasculature.

Nevertheless, the chemical properties and the stoichiometry of NA do not exclude the existence of other metal binding molecules or proteins. Indeed, in the phloem sap Fe appears to be mostly bound to the protein fraction, in particular to a specific protein called ITP (iron transport protein) belonging to the late embryogenesis abundant family (Krüger et al. 2002). ITP is a dehydrin and has been identified in the phloem sap of seven day-old castor bean shoots. It is expressed in the shoots of seedlings and adult plants. Most of the knowledge about ITP has been obtained in experiments with radiolabeled Fe. By applying ^{55}Fe to the cotyledons, nearly the complete radioactivity was recovered in the phloem sap associated with the 17 kD ITP protein, indicating that Fe moves quickly to the phloem and nearly all is bound by ITP. The purified ITP protein was found to preferentially bind Fe(III) but not Fe(II) (Krüger et al., 2002). Unfortunately, obtaining large amounts of phloem sap from plant model organisms is difficult, and ITP remains reported only in castor beans. The most similar genes in *Arabidopsis* have annotations related to stress, and several genes are highly upregulated in response to Fe deficiency in the root (BTI1, BTI2, At1g54410, At2g44060), although none are specific to the stele (Dinnyen et al., 2008). But, working under the assumption that an ITP exists in other plant species, it has been proposed that NA serves as a

1. Introduction

shuttle, facilitating Fe movement in and out of the phloem or more generally entering a symplastic route, while the actual long-distance transport of Fe within the phloem occurs bound to ITP, but this remains to be proven.

1.2.4.3.2 The role of NA in Fe seed loading

The studies on mutants with altered NA content like *chloronerva* and the transgenic tobacco *naat* showed that NA is essential for flower and seed development. The loss or depletion of NA results in deformed flowers and sterility, as well as significant decreases in floral Fe accumulation (Ling et al. 1999; Takahashi et al. 2003). Indicative for a role of NA in reproduction is also the *NAS* expression pattern in tobacco with highest expression in flowers, especially in anthers and pollen (Takahashi et al., 2003). Interestingly, the grafting of NA-depleted tobacco shoots onto *NAS* overexpressing basis restored Fe mobilization in leaves and flower development but could not completely rescue the impaired seed set (Takahashi et al., 2003). This experiment emphasizes the requirement of the Fe-NA complexes, which is particularly high for normal seed development.

Since Fe-NA complexes are critical in seed development, YSLs may play an important role in the delivery of Fe-NA to the developing seed. In *Arabidopsis* *YSL1* is expressed in the flowers, in pollen, young siliques, embryo and in and around the leaf veins, especially in senescent leaves (Le Jean et al., 2005). This expression pattern suggests a role in Fe remobilization from senescent leaves for the transport to developing seed. Indeed, the seeds of the *ysl1* loss of function mutant lines contained 30-65% less Fe and germinated more slowly on Fe-deficient medium. Watering plants with exogenous Fe could not restore Fe accumulation in the seeds, indicating that YSL1 plays a role in seed loading that cannot be compensated by other transporters or chelators. The expression pattern of YSL3 is somewhat similar to that of YSL1: in the vasculature of shoots and in pollen and anthers (Waters et al., 2006). The *ysl1ysl3* double mutant was chlorotic, and most flowers did not produce siliques. The few resulting seeds were small and irregular and have germination rate of 20% compared to wild-type seeds. These phenotypes are similar to the floral deformity and sterility seen in plants lacking NA (Ling et al., 1999; Takahashi et al., 2003) indicating that seed development requires not just the availability of NA but also specific Fe-NA transporters. Just recently, dual roles of YSL1 and YSL3 in reproduction have been shown by Chu et al. (2010) with inflorescence grafting techniques. On the one hand, their activity in the leaves is

1. Introduction

required for normal fertility and normal seed development and their activity in the inflorescences themselves is required for proper loading of metals into the seeds on the other hand, which was also predicted before by Waters et al. (2006). This study using the double mutant *ys1/ys3* demonstrated that both of these transporters play a role in Fe, Cu and Zn remobilization from leaf tissue, which fits to the results of DiDonato et al. (2004) showing reduced levels of these metals in seeds in the absence of YSL1 and YSL3.

A further candidate in the transport of Fe-NA complexes is OPT3. OPT3 is a member of the oligopeptide transporter family that includes ZmYS1 and the AtYSLs (M. G. Stacey 2002; Yen, Tseng, and Saier 2001; Saier 2000). *OPT3* is expressed in roots and the shoot, in pollen, the silique vasculature and the developing embryo at which the expression in the root and shoot vasculature is upregulated in response to Fe deficiency (Stacey 2002; Stacey et al. 2006). A recent study has demonstrated that OPT3 plays an important role in Fe transport (Stacey et al. 2008) and while it has not been established what form of Fe is transported, it is likely to be chelated to NA or an oligopeptide as the name of these transporter predicted. Unlike the *ysl* single mutants, the *opt3* null mutant is embryo lethal, indicating an essential role for AtOPT3 in seed development. An *opt3* knock down line, *opt3-2*, allowed embryo formation in seeds, but these accumulated significantly less Fe (Stacey et al., 2008). The *opt3-2* plants also exhibit constitutive expression of genes involved in the root Fe deficiency response, regardless of exogenous Fe supply. This leads to the accumulation of very high levels of Fe in leaves, resulting in brown necrotic spots, especially during the seed-filling stage. The substrate of OPT3 is unknown, but its phenotypes and relation to the YSLs suggests it likely transports chelated Fe or a Fe chelator. There are eight other members of the Arabidopsis OPT subfamily, and many are expressed in the vasculature and reproductive organs. None of them, however, have reported phenotypes, most likely due to functional redundancy. Although yeast studies with OPT3 have suggested that it can transport Cu as well (Wintz et al., 2003), OPT3 does not seem to play a direct role in Zn or Cu loading, as *opt3-2* seeds indeed accumulate increased levels of these two metals (Stacey et al., 2008).

1.2.5 Intracellular transport and storage of Fe

Once Fe and Cu have reached their destination tissue, they must be properly distributed at the sub-cellular level. This covers the demand of Fe for metabolic processes in the

1. Introduction

different cell compartment and protects the cell from oxidative stress in times of excess. Following paragraphs will describe for which proteins and clusters Fe and Cu are needed and what is known about the metal transporters of the different cell compartments. For an overview of transporters involved in intracellular transport compare Fig. 1.6.

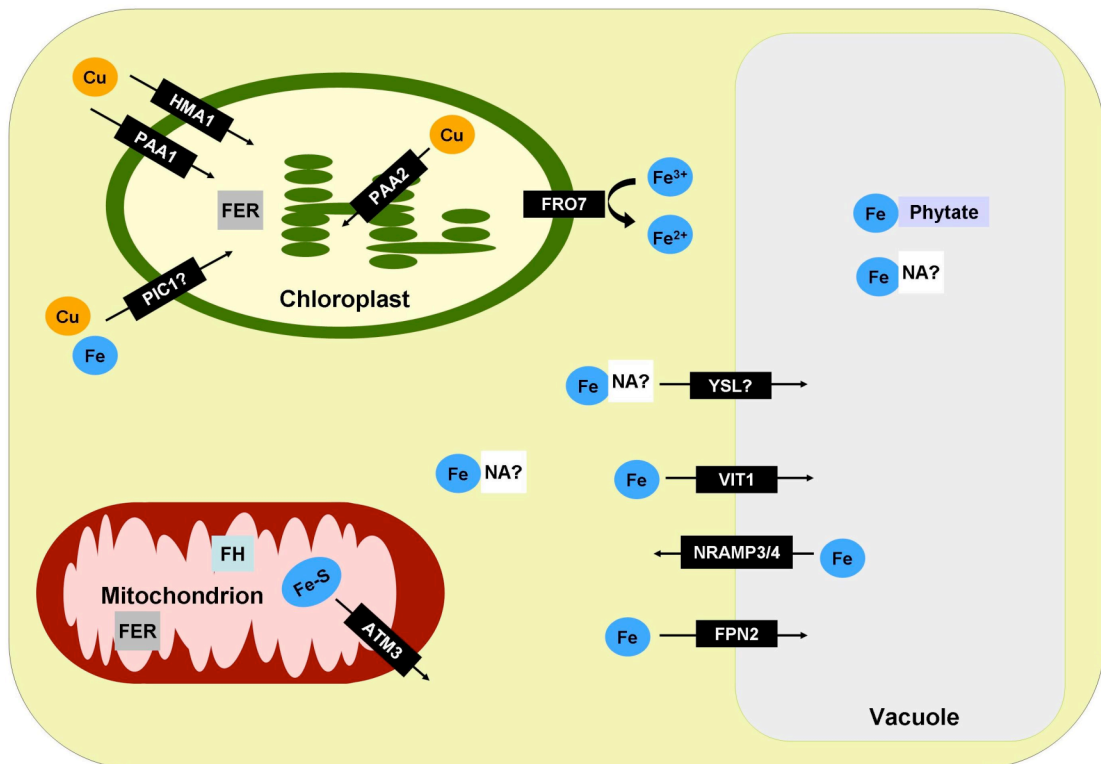


Fig. 1.6: Intracellular metal transport and sequestration (modified from Palmer and Guerinot, 2009)

Fe is transported into the vacuole by FPN2 and VIT1 and is remobilized from the vacuole by NRAMP3 or NRAMP4. Fe is possibly bound to nicotianamine (NA) in the cytosol and transported via YSL transporters into the vacuole. Fe-NA and Fe-phytate are most likely the main storage forms of Fe in the vacuole. Transport into the chloroplast is best characterized for Cu, which is transported into the chloroplast by HMA1, PAA1 and possibly PIC1. PAA2 is thought to transport Cu across the thylakoid membrane. Transport of Fe into the chloroplast is known to require reduction by FRO7 and may involve transport by PIC1. Within the chloroplast, Fe is sequestered in ferritin (FER). Very little is known about transport in and out of the mitochondria, though ATM3 is well established as Fe-S cluster exporter. In the mitochondria, Fe is sequestered by FER and frataxin (FH), most likely to minimize oxidative stress. FH also plays a role in Fe-S cluster assembly or repair. References reside in the text.

1.2.5.1 Chloroplast

Because of the immense Fe demand in the green parts of the plant, nearly 90 % of plants Fe is located to the chloroplast, where it is required for photosynthesis, the Fe-S cluster assembly of the electron transport chain and the synthesis of chlorophyll, heme and Fe-S clusters (Kim and Guerinot 2007; Terry and Abadia 1986). Cu and Fe are in addition needed as cofactors for the superoxide dismutases (SODs) located to the

1. Introduction

chloroplast. They catalyze the conversion of superoxides to hydrogen peroxide, preventing cellular damage by the extremely reactive hydroxyl radical species normally produced from the electron transport chain (Alscher 2002). Two different kinds of SODs are known to protect the cell from ROS damage: Fe-SODs and CuZn-SODs. Under limiting conditions of metals, plants are able to synthesize both (Cohu and Pilon 2007; Myouga et al. 2008; Puig et al. 2007). This flexible mechanism of metal utilization as cofactor underlies a differential control of Cu enzymes by micro RNAs (Abdel-Ghany and Pilon 2008; Yamasaki et al. 2007; Yamasaki et al. 2009).

Metal transport into the chloroplast

Recently, it has been shown that reduction of Fe by FRO7 is required for uptake into the chloroplast (Jeong et al. 2008). *fro7* mutants contain 30% reduced Fe in the chloroplast and show photosynthetic defects, including perturbed photosystem components and compromised electron transport. Most importantly, FRO7 is required for seedling survival under Fe-limiting conditions. These findings, along with the identification of a reductase in the mitochondrial proteome (Heazlewood et al. 2004), as well as the abundance of other FROs (Mukherjee et al. 2006) and the transport of Fe in form of Fe(III)-citrate chelates (Durrett et al., 2007) raises the possibility that Fe must be reduced at each of the membranes that it has to cross.

Very little is known about the transporters, which supply the chloroplast with Fe. The only known transporter is PIC1, which has earlier been identified as a component of a protein translocation complex. It was found to immunoprecipitate with the major components of the Toc and Tic translocon (Teng et al. 2006; Daniela Duy et al. 2007), indicating that the permease PIC1 (Tic21) localizes to the inner chloroplast envelope.

PIC1 was able to complement the yeast Fe uptake mutant *fet3fet4*, but moreover it was also able to complement the yeast Cu uptake mutant *ctr1* as well (Duy et al., 2007). It remains to be shown whether PIC1 can transport Fe and/or Cu in plants. Although overall Fe levels in the leaf do not change in the *pic1* mutant, the plants are dwarfed and chlorotic, with impaired chloroplast development. These plastids were also found to have elevated levels of ferritin and lacked thylakoids, which suggests a disturbed Fe recovery in the plastid resulting in the accumulation in ferritin. This mislocalization of Fe in *pic1* also changes the expression of non-plastid, Fe-regulated genes in the shoot cells, and led to the reduced expression of the root Fe uptake transporter *IRT1*, indicating that the chloroplast is integral to the Fe sensing mechanism, because the Fe

1. Introduction

status of the chloroplast affects the Fe homeostasis of the entire cell, in addition to the expression of Fe deficiency response genes in the root (Duy et al. 2007; Duy et al. 2011).

The Cu transport into different cell compartment is better understood than the Fe transport. PAA (HMA6) and PAA2 (HMA8), two members of the Cu-transporting P_{1B}-type ATPase family, have been shown to be as essential for the Cu delivery to plastocyanin in the chloroplast (Abdel-Ghany and Pilon 2008; Shikanai 2003). PAA1 localizes to the inner chloroplast envelope, while PAA2 localizes to the thylakoid membrane. The fact, that the Cu transport into the chloroplast in *paal1paal2* mutants is not completely abolished, suggests the existence of other transporters. Another family member of PAA1 is HMA1, which localizes to the chloroplast envelope and shows increased ATPase activity in the presence of Cu and Zn (I Moreno et al. 2008; Seigneurin-Berny et al. 2006). HMA1 has been identified to be a Ca⁺/heavy metal pump in yeast and may play a specialized role in Cu delivery to superoxide dismutase, as *hmal* mutants show reduced chloroplastic CuZn-SOD activity but normal plastocyanin content (Seigneurin-Berny et al., 2006; Moreno et al., 2008).

1.2.5.2 Mitochondria

In Mitochondria Fe and Cu are needed in the respiratory electron transport chain and in synthesis of Fe-S clusters (Balk and Lobréaux 2005). Flower development, especially microsporogenesis, is highly dependent on energy from the mitochondria (Ray J Rose 2007). Maintaining mitochondrial Fe levels is thus of high importance, because Fe deficiency produces deformed mitochondria in rice pollen and reduces seed yield (Mori et al., 1991). Appropriately, many Fe-related genes are highly expressed in the anthers, such as NtNAS, AtOPT3, AtYSL1, AtYSL3, and AtIRT1 (Vert et a., 2002, Takahashi et al., 2003; Waters et al., 2006; Stacey et al., 2006).

Metal transport into the mitochondria

As in the chloroplast, very little is known about the mitochondrial metal transporters. In Arabidopsis, ATMs, half-molecule ABC proteins, which are orthologs of ScATM1 are the only identified mitochondrial Fe transporter (Kispal et al. 1997). The Arabidopsis ATMs were first identified by the chlorotic, dwarf phenotype of the *atm3* loss of function mutant (or *sta1*). Like *atm1* yeast mutant, mitochondria of these plants accumulated more nonheme, nonprotein Fe than those of wild-type plants, resulting in

1. Introduction

increased oxidative stress. AtATM3 (STA1), an ABC transporter orthologous to the yeast ATM1p, has been implicated in the export of Fe-S clusters and can rescue yeast *atm1* mutants (Kushnir et al. 2001).

Nothing is known so far about the Cu transport into mitochondria, but the Cu chaperone Cox17 has been implicated in Cu delivery within the mitochondria (Maxfield, Heaton, and Winge 2004).

Frataxin was recently identified in *A.thaliana* (Busi et al. 2004) and is a conserved mitochondrial protein implicated in cellular iron homeostasis. It has been involved as the iron chaperone that delivers Fe for the Fe-S cluster and heme biosynthesis (Busi et al. 2006). However, its role in iron metabolism remains unclear, especially in photosynthetic organisms. Like FER4, frataxin is expressed in the mitochondria of the flowers (Busi et al., 2004) in addition to the developing embryo (Vazzola et al. 2007). Unlike mitochondrial ferritin, frataxin is not Fe-regulated, and its loss is embryo lethal (Vazzola et al., 2007, Busi et al., 2006). The knock-down of frataxin in *Arabidopsis* is not lethal but results in increased ROS and decreased vegetative growth and seed set (Busi et al., 2006; Martin et al., 2009). Frataxin is essential to growth because it has functions beyond mitochondrial Fe sequestration. In addition to sequestering Fe, frataxin is believed to serve as a chaperone, mediating Fe delivery to the Fe-S cluster assembling complex (Bencze et al. 2006).

Ferritin has been localized to the mitochondria in several organisms (S Levi et al. 2001; Missirlis et al. 2006; Santambrogio et al. 2007) including *Arabidopsis* (Zancani et al. 2004). They appear to play a very important role in metal homeostasis not only in the mitochondria, but also in the whole cell. *Arabidopsis* is synthesizing four ferritins FER1, FER2, FER3 and FER4. FER1, FER2, and FER3 are predicted to localize to the plastid, while FER4 is predicted to localize to the mitochondria, or be dually targeted to both organelles (Petit et al. 2001). The *fer4* loss of function mutant does not have a phenotype, perhaps because one or more of its paralogs are also targeted to the mitochondria or frataxin is able to compensate. It is expressed in response to Fe overload, but is downregulated in response to oxidative stress (Petit et al., 2001). The expression of *FER4* diverges importantly from what is described for the other three *FER* genes. Like the mitochondrial ferritin in humans and fruit flies (Levi et al., 2001; Missirlis et al., 2006), FER4 appears to play an important role in the mitochondria-rich reproductive organs, because *FER4* expression is restricted to the flowers and the floral

1. Introduction

stalk with a maximum after pollination. The differentiated roles of the four ferritin paralogs is likely controlled by their localization and regulation: *FER2* is only expressed in the seeds, while the other three ferritins are expressed in the shoots and flowers, while *FER1* is the only ferritin expressed in roots (Petit et al., 2001). Additionally, the expression of the three nonseed ferritins increases in response to high Fe levels, whereas the seed *FER2* is expressed in response to the plant hormone ABA (Petit et al., 2001). Ferritins appear to buffer Fe levels and sequester excess free Fe to prevent oxidative stress, as mentioned before in section 1.2.2.2 (Ravet et al. 2009). When the three genes encoding non-seed ferritins were knocked out, the *fer1fer3fer4* triple mutant showed a shift in Fe accumulation from stem to flower when supplemented with Fe, resulting in increased oxidative stress and deformed flowers. This supports the hypothesis that chloroplasts are an important Fe sink and that ferritins may sequester some Fe in the leaf plastids. This could prevent an excess Fe movement to the flower, although it is unclear whether this is by physically sequestering Fe in the shoot or whether the Fe status of the plastid regulates long-distance Fe transport to the flower. Ferritins are not essential for chloroplast development, since *fer1fer3fer4* showed no decrease in photosynthesis (Ravet et al., 2009). Instead, the ferritins prevent excess free Fe from accumulating in the flower, where it causes damage.

1.2.5.3 Vacuole

The vacuole represents an essential storage compartment in seeds. In early seed development the vacuole is functioning as an initial store of metals for the plant before it switches to the uptake by the root. The storage state of Fe in *Arabidopsis* seeds was unknown, although it was long assumed to be stored in ferritin in the plastid. This was based on earlier experiments in legumes that found as much as 90 % of Fe in ferritin (J F Briat et al. 1999). Recent work in *Arabidopsis* has found that there is only very little ferritin in seeds (Ravet et al., 2009), which raises the possibility that in *Arabidopsis* most seed Fe is bound by phytate, NA or some other chelator in the vacuole. Ferritin was estimated to account for only 5 % of total seed Fe (Ravet et al., 2009). Thus, ferritin likely serves more as a Fe buffer, sequestering free Fe to prevent oxidative stress. But, although ferritin is not acting mainly as storage protein in seeds, it is of great importance in agronomic food science (discussed in section 1.3).

1. Introduction

Vacuolar transporter

In *Arabidopsis*, VIT1 transports Fe(II) into the vacuole, and is expressed in the vasculature, especially during embryo and seed development (SA Kim et al. 2006). While the loss and the overexpression of VIT1 do not affect total Fe levels in seeds, Fe is severely mislocalized in the loss of function mutant. The visualization of Fe distribution by synchrotron X-ray fluorescence microtomography (T Punshon, M L Guerinot, and A Lanzirotti 2009) showed Fe concentrated in provascular strands of the embryo in wild-type seeds, while in the *vit1* mutant, Fe was not associated with the vascular system, but rather was seen throughout the hypocotyl and radicle and was concentrated in a layer of cells just inside the abaxial epidermis of the cotyledons (SA Kim et al., 2006). Within the epidermis, the divalent metal effluxer FPN2 is expressed during Fe deficiency on the vacuolar membrane and may serve to buffer Fe uptake by sequestering excess free Fe in the vacuole (Schaaf et al. 2006). When expressed in yeast, FPN2 confers tolerance to Ni (Schaaf et al., 2006) and Co (Morrissey et al., 2009). The Fe-regulated expression pattern and root localization of *FPN2* suggests that it serves as an adaptation to the influx of Ni and Co during Fe deficiency. Accordingly, the loss of FPN2 results in increased sensitivity to Ni and Co (Morrissey et al. 2009). While VIT1 and FPN2 were shown to load Fe into the vacuole, two *Arabidopsis* transporters, namely NRAMP3 and NRAMP4, function in the remobilization of vacuolar Fe in times of Fe deficiency (Thomine et al. 2003; Lanquar et al. 2005). Like *vit1*, the *nramp3 nramp4* double mutant seeds contain the same level of Fe as wild-type but show a 90 % lethality rate when germinated on Fe-deficient soils, while single mutants show no phenotype (Lanquar et al., 2005).

1.3 Improving Fe bioavailability in crop plants

As the world's population grows and the demand for food increases, it will become imperative that we perform the research needed to design agricultural systems that not only provide enough food to meet energy needs but also provide healthy foods to prevent nutrient deficiencies and the chronic diseases associated with inappropriate diets and low quality food products. Approximately two billion people worldwide suffer from Fe deficiency anaemia. Hence, a solution needs to be found to combat this disease. A large-scale medication of pharmaceutical products would be a possible solution to combat deficiency disorders, but it requires a fully-developed infrastructure, which is a

1. Introduction

limiting factor in developing countries. Moreover, these countries are not able to afford such immense transport and purchase costs.

A superior approach to cure human malnutrition is the improvement of crop plants which indirectly enhances human diets. As mentioned in section 1.1, Fe deficiency is also the predominant micronutrient malnutrition in plant. The foliar application of Fe chelators such as Fe-EDTA or Fe-EDDHA has been recommended to cure Fe deficiency of crops growing on calcareous soils. Indeed, the deficiency can get cured to some extent with fertilizers, but these chemicals are very expensive for extensive use and furthermore can be toxic for the environment. Additionally, such treatments are expensive and cannot be precisely targeted to the deficient parts of the plant, causing, in some cases, Fe excess followed by yield reduction.

To have significant impact on Fe nutrition of humans, improvement strategies are under way to develop new varieties of major crops with increased amounts of bioavailable Fe. The technical term 'biofortification' designates the generation of plants that fortify themselves with nutrients and other health promoting factors during their growth. Biofortification is therefore an agricultural tool to combat human malnutrition in the world. Biofortification focuses on breeding major staple food crops that would produce edible products enriched in bioavailable amounts of iron, zinc and provitamin A carotenoids. In the biofortification process three challenges have to get overcome. First, the plants have to take up more of the nutrients. Second, the nutrient should become accumulated in the edible parts of the plant and third, the nutrient should stay bioavailable for the human body. To achieve this goal, scientists need to acquire a better understanding of the underlying mechanisms of plants metal homeostasis to provide a basis for future biotechnological and conventional breeding approaches.

1.3.1 Approaches for Fe biofortification of plants

Some organic compounds like Phytic acid (PA) (described in section 1.2.2) can decrease the availability of nutrients in the plant. PA is the primary storage compound of phosphorus in seeds accounting for up to 80 % of the total seed phosphorus and contributing as much as 1-2% to the seed dry weight (Hurrell 2002). The negatively charged phosphate in PA strongly binds to metallic cations of Ca, Fe, K, Mg, Mn and Zn making them insoluble and thus unavailable as nutritional factors (Urbano et al. 2000). Seeds of many staple crops, including maize embryo and the aleurone cells of wheat, rice and barley, accumulate large amounts of PA (Bohn et al., 2008) which poses

1. Introduction

a serious impediment to dietary Fe uptake. In developing countries, the prevalence of PA in the plant-based diet is believed to contribute to the high rate of Fe deficiency and anemia (Brown et al., 1991). Conversely, the presence of ferritin has the opposite effect to PA. Fe stored in ferritin is believed to be safe and have high bioavailability (E C Theil 2004). Ferritin was utilized to fortify rice, wheat, and lettuce with bioavailable Fe in several studies (Drakakaki et al., 2000; Goto et al., 1999a; Masuda, Goto et al., 2001) through an accumulation of the ferritin subunit in the seeds and the vegetative parts of the plants. There is also evidence that ferritin supports the plant's Fe availability and combats oxidative stress resulting from biotic and abiotic stress (Deák et al. 1999; Lönnnerdal 2009; Ravet et al. 2009). Therefore, several strategies have been employed to reduce the amount of PA in seeds and increase the amount of ferritin.

The first approach was the disruption of PA biosynthesis. This approach successfully reduced the accumulation of PA in seeds, but also the total amount of PA in the plants, which led to poor germination and an increased susceptibility to stress (Raboy 2007). In the work of Stevenson-Paulik et al. (2005) two *Arabidopsis* inositol polyphosphate kinases ATIPK1 and ATIPK2 have been disrupted, which are required for the later steps of PA synthesis. These mutants were found to produce 93 % less PA in seeds, while their seed yield and germination was not affected, but the loss of the PA precursors did alter phosphate sensing. Numerous examinations have to follow to find a solution to exclude all negative influences on plant growth and altered nutrient homeostasis. How the reduction of PA in seeds affects Fe homeostasis has not been examined, but it would be interesting to look at the interplay between vacuolar and plastid Fe pools in these mutants.

Another approach to enrich edible plant parts with bioavailable iron is the overexpression of ferritin in seeds (section 1.2.2 and 1.2.4). The Fe clusters or the protein alone help the meals survive digestion. Existing reports endorse, that Fe is transiently stored in ferritins and utilized for the accumulation of Fe-containing proteins. It has been documented that ferritin functions as a temporary Fe buffer in the developmental processes of plants (Buchanan-Wollaston and Ainsworth 1997; Strozycki et al. 2003), while seed formation studies showed that ferritins are also key proteins in long-term Fe storage (Lobreaux and Briat 1991; Marentes and Grusak 1998). Recent reports indicate the potential role of ferritin as a protector of the genome (Surguladze et al. 2005). Since ferritin Fe is separated from the Fe-binding components in food by its protein coat, it is less sensitive to chelators such as phytates (Theil, 2000)

1. Introduction

and therefore ferritin has consequently been viewed as a means of increasing bioavailability of Fe in staple crops. The overexpression of soybean and bean ferritins in rice seeds resulted in 2-3 fold increases in seed Fe content (F Goto, T Yoshihara, Shigemoto, Toki, and F Takaiwa 1999b; Lucca, R Hurrell, and Potrykus 2001; Murray-Kolb et al. 2002). Ferritin and soybean feeds were used as dietary treatment for Fe deficiency in rats. The evaluation indicated a significant increase in tissue Fe levels after a 28-day treatment and rats fully recovered from anemia (Beard et al., 1996; Murray-Kolb et al. 2003; Lucca et al., 2002). The overexpression of soybean ferritin in tobacco resulted in a constitutive Fe deficiency response, causing greater Fe uptake and accumulation. But when the plants were grown on contaminated soil, also a 2-fold increase in Cd could be observed. At the same time, the increase in sequestered Fe produced improved resistance to oxidative stress (van Wuytswinkel et al. 1999; Vansuyt 2000). An overexpression of alfalfa ferritin in tobacco produced an increased resistance to Fe overload, oxidative stress, and pathogen invasion (Deak et al., 1999). Ferritin overexpression with more powerful promoters produced the same fold increase in Fe as transgenics with weaker promoter constructs, suggesting that a further increase of Fe accumulation is limited by Fe uptake and transport and not by ferritin levels (Qu et al. 2005).

Finally, a combination of the two approaches has been undertaken. Maize plants were transformed with *Aspergillus* phytase and soybean ferritin, both driven by an endosperm specific promoter (Drakakaki et al., 2005), and indeed this led to increased total Fe content in seeds by 20-70% and resulted in the degradation of nearly all endogenous phytate. When paste from the resulting seeds was fed to cultured human cells, Fe uptake was significantly higher compared with those fed wild-type seed paste. Thus, attempts to increase bioavailable Fe in seeds are becoming more successful.

The increase of Fe uptake and its accumulation in the plant has been achieved with several approaches. Following studies could demonstrate an accumulation of Fe by overexpressing several factors of Fe homeostasis: Fe-Reductase (Samuelsen et al., 1998; Connolly et al., 2003), Ferritin (Deak et al., 1999; van Wuytswinkel et al., 1999), NAAT (Takahashi et al., 2001), NAS (Douchkov et al. 2001). Unfortunately these plants enriched Fe only in the vegetative parts of the plants since there is no natural reason to transport excess Fe into the seed. Therefore increasing Fe transport into the seed is a further challenge to overcome.

1. Introduction

In this respect, understanding the control of Fe-homeostasis mechanisms in plants is of vital importance for efficient Fe fortification efforts. It would help to address the Fe-deficiency problem in a better way leading to a specific and more effective solution.

1.3.3 Manipulation of the *NAS* genes as biotechnological approach

NA is considered to be a key compound of metal homeostasis in plants. It contributes to all important sub-processes of plant metal homeostasis: Mobilization and uptake, intercellular- and intracellular transport, sequestration, storage and detoxification of metals. Several studies did already present positive effects of NA on iron uptake and accumulation in plant roots and seeds (Douchkov et al. 2005; Cheng et al. 2007). Therefore, NA is supposed to be a potential biofortification factor of essential nutrients like Fe and Zn in edible portions of crop plants, because it might be able to improve Fe bioavailability to animal or humans by chelating Fe to form a soluble NA-ferrous complex. Lee et al. (2009) showed that activation of *OsNAS3* led to increase of Fe, Zn in both green tissue and mature seed. Anemic mice fed with the *OsNAS3* transgenic rice seeds recovered to normal levels of hemoglobin and hematocrit within 2 weeks. Just recently, the study of Zheng et al. (2010) showed a positive influence of NA on the bioavailability of Fe. In this study an elite rice line cultivated in Southern China has been transformed with the rice nicotianamine synthase gene (*OsNAS1*) fused to a rice glutelin promoter. Endosperm overexpression of *OsNAS1* resulted in a significant increase in NA concentrations in both unpolished and polished grain. Bioavailability of Fe from the high NA grain, as measured by ferritin synthesis in an *in vitro* Caco-2 cell model that simulates the human digestive system, was twice as much as that of the control line. When added at 1:1 molar ratio to ferrous Fe in the cell system, NA was twice as effective when compared to ascorbic acid (one of the most potent known enhancers of Fe bioavailability) in promoting more ferritin synthesis. Especially these data propose that NA is a novel and effective promoter of iron utilization (Zheng et al. 2010). Biofortified, polished rice with this compound has great potential in combating global human Fe deficiency in people dependent on rice for their sustenance. Therefore, the elucidation of the versatile functions of the small chelator molecule NA is from vital importance since the knowledge about NA function is fundamental for manipulation approaches to modify Fe homeostasis through alteration of the *NAS* genes.

However, in which processes of metal homeostasis NA has an essential or only a supportive functions is still not fully understood. To get a full understanding of NA

1. Introduction

function, the mutants existing represent a limiting factor. Work with transgenic tobacco or tomato like *naat* and *chloronerva*, respectively plants is limited concerning the availability of molecular genetic tools to investigate the consequences of the loss of NA function on molecular-physiological level in the whole plant. Furthermore, the cost and time expences connected with the molecular genetic work on tomato and tobacco restrict these NA mutants as model organism. The most efficient way to fill the gaps in the understanding of NA function is by exploiting the scientific and practical advantages of the model organism *A. thaliana* (see section 1.5).

1.4 The use of *A.thaliana* as a model plant to investigate NA function

A. thaliana is a small dicotyledonous species, a member of the mustard family (*Cruciferae* or *Brassicaceae*) with a broad natural distribution throughout Europe, Asia and North America. Many different ecotypes (accessions) have been collected from natural populations and are available for experimental analysis. The Columbia (Col-0) and Landsberg (Le) ecotypes are the accepted standards for genetic and molecular studies. It has been the focus of intense genetic, biochemical and physiological study for over 40 years because of several traits that make it very desirable for laboratory study. The entire life cycle, starting with seed germination and ending with the production of mature seeds, is completed after six weeks. Arabidopsis produces thousands of progenies by self-pollination (selfing), has very limited space requirements and is easily grown in a greenhouse or indoor growth chamber maintained in pots with soil or in petri plates. With a size of 157 Mbp (Bennett 2003) Arabidopsis possesses a relatively small genome and a small amount that can be manipulated through genetic engineering, much more easily and rapidly than any other plant genome. The sequencing of the *A.thaliana* genome has been completed in 2000 by the Arabidopsis Genome Initiative (the Arabidopsis Genome Initiative (2000)). A large community of scientists is studying the Arabidopsis genome. Numerous high throughput techniques and genetical tool came up which allow scientists to exploit the Arabidopsis genome, transcriptome, proteome and metabolom which introduced the era of functinal genomics in plants.

The Arabidopsis research community has developed most of the methods and resource materials expected of a model genetic organism. These include simple procedures for chemical and insertional mutagenesis, efficient methods for performing crosses and introducing DNA through plant transformation, extensive collections of mutants with

1. Introduction

diverse phenotypes, and a variety of chromosome maps of mutant genes and molecular markers (Koncz et al. 1989).

1.4.1 Functional genomics in Arabidopsis

The absence of an efficient system for gene replacement through homologous recombination was in earlier times a limitation shared by other model organisms such as *Drosophila* and *Caenorhabditis elegans*. Chemical or X-ray mutagenesis was the method of choice in the past being suitable because of the high amount of progenies and the short life cycle of Arabidopsis. Promising advances in this important area of Arabidopsis research have nevertheless been reported (Kempin et al., 1997) as insertional mutagenesis with transferred DNA (T-DNA) from *Agrobacterium tumefaciens* (since 2001 *Rhizobium radiobacter* (Young et al. 2001) has become routine through development of whole-plant transformation methods (Bechthold 1994) that avoid the pitfalls associated with plant regeneration in culture. In this effective method of transformation through the simple dipping of the flower to the bacterial culture (Clough and Bent 1998), the bacterium infects the plant through its Ti plasmid, which integrates a segment of its DNA, known as T-DNA, into the chromosomal DNA of its host plant cell. Instead of mutagenesis, the transformation with a transgene is also possible with *A. tumefaciens*. The sequence of interest has to get inserted into the Ti plasmid of the bacterium and can get transformed transiently by injection into the leaves of Arabidopsis, tobacco or other plant species or stable by dipping the flowers into the bacterial culture. These days, the T-DNA insertions mutagenesis is the method of choice to do functional genomics by „Reverse genetics“ in Arabidopsis.

With high-throughput random T-DNA mutagenesis projects, performed by public (SALK (Alonso et al. 2003) and GABI-kat (Li et al. 2003)) and commercial institutions (Syngenta (Sessions et al. 2002)), about 500000 different, mapped T-DNA insertion mutants are available. Most likely a T-DNA insertion mutant for almost all of the 27000 Arabidopsis genes could be found which represents a great step forward in plant functional genomics. The mutagenized seeds are stored in public stock centers and all informations about available mutants, linked with publications, annotations and sequences are collected, deposit in a database namely TAIR (Rhee et al. 2003) and are accessible to the scientific community under www.arabidopsis.org. Several thousand

1. Introduction

mutants of *Arabidopsis* defective in almost every aspect of plant growth and development have been identified over the past 20 years.

1.4.2 High throughput transcriptome analysis

In functional genomics, technological innovations such as the use of DNA chips and microarrays to study global patterns of gene expression gain of vital importance. With the release of the ATH1 chip of the company Affymetrix in 2002, it has become possible to investigate the transcript levels of 22500 genes in parallel. The method of whole transcriptome profiling has strongly advanced our understanding of complex networks of gene interactions in many biological processes.

For the collection of the vast amount of expression data, many repositories have been developed, including the Gene Expression Omnibus (GEO) (Edgar et al., 2002) or Stanford Microarray Database (SMD) (Sherlock et al. 2001). To meet also the interpretation of data, the development of suitable tools became necessary to extract information beyond the single gene level out of the huge amount of data, in order to address questions on the co-regulation of genes, on the identification of gene networks and entire extensive pathways of genes acting in the same physiological process. It has become a routine for researchers to consult published microarray expression data for theoretical modeling of regulatory networks involving their favourite genes prior to experimentation (Winter et al. 2007; Zimmermann et al. 2004). Specialized software tools like Genevestigator (Zimmermann et al., 2004), the Botany Array Resource (BAR) (Toufighi et al. 2005), MapMan (Thimm et al. 2004) or ATTED-II (Obayashi et al. 2009; Obayashi et al. 2007) or for example have been developed to answer such complex questions in plants and are nowadays indispensable in dealing with microarray experiments.

With continued progress in genomics, biology, and database management, it nevertheless appears, that *Arabidopsis* became an important model for higher eukaryotes, not only for understanding of plant structure and function, but also for addressing more universal questions concerning the nature and origin of biological complexity.

1. Introduction

1.5 Prerequisites for this work

1.5.1 Predicted roles of NA in Fe and Cu homeostasis

NA has an evidenced role in Strategy II plants (Graminaceae) being the first intermediate in the synthesis of PS, which mediate Fe uptake in grasses (S Mori 1999; Shojima et al. 1990) (see section 1.2.1.2). However, its function in Strategy I plants is less clear, but of central importance as illustrated in the studies of *chloronerva* and the transgenic tobacco *naat* (compare section 1.2.3). NA is supposed to participate in numerous processes of metal homeostasis like the long-distance transport, the inter- and intracellular transport of metals, reproduction and Fe seed loading. But none of these functions could be proven *in planta* thus far. Investigations of *chloronerva* strongly suggest an essential function of NA in long-distance transport of Cu (described in section 1.2.4.2) and the inter- and intracellular transport of Fe (described in section 1.2.4.3 and 1.2.5.3). Interestingly, the interveinal leaf chlorosis of *chloronerva* is only visible in young leaves and decreases with age of leaves and NA concentration is always highest in meristematic tissues (apical zones of shoots and roots) (Curie et al., 2009). If NA is indeed needed for the phloem transport, these phenotypes could be explained with the slower differentiation of xylem compared to phloem. It is possible, that young developing tissues and apical meristems are mostly fed with Fe by the phloem until the vasculature is fully developed (Curie et al., 2009). The investigations of *naat* also support the role of NA in the intracellular transport. In *naat* mutants, the distribution of ^{59}Fe was monitored in detached leaves fed with different Fe chelates. When provided alone, Fe was restricted to the main veins whereas a co-incubation of Fe and NA induced a widespread distribution of Fe in the mesophyll cells (Takahashi et al., 2003). These findings highlight the importance of NA in the distribution of Fe at the cellular level or in its entry in the ‘symplastic compartment’. In order to find out if NA is involved in the uptake of metals, Fe for instance, on the plasma membrane Pich and Scholz (1991) compared the Fe acquisition of protoplasts prepared from *chloronerva* and its wild-type parent Bonner Beste. Surprisingly, the authors found that the Fe uptake was even higher in *chloronerva* protoplasts compared to wild type and they could not see a difference in the activity of the plasma membrane ferric reductase in both genotypes. Moreover, the addition of NA to the uptake medium had no effect on the absorption of Fe, showing that NA is not essential for the transport of Fe at the plasma membrane level. Finally, the comparison of Fe content between protoplasts and

1. Introduction

whole leaves, which is an approximation of the apoplastic Fe concentration, has shown that the lack of NA in cells provokes a high accumulation of Fe in symplastic and apoplastic pools (Pich and Scholz 1991). The function of NA over short-distance ranges might also be an explanation for its role in the reproduction process, since the reproductive organs possibly rely on the metal supply by NA. Taken together, if NA is not directly involved in the uptake of Fe at the cell level, this strongly suggests a role of NA in the regulation of its distribution between apoplastic and symplastic compartments which remains to be proven.

Discovering the distinct function and place of activity for NA proved to be very difficult within the last two decades. This is caused by the affinity of NA to a variety of metals on one hand (section 1.2.3.1) and the mutants available to study NA function on the other hand. Numerous predictions of NA function could be obtained with the tomato mutant *chloronerva* and the transgenic tobacco plant *naat* (see section 1.2.3). The specific classification of NA function in the complex network of genes involved in metal homeostasis requires the switch to another model organism, which provides more and better molecular genetic methods and functional genomic tools. Moreover, in the transgenic tobacco secondary effects of the transgene cannot get excluded. Therefore, the generation of an *A.thaliana nas* mutant has been chosen as model organism to investigate NA function, since Arabidopsis provides most of the molecular genetic methods and genomic tools for plant science (see section).

1.5.2 The Arabidopsis *NAS* gene family

The Arabidopsis *NAS* gene family comprises four members. *NAS1* and *NAS2* are located on chromosome V, while *NAS3* and *NAS4* are located on chromosome I, each on the opposite chromosome arm (see Fig. 1.7A). Each *NAS* gene consists of only one exon without any introns. *NAS1*, *NAS2* and *NAS3* have a length of 963 bp, while *NAS4* is 975 bp long. Multiple alignment (CLUSTALW) showed a close relation between *NAS* genes located on the same chromosome with 83 % identity while alignment of genes located not on the same chromosome showed an identity of 69 % (dissertation Marco Klatter, 2008). Gene mapping between *Solanum esculentum* and *A.thaliana* demonstrated that the four Arabidopsis genes, as well as the single tomato *NAS* gene originated from a common primary *NAS* gene. The major location of COS (conserved orthologous set) markers could be found for SeNAS and AtNAS3 (P Bauer et al. 2004). This finding hints to a gene duplication event in the evolution of *A.thaliana*, followed

1. Introduction

by two other independent gene duplication events which finally led to four *NAS* genes in *A.thaliana* (Bauer et al., 2004). Despite the strong sequence conservation the four *NAS* genes show differential regulation and thus form a partially redundant gene family (Suzuki et al., 2001).

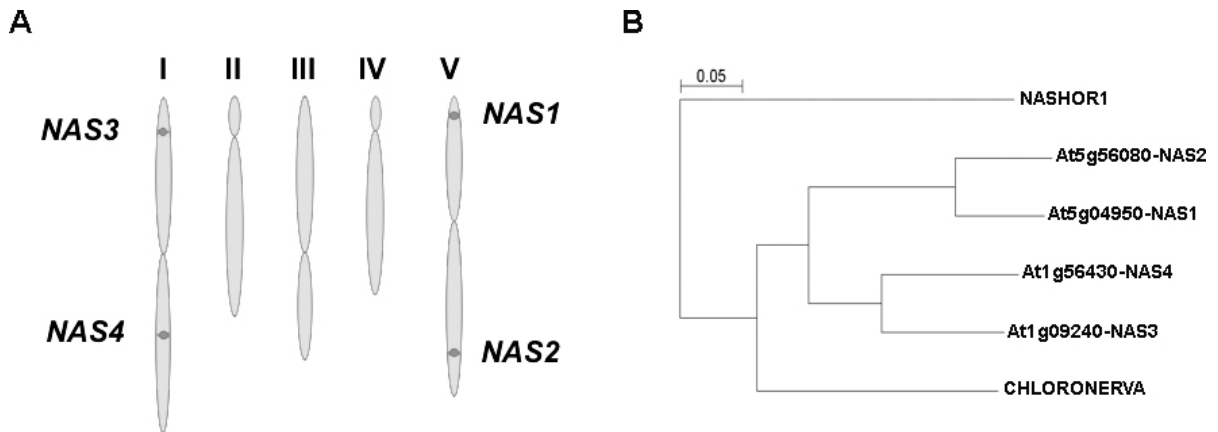


Fig. 1.7: The *NAS* gene family of *Arabidopsis thaliana*

A) Schematic presentation of the five chromosomes of Arabidopsis. Dots mark the localization of the four *NAS* genes on chromosomes I and chromosome V. **B)** Phylogenetic tree of Arabidopsis, tomato and barley *NAS* genes, generated with CLUSTALX (Bauer et al., 2004)

Although the absence of single functional *NAS* genes did not show obvious phenotypes under control conditions (Bauer et al. 2004, dissertation Marco Klatte 2008), the upregulation of individual gene family members such as observed in the metallophyte and zinc hyperaccumulator *A. halleri*, for instance, may lead to discrete dominant phenotypes (Becher et al., 2004, Talke et al 2006, van de Mortel et al., 2006).

With the aim to study NA function in Arabidopsis, four single *nas* T-DNA insertion mutants were identified (Fig. 1.8) and were crossed in order to generate a homozygous quadruple mutant. The crossing procedure is described in detail in the dissertation of Marco Klatte (2008) and in Klatte et al. (2009). First, a quadruple homozygous mutant was identified as *nas1-1^{-/-}nas2-1^{-/-}nas3-1^{-/-}nas4-1^{-/-}* and termed *nas4x-1*. To verify the mutations full-length cDNA studies have been deduced. For the selected *nas1-1*, *nas3-1* and *nas4-1* lines it was shown that the positions of the T-DNA insertions in the exons (Fig. 1.8) led to a full loss of function for these three *NAS* genes. However, in case of the *nas2-1* line, there was still a fragment synthesized which contained the full-length *NAS2* region due to the position of the T-DNA insertion in the 5'UTR of the gene. Moreover, the transcript made by the *nas2-1* allele could be detected not only in the roots like in the wild type situation it was also ectopically expressed in leaves of the mutant (Klatte et al. 2009). In conclusion, the T-DNA insertion of *nas1-1*, *nas3-1* and

1. Introduction

nas4-1 in the exon region fully knocked out their gene function while in case of the *nas2-1* it remained unclear if a functional *NAS2* protein was still synthesized (Fig. 1.8). While the generation of the *nas4x-1* has already been progressed in the previous work, another single T-DNA insertion line of the *NAS2* gene could be identified later on in the project, namely *nas2-2* harboring a T-DNA insertion in the exon-region of the *NAS2* gene (Fig. 1.8). The new *nas2-2* single mutant has been crossed to the *nas4x-1* mutant in order to generate a second quadruple *nas* mutant with a full loss of *NAS* function. Therefore another heterozygous quadruple mutant *nas1-1^{-/-}nas2-2^{-/-}nas3-1^{+/-}nas4-1^{+/-}* segregating for *NAS3* and *NAS4* was available as well at the beginning of this project. During the crossing and selection procedure of the quadruple *nas* mutant, all possible combinations of double and triple *nas* mutants were generated and were additionally available (Klatte et al., 2009), namely *nas1/2*, *nas1/3*, *nas1/4*, *nas2/3*, *nas2/4*, *nas1/2/3*, *nas1/2/4*, *nas1/3/4*, *nas2/3/4* for the further investigation of an individual function of the four *NAS* genes.

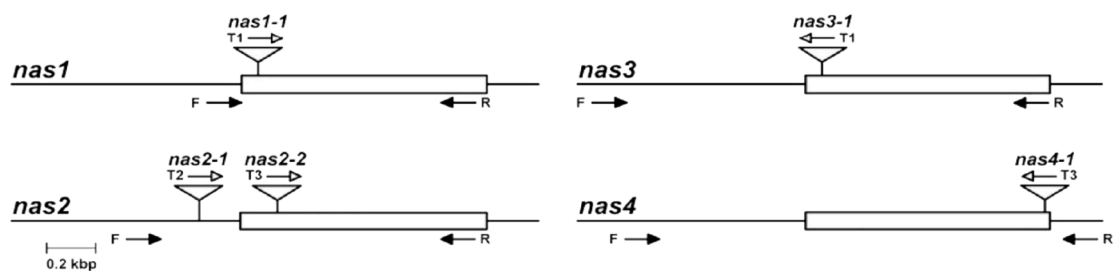


Fig 1.8: Genetic composition of *nas4x-1* mutant plants

Localization of T-DNA insertions in *nas* alleles: *nas1-1* (GABI_223A09), *nas2-1* (SAIL_156C08), *nas2-2* (SALK_066962), *nas3-1* (GABI_010A10) and *nas4-1* (SALK_135507). Arrows indicate the primer positions used for genotyping.

nas4x-1 plants were initially characterized in previous study (dissertation Marco Klatte, 2008, Diplomarbeit Mara Schuler 2007). *nas4x-1* were still fertile and showed an interveinal leaf chlorosis primarily appearing upon transition to reproductive growth stage (Fig. 1.9). Preliminary NA measurements showed that leaves of vegetative stage and the reproductive parts of the plant like siliques and seeds contained residual NA contents, which could be presumably traced back on the activity of the *nas2-1* allele. Thus, it was clear at the beginning of this project that *nas4x-1* was not a full knock out mutant. Nevertheless, the intermediate phenotype of *nas4x-1* and its fertility still allowed the investigation of seed metal and NA contents and therefore *nas4x-1* was a valuable model to study NA function in late phase of plant development.

Furthermore, the exposure of *nas4x-1* mutants to Ni excess and Fe deficient growth medium revealed that *nas4x-1* mutants showed an increased susceptibility to Ni excess and an increased susceptibility to Fe deficiency (Klatte et al, 2009).

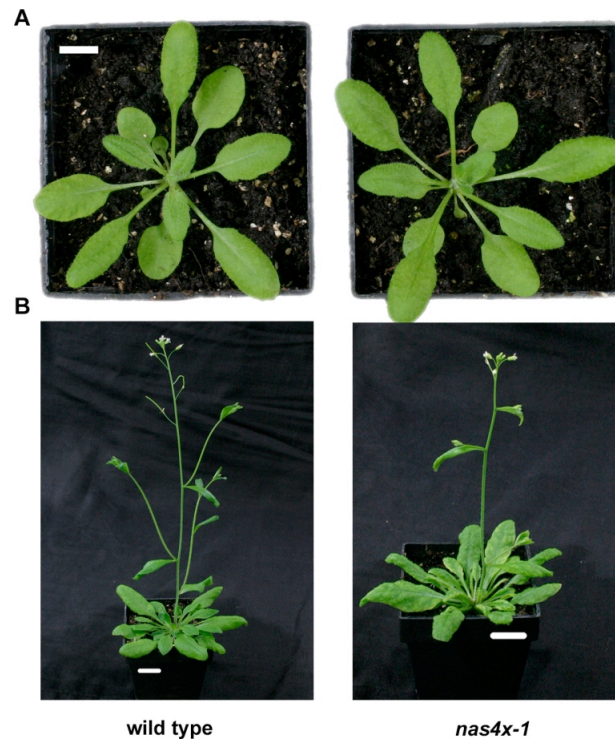


Fig. 1.9: Phenotypes of soil-grown *nas4x-1* plants compared to wild type

A) Four week-old plants in vegetative growth stage grown under long-day conditions. **B)** Six week-old plants in reproductive growth stage grown under long-day conditions. Bar = 1cm

2. Aims of this project

2. Aims of this project

The ability of NA to chelate divalent metal ions and its putative role in maintaining the solubility of essential metals like Fe, Cu and Zn and thereby increasing its bioavailability in plants make the *NAS* genes appealing for biofortification approaches.

The goal of this project was the localization of NA activity and the elucidation of a concrete function of NA in Fe and Cu transport throughout the plant and to reproductive organs using the model plant *A. thaliana*.

The concrete aims of this project were as follows:

Aim 1: Supportive investigation and further characterization of the quadruple *nas* mutant *nas4x-1*

The available plant material to investigate NA function at the beginning of this project was the homozygous *nas4x-1* mutant with reduced NA content due to reduced NAS activity. Previous experiment (dissertation Marco Klatte, 2008) required a repetition under controlled physiological conditions. The striking interveinal leaf chlorosis of *nas4x-1* plants which primarily occurred upon the switch from the vegetative to the reproductive growing phase suggested a differential importance of NA function depending on the growing stage. Therefore, measurements should be repeated simultaneously from the two developmental stages and compared to each other. These results should verify the hypothesis that NA is involved in the mobilization of Fe from leaves to developing seeds.

Furthermore, the enhanced susceptibility of *nas4x-1* plants to Fe deficiency which has already been shown in previous studies should be verified as well. Since NA is also able to form complexes with Zn and Cu the effects of Zn and Cu deficiency on *nas4x-1* were to be compared to wild type plants in order to investigate the role of NA in the homeostasis of these metals.

Aim 2: Analysis of global changes in *nas4x-1* mutants on transcriptional level

To integrate the function of NA in a broader physiological context, transcriptomes of *nas4x-1* and wild type plants should be compared in a gene chip experiment. In this comparative microarray study, transcriptomes of *nas4x-1* mutant and wild type plants should be compared in response to Fe deficiency or sufficient Fe supply.

2. Aims of this project

First, the data evaluation should target on the identification of functional categories in comparative transcriptome data of roots and leaves of mutant versus wild type plants and Fe deficiency versus Fe supply conditions in order to uncover whole functional pathways or biological processes, which show an alteration in response to the *nas* mutation or Fe deficiency, respectively. In cooperation with the bioinformatic group of Prof. Dr. H.P. Lenhof, a web-based tool named GeneTrail should be set up for the use of *Arabidopsis thaliana*. With the transcriptome data the functionality of GeneTrail for plant specific analysis was to be tested. Second, differentially expressed genes should be selected in pair-wise comparisons of transcriptome data and should be evaluated with the focus on alteration of gene expression patterns of metal homeostasis genes in order to integrate NA function in the network of metal homeostasis.

Aim 3: Analysis of individual and overlapping functions of the four *NAS* genes

To study individual functions of *NAS* genes the collection of all single and multiple *nas* mutants, generated in a previous study (dissertation Marco Klatte, 2008), should be utilized. Since previous study showed that *NAS* gene expression underlies a differential regulation and was moreover shown to be tissue specific, it should be investigated whether all four *NAS* genes undertake overlapping functions in the plant or if specific *NAS* genes might have gained individual functions e.g. in response to specific environmental cues during evolution. Analysis of the previous study had shown that *NAS3* and *NAS4* isoforms showed nonredundant functions in dealing with Ni excess conditions, whereas *NAS1* and *NAS2* could be neglected. To investigate if *NAS3* and *NAS4* also have individual functions in the Fe deficiency response, all single and multiple *nas* mutants should be exposed to Fe deficiency to evaluate the degree of their chlorosis.

Transgenic reporter lines expressing fusion proteins with GUS and GFP should be generated for *NAS3* and *NAS4* in order to confirm their particular importance. With *NAS3* and *NAS4* reporter fusions *NAS* protein levels should be compared to their respective gene expression levels in order to investigate the possibility of a posttranscriptional control of the *NAS* proteins.

2. Aims of this project

Aim 4: Verification and detailed characterization of an NA-free mutant, termed *nas4x-2*

A new homozygous quadruple *nas* mutant, namely *nas4x-2* was to be selected from *nas1^{-/-}nas1^{-/-}nas3^{+/-}nas4^{+/-}* segregating lines. *nas4x-2* plants should be analyzed to confirm the full loss of *NAS* activity in *nas4x-2* plants. Next, *nas4x-2* plants should undergo a detailed physiological analysis in comparison to *nas4x-1* mutants. With molecular-physiological analysis including metal measurements of all plant organs, gene expression analysis of marker genes and *in situ* Fe stainings we aimed to discover alterations of Fe distribution occurring in response to the loss of NA. These analyses should be utilized first, to elucidate NA function in the long-distance and short-distance intercellular Fe transport in order to uncover the place of NA action. The investigation of long-distance transport function of NA should take a complementary function by citrate into account.

Second, the role of NA in reproduction should be investigated. Since *nas4x-2* was found to be sterile, it was to be elucidated whether the loss of NA in the female tissue of the pistil or its loss in the male tissue of the anthers caused the fertilization defect.

3. Material and Methods

3.1 Material

3.1.1 Plant material:

- *Arabidopsis thaliana* ecotype Columbia (Col-0) has been used as wild type
- *Arabidopsis* T-DNA insertion lines:

Abbreviation	Name	Gene	AGI code	Position
<i>nas1-1</i>	GABI-kat 223A09	<i>NAS1</i>	At5g04950	Exon, 69 bp downstream of ATG
<i>nas2-1</i>	Syngenta SAIL 156C08	<i>NAS2</i>	At5g56080	5'-UTR, 70 bp upstream of ATG
<i>nas2-2</i>	SALK 066962	<i>NAS2</i>	At5g56080	Exon, 144 bp downstream of ATG
<i>nas3-1</i>	GABI-kat 010A10	<i>NAS3</i>	At1g09240	Exon, 69 bp downstream of ATG
<i>nas4-1</i>	SALK 135507	<i>NAS4</i>	At1g56430	Exon, 19 bp upstream of TAG

- *frd3-1 (man1-1)* (EMS mutant; described in Rogers and Guerinot, 2002a, ordered from stock center (ABRC): stock CS6584)
- Mutation: C-to-A transversion in the second exon, substitution of Asp for Ala at position 54 in the first transmembrane domain of the protein.

3.1.2 Bacterial strains for molecular cloning

- *E. coli*, *ccdB* one shot survival T1-Phage resistant cells (Invitrogen)
F-mcrA (mrr-hsdRMS-mcrBC) 80lacZ M15 lacX74 recA1 ara 139 D (ara- leu) 7697 galU galK rpsL (StrR) endA1 nupG tonA::Ptrc -ccdA
- *E. coli* INV α F' (Invitrogen) F' endA1 recA1 hsdR17 (rk-, mk+) supE44 thi-1 gyrA96 relA1 ϕ 80lacZ_M15_(lacZYAargF) U169 λ -
- *Agrobacterium tumefaciens*: C58C1; GV2260/pGV2260

3.1.3 Plasmids

Detailed information about Gateway vectors are available under:

http://botserv1.uzh.ch/home/grossnik/curtisvector/index_2.html

3. Material and Methods

- pDONR207 (Gateway cloning system, Invitrogen)
 - Size: 5.5 kb
 - Entry vector containing Gateway cassette with P1 and P2 attachment sites
 - Selection marker: *ccdb* suicidal gene: insertion control, Gm^R: transformation control in bacteria
- pMDC107 (Gateway cloning system, Invitrogen)
 - Size: 11.7 kb
 - Binary destination vector for expression of native promoter-gene-of-interest-GFP C-terminal fusions
 - Selection marker: *ccdb* suicidal gene: insertion control, Kan^R: transformation control in Bacteria, Hygromycin^R: transformation control in plants
- pMDC162 (Gateway cloning system, Invitrogen)
 - Size: 12.9 kb
 - Binary destination vector for expression of native promoter-gene-of-interest-GUS C-terminal fusions
 - Selection marker: *ccdb* suicidal gene: insertion control, Kan^R: transformation control in Bacteria, Hygromycin^R: transformation control in plants

3.1.4 Oligonucleotides

All primers were ordered in a concentration of 100 µM.

Table 3.1: List of primer sequences for standard-PCR reactions.

Primers were used for genotyping (G) or amplification of a full-length transcript (FL)

Gene/ T-DNA	Primer name	Sequence
NAS1 (G)	NAS1-60-5'	5`-GCCAAGAATTGACCCCACG-3`
	NAS1-60-3'	5`-ACGGTTGTTTCATGATCGCG-3`
NAS2 (G)	NAS2-60-5'	5`-TGGAACATATCGCGATTTTTAGTTG-3`
	NAS2-60-3'	5`-TCGATGGCACTATACTCCTCGATC-3`
NAS3 (G)	NAS3-60-5'	5`-TGTCGCAAGTCATGCACATTTC-3`
	NAS3-60-3'	5`-TTCAGCCCAACAGTGTCGC-3`

3. Material and Methods

<i>NAS4</i> (G)	NAS4-60-5'	5'-AACTATGCACCCCGTAGAGCC-3'
	NAS4-60-3'	5'-CCCACCCTTTGCAAATTGC-3'
GABI-kat T-DNA (G)	GABI-TDNA check	5'-CCCATTTGGACGTGAATGTAGACAC-3'
SALK T-DNA (G)	Salk LB1	5'-GCGTGGACCGCTTGCTGCAACT-3'
Syngenta T-DNA (G)	Syn-LB3short	5'-TAGCATCTGAATTTTCATAACCAATCT-3'
<i>NAS2</i> (FL)	NAS2-cDNA-check 5'	5'-ACAATTTCAAACACTCAATATTCTCTC-3'
	NAS2-cDNA-check 3'	5'-AAGGGCAAACATAAACACAT-3'

Genotyping (G); full-length cDNA test (FL)

Table 3.2: Primer sequences for Real Time RT-qPCR.

Primers were used for standard amplification (STD) or for quantification (Q) in real time RT-qPCR.

Gene	Primer name	Sequence
<i>EF1B-alpha-g</i> (STD)	AtEF-gen-3'(2726)	5'CCGGGACATATGGAGGTAAG-3'
	AtEF-gen-5'(2522)	5'-TCCGAACAATACCAGAACTACG-3'
<i>EF1B-alpha-g</i> (Q, gDNA)	AtEF-gen-3'(2726)	5'-CCGGGACATATGGAGGTAAG-3'
	AtEF-gen-5'(2522)	5'-TCCGAACAATACCAGAACTACG-3'
<i>EF1B-alpha</i> (STD)	AtEF-c-5'(2125)	5'-ACTTGTACCAGTTGGTTATGGG-3'
	AtEF-c-3'(2251)	5'-CTGGATGTACTCGTTGTTAGGC-3'
<i>EF1B-alpha</i> (Q, cDNA)	AtEF-c-5'(2125)	5'-ACTTGTACCAGTTGGTTATGGG-3'
	AtEF-c-3'(2251)	5'-CTGGATGTACTCGTTGTTAGGC-3'
<i>UBP6</i> (STD)	AtUBP6-c-5'(975)	5'-GAAAGTGGATTACCCGCTG-3'
	AtUBP6-c-3'(1066)	5'-CTCTAAGTTTCTGGCGAGGAG-3'
<i>UBP6</i> (Q)	AtUBP6-c-5'(975)	5'-GAAAGTGGATTACCCGCTG-3'
	AtUBP6-c-3'(1066)	5'-CTCTAAGTTTCTGGCGAGGAG-3'
<i>FRO2</i> (STD)	AtFRO2-c-3'(1927)	5'-AAGATGTTGGAGATGGACGG-3'
	AtFRO2-c-5'(1806)	5'-CTTGGTCATCTCCGTGAGC-3'
<i>FRO2</i> (Q)	AtFRO2-c-5'(1806)	5'-CTTGGTCATCTCCGTGAGC-3'
	AtFRO2-c-3'(1927)	5'-AAGATGTTGGAGATGGACGG-3'
<i>IRT1</i> (STD)	AtIRT1-c-3'(1622)	5'-TTAGGTCCCATGAACTCCG-3'
	AtIRT1-c-5'(1523)	5'-AAGCTTTGATCACGGTTGG-3'

3. Material and Methods

<i>IRT1</i> (Q)	AtIRT1-c-5'(1523)	5'-AAGCTTTGATCACGGTTGG-3'
	AtIRT1-c-3'(1622)	5'-TTAGGTCCCATGAACTCCG-3'
<i>FIT</i> (STD)	AtFRU-c-5'(1392)	5'-GGAGAAGGTGTTGCTCCATC-3'
	AtFRU-c-3'(1483)	5'-TCCGGAGAAGGAGAGCTTAG-3'
<i>FIT</i> (Q)	AtFRU-c-5'(1392)	5'-GGAGAAGGTGTTGCTCCATC-3'
	AtFRU-c-3'(1483)	5'-TCCGGAGAAGGAGAGCTTAG-3'
<i>NAS1</i> (STD)	AtNAS1-RT600-3'	5'-AACGACGTCATATTGGTCAAG-3'
	AtNAS1-RT541-5'	5'-ATCTTCCACACAACGGACG-3'
<i>NAS1</i> (Q)	AtNAS1-RT541-5'	5'-ATCTTCCACACAACGGACG-3'
	AtNAS1-RT600-3'	5'-AACGACGTCATATTGGTCAAG-3'
<i>NAS2</i> (STD)	AtNAS2-RT943-3'	5'-CCTCGATCAAATTCTTCTCCAT-3'
	AtNAS2-RT854-5'	5'-AGATCGGACGGTGTGTGG-3'
<i>NAS2</i> (Q)	AtNAS2-RT854-5'	5'-AGATCGGACGGTGTGTGG-3'
	AtNAS2-RT943-3'	5'-CCTCGATCAAATTCTTCTCCAT-3'
<i>NAS3</i> (STD)	AtNAS3-RT953-3'	5'-TGTTCCCTCCCTAGCTCCG-3'
	AtNAS3-RT836-5'	5'-CAATTGGGAATGTTGGTGG-3'
<i>NAS3</i> (Q)	AtNAS3-RT836-5'	5'-CAATTGGGAATGTTGGTGG-3'
	AtNAS3-RT953-3'	5'-TGTTCCCTCCCTAGCTCCG-3'
<i>NAS4</i> (STD)	AtNAS4-RT810-5'	5'-TGTAATCTCAAGGAAGCTAGGTG-3'
	AtNAS4-RT893-3'	5'-CAGTTACACGCGAGATCCG-3'
<i>NAS4</i> (Q)	AtNAS4-RT810-5'	5'-TGTAATCTCAAGGAAGCTAGGTG-3'
	AtNAS4-RT893-3'	5'-CAGTTACACGCGAGATCCG-3'
<i>YSL1</i> (STD)	YSL1-STD-(1681)-5'	5'-TATTGTAGCTTACATTTTCGCG-3'
	YSL1-STD-(2705)-3'	5'-CCGAGCCCATAACAGTTTC-3'
<i>YSL1</i> (Q)	YSL1-RT-(2429)-5'	5'-TTCTTAGCTTCATAGGATCAGTCAA-3'
	YSL1-RT-(2552)-3'	5'-GTTCTTGTTTCAGAAGTCTACCTGTT-3'
<i>YSL2</i> (STD)	YSL2-STD-(1576)-5'	5'-GATGGCTTGTGTCGGATACTTA-3'
	YSL2-STD-(2591)-3'	5'-ACCAACTCTCTTTCTGTTTCATTCTTA-3'
<i>YSL2</i> (Q)	YSL2-RT-(2246)-5'	5'-TGTATCGGGAGCTTAGTGGTATA-3'
	YSL2-RT-(2431)-3'	5'-GCCTTAATGAGCCGCAGT-3'
<i>YSL3</i> (STD)	YSL3-STD-(2100)-5'	5'-ATTGTATCGATTTCTTCTGACCTAAT-3'
	YSL3-STD-(3103)-3'	5'-AATATGACGTGTGCTGAATTGAC-3'
<i>YSL3</i> (Q)	YSL3-RT-(2530)-5'	5'-CTTGGAATATGAGAGATCGAGTTAA-3'
	YSL3-RT-(2690)-3'	5'-CGAATATTTACTCGGCATGAA-3'

3. Material and Methods

<i>OPT3</i> (STD)	5' STD cOPT3	5'-GGTCTGCAGTGAACACCACGA-3'
	3' STD cOPT3	5'-CAGGGCGAAGAACAAGAGCA-3'
<i>OPT3</i> (Q)	5' RT cOPT3	5'-CCCAAACAAGAAGTGGATCCC-3'
	3' RT cOPT3	5'-GTGACCAACCAGCTGGCAAT-3'
<i>FRD3</i> (STD)	5' STD_FRD3_cDNA	5'-GCATCTTTCGTGGATTCAAGGA-3'
	3' STD_FRD3_cDNA	5'-AAGGAAGAAGAGATGCAACTCGTT-3'
<i>FRD3</i> (Q)	5' RT_FRD3	5'-ATGGCCATCGGAATACCGTT-3'
	3' RT_FRD3	5'-CTAGGAAGATGAAGAGGATGATCGT-3'
<i>FER1</i> (STD)	FER1 STD Real Time 5'	5'-GCGGCTCAACACTATCCTCT-3'
	FER1 STD Real Time 3'	5'-ACAGAGCCAACCTCCATTGCT-3'
<i>FER1</i> (Q)	5' RT FER1	5'-ACGCACTCTCGTCTTTCACC-3'
	3' RT FER1	5'-GAAAGGCTGGAACACGACTC-3'

Standard amplification (STD); Quantification (Q)

Table 3.3: Primer sequences for molecular cloning.

Primers were used for insert amplification and adherence of attachment sites.

Gene	Primer name	Primer sequence
<i>NAS3</i>	5'-attB1-NAS3-GS	5'-GGGGACAAGTTTGTACAAAAAAGCAGGCTCC GGAATCCATTGACTGACAACCACA-3'
	3'-attB2-NAS3-GS	5'-GGGGACCACTTTGTACAAGAAAGCTG GGTCAGACAACCTGTTCCCTAGCTCC-3'
<i>NAS4</i>	5'-attB1-NAS4-GS	5'-GGGGACAAGTTTGTACAAAAAAGCAGGCTC CATCAATCAAATCCATTGTTCAAGTTC-3'
	3'-attB2-NAS4-GS	5'-GGGGACCACTTTGTACAAGAAAGCTGGGTC GGTAAGTTGTTCTTCATTAGCACCTGC-3'

Table 3.4: Primer sequences for Sequencing

Plasmid	Primer name	Sequence
<i>NAS3</i> inserted in pDONR207	5' pDONR check	5'-CCTGGCAGTTCCTACTCTC-3'
	5' Atnas1aSG1	5'-TGTTTTTCGGTCAAGCAACTTG-3'
	5' Atnas1aSG3	5'-AACAGTTCACACCACCCGAGAA-3'
	3' pDONR check	5'-CTGCAGCTGGATGGCAAATA-3'
	3' Atnas1aSG2	5'-GACTTGTGTGAACATGGATTAGATCC-3'

3. Material and Methods

	5` pDONR check	5`-CCTGGCAGTTCCTACTCTC-3`
	5`Atnas1bSG1	5`-GAATGGGCATCTCGTAGAACTGA-3`
	5`Atnas1bSG3	5`-GGTTATTGCCAAGACGACCAAC-3`
NAS4 inserted in pDONR207	5`AtNAS4-RT810-5`	5`-TGTAATCTCAAGGAAGCTAGGTG-3`
	3`pDONR check	5`-CTGCAGCTGGATGGCAAATA-3`
	3`Atnas1bSG4	5`-AGGGAGAGGACCAGAGCCAAT-3`
	3`Atnas1bSG2	5`-ATACCCAGCACAATAAATTAATGAAGTG- 3`

3.1.5 Enzymes and Kits

Application	Description	Manufacturer
cDNA synthesis	RevertAid First Strand cDNA Synthesis Kit	Fermentas
DNase I treatment	DNase I, RNase-free	Fermentas
RNA Isolation (RT-qPCR)	Spectrum Plant Total RNA Kit	Sigma-Aldrich
RNA Isolation (Microarray experiment)	RNeasy Plant Mini Prep Kit	Qiagen
Standard PCR	JumpStartREDTag Ready Mix	Sigma-Aldrich
Real time RT-qPCR	Premix ExTaq	TaKaRa
Cloning (Insert Amplification)	Phusion DNA Polymerase	Finnzymes
BP reaction (Gateway cloning)	Gateway BP clonase II Enzyme Mix	Invitrogen
LR reaction (Gateway cloning)	Gateway LR clonase II Enzyme Mix	Invitrogen

3. Material and Methods

3.2 Methods

3.2.1 Plant Methods

3.2.1.1 Plant Growth

Seeds were surface-sterilized and stratified for 2-3 days at 4°C. Arabidopsis plants were grown on soil, agar plates or hydroponic system.

Following Hoagland salt concentrations have been used for the preparation of Hoagland medium: 0.1875 mM MgSO₄ x 7 H₂O, 0.125 mM KH₂PO₄, 0.3125 mM KNO₃, 0.375 mM Ca(NO₃)₂, 12.5 μM KCL, 12.5 μM H₃BO₃, 2.5 μM MnSO₄ x H₂O, 0.5 μM ZnSO₄ x 7 H₂O, 0.375 μM CuSO₄ x 5 H₂O, 0.01875 μM (NH₄)₆Mo₇O₂₄ x 4 H₂O. pH has been set to 6.0.

- The growth on agar plate system was performed using 1x Hoagland solution with a concentration of 0.8 % plant agar supplied with 50 μM FeNa-EDTA (control) and 1% sucrose. Cultivation took place on square plates placed at 21°C/19°C and 16 h light, 8 h dark cycles (long-day condition) in plant chambers of *CLF Plant Climatics*.
- For the hydroponic growth system seedlings were germinated on ¼ x Hoagland agar medium in 500 μl support tubes containing a hole at the bottom for root growth. After two weeks plants were placed into ¼ x Hoagland liquid medium for another 2 weeks (Fig. 3.1). Medium was exchanged weekly. ¼ x Hoagland medium contained a quarter of the Hoagland salts and 10 μM FeEDTA (control). Solid germination medium of the hydroponic system contained no sucrose and 0.6 % plant agar. Four weeks after germination, plants were exposed for another week to plant medium containing either 10 μM FeNa-EDTA (+ Fe) or without Fe (- Fe). Cultivation took place at 21°C/19°C and 16 h light, 8 h dark cycles (long-day condition) or 8 h light, 16 h dark cycles (short-day condition), respectively and a light intensity of 150 μmol x m⁻² x s⁻¹ and a humidity of 60 %.
- For the growth on soil, a turf substrate was mixed with vermiculite (3:1).

3. Material and Methods

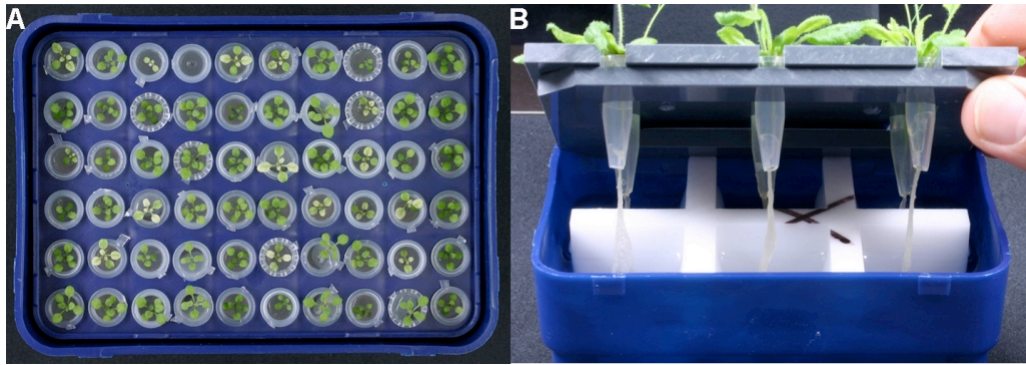


Fig.3.1: Hydroponic growth system for Arabidopsis

A) Seedlings were germinated on $\frac{1}{4}$ x Hoagland agar medium in 500 μ l support tubes containing a hole at the bottom for root growth. **B)** After two weeks plants were placed into $\frac{1}{4}$ x Hoagland liquid medium for further growth.

3.2.1.2 Metal measurements

For metal determination plant material was harvested and dried over night at room temperature (RT) and again dried for 1 d at 120°C in the oven. Roots were washed with 100 mM $\text{Ca}(\text{NO}_3)_2$ before harvest to eliminate metal residues from the growth medium. For determination of metal contents dry plant material was powdered with an Ahart mortar. Metal contents were finally determined from plant material with Inductively-Coupled Plasma Atomic Absorption Spectroscopy (ICP-AAS) at the Leibniz Institute für Neue Materialien (INM, Saarbrücken).

3.2.1.3 Collection of xylem sap

For xylem sap collection plants were grown on soil as described above (3.2.1.1). Xylem sap was collected from plants in reproductive stage (6 week-old wild type and *frd3* plants; 9 week-old *nas4x-2* and *nas4x-2/frd3* plants). To increase root pressure for the collection of xylem sap, the relative air humidity was increased by covering soil grown plants with a dome 2 days before xylem sap collection. Xylem sap was collected by excision of the hypocotyls below the rosette with a sharp scalpel (Fig. 3.2 A). The first droplet was discarded with a tissue paper without touching the plant (Fig. 3.2 B). For xylem sap collection a pipette tip was carefully mounted over the stem (pipette tip was adjusted according to the stem diameter to an internal diameter of 1.0 to 1.5 mm with a razor blade) (Fig. 3.2 C). Capillary forces subsequently soak xylem sap into the mounted pipette tip. Exuding sap was sampled over a period of 30 min in a pipette tip. The mounting procedure can be facilitated by fixing the small stem with a forceps (Fig. 3.2C). Subsequently, xylem exudates were pooled from 5-7 plants, giving one

3. Material and Methods

biological replicate and were collected in a 200 µl Eppendorf tube which was stored on ice. Volumes of collected xylem exudate samples were determined and then stored at -20°C. Determination of organic acids concentration was performed in cooperation with the group of Dr. Javier Abadia at the CSIC in Zaragoza Spain using a newly established liquid chromatography-electrospray ionization time-of-flight mass spectrometry method (HPLC-TOFMS), which enables the quantification of low molecular mass carboxylates in plant extracts (Rellan-Alvarez and Lopez-Gomollon, unpublished data).



Fig. 3.2: Collection procedure of xylem sap

A) Excision of the hypocotyls below the rosette with a sharp scalpel. **B)** Removal of the first droplet with a tissue paper. **C)** Mounting an adjusted pipette tip over the decapitated stem while careful fixation of the stem with a wide forceps.

3.2.1.4 Perls stain method

The Perls method was used to stain blue Fe deposits in the tissues (Durrett et al., 2007; Roschttardt et al. 2009; Rogers and Guerinot 2002). Potassium ferrocyanide, the so called perls reagent, can react with Fe(III) to form an insoluble pigment known as Prussian blue. Perls stain is a well suitable method to detect hyperaccumulating Fe in tissues. Leaves and flowers were harvested freshly and were vacuum infiltrated for 1 h with equal volumes of the Fixative (Methacarn: Methanol/Chloroform/ pure acedic acid (6:3:1)) at RT. Fixativ was removed and plant organs were washed 3 x with distilled water and subsequently vacuum infiltrated with equal volumes of Perls stain solution (4% HCl and 4% K-ferrocyanide) (1:1) for 15 min to 5 h at RT (Stacey et al., 2008). The reaction was stopped by rinsing 3 x with distilled water.

Microscopic Analysis

The stained plant organs were dehydrated in successive baths of 10 %, 30 %, 50 %, 70%, 90 %, 95 %, and 100 % ethanol, butanol/ethanol (1:1), and 100% butanol. Then, the plant organs were embedded in the Technovit 7100 resin (Kulzer) according to the manufacturer's instructions and thin sections (7 mm) were produced using a rotation

3. Material and Methods

microtome. Sections were analyzed and photographed with a Leica microscope.

3.2.1.5 Pollen germination assay

Pistils were collected 24 h after pollination and fixed in solution containing 70% ethanol, 3.7% formaldehyde (Sigma-Aldrich), and 10% acetic acid (Sigma-Aldrich) for 24 h. The fixed material was then briefly washed and incubated for 24 h in 10 M NaOH and for another 24 h in destained aniline blue solution (0.1% aniline blue in 0.1M K₃PO₄, pH 7.0). Pollen tube growth was observed under UV light with a Leica microscope.

3.2.1.6 Fluorimetric GUS Assay

For GUS activity measurement, protein was isolated from transformed tobacco leaves with 200 µl of GUS extraction buffer. 2 mM 4-methylumbelliferyl-β-d-glucuronide (MUG) was used as a substrate for GUS measurement. The formation of fluorescent product methyl-umbeliferone-D-glucoronide (MU) was quantified by fluorimetry (365 nm excitation/ 456 nm emission). GUS activity was calculated with a MU standard curve (1-10 nmol MU/ 10µl) and was normalized to the protein concentration in the extract and determined according to Bradford method (Bradford 1976). GUS activity was presented in MU product development in µmol MU/min/mg protein.

3.2.1.7 Harvest of Arabidopsis floral organs for expression analysis

Plants were grown on soil under long-day conditions until they produced flowers. Floral organs were harvested under the binocular microscope over a time range of one week to obtain 30 mg per sample for gene expression analysis. To facilitate the harvesting procedure, plant material was put on 3% agar plates (Fig. 3.3). Every second hour, harvested plant material was collected with a forceps in an Eppendorf tube put in liquid nitrogen and was stored in – 80 °C for further processing.

3. Material and Methods



Fig. 3.3: Harvest of floral organs on 3% agar plates

3.2.2 DNA and RNA techniques

Standard methods such as PCR, cDNA synthesis, Western blot analysis and enzyme digestion were performed according to manufacturer's instructions and standard protocols (Sambrook, Fritsch, and Maniatis 1989).

3.2.2.1 Molecular cloning

Two protein fusion constructs were generated using the Gateway cloning system (Invitrogen) (Curtis and Grossniklaus 2003). First, *NAS3* and *NAS4* genomic DNA sequences including the native promoter regions (1500 bp upstream of ATG) were introduced by Gateway cloning (Invitrogen) into the pDONR207 vector (http://www.lablife.org/p?a=vdb_view&id=g2.d7DVqHv0lrxioVcDoYgxK0fpBlk). To obtain protein-GFP and protein-GUS fusion constructs of the respective *NAS* genes, the inserts were transferred by Gateway cloning into the binary vectors pMDC107 and pMDC162, respectively (http://botserv1.uzh.ch/home/grossnik/curtisvector/index_2.html). *pNAS3::NAS3::GFP* and *pNAS4::NAS4::GFP* fusion constructs were obtained with the pMDC107 vector and *pNAS3::NAS3::GUS* and *pNAS4::NAS4::GUS* fusion constructs were obtained with the pMDC162 vector. Both destination vectors were transferred into *Agrobacterium tumefaciens* strain GV2260 (containing pGV2260). The transformation of *Arabidopsis thaliana* plants (ecotype Col-0) was performed following the “floral dip” method (Clough and Bent 1998). Selection of transgenic seeds was based on hygromycin resistance for the pMDC transformants. Transgenic *Arabidopsis* lines were multiplied to homozygosity.

3. Material and Methods

3.2.2.2 Microarray experiment

RNA extraction and microarray hybridization

Total RNA was extracted from 100 mg of root or leaf material with the Qiagen RNeasy Plant Mini Prep Kit according to the manufacturer's protocol. 5 µg RNA were processed into biotin-labeled cRNA and hybridized to Affymetrix GeneChip Arabidopsis ATH1 Genome Arrays (Affymetrix, High Wycombe, U.K.), using the Affymetrix One-Cycle Labeling and Control (Target) kit according to the manufacturer's instructions. Microarray signals were determined using Affymetrix Microarray Suite 5.1.(MAS 5.1) and made comparable by scaling the average overall signal intensity of all probe sets to a target signal of 100 (Affymetrix GeneChip Operating software, GCOS) (Clausen et al. 2004; Duy et al., 2007). Normalized microarray data are available under <http://www.ncbi.nlm.nih.gov/geo/query/acc.cgi?acc=GSE24348>.

Statistical analysis of microarray expression data and calculation of fold changes

Microarray data were pre-processed with quantile normalization (Bolstad et al. 2003). Median values were calculated from the normalized expression signals of the three biological replicates. Fold changes were calculated from median values for eight comparisons of the eight data sets, namely - Fe vs. + Fe (WT), - Fe vs. + Fe (*nas4x-1*), *nas4x-1* vs. WT (+ Fe), *nas4x-1* vs. WT (- Fe), for roots and leaves, respectively.

Data analysis

GeneTrail

The web-based application GeneTrail (Backes et al. 2007; Keller et al. 2008) provided two basic approaches for assessing the enrichment or depletion of gene sets: the unweighted Gene Set Enrichment Analysis (GSEA) and the Over-Representation Analysis (ORA).

GeneTrail supported a variant of unweighted GSEA (Keller, Backes, and Lenhof 2007). The input for a GSEA was a list of genes that were sorted by an arbitrary criterion (e.g., fold changes of expression values). For computing the statistical significance of a biological category, a Kolmogorov-Smirnov-like test was used that computed whether the genes in the category were equally distributed (category was not enriched) or accumulated on or on bottom of the list. To this end, a running sum was computed as

3. Material and Methods

follows: When processing the input list from top to bottom, the running sum was increased each time a gene belonged to the biological category, otherwise the running sum was decreased. Red graphs with a ‘mountain-like shape’ illustrated a specific category predominantly containing top-ranked genes. In contrast, green graphs with a ‘valley-like shape’ illustrated a specific category predominantly containing bottom-ranked genes). The enrichment of a category did not imply a differential expression of all genes of this category. The expression values of every single gene were interpreted and evaluated individually. For estimating the statistical significance, the maximal deviation from zero of the running sum was considered. If this maximal deviation was positive, the category was enriched for the test set genes, otherwise it was depleted. In GeneTrail, the p-value was computed as the probability that any running sum reached a larger or equal absolute maximal deviation from zero. To perform GSEA fold changes were generated to compare two samples, which were then sorted according to values from highest to lowest. Sorted gene identifiers were uploaded as text file prior to performing GSEA.

An ORA compares a set of interesting genes (test set) to a background distribution (reference set) concerning a certain biological category (e.g. a metabolic pathway). The distribution of test set genes that were contained in the considered biological category were compared to the genes of the reference set having this property. If more genes in the test set belonged to the considered biological category than expected, this category was enriched or over-represented, otherwise the category was depleted or under-represented in the test set. In GeneTrail, the statistical significance was assessed by computing a one-tailed p-value using the hypergeometric distribution.

If not mentioned otherwise, we performed all analyses with GeneTrail using the following parameters: p-value adjustment: FDR, significance threshold: 0.05. The number of two genes per category was set as minimum number for all analyses. As reference set for performing an ORA, we used all genes present on the ATH1 chip. All analysis results computed with GeneTrail are available on the web-site <http://genetrail.bioinf.uni-sb.de/paper/ath/>, where links to GSEA and ORA results are provided (The original GeneTrail results pages can be accessed under the file named SummaryPage.html for all comparisons).

3. Material and Methods

NIA Array Analysis Tool

For statistical treatment and identification of differentially expressed genes from pairwise comparisons, the web-based software NIA Array Analysis tool developed by the National Institute on Aging (Sharov, Dudekula, and MS Ko 2005); available at <http://lgsun.grc.nia.nih.gov/ANOVA/index.html> was utilized. The statistical analysis performed with this online tool was based on the single-factor ANalysis Of VAriance (ANOVA). The statistical significance was determined using the False Discovery Rate (FDR) method. The data were statistically analyzed using the following settings: error model 'max (average, actual)', 0.01 proportion of highest variance values to be removed before variance averaging, 10 degrees of freedom for the Bayesian error model, 0.05 Benjamini and Hochberg False discovery rate (FDR) threshold, zero mutations.

3.2.2.3 Real-time Reverse transcription quantitative PCR (RT-qPCR)

To study gene expression levels of marker genes, we used Reverse transcription real-time quantitative PCR (RT-qPCR). Compared to previous methods to quantify mRNA levels, RT-qPCR is nowadays the most sensitive method with a theoretical detection limit of one single molecule per reaction tube. All steps of the establishing RT-qPCR were performed with consideration of recommendations for accurate RT real-time quantitative PCR of Marco Klatte and Petra Bauer 2008, Plant signal Transduction, Methods in Molecular Biology, Issue 479).

RNA isolation and cDNA synthesis

For RNA extraction about 100 mg deep frozen plant material was powdered and homogenized under liquid nitrogen using a homogenizer stick. RNA was isolated from homogenized powder with the Spectrum Total RNA Kit from Sigma-Alrich according to the manufacturer's protocol. To reduce genomic DNA contaminations in the samples, a DNA digestion was performed. RNA concentration was measured and 1µg of DNaseI-treated total RNA was used for cDNA synthesis. cDNA was diluted 1:10 for RT-qPCR quantification, which was recommended, when the Fermentas cDNA synthesis kit was used for cDNA synthesis.

3. Material and Methods

Primer-Design

Primers for real-time RT qPCR were designed using the software DNA Star. Primers were 17-23 bp long, have a GC content of 40-60 % and a T_m of 54-56°C. The length of the amplicons was 80-300 bp. Primer sequence specificity has been confirmed by BLAST searches against available databases on the TAIR website (www.arabidopsis.org). Primers were ordered in HPLC purified quality in a concentration of 100 µM.

For generation of standards for RT-qPCR, another set of primers was designed which did not amplify more than 1 kb and included the target sequence for transcript quantification in RT-qPCR. Template for standard amplification was cDNA.

Standard-preparation

To generate standards we performed 3 parallel 25 µL PCR reactions with 30-35 cycles and separated PCR fragments on a 1% agarose gel. Bands were cut out and DNA was extracted using the innuPREP Gel extraction Kit (Analytik Jena) according to the manufacturer's protocol. Extracted PCR-products were quantified and their purity was verified by UV-spectroscopy (A260 and A280). The quantity of PCR product was confirmed in gel electrophoresis with a mass ruler using 1.5 % agarose and low voltage. The molecular weight of the PCR product was determined with a DNA calculation tool (e.g. Oligo Analyzer, available under <http://eu.idtdna.com/analyzer/Applications/OligoAnalyzer/default.aspx>), which provided the M_r (g/mol), the G/C content (%) and the length of the PCR-product. By dividing the molecular mass (M_r) through the Avogadro number (6.023×10^{23}) and subsequent multiplication with 10^{18} ($(M_r / 6.023 \times 10^{23}) \times 10^{18}$) we calculated the weight of 10^9 molecules (ng/ 10^9). To adjust the concentration of the PCR product to 10^9 molecules per 10 µL in the final stock solution, the calculated weight of 10^9 molecules (ng/ 10^9) has been divided through the initially determined concentration of the PCR product (ng/µl) and multiplied with the volume of the final solution (µl) and filled up with the final volume. Finally, a serial dilution was obtained from the 10^9 stock: 10^7 , 10^6 , 10^5 , 10^4 , 10^3 and 10^2 molecules per 10 µL solution. 30 µL of each serial dilution were aliquoted in PCR strips.

3. Material and Methods

Determination of optimal primer concentration

In order to achieve a high efficiency in RT-qPCR, we generated a primer matrix to determine the optimal concentration of 5' and 3' primer. Therefore, we performed RT-qPCR reactions with primer concentrations ranging from 50 to 300 nM and selected the primer constellation with the highest efficiency.

Reaction mix for primer matrix:

10 µl Takara Premix
0.1 µl SYBR green
1 µl standard $10^4/10\mu\text{l}$

Experimental setup

Mastermix for real time RT-qPCR:

10 µl Takara Premix
0.2 µl Primer 5'
0.2 µl Primer 3'
0.1 µl SYBR green
10.5 µl total volume

Table 3.5: Thermoprofile of RT-qPCR

Initial Denaturation	95 °C	3 min	
Denaturation	95 °C	10 s	40 x
Annealing	58 °C	18 s	
Elongation	72 °C	18 s	
Final Elongation	72 °C	7 min	
Melt curve analysis	55 °C -95 °C		
Cooling	12 °C	forever	

Samples were pipetted with a multichannel pipette by mixing 10 µl mastermix with the sample 10 µl cDNA or standard cDNA, respectively. RT-qPCR was performed using the Biorad IC cycler in 96 well PCR plates sealed with ICycleriQ™ Optical Tape.

3. Material and Methods

Data evaluation

Expression data were exported from the Biorad operating software into Microsoft Excel. Sample names and absolute expression values (SQ mean values) were extracted. Water controls and expression values obtained from genomic DNA were subtracted from expression raw values.

The normalization factors were determined by dividing the absolute expression values of a control sample (e.g. wild type, root, standard condition) by the absolute expression of each individual sample of the housekeeping gene (*EFc/ UBP6*). The obtained normalization factors were multiplied with the respective expression values of all measured genes. Mean values and standard deviation were finally calculated from biological replica and absolute normalized expression values were presented in bar diagrams.

3.2.3 Protein techniques

3.2.3.1 Western analysis

Total plant protein extracts were obtained as follows: Leaves and roots were harvested and weighed after grinding. The plant material was extracted in 2x Laemmli loading buffer and subsequently centrifuged for 5 min at 10000 x g. The amount of 2x Laemmli loading buffer added was adjusted according to the weight of ground material. Equal amounts of the supernatants containing the total protein extracts were denatured at 95°C for 5 min and loaded onto a 12 % SDS-polyacrylamide gel for separation. Samples were transferred to Protran nitrocellulose membrane (Schleier & Schuell), stained with Ponceau S (Sigma-Aldrich), and photographed to control loading. Subsequently, the membranes were probed with anti-GFP (Roche, 1:1000) (according to the concentration of the eluate used) followed by goat anti-mouse horseradish peroxidase secondary antibody (Pierce Chemical, 1:5000). Western blots were developed using ECL chemiluminescence detection reagents (GE Health Care) according to the manufacturer's instructions. The accuracy of loading was further controlled by Coomassie Blue staining of protein gels loaded with the same amounts of protein samples as used for Western blots.

3. Material and Methods

3.2.4 Determination of NA contents

NA contents were determined with High Pressure Liquid Chromatography (HPLC). The measurements were supervised by Dr. Markus Wirtz and performed in the laboratory of Prof. Dr. R. Hell at the University of Heidelberg.

NA was extracted by using a modified protocol based on Neumann et al. (1999). Plant tissue (0.1 g) was grinded to a fine powder in liquid nitrogen and extracted in 1 ml H₂O for 20 min at 80 °C, followed by sonification for 15 min in a waterbath. Cell debris was removed by two centrifugation steps for 20 min at 15000 x g. 25 µL of the resulting supernatant were diluted with 75 µL of 0.5 M sodium-borate buffer (pH 7.7), containing 50 mM EDTA and derivatized for 45 s by the addition of 50 µL 12 mM 9-fluorenylmethyl chloroformate (FMOC, Sigma) according to Gustavsson and Betner (1990). Excess of FMOC was precipitated by the addition of 50 µL 40 mM adamantan-1-amine hydrochloride (ADAM, Sigma) in acetone: water (3:1, v/v) and removed by two centrifugation steps for 30 min at 15,000 x g and 4 °C. The derivatisation-assay (10 µl) was injected on a Nucleosil 100-5 C18, 250/4 column (Macherey- Nagel, Düren, Germany) that was connected to a Waters 600E HPLC system. After equilibration of the column for 8 min in buffer A (20 % (v/v) acetonitrile in 50 mM sodium acetate buffer pH 4.2) NA was separated by using the following binary gradient with a flow rate of 1 ml per minute: 0-5 min (0 % B), 5-15 min (20 % B, linear), 15-20 min (100 % B, linear), 20-22 min (100 % B). 80 % (v/v) acetonitrile in 50 mM sodium acetate buffer pH 4.2 served as buffer B. Fluorescence of FMOC-derivatives was detected by using a fluorescence detector (Jasco FP 920, excitation: 263 nm, emission: 313 nm, Gain: 10, Response: Fast) and quantified by external NA standards (T. Hasegawa Co., Tokyo, Japan). Data were collected and processed with the Millennium32 software (Waters). The identity of NA was evidenced by spiking of chemically synthesized NA to plant samples. The NA-free tomato mutant *chloronerva* was used as a control. In leaves of Arabidopsis, a recovery rate of 98% ± 7% was achieved after addition of external standard to the plant sample prior to NA extraction.

4. Results

4. Results

4.1. Verification and further physiological characterization of *nas4x-1* mutants (published in Klatte, Schuler et al., 2009)

4.1.1 Supportive physiological investigation of *nas4x-1* mutants

4.1.1.1 Determination of NA contents in *nas4x-1* mutants

To verify whether the T-DNA insertion in the four NAS genes indeed destroyed their gene function, we analyzed NA contents of leaves of *nas4x-1* plants compared to wild type. Plants were grown for four weeks on soil under different light periods. Plants were grown in short-day conditions (8 h light, 16 h dark) persisting in the vegetative growing stage and under long-day conditions (16 h light, 8 h dark) turning to reproductive growing stage. Rosette leaves were harvested from plants of both growing stages for determination of NA contents using High Pressure Liquid Chromatography (HPLC).

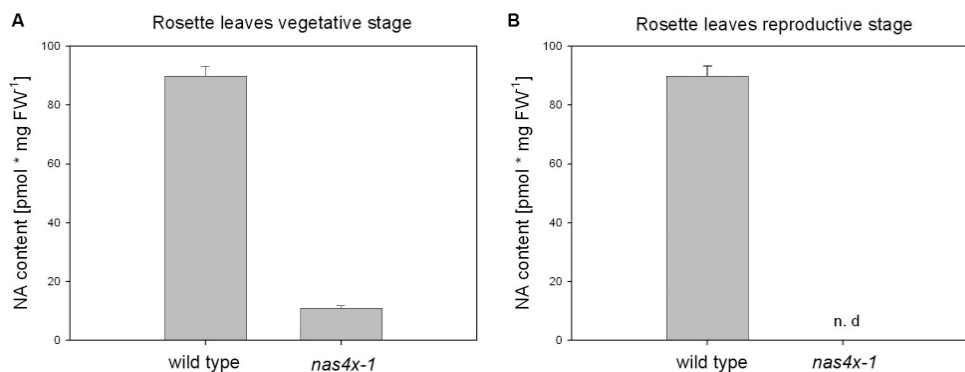


Fig. 4.1.1: Nicotianamine (NA) contents in rosette leaves of wild type and *nas4x-1* plants

Plants were grown for five weeks on soil (n=5). **A)** NA contents of *nas4x-1* compared to wild type harvested from vegetative stage. **B)** NA contents of *nas4x-1* compared to wild type harvested from vegetative stage.

Rosette leaves harvested from *nas4x-1* plants in the vegetative stage contained 12 % NA levels of wild type NA contents (Fig. 4.1.1A), while no NA was detectable at the reproductive stage in leaves (Fig. 4.1.1B). This finding fits to the time point of the development of interveinal leaf chlorosis which primarily occurred when *nas4x-1* plants turned to the reproductive stage where NA was depleted. However, the NA measurements of *nas4x-1* leaves at the vegetative stage indicated that NAS function was not fully disrupted.

4. Results

4.1.1.2 Determination of Fe and Cu contents in *nas4x-1* mutants

The development of the interveinal leaf chlorosis hints to altered Fe contents in leaves of *nas4x-1* plants compared to wild type plants. Since the main defects of the tomato mutant *chloronerva* could be traced back on disturbed Fe and Cu transport, we determined the content of these metals in *nas4x-1* plants. To investigate whether low NA levels influenced the transport and in consequence the contents of Fe and Cu in *nas4x-1* plants, we performed metal measurements. In previous study a significantly reduced Fe content could be detected in flowers (13 %), in siliques (13%) and in seeds (46 %) of *nas4x-1* plants compared to wild type. No changes were detected in roots between *nas4x-1* and wild type. To complete the analysis of all plant organs, we measured metal contents of rosette leaves. Therefore, *nas4x-1* and wild type plants were grown for five weeks in hydroponic system under control conditions (10 μ M FeNa-EDTA). Since the interveinal leaf chlorosis was primarily occurring in reproductive stage, we compared metal contents of rosette leaves of vegetative and reproductive growing stages. Therefore, plants were grown under short-day conditions (8 h light, 16 h dark) residing in the vegetative growing stage and under long-day conditions (16h light, 8 h dark) turning to the reproductive growing stage, respectively and rosette leaves (L3/L4) were harvested from plants from both growing stages for Fe and Cu determination.

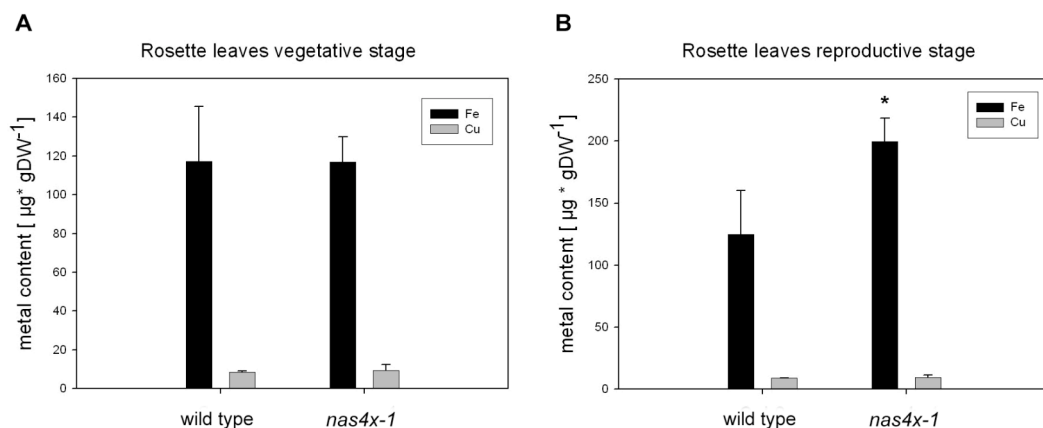


Fig. 4.1.2: Determination of Fe and Cu contents in leaves of *nas4x-1* and wild type plants

Plants were grown in hydroponic system supplied with 10 μ M FeNa-EDTA (n=4). **A)** Metal contents of rosette leaves harvested from plants in vegetative growing stage grown under short-day conditions (8 h light, 16 h dark). **B)** Metal contents of rosette leaves harvested from plants in the reproductive growing stage grown under long-day conditions (16 h light, 8 h dark). * $P < 0.05$ using unpaired t-test

In the vegetative stage, no significant differences in metal contents of rosette leaves could be determined between wild type and *nas4x-1* plants (Fig. 4.1.2A), whereas in the reproductive stage *nas4x-1* leaves had a 1.6-fold increase in Fe content compared to

4. Results

wild type. The Cu content was unchanged between wild type and *nas4x-1* plants (Fig. 4.1.2.B) in both growing stages. The significant increase of Fe content in rosette leaves of the reproductive phase in combination of findings of the previous study that flowers, siliques and seeds of *nas4x-1* plants had decreased Fe contents (dissertation Marco Klatte, 2008), demonstrated that NA was not needed to take up and transport Fe to leaves but it was required to efficiently mobilize Fe from leaves during reproductive phase to flowers and seeds.

4.1.1.3 Comparison of *NAS* gene expression in *nas4x-1* mutants in vegetative and reproductive growing stage

In previous work it has been determined that seed NA levels of *nas4x-1* plant were 40% of those in the wild type. Thus, the loss of NA content in rosette leaves of *nas4x-1* during the reproductive phase could be explained by the removal of NA through remobilization transport out of leaves to the reproductive organs, but can also be explained with a reduced production. To analyze this, we compared expression levels of all four *NAS* genes in roots and leaves of wild type and *nas4x-1* plants in vegetative and reproductive stage. Therefore, plants were grown in hydroponic system for six weeks under either short-day conditions (8-h light period, harvest at the vegetative stage) or long-day conditions (16-h light period, harvest at the reproductive stage) and *NAS* gene expression was analyzed with RT-qPCR from roots and leaves of *nas4x-1* plants.

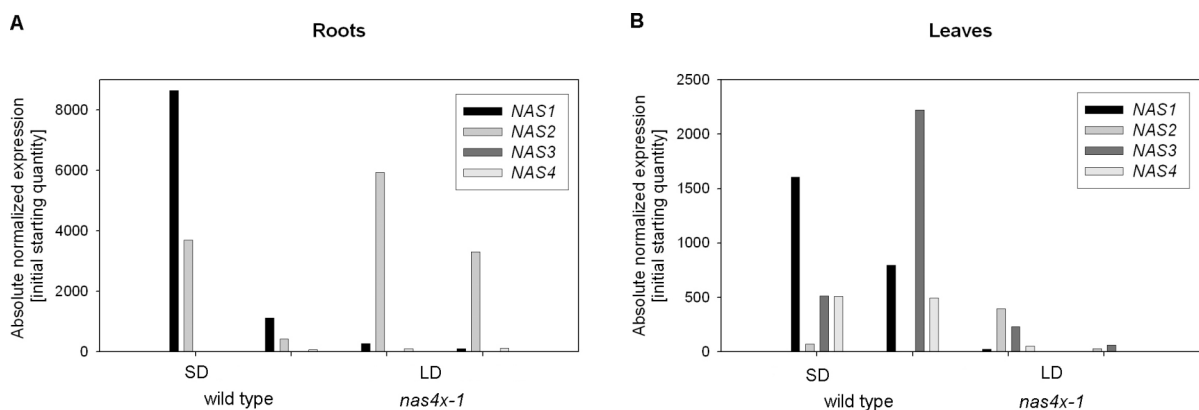


Fig. 4.1.3: *NAS* gene expression in *nas4x-1* mutants compared to wild type plants in roots and leaves **A)** Expression of four *NAS* genes in roots of *nas4x-1* mutants compared to wild type plants under short-day (SD) conditions and long-day (LD) conditions. **B)** Expression of *NAS* genes in leaves of *nas4x-1* mutants compared to wild type under SD conditions and LD conditions

The analysis showed that *NAS1* and *NAS2* were expressed at 8- to 10- fold higher levels in roots at the vegetative stage than in the reproductive stage. *NAS3*, on the other hand, was expressed at about 4-fold higher levels in leaves at the reproductive stage than at

4. Results

the vegetative stage. *NAS4* was expressed at a similar level in the two stages. These results are in agreement with the microarray data available from public databases (compare data from genevestigator). In the *nas4x-1* plants, *NAS2* was expressed 2-fold higher upon the vegetative stage than the reproductive stage, whereas all other *NAS* genes were downregulated due to the mutations (Fig. 4.1.3). Thus, *NAS* genes were differentially expressed with respect to the growth stage. At every stage, at least two *NAS* genes were expressed in the wild type. *nas4x-1* showed higher *NAS2* expression in roots than in leaves, whereas expression in roots was lower upon the reproductive phase than the vegetative stage. Therefore, reduced NA production along with increased transport of NA away from leaves may explain the leaf chlorosis phenotype appearing upon transition to reproductive phase.

These results, together with significant alteration of metal and NA contents suggest an important role of NA in seed metal homeostasis.

4.1.2 Investigation of Fe, Zn and Cu deficiency effects on *nas4x-1* mutants

NA is able to chelate Fe, Cu and Zn (von Wiren et al., 1999). Therefore we tested whether deficiency of these metals may play a role in the expression of the mutant phenotype. The development of a phenotype under deficiency conditions may hint to a role of NA in the mobilization of internal metal stores.

We have grown wild type and *nas4x-1* plants under long-day conditions (16 h light, 8 h dark) in a hydroponic system for four weeks under control conditions (10 μ M FeNa-EDTA) and then exposed the plants for one week to control medium (+ Fe) or Fe deficiency (- Fe), Zn and Cu deficiency.

4. Results

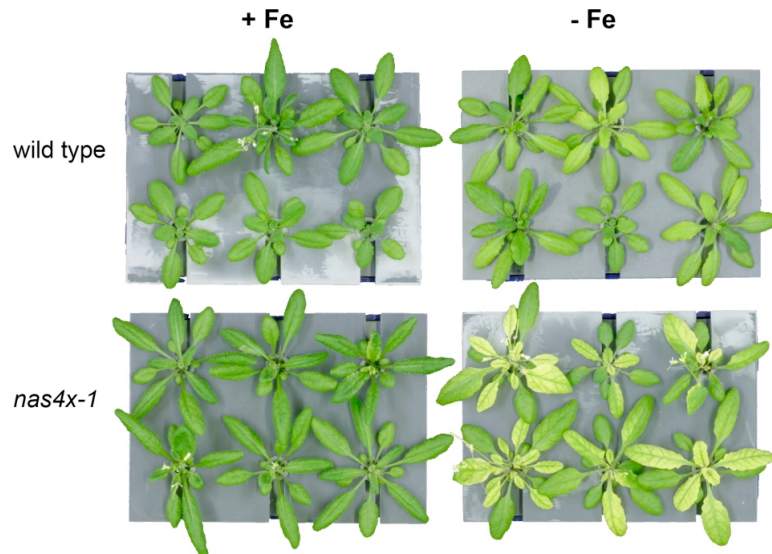


Fig. 4.1.4: Phenotypes of *nas4x-1* mutant in comparison to wild type plants

nas4x-1 and wild type plants were grown in hydroponic system for four weeks on control medium (10 μ M FeNa-EDTA) and were transferred for one week on control (+ Fe) and Fe deficient medium (- Fe).

During vegetative growth *nas4x-1* plants did not show any signs of Fe deficiency neither under + Fe, nor under – Fe conditions (not shown). When *nas4x-1* plants turned to reproductive stage, a slight interveinal leaf chlorosis was visible under + Fe and a strong interveinal leaf chlorosis appeared under – Fe conditions (Fig. 4.1.4). Additionally, *nas4x-1* showed curled leaves under + Fe conditions and produced numerous small, young rosette leaves upon the switch from vegetative to reproductive stage which could not be observed in wild type plants.

Next we tested effects of *nas4x-1* plants exposed to Zn and Cu deficiency, but we did not observe any strong leaf chlorosis in the mutant after one week of exposure to deficiency. These results demonstrated that *nas4x-1* mutants were sensitive to Fe deficiency but not to deficiency of Cu and Zn. Hence, in *nas4x-1* plants, NA is present in insufficient amounts to properly distribute the low Fe, whereas no problem exists for distribution of low Cu and low Zn.

The severe interveinal leaf chlorosis of *nas4x-1* mutants upon Fe deficiency pointed to a disruption of Fe homeostasis due to reduced NAS activity, which seems to be dependent on the developmental stage of the plant. The increased sensitivity of *nas4x-1* plant to Fe deficiency presumably hints to a function of NA in the mobilization of internal Fe stores from the vacuole upon Fe deprivation.

4. Results

4.2 Genome wide expression study of *nas4x-1* mutants compared to wild type plants in a comparative gene chip experiment

To get a global view on transcriptional changes occurring upon the reduction of NA level, we investigated *nas4x-1* plants compared to wild type plants in a gene chip experiment. Since NA is supposed to be involved in numerous processes like long-distance phloem Fe-transport, long-distance Cu-transport, reproduction and intracellular sequestration of metals, we aimed at integrating NA function in the network of metal homeostasis. Therefore, *nas4x-1* and wild type plants were grown in the hydroponic system for five weeks under + Fe and – Fe conditions (as described under 4.1.2). Since we found in previous experiments that *nas4x-1* plants were mainly affected in the homeostasis of Fe (Fig. 4.2.1), rosette leaves and roots of wild type and *nas4x-1* mutant plants were harvested separately from Fe deficient (- Fe) and plants which were grown under control conditions (10 μ M FeNa-EDTA; + Fe) in order to obtain whole transcriptome data with a microarray experiment (Fig. 4.2.1). The experiment was performed three times in three consecutive weeks and respective samples were harvested to obtain three biological replica (n= 3; Fig. 4.2.1). The data of the microarray experiment are available under <http://www.ncbi.nlm.nih.gov/geo/query/acc.cgi?acc=GSE243>.

4. Results

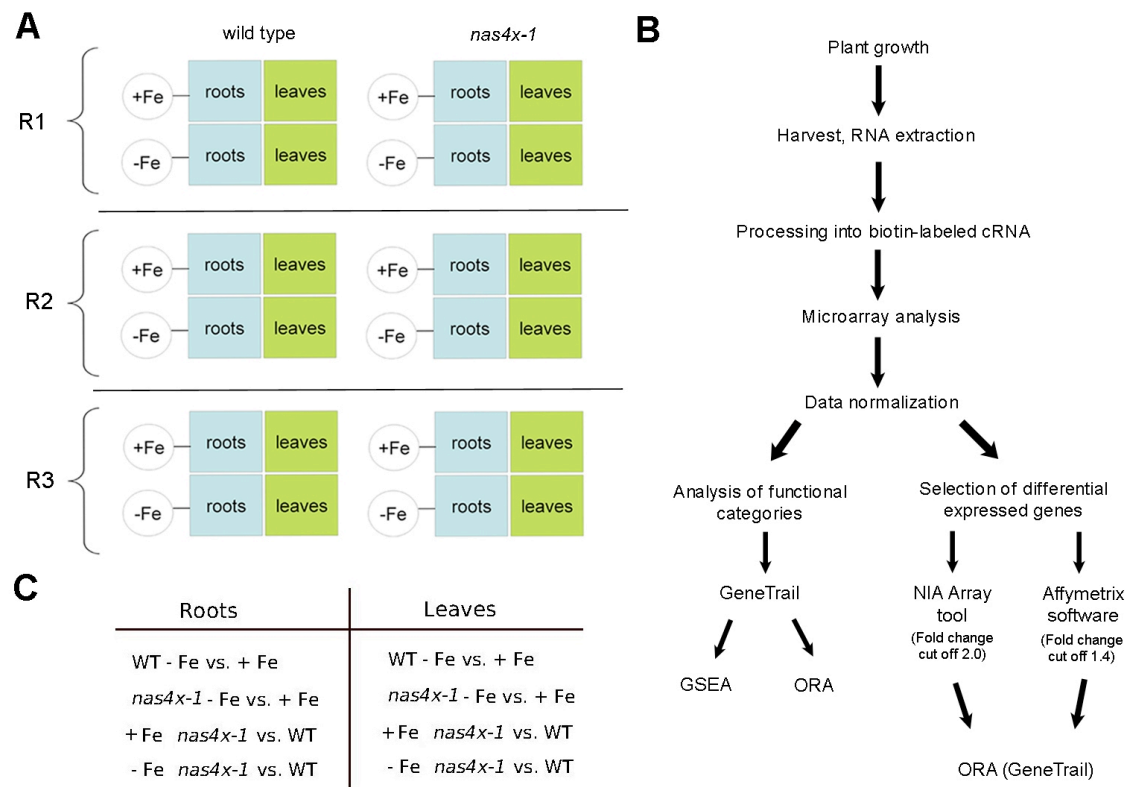


Fig. 4.2.1: Overview of the experimental setup

A) Experimental plan indicating biological experiments with biological repetitions (R1-R3). Roots and leaves from wild type and *nas4x-1* plants grown under Fe supply (+ Fe) and Fe deficiency conditions (- Fe) were harvested, resulted in eight samples for microarray analysis. **B)** Flow scheme of gene chip experiment and data evaluation. **C)** Meaningful pair-wise comparisons.

4.2.1 Transcriptome analysis using the web-based tool GeneTrail

(published in Schuler et al., 2011)

In order to identify whole pathways and biological processes affected in consequence of the reduction of *NAS* gene activity in the *nas4x-1* mutant we searched for functional categories enriched in *nas4x-1* mutants compared to wild type plants. We used the online tool GeneTrail (Backes et al., 2007) (available under: <http://genetrail.bioinf.uni-sb.de/>), which has been adapted for the use of our Arabidopsis microarray data. The tool offers the possibility to test categories from public data bases as well as self-assembled categories, which can be uploaded for own analysis. With our data analyses we tested both analyses to identify functional categories in our samples and to evaluate GeneTrail for plant-specific approaches (published in Schuler et al., 2011).

Normalized expression values (available from GEO under <http://www.ncbi.nlm.nih.gov/geo/query/acc.cgi?acc=GSE24348>) were processed and first analyzed in GeneTrail. Second, data were screened for differentially expressed

4. Results

genes using two different tools: the NIA array tool and the Affymetrix software, using a different fold change-threshold in each case. Selected differentially expressed genes were subsequently used for GeneTrail (see experimental outline in Fig. 4.2.1B). A total of eight meaningful pair-wise comparisons between the eight data sets was considered in our analysis, namely - Fe vs. + Fe (WT), - Fe vs. + Fe (*nas4x-1*), *nas4x-1* vs. WT (+ Fe), *nas4x-1* vs. WT (- Fe), for roots and leaves, respectively (Fig.4.2.1C).

4.2.1.1 Adaptation of GeneTrail for the use of *A. thaliana*

In order to utilize GeneTrail for *A. thaliana*, we extended GeneTrail such that, besides our supported default identifiers, Arabidopsis-specific identifiers (AGI gene codes from TAIR, transcript IDs from the ATH1 microarray) could be used. In addition, we allowed for the usage of the ATH1 chip as pre-defined reference set. Moreover, we improved the handling of individually defined categories. As default analyses for Arabidopsis, we included KEGG, GO, Homologene, and the search for an arbitrary amino acid sequence motif.

4.2.1.2 Gene Set Enrichment Analysis (GSEA) using general biochemical and cell biological categories from KEGG, TRANSPATH, GO and TRANSFAC

To identify functional categories enriched among the transcriptomic data, Gene Set Enrichment Analyses (GSEA) has been performed. GSEA is searching for functional categories enriched among an uploaded test set of fold changes generated of one pair-wise comparison. Functional categories from public data bases like KEGG, GO, TRANSPATH and TRANSFAC include mainly biochemical or cellular processes were initially tested.

Tables of all categories enriched in this experiment are available in the supplemental data of Schuler et al. (2011) (files were not included for reasons of space). Comparing – Fe versus + Fe in wild type we could identify nine induced categories belonging to four different areas (carbohydrate and energy, oxidoreductase activity, defense response, nitrate and amino acid metabolism), and 17 repressed categories belonging to 11 different areas (dolichol metabolism, cold response, prenol metabolism, chloroplast, flavonoid metabolism, nucleoside metabolism, COP1, cellulose activity, fatty acid metabolism, phototropism, DNA polymerase) (Table 2). When comparing *nas4x-1* samples, - Fe vs. + Fe, we identified five categories of three different areas (Fe transport, protease, secondary metabolism) that were induced, whereas three categories

4. Results

of two different areas (hormone/auxin transport, tubulin) were repressed (Table 1). When comparing + Fe samples, *nas4x-1* vs. wild type, we found that 16 categories of five different areas (pyrimidin metabolism, nutrient reservoir, metal homeostasis, defense/glucosinolate/chitinase, general metabolism) were induced while five categories of three different areas (sucrose, fatty acid, protein synthesis) were repressed (Table 1). Finally in the comparison of – Fe samples, *nas4x-1* vs. wild type, only five categories of two different areas (metal, ATPase) were induced, and no categories were found repressed (Table 1). From these data we can conclude that the number of differentially regulated categories was highest in the comparisons of wild type – Fe vs. + Fe (in total 26 categories belonging to 15 areas, Table 1) and of + Fe, *nas4x-1* vs. wild type (in total 21 categories belonging to eight areas, Table 1) suggesting that cellular physiology of the plants from which the samples had been taken had been drastically affected by the treatment (wild type + vs. - Fe) and by the mutation (+ Fe *nas4x-1* vs. wild type). On the other hand, the number of differentially regulated categories was low when comparing *nas4x-1* samples with each other (in total eight categories belonging to five areas, Table 1) and *nas4x-1* with wild type at – Fe (in total five categories belonging to two areas, Table 1). The latter observation suggests that few cell physiological changes had occurred between the samples which were therefore physiologically more similar to each other at cellular level.

When comparing leaf samples the majority of categories were also affected between wild type + and – Fe (in total 31 categories belonging to 15 areas), while an intermediate number of categories was hit between *nas4x-1* samples (in total 12 categories belonging to 10 areas) and between *nas4x-1* and wild type at – Fe (in total 14 categories belonging to eight areas) (Tables 1 and S1). Few changes of categories were found between *nas4x-1* and wild type leaves at + Fe (in total five categories belonging to five areas) (Tables 1 and S1). These comparisons therefore suggest that wild type + and – Fe leaf samples were physiologically very different, whereas *nas4x-1* leaf samples (+ or – Fe) and – Fe samples (*nas4x-1* or wild type) were only partially physiologically distinct. Little physiological difference was detected between *nas4x-1* and wild type leaves upon + Fe. Therefore, roots and leaves reacted with similar strength to + and – Fe. The *nas4x-1* mutation had resulted in an approximation of the – Fe wild type situation in roots and of the + Fe wild type cell physiological situation in leaves.

4. Results

Due to the high diversity and the little overlap of cellular categories in between the different comparisons it was not possible to represent the results in Venn diagrams in any reasonable manner.

4. Results

4.2.1.3 GSEA of transcriptome data testing specific plant physiology categories from MapMan

The GeneTrail-predefined categories utilized in the previous paragraph reflected the physiological status at cellular level but did not appear sufficient for the investigation at whole organism level. To circumvent this obstacle, we next performed GSEA with categories that had been developed for the plant-specific visualization tool MapMan (Thimm et al., 2004) including plant-specific response pathways.

MapMan categories could be incorporated into the GSEA tool of GeneTrail as individually defined categories. Contrary to the GeneTrail-predefined categories the genes of MapMan categories had been grouped according to physiological aspects and pathways relevant for plants.

Tables of all enriched MapMan categories in this experiment are available in the supplemental data of Schuler et al., 2011 (files were not included for reasons of space). The number of MapMan categories affected in the eight meaningful comparisons was determined as in the previous paragraph (Table 1). We found that between one and seven MapMan categories (induced and repressed counted together) were hit in the eight comparisons (Tables 1). The majority of MapMan categories affected was found when comparing wild type roots + and – Fe (six categories) and leaf *nas4x-1* vs. wild type (six and seven categories for + and – Fe, respectively) (Table 1). Only one MapMan category was hit in the comparison of leaf + vs. – Fe, while all other comparisons gave intermediate numbers of MapMan categories hit (four to five) (Table 1). In total we identified 15 different MapMan categories in all comparisons of root samples and 17 different MapMan categories in all comparisons of leaf samples. The data were represented in Venn diagrams (Fig. 4.2.2). This representation shows that among the 15 categories affected in root samples three MapMan categories were shared between at least two comparisons, namely biotic stress, metal transport and carbohydrate metabolism (Fig. 4.2.2A, C). The biotic stress category was found induced in comparisons of – Fe vs. + Fe (in wild type and in *nas4x-1*) and in *nas4x-1* vs. wild type at + Fe, indicating that biotic stress responses were generally induced by Fe deficiency. The metal transport category was induced in comparisons of *nas4x-1* vs. wild type and between *nas4x-1* - and + Fe, showing that metal transport processes were reoriented in *nas4x-1*. Finally, carbohydrate metabolism was induced in *nas4x-1* – Fe

4. Results

vs. + Fe and vs. wild type – Fe suggesting that in *nas4x-1* plants carbohydrate metabolism was altered in response to – Fe.

Among the 17 MapMan categories affected in leaf samples only two categories were hit in at least two comparisons as deduced from the Venn diagram (Fig. 4.2.2B, D). The photosystem category was induced in leaves in the comparisons of *nas4x-1* – Fe vs. + Fe and *nas4x-1* vs. wild type at – Fe indicating that *nas4x-1* leaves at – Fe experienced a remodeling of the photosynthetic apparatus. The MapMan category biotic stress was induced in wild type – Fe vs. + Fe and at + Fe in *nas4x-1* vs. wild type indicating that – Fe conditions resulted in a need for stress defense.

Table 1: Numbers of significantly enriched categories in GSEA

General biochemical and cellular categories from KEGG, GO, TRANSPATH and TRANSFAC						
Comparisons	Roots			Leaves		
	induced	repressed	Σ	induced	repressed	Σ
WT - Fe vs. + Fe	9 (4)	17 (11)	26 (15)	18 (11)	13 (4)	31 (15)
<i>nas4x-1</i> - Fe vs. + Fe	5 (3)	3 (2)	8 (5)	10 (8)	2 (2)	12 (10)
+ Fe, <i>nas4x-1</i> vs. WT	16 (5)	5 (3)	21 (8)	3 (3)	2 (2)	5 (5)
- Fe, <i>nas4x-1</i> vs. WT	5 (2)	-	5 (2)	11 (6)	3 (2)	14 (8)
MapMan categories						
Comparisons	Roots			Leaves		
	induced	repressed	Σ	induced	repressed	Σ
WT - Fe vs. + Fe	5	1	6	1	-	1
<i>nas4x-1</i> - Fe vs. + Fe	3	1	4	4	1	5
+ Fe, <i>nas4x-1</i> vs. WT	3	2	5	4	2	6
- Fe, <i>nas4x-1</i> vs. WT	4	-	4	3	4	7

The numbers were obtained by counting induced and repressed categories of Table S1 and Table S2, available in Schuler et al., 2011. In brackets are the numbers of areas into which the corresponding enriched categories were grouped.

This analysis indicated that the incorporation of plant-specific physiological categories into GSEA added possibilities for novel physiological interpretations at whole organism level that were not achieved by merely concentrating on cellular categories.

Surprisingly, GSEA of MapMan categories did not reveal hits of the transport metal

4. Results

category in each of the eight meaningful comparisons. One possible explanation could be that metal transport was not affected in all comparisons. However, an alternative interpretation could be of technical nature that simply the transport metal MapMan category was not complete. Indeed, this MapMan category only contained 47 genes involved in uptake, transport and allocation of metal ions (further information at <http://genetrail.bioinf.uni-sb.de/paper/ath/>), whereas the list of published genes that were affected by altered metal distribution was larger.

4.2.1.4 GSEA of transcriptome data using an individually designed metal homeostasis category

Since GeneTrail allowed the upload of individually assembled categories, we intended to test a large metal homeostasis category in GSEA. To obtain such a category, we assembled a nearly complete set of genes from published data of metal homeostasis genes and their homologous genes based on sequence similarities and created an individual, new functional category, that has been named „metal homeostasis“ (the gene list of this category has been provided as Additional data file 1, named „Gene list of the individually defined category metal homeostasis.txt“ in Schuler et al., 2011). When performing GSEA this individually defined metal homeostasis category showed enrichment in all eight meaningful pair-wise comparisons (Fig. 4.2.2; results are available at <http://genetrail.bioinf.uni-sb.de/paper/ath/>). The category was found induced in all comparisons of root samples with – Fe vs. + Fe and *nas4x-1* vs. wild type, as well as of leaf samples with wild type – Fe vs. + Fe and + Fe *nas4x-1* vs. wild type (Fig. 4.2.2). The category was repressed in leaf comparisons of *nas4x-1* – Fe vs. + Fe and – Fe *nas4x-1* vs. wild type (Fig. 4.2.2).

Thus, changes in external Fe supply or in internal regulators of metal chelation and transport resulted in significant alterations of gene expression patterns of an entire category of genes representing the components for metal homeostasis.

4. Results

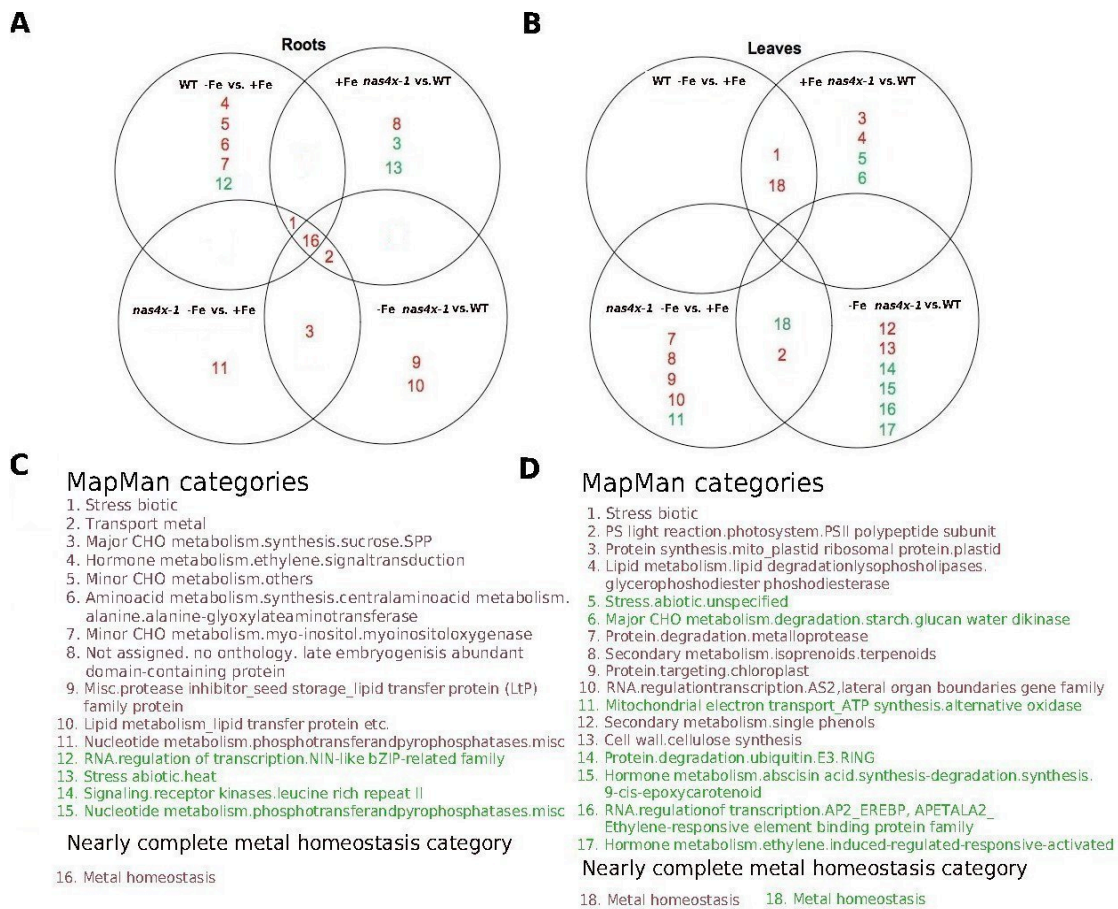


Fig. 4.2.2: **A, B)** Venn diagrams summarizing co-regulation data of enriched categories in pairwise comparisons of **(A)** root and **(B)** leaf transcriptome data. Each circle represents the pairwise comparison indicated. The numbers indicate the respective categories that were found enriched (see **C, D**). In case categories were enriched in more than one comparison the respective number is found in the overlap region of the circles. **C, D)** Designation of categories that were found enriched in **(C)** root comparisons and **(D)** leaf comparisons. Red coloured numbers indicate induced categories, green coloured numbers indicate repressed categories.

4.2.1.5 Over Representation Analysis (ORA) of 258 differentially expressed genes

GSEA is testing a sorted fold change list of two samples compared to each other in order to identify genes belonging to a functional category enriched on top or on bottom on the sorted list. GSEA only enables the use of large test sets. Thus, GSEA enriched functional categories have to be tested of their statistical significance, which is very labor intensive. Finally, we aimed at utilizing GeneTrail to identify functional categories only among selected significantly differentially expressed genes. To identify a list of significantly differentially expressed genes we first used the NIA array analysis software tool to analyze the eight meaningful pair-wise comparisons (A fold change-threshold > 2.0 were selected as upregulation and a threshold > 0.5 were selected as

4. Results

downregulation of a gene). Root and leaf samples were considered separately from each other. The pair-wise comparisons of expression values revealed a total number of 226 leaf-specific and 32 root-specific differentially expressed genes (Additional data file 2 in Schuler et al., 2011, named “Gene list of 258 NIA selected genes.txt”). These 258 genes showed a differential expression in at least one single pair-wise comparison in the NIA Array analysis. With this data set we performed an Over Representation Analysis (ORA) to test whether among the 258 differentially expressed genes specific biological categories or pathways were affected. When an ORA was performed with the GeneTrail-predefined categories from KEGG, GO, TRANSPATH and TRANSFAC no category was enriched within the 258 selected genes compared to all the genes on the ATH1 gene chip. Upon ORA with MapMan categories seven MapMan categories were enriched (Table 2). Among the enriched categories were two metal specific categories, named „metalhandling, binding, chelation and storage“ and „transport metal“, two different oxidative stress categories, both named „redox.dismutases and catalases“, a cell division, a GCN5-related N-acetyltransferase and a non-assigned category (Table 2). We also performed ORA with the metal homeostasis category that we have designed individually as described above. This category was found enriched as expected. Hence, we conclude from ORA analysis of the differentially expressed genes that metal homeostasis as a category was preferentially affected in our experimental conditions. In conclusion, ORA of pre-selected genes allowed the interpretation of transcriptome data in meaningful physiological contexts.

4. Results

Table 2: Enriched MapMan categories testing the 258 NIA pre-selected genes compared to all the genes present on the ATH1 gene chip in the ORA

Enriched categories	Associated genes
metalhandling.binding,chelationandstorage	NAS3, ATCCS, ATFER4, ATFER3, CCH, ATFER1, NAS1, NAS2
redox.dismutasesandcatalases	ATCCS, CSD2, FSD1
redox.dismutasesandcatalases	WRKY60 WRKY46 WRKY47 WRKY53 WRKY48
transport.metal	NRAMP3, MTPA2, IRT2, ZIP5, HMA5, YSL1
cell.division	AT1G49910 AT1G69400 CDKB1;2 APC8 ATSMC3
misc.gcN5-related N-acetyltransferase	AT2G32020 AT2G32030 AT2G39030
notassigned.noontology	AT3G07720 AT5G52670 AT1G09450 CENP-C COR414-TM1ZW9 AT1G76260 ATNUDT6 ATEXO70H4 AT3G14100 ATNUDX13 AT4G36700

The table illustrates those genes among the 258 NIA preselected genes, which are associated with enriched categories.

4.2.2 Analysis of differentially regulated genes on single gene level (unpublished data)

To further analyze microarray data on single gene level we tested the selection of differentially regulated genes with the Affymetrix software using an extended cut off (Fig. 4.2.1B). Therefore, we performed again eight pair-wise comparisons: - Fe versus + Fe (WT), - Fe versus + Fe (*nas4x-1*), *nas4x-1* versus WT (+ Fe), *nas4x-1* versus WT (- Fe) for roots and leaves, respectively. Microarray signals of the different samples (n = 3) were compared with each other by Affymetrix Data Mining Tool (DMT) and GeneChip Operating (GCOS) software. Statistical significance of signal differences was first analyzed by unpaired t-tests (p<0.05) using the DMT software (MAS5.0). The GCOS software uses a change algorithm (Wilcoxon's Signed Rank test) in combination with a signal log ratio algorithm (one-step Tukey's Biweight method). Signal differences with a signal log ratio > 0.5 (1.4 fold change) and a change p-value of 0-

4. Results

0.005 were selected as up-regulation, while a signal log ratio < -0.5 (0.7 fold change) and a change p-value of 0.995-1.0 designated down regulation of genes. Tables of differentially expressed genes of all eight meaningful comparisons of roots and leaves samples are presented in the appendix (Table A2.1; A2.2; A2.4; A2.5). The amount of genes differentially expressed in the pair-wise comparisons is summarized in Venn diagrams shown in Fig. 4.2.3. The numbers of differentially expressed genes in one pair-wise comparison have been matched with other pair-wise comparison. The numbers in the intersections represent the extent of the overlap between two analyses.

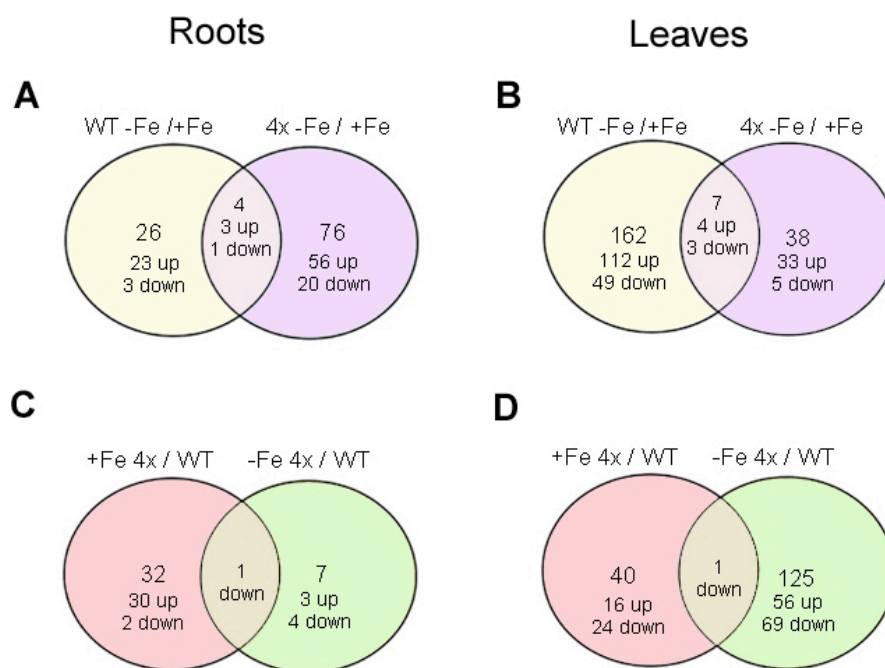


Fig. 4.2.3: Venn diagrams summarizing the microarray analysis of pair-wise comparisons in roots and leaves. The numbers of differentially expressed genes in one pair-wise comparison have been matched with each other pair-wise comparison. The numbers in the intersections represent the extent of the overlap between two analyses. Gene transcripts were tallied whose P value was less than 0.05 and that were up- or down-regulated by greater than 1.4-fold. Plants were grown in hydroponic system supplied with 10 μM FeNa-EDTA (+ Fe) for four weeks and transferred for one week to + Fe and Fe deprived medium (- Fe). WT= wild type; 4x = *nas4x-1* mutant

Among the 22746 genes present on the ATH1 chip, a total number of 462 genes were differentially regulated, 125 in roots and 337 in leaves. Most of the genes were upregulated under - Fe conditions and in the *nas4x-1* mutant compared to wild type plants. Most of the genes are differentially regulated in the comparison between - Fe and + Fe in leaves of wild type plants (162) and under - Fe in the comparison of *nas4x-1* and wild type plants in leaves (125). Generally more differentially expressed genes could be found in leaf samples than in root samples (Fig. 4.2.1) which suggests that

4. Results

most of the changes on molecular level occurring in the above ground plant organs which presumably more suffer from Fe deficiency and reduced NA reduction in case of the mutant. By comparing how many genes are differentially expressed in response to Fe deficiency in wild type compared to *nas4x-1* samples (Fig. 4.2.1 A, B), we observed that more genes were differentially expressed in the mutant compared to wild type in roots (Fig. 4.2.1 A), whereas in leaves more genes were differentially expressed in wild type leaf samples compared to *nas4x-1* (Fig. 4.2.1 B). These results indicated that NA-reduced *nas4x-1* plants underlie a stronger alteration on transcriptional level in roots to deal with Fe deficiency than in leaves. In previous work of Marco Klatte, it has been already shown that *nas4x-1* plants show an induction of the Fe uptake machinery: the Fe transporter IRT1 (Eide et al., 1999; Vert et al., 2002) and the Ferric reductase FRO2 (Robinson et al., 1999) which are up-regulated by Fe deficiency dependent on the transcription factor *FIT* (Colangelo and Guerinot 2004; Jakoby et al. 2004; Yuan et al. 2005), which also showed induction in roots, even upon sufficient Fe supply (dissertation Marco Klatte, 2008). Possibly *nas4x-1* leaf mesophyll cells were more affected by Fe deficiency than wild type leaves and therefore send a constitutive Fe deficiency signal to roots, which in consequence induce all factors responsible for increased Fe uptake and mobilization. But since no Fe is available in the growth medium, less Fe reaches the shoot. Internal Fe stores can presumably rescue wild type plants from severe chlorosis upon Fe deficiency, but since *nas4x-1* plants are presumably not able to mobilize and distribute Fe to target leaf cells they suffer from severe interveinal chlorosis upon - Fe. When comparing *nas4x-1* and wild type samples upon + Fe and - Fe in roots (Fig. 4.2.3C), we observed that more genes were differentially regulated upon + Fe in roots compared to - Fe. This could be explained with the reduced ability of *nas4x-1* plants to sequester Fe into the vacuole and to properly distribute Fe to their target cell or organell, respectively which might cause local Fe overload and might cause oxidative stress, which intensifies upon Fe supply and might be neglected upon Fe deprivation. Upon Fe supply conditions *nas4x-1* plants additionally have to react to an increased Fe income presumably due to increased Fe uptake machinery compared to wild type plants. However, the same comparison in leaves showed that more genes were differentially expressed upon - Fe when comparing leaves of *nas4x-1* and wild type as upon + Fe (Fig. 4.2.3D). However, among the 125 differentially expressed genes, about 60 % were downregulated in *nas4x-1* compared to wild type. Since *nas4x-1* plants suffer from severe leaf chlorosis

4. Results

upon – Fe (Fig. 4.1.4), it is possible that Fe containing components of the electron transport chains or metalloproteins like ferredoxins or superoxide dismutases, components of chlorophyll biosynthesis and cytochromes were downregulated after a period of Fe deprivation since without NA even Fe stores cannot get mobilized (Table A2.2; A2.5).

In the analysis on single gene level, we focused on metal homeostasis genes among the differentially expressed genes. The induction of *IRT2* and *NRAMP3* in the comparison of *nas4x-1* to wild type plants under + Fe confirmed that *nas4x-1* plants suffer from Fe deficiency even under + Fe conditions. The induction of the transcription factors *BHLH39* and *BHLH101*, which were induced in this comparison, was already reported by Wang et al. (2007). The elevation of transcript levels of *ZIP1* and *ZIP4* involved in the detoxification process of Zn excess in roots of *nas4x-1* hints indirectly to a Fe deficiency caused by the enhanced activity of the unselective transporter *IRT1* in the root which also imports Zn in Fe deprived medium. *FRD3*, a gene coding for a citrate effluxer located in the pericycle (Durrett et al., 2007) also showed induction in *nas4x-1* compared to wild type under + Fe indicating an increased citrate efflux into the xylem of *nas4x-1* roots. The induction of *NAS2* in the mutant, which was confirmed in RT-qPCR in previous work, was a further control for the accuracy of the microarray experiment (Table A2.2). The differential expression of all mentioned metal homeostasis genes further suggests that leaves and roots of *nas4x-1* plants obviously sense opposite Fe status. For example *FER3*, a Fe excess marker was induced in *nas4x-1* leaves compared to wild type under + Fe (Table A2.3), whereas *IRT2* and the transcription factors *BHLH39* and *BHLH101* are induced in the roots of *nas4x-1* mutant compared to wild type indicating that *nas4x-1* roots sense Fe deficiency, whereas *nas4x-1* leaves sense Fe excess. Comparison of *nas4x-1* leaves between – Fe and + Fe show an induction of four oxidative stress related marker genes: the Cu / Zn superoxide dismutases *CSD1* and *CSD2*, and the copper chaperone *CCS* which indicates that a reduction of NA might lead to oxidative stress in leaves of *nas4x-1* plants.

The gene coding for cytochrome CYP7110A2 belonging to the P450 cytochrome family and the *FDI* gene, coding for ferredoxin 1 were repressed in *nas4x-1* leaves which confirmed that Fe containing complexes were downregulated in *nas4x-1* leaves due to local Fe deprivation (Table A2.2; A2.4).

4. Results

The induction of the oligopeptide transporter OPT3 which is a putative candidate to transport Fe-NA complexes might also be an indicator for the lack of NA-Fe in certain tissue. Generally the analysis on single gene level could verify that plants indeed suffer from Fe deficiency upon chosen growth conditions. The results show further that *nas4x-1* plants are disrupted either in proper Fe distribution throughout the plant or Fe sensing since they obviously suffer from Fe deficiency in roots and from Fe excess and oxidative stress in leaves. All in all, these results suggest that NA is responsible for the transport of Fe to their target cells and the mobilization of internal Fe stores in leaves

4.2.2.1 Over Representation Analysis (ORA) of 462 differentially expressed genes

To test whether among the extended set of 462 selected, differentially expressed genes specific biological categories or pathways were affected, we performed an ORA with this extended list. The ORA has been performed separately with root and leaf genes using the GeneTrail-predefined and MapMan categories. 53 pre-defined GO categories were found to be enriched among the 125 selected root specific genes and 89 pre-defined GO categories were found to be enriched compared to all the genes on the ATH1 gene chip (Table A2.3). No MapMan category was enriched by testing root and leaf genes separately, whereas 7 MapMan categories were enriched when testing 462 differentially expressed genes together (Table A2.3). Enriched GO categories revealed by ORA in roots and leaves were assigned to biological processes and are presented in Table A and summarized in pie charts in Fig. 4.2.4). The sub-categories were assigned to six biological processes, named stress response, metal homeostasis, oxidative stress, small organic acid metabolism, NA biosynthesis and DNA modification. All categories describing unspecific biochemical, intracellular processes which could not get related to specific biological processes were summarized among `Others`. Among 125 root specific genes were 21% of the categories assigned to metal homeostasis including metal transport and metal binding categories, 11% of the enriched categories were related to a general stress response, 15% to oxidative stress, 22% to small organic acid metabolism, 6% to NA biosynthesis, 6 % were assigned to DNA modification and the residual 19% were summarized among `Others` (Fig. 4.2.4A). Among the 337 leaf specific genes we found to a large extend the same categories enriched than in roots, whereas the portion of unspecific biochemical, cellular categories was larger than in roots. Among 337 leaf specific genes were 15% of the categories assigned to metal homeostasis, 7% of the enriched categories were related to a general stress response, 9%

4. Results

to oxidative stress, 12% to small organic acid metabolism, 3% to NA biosynthesis, 3% were assigned to DNA modification and the residual 51% were summarized among 'Others' (Fig. 4.2.4B). As a control, we also performed ORA with the metal homeostasis category that we have designed individually as described above. This category was found enriched among the pre-selected differentially expressed root and leaf genes, as expected. Hence, we conclude from ORA analysis of the differentially expressed genes that metal homeostasis as a category was preferentially affected in our experimental conditions. In conclusion, ORA of pre-selected genes allowed an interpretation of transcriptome data in meaningful physiological contexts. Put together, ORA revealed that *nas4x-1* mutants are mainly impaired in metal homeostasis in roots as well as in leaves and suffer from oxidative stress and induce a general stress response. We can also hypothesize that *nas4x-1* plants presumably try to compensate the loss of the chelator molecule NA with an enhanced biosynthesis and transport of small organic molecules. These results demonstrate that the reduction of NA exclusively disturbed metal homeostasis itself, whereas no other specific biological pathway could be found to be affected by the reduction of NA.

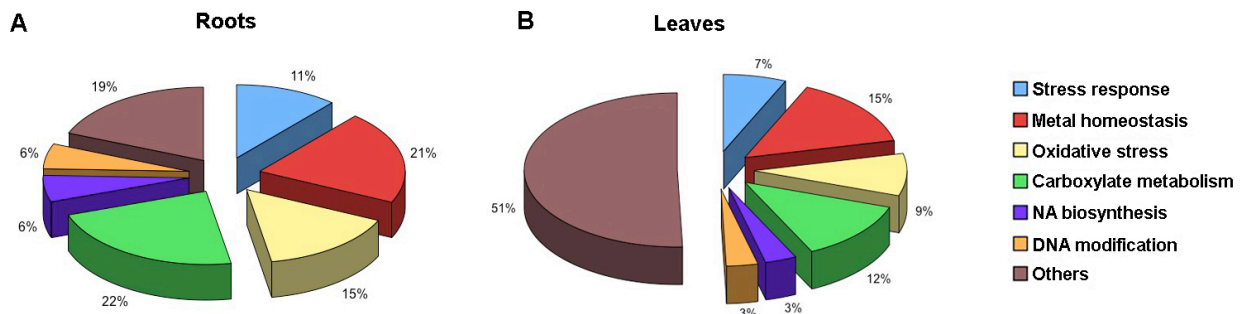


Fig. 4.2.4: Association of over-represented functional categories in 462 differentially expressed genes of microarray data of roots and leaves. Pie charts represent the portion of functional categories which could be assigned to several relevant biological processes **A)** among 125 root specific differentially expressed genes and **B)** among 337 leaf specific differentially expressed genes.

4. Results

4.3 Analysis of individual and overlapping functions of the four *NAS* genes

4.3.1 Determination of NA contents in single and triple *nas* mutants

The differential expression of *NAS* genes (Bauer et al., 2004; dissertation Marco Klatte, 2008) suggests that *NAS* isoforms may have acquired specific functions during their evolution. However, gene expression studies and the fact that single mutants, double and triple mutants look similar to wild type plants when grown under control conditions (Bauer et al., 2004; dissertation Marco Klatte, 2008) indicated that the *NAS* genes are functionally redundant. Therefore, we assessed the contribution of individual *NAS* isoforms to NA production by measuring NA contents in the four single mutants with a single *nas* gene knockout and in the triple mutants containing only one single active *NAS* gene.

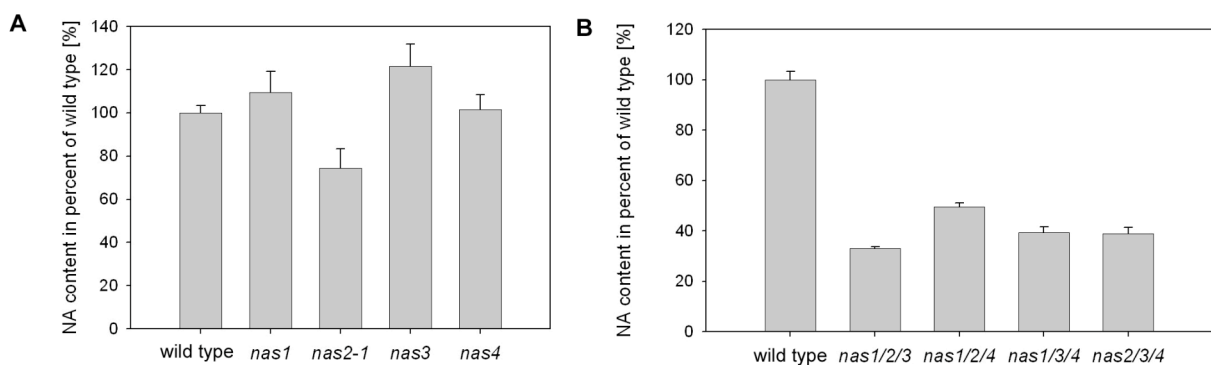


Fig. 4.3.1: *nas* mutant's nicotianamine (NA) contents in percent of wild type's NA contents. Plants were harvested from vegetative stage of five week-old plants (n=5). **A)** Single *nas* mutant's NA contents. **B)** Triple *nas* mutant's NA contents.

The single mutants did not show a significant difference in NA content compared to wild type (Fig. 4.3.1A). All triple mutants show about 30 %-50 % of wild type NA content. From these measurements it can be assumed that none of the single *NAS* genes has any predominant contribution to the overall NA content indicating that the other three *NAS* genes might compensate the loss of one *NAS* gene. These results also give information about the function of *nas2-1* allele in the *nas4x-1* mutant since the triple mutant *nas1/3/4* had 35 % NA compared to wild type whereas *nas4x-1* mutants only contain 12 % of wild type's NA content (Fig.4.3.1B) which means that *NAS2* activity in the *nas4x-1* mutant may be reduced compared to the wild type plants, although expression levels are elevated (Table A2.1; A2.4). Since the NA contents of the single

4. Results

nas2-1 mutant is not higher than the wild type NA content, the *nas2-1* T-DNA insertion does not lead to an increased NA production.

4.3.2 Differential expression of *NAS* genes in multiple *nas* mutants compared to wild type plants

To test whether the redundancy of the *NAS* genes could be due to compensatory effects of *NAS* genes' transcription levels, we tested *NAS* gene expression in the single and triple mutant background compared to the quadruple *nas* mutant and wild type plants. Additionally, we verified the down-regulation of the respective *NAS* genes in the collection of single and multiple mutants and analyzed the differential expression of wild type *NAS* genes. Therefore, wild type plants, single, triple and *nas4x-1* plants were grown on Hoagland agar plates supplied with 50 μ M FeNa-EDTA for two weeks. Leaves and roots were harvested separately in liquid nitrogen, total RNA was extracted and transcribed into cDNA. Transcript levels of *NAS1*, *NAS2*, *NAS3* and *NAS4* were determined via RT-qPCR.

4. Results

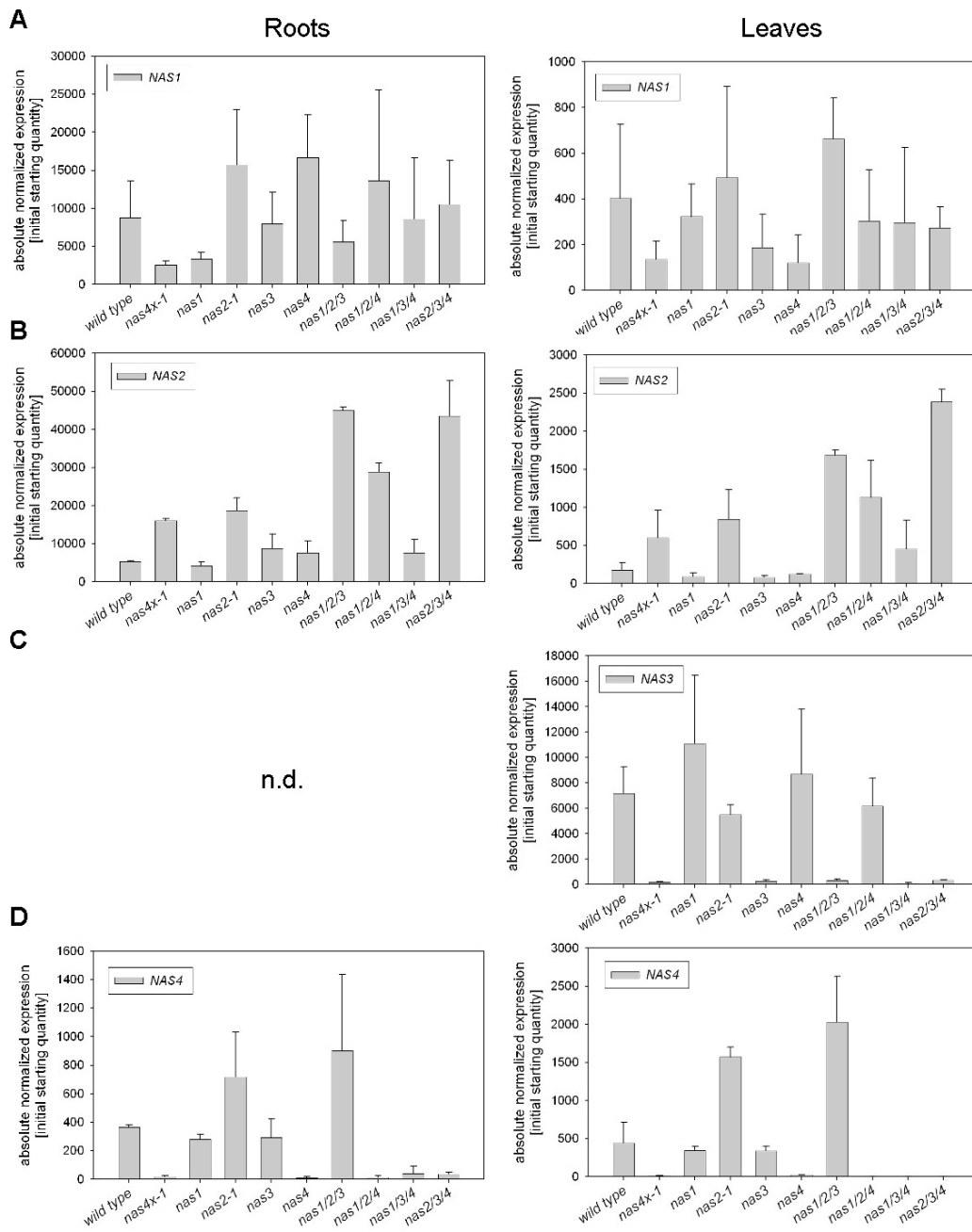


Fig. 4.3.2: Expression levels of *NAS* genes in roots and leaves of wild type plants, single, triple and the *nas4x-1* mutant (n=2). **A)** *NAS1* gene expression in leaves and roots. **B)** *NAS2* gene expression in leaves and roots. **C)** *NAS3* gene expression in leaves. *NAS3* expression was not detectable (n.d.) in roots. **D)** *NAS4* gene expression in leaves and roots

In previous work it has been shown that in wild type plants *NAS1* and *NAS4* are expressed in roots and leaves, while *NAS2* is exclusively expressed in roots and *NAS3* is exclusively expressed in leaves (dissertation, Marco Klatte, 2008). *NAS3* and *NAS4* gene expression was as expected clearly downregulated in all respective mutants in consequence of the T-DNA insertion. Residual *NAS1* expression in all *nas1* mutants (Fig. 4.3.2A) can be traced back on the cross-reaction of *NAS1* primer with *NAS2* gene,

4. Results

which was noticed later on in this study. As expected from previous full length cDNA analysis of Marco Klatte, *NAS2* was in general upregulated in roots of respective *nas* mutants and was in addition ectopically expressed in leaves of all mutants carrying the mutated *nas2-1* allele.

Concerning a compensatory effect we observed that the presence of other mutant *nas* alleles did not affect gene expression of *NAS2* and *NAS3*. *NAS1* expression levels did not seem to be influenced by other *nas* mutations too, but due to high variation of *NAS1* expression in the biological replica, no clear conclusion was possible. The only case where *NAS* gene expression may have been influenced was that of *NAS4* wild-type allelic expression in the background of a *nas2-1* and the *nas1/2/3* mutation (Fig. 4.3.2D). These control experiments indicated that redundancy of the four *NAS* genes was presumably due to compensation of defective *NAS* genes by increased expression of *NAS2* and *NAS4* upon control conditions.

4.3.2 Effects of Fe deficiency to *nas* multiple mutants

In previous study it has been confirmed that NA is involved in the detoxification of Ni through induced Ni sensitivity of *nas4x-1* plants. Other studies reported Ni tolerance upon increased NA levels in Arabidopsis or tobacco (Douchkov et al., 2005; Kim et al., 2005; Pianelli et al., 2005, Mari et al., 2006). By investigating Ni tolerance, previous study demonstrated that *NAS* genes have nonredundant functions. *NAS4* and to a lower degree *NAS3* contributed essentially to Ni tolerance, whereas *NAS1* and *NAS2* could be neglected. Ni may directly affect *NAS* function, so perhaps *NAS3* and *NAS4* could be the Ni-tolerant *NAS* isoforms. Upon Ni treatment, increased NA might have been needed for Fe mobilization. Indeed, it was also shown that *FRO2* was induced upon Ni excess conditions (dissertation Marco Klatte, 2008) indicating that Ni treatment caused Fe deficiency, perhaps through competition of binding sites to NA and other compounds in the cells. Interestingly, further studies reported that increased NA in Arabidopsis not only resulted in tolerance to Ni but also in tolerance to Fe deficiency (Douchkov et al., 2005; Kim et al., 2005). To further test whether the same *NAS* isoforms have nonredundant functions in the tolerance to Fe deficiency, we tested the effect of Fe deficiency on the whole collection of single and multiple *nas* mutants to study whether certain mutants indicate more severe phenotypical effects in response to Fe deficiency than others. Therefore, we have germinated and grown all single and

4. Results

multiple *nas* mutants for two weeks on Fe deprived Hoagland agar plates. The degree of leaf chlorosis has been rated using a chlorosis scale, which enabled the classification of plant phenotypes. Three levels of leaf chlorosis have been considered: light green leaves, slight interveinal leaf chlorosis and intensive interveinal leaf chlorosis. The rating of chlorosis intensities of the entire collection of single and multiple *nas* mutants is presented in Fig.4.3.3.

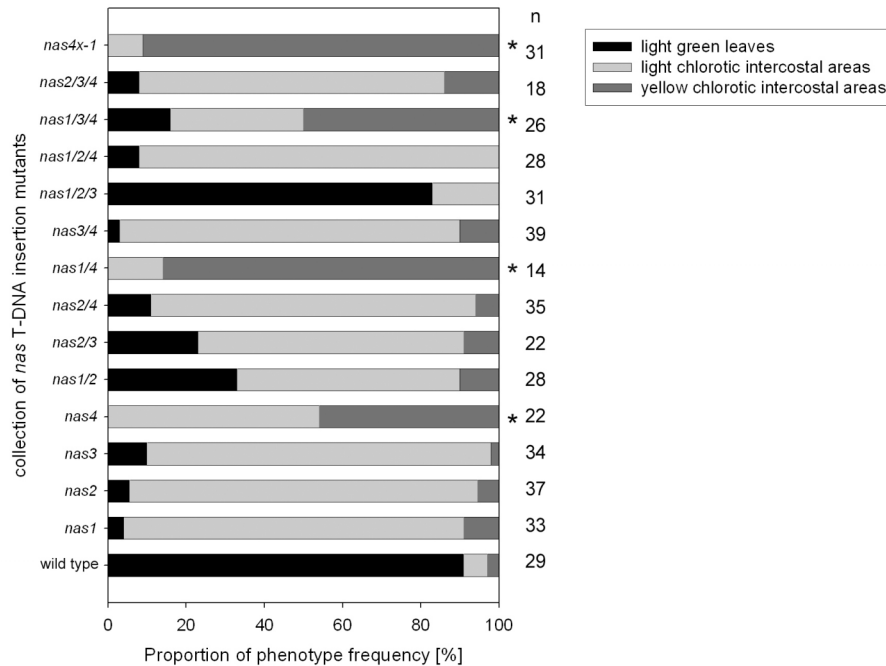


Fig. 4.3.3: Rating of chlorosis intensities of *nas* multiple mutants by chlorosis scales

Plants were grown for two weeks on Hoagland agar plates without Fe supply. The plant's leaf were classified in: light green leaves, light chlorotic intercostals areas, yellow chlorotic intercostals areas. Mutants hypersensitive to Fe deficiency are labeled with a star.

90 % of the *nas4x-1* plants developed a strong interveinal leaf chlorosis and thus they were, as expected, the most Fe deficiency affected plants among all multiple mutants. The multiple mutant analyses showed compensatory interactions of *nas* mutant alleles. The single and multiple mutant combinations with *nas4-1* were most severely affected, even in the single *nas4-1* mutant (labeled with a star), whereas no significant impairment could be detected in single or multiple mutants containing *nas1-1*, *nas2-1* or *nas3-1*. This experiment confirmed a nonredundant function for NAS4 in Fe deficiency tolerance, whereas NAS1, NAS2 and NAS3 function might be compensated by other NAS proteins. Nevertheless, the two processes of Ni excess and Fe deficiency could indeed be physiologically linked.

4. Results

4.3.3 Generation of NAS3 and NAS4 reporter constructs

Previous results indicated that NAS4 might be an important function in the tolerance to Fe deficiency and Ni excess. *NAS3* was also detected as an important factor in Ni tolerance in previous study and moreover it is the only *NAS* gene, which is expressed in the inflorescence. Thus, we decided to generate reporter constructs from the NAS3 and NAS4 isoform and cloned the whole genomic sequence including the native promoter sequence. To monitor, quantify and localize NAS3 and NAS4 protein expression *in planta* we generated per NAS isoform two different NAS reporter construct were generated: pNAS3::NAS3-GFP; pNAS3::NAS3-GUS; pNAS4::NAS4-GFP and pNAS4::NAS4-GUS.

4.3.3.1 Verification of generated NAS3 and NAS4 reporter constructs

4.3.3.1.1 Transient transformation of tobacco leaves

The expression of pNAS3::NAS3-GFP, pNAS4::NAS4-GFP, pNAS3::NAS3-GUS and pNAS4::NAS4-GUS recombinant fusion proteins, was first verified by transient transformation of *Agrobacterium tumefaciens*- mediated infiltration into tobacco leaves.

Green fluorescent protein (GFP) signals of tobacco leaves were investigated two days after infiltration under the fluorescence microscope (Fig.4.3.4).

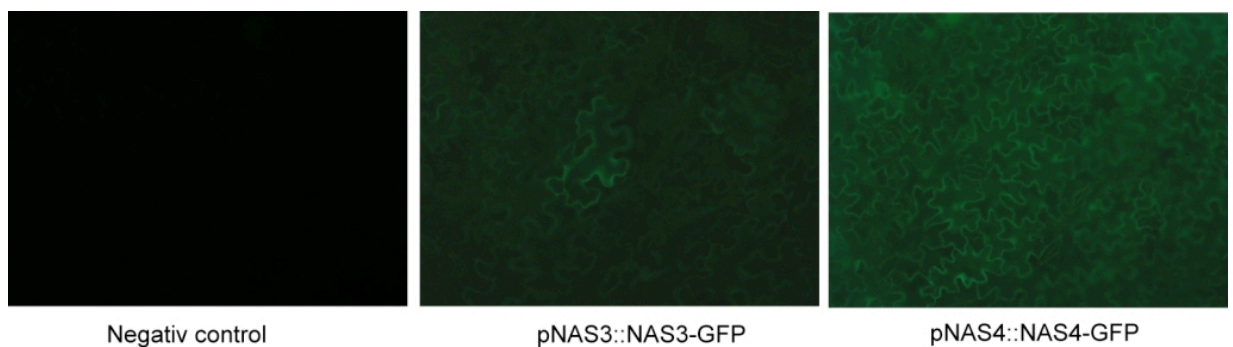


Fig.4.3.4: GFP signals of transiently transformed tobacco leaves

Tobacco leaves were infiltrated with a solution of *Agrobacteria* containing the reporter constructs pNAS3::NAS3-GFP and pNAS4::NAS4-GFP. After two days expression of GFP fusion proteins has been visualized under fluorescence microscope.

Fig. 4.3.4 showed the successful expression of both constructs. Most of the green fluorescence signal could be localized to the cytoplasm of tobacco leaf cells indicating that NAS activity resides in the cytoplasm.

Expression of pNAS3::NAS3-GUS and pNAS4::NAS4-GUS recombinant proteins in tobacco leaves was verified by determination of fluorimetric GUS activity after 2 days.

4. Results

For the NAS3-GUS fusion we could detect a slight GUS activity of 26,3 $\mu\text{mol MU}/\text{min}/0,005\text{mg}$ protein and for the NAS4-GUS fusion we detected a GUS activity of 29 $\mu\text{mol MU}/\text{min}/0,005\text{mg}$, whereas untransformed control leaves did not show any GUS activity. This control experiment proved the functional expression of both constructs

4.3.3.1.2 Stable transformation of Arabidopsis plants

After verification of recombinant expression of all four constructs, we tested the functionality of the constructs in functional complementation studies. Therefore, we transformed the segregating *nas* line $nas1^{-/-}2^{-/-}3^{-/-}4^{+/-}$ with all four constructs to obtain transformants in the *nas4x-2* background.

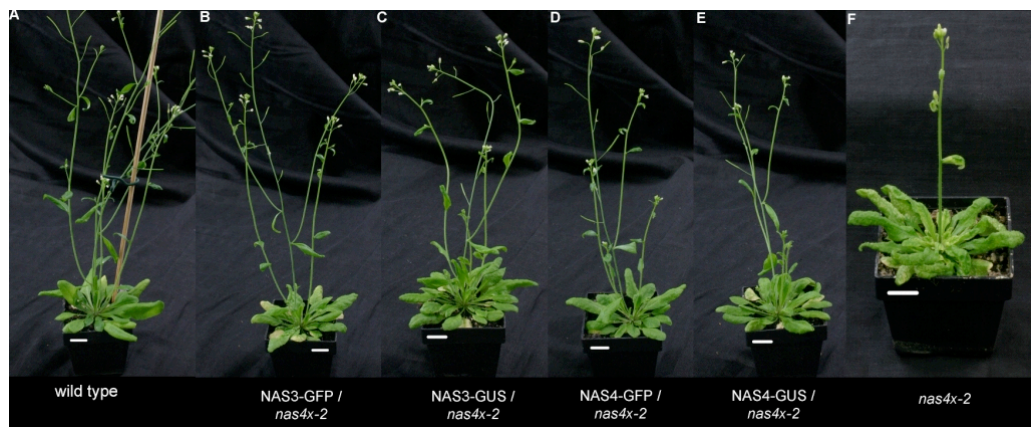


Fig. 4.3.5: Functional complementation of *nas4x-2* mutants by **B)** pNAS3::NAS3-GFP **C)** pNAS3::NAS3-GUS **D)** pNAS4::NAS4-GFP **E)** pNAS4::NAS4-GUS. **A)** Wild type control **F)** *nas4x-2* control

We screened positive plants on Hygromycin-selective medium and tested resistant plants via genotyping whether they were homozygous for all four *nas* mutations. Positive plants could be selected for all four constructs (Fig. 4.3.5). The expression of the constructs was able to reverse the sterility, but it only partially rescued the interveinal leaf chlorosis, which was still visible in the reproductive phase of the plant, reminiscent on the phenotype of *nas4x-1* plants. Therewith, we could prove the functionality of all four generated constructs. Three complemented *nas4x-2* lines were obtained with the NAS3-GUS construct, four with the NAS4-GUS, three with the NAS3-GFP construct and four with the NAS4-GFP construct.

For further analysis on protein level we transformed corresponding wild type (Col-0) plants as well with each of the four constructs in order to investigate protein abundance in mutant and wild type background. For each of the constructs positive plants could be

4. Results

selected to homozygosity in the wild type background. Five transformants were obtained with the NAS3-GUS construct, four with the NAS4-GUS, three with the NAS3-GFP construct and only one with the NAS4-GFP construct.

4.3.3.1.3 Identification of NAS4-GFP fusion protein in Western blot analysis

In order to verify the production of functional fusion proteins in the correct size, we performed immunoblot analysis on leaf and root proteins probed with anti-GFP antibodies. Due to time restriction it was only possible to test the functionality of the NAS4-GFP fusion protein in the background of Col-0. Since we also wanted to test the influence of different growth conditions on the protein quantity we plated seeds of NAS4-GFP transformants in the wild type (Col-0) background (Col-0 / NAS4-GFP) on Hoagland agar plates with Fe supply (+ Fe), without Fe supply (- Fe) and with a high Ni content (++ Ni). As negative control we utilized protein extracts of untransformed wild type plants. After two weeks, we extracted total proteins from roots and leaves and performed western blot analysis with an anti-GFP antibody. Fusion protein could be detected at the correct size of 63 kDa (Fig.4.3.6).

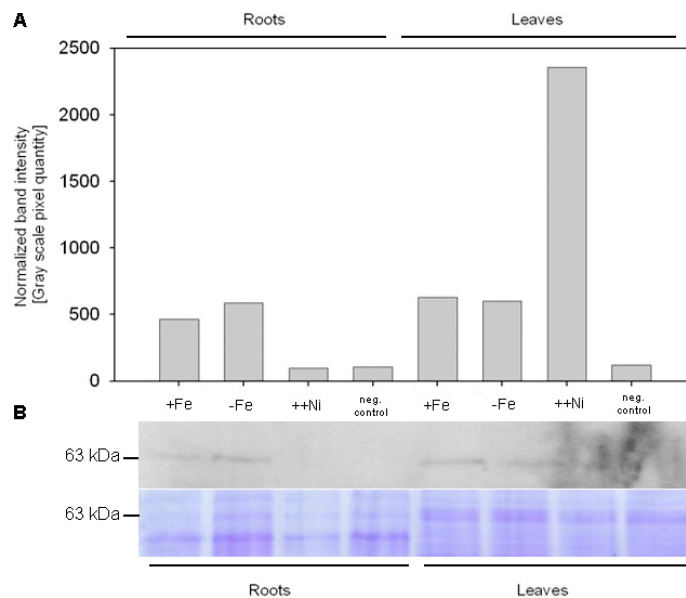


Fig. 4.3.6: NAS4-GFP protein abundance in the wild type background

Col-0 / NAS4-GFP and untransformed Col-0 (neg.control) plants were grown on Hoagland agar plates with supplied with 50 μ M FeNa-EDTA (+ Fe), without Fe supply (- Fe) and with 60 μ M Ni (++ Ni). Protein quantity was measured from leaves and roots of two week-old plants. **A**) Quantification of band intensities by measuring gray scale pixel quantity using Image J. **B**) Western blot analysis using anti-GFP antibody. The Coomassie loading control is presented below.

Total protein quantity appeared low, presumably since NAS4-GFP gene was under the control of its native promoter. NAS4-GFP protein abundance was similar at + Fe and –

4. Results

Fe conditions, whereas NAS4 protein was downregulated in roots upon Ni excess. In leaves, we could again observe no difference in protein levels between + and – Fe in leaves, whereas the protein quantity under Ni excess in leaves seemed to be 4-fold higher than under + Fe and – Fe conditions, but because of the high background signal the quantification has to be repeated. However, this analysis verifies the successful cloning and expression of the NAS4-GFP fusion construct with the correct size in Arabidopsis.

Further studies with these tagged lines are needed for analyzing the regulation of NAS3 and NAS4 proteins. With future comparison of the fusion constructs we will approve protein localization and quantification with two different imaging and quantification techniques (GUS and GFP), which will allow us to evaluate secondary effects due to the protein fusion or technical problems (e.g. the antibody stability).

4.4 Verification and detailed characterization of the second quadruple *nas* mutant *nas4x-2*

4.4.1 Verification of *nas4x-2* mutants

Homozygous *nas4x-2* plants could be identified due to strong interveinal leaf chlorosis occurring 2-3 weeks after germination from individuals of the F3 generation. Like the tomato mutant *chloronerva*, *nas4x-2* plants are completely sterile. Therefore, the segregation line *nas1-1^{-/-}nas2-2^{-/-}nas3-1^{-/-}nas4-1^{+/-}* had to be maintained to multiply *nas4x-2* plants.

Due to the T-DNA insertion in the exon region of the *NAS2* allele, it was expected that *nas4x-2* did not express any full-length *NAS2* transcript. To test this we performed a full length *NAS2* gene expression analysis of *nas4x-1*, *nas4x-2* and wild type cDNA. Therefore, wild type, *nas4x-1* and *nas4x-2* plants were grown for four weeks in hydroponic system under long-day conditions and were transferred for one week on Fe supply (+ Fe) and Fe deficient (- Fe) medium, respectively. Roots and leaves of five week-old plants were harvested separately, RNA was extracted and transcribed into cDNA. The presence of full-length *NAS2* transcript was tested by PCR amplification of *nas4x-1*, *nas4x-2* and wild type root and leaf cDNA.

4. Results

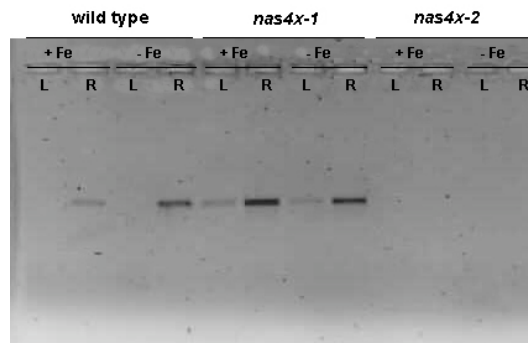


Fig. 4.4.1: Verification of *NAS2* full-length cDNA by PCR

Plants were grown for four weeks in hydroponic system under long-day conditions and transferred for one additional week on Fe supply (+ Fe) and Fe deficient (– Fe) medium. Roots and leaves of five week-old plants were harvested separately, RNA was extracted and transcribed into cDNA. The presence of *NAS2* full-length transcript was tested by PCR amplification of *nas4x-1*, *nas4x-2* and wild type cDNA.

The *NAS2* gene was exclusively expressed in roots and not in leaves of wild type plants (Fig. 4.4.1). The PCR results confirmed that T-DNA insertion of *nas2-1* in the 5'UTR of the gene led to ectopic expression of *NAS2* in leaves (Klatte et al., 2009) which was also previously demonstrated in quantitative RT-PCR (Fig. 4.4.1), whereas no transcript could be detected in the new quadruple mutant *nas4x-2*. This finding suggests that the T-DNA insertion in the exon region of the *NAS2* allele indeed led to a loss of *NAS2* gene activity.

Next, we determined whether the exchange of the *nas2-1* to the *nas2-2* allele indeed led to a full loss of *NAS* activity and led in consequence to a loss of NA production. Therefore, we measured NA contents of *nas4x-2* rosette leaves. Since vegetative growth resulted in highest ratio of NA levels in *nas4x-1* mutants versus wild type plants, we analyzed *nas4x-2* NA contents at the vegetative stage. Therefore, we have grown *nas4x-1*, *nas4x-2* and wild type plants on soil in short-day conditions, persisting in the vegetative growing phase. Rosette leaves were harvested from six week-old plants and NA contents were determined using HPLC.

4. Results

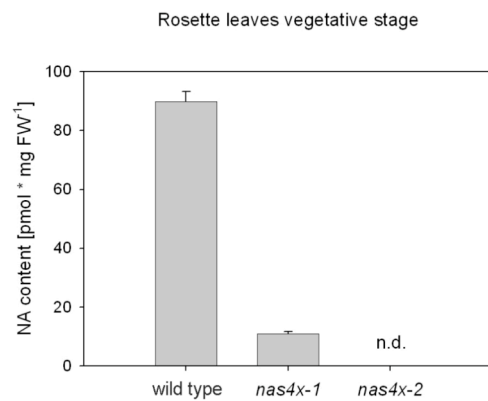


Fig. 4.4.2: Nicotianamine (NA) contents of rosette leaves of *nas4x-1*, *nas4x-2* and wild type plants. Plants were grown on soil under short-day conditions (16 h dark, 8 h light) residing in the vegetative stage. Six week-old plants were used for analysis (n=5)

The NA measurement clearly demonstrated (Fig. 4.4.2) the elimination of NA in leaves of the *nas4x-2* mutant which proved that the T-DNA insertion in *nas2-2* finally led to a full loss of *NAS* function in *nas4x-2* mutant. The genetic composition of *nas4-1* and *nas4x-2* mutants is opposed in Fig. 4.4.3

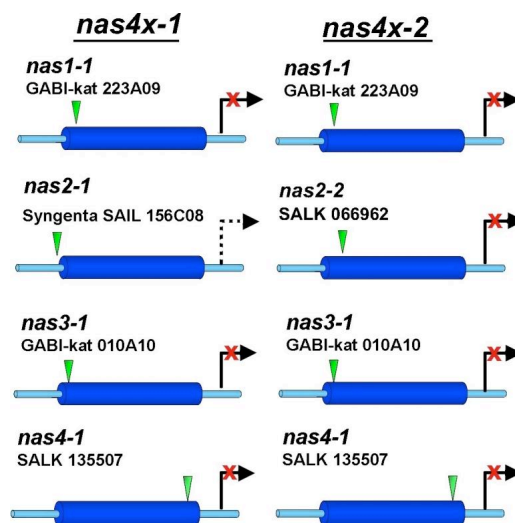


Fig. 4.4.3: Genetic composition of *nas4x-1* and *nas4x-2* mutant plants

The *nas2-1* allele of *nas4x-1* plants harbours a T-DNA insertion in the 5' UTR of the gene leading to a rest activity of the gene, whereas *nas2-2* of *nas4x-2* plants harbours a T-DNA insertion in the exon region of the gene leading to a full loss of gene function.

4. Results

4.4.2 Detailed physiological characterization of *nas4x-2* plants

4.4.2.1 Phenotypical characterization of *nas4x-2* plants

The interveinal leaf chlorosis, which occurred 2-3 weeks after germination, was reminiscent of the interveinal leaf chlorosis of the tomato mutant *chloronerva*. The interveinal leaf chlorosis of *chloronerva* was described to decrease with age (Pich et al., 1994; Ling et al. 1999). To test this in the NA-free Arabidopsis mutant, we documented the phenotypes of *nas4x-2* plants over their entire life cycle (Fig. 4.4.4). Like *chloronerva*, *nas4x-2* showed reduced growth and a complete sterility (Fig.4.4.4). Both *nas4x-2* phenotypes, the interveinal leaf chlorosis and the sterility, could be reverted by daily application of 5 μ M NA on leaves (not shown). The interveinal leaf chlorosis could also be reduced by spraying Fe fertilizer on leaves (Flory 72, Fe-EDDHA, concentration: 0.5g/l), whereas the sterility could not be rescued by Fe treatment (not shown). L2 leaves first exhibited a chlorosis 2-3 weeks after germination (Fig. 4.4.4). During the expansion of the young leaves the interveinal leaf areas re-greened, whereas the leaf veins stayed dark green (Fig. 4.4.4). All young leaves of the mutant developed over the entire life cycle were chlorotic and re-greened with age (Fig. 4.4.4). Older leaves of *nas4x-2* are curled compared to wild type leaves (Fig. 4.4.4). The observation of *nas4x-2* plants over their life cycle revealed that they show significant differences in their development compared to wild type plants. While five week-old wild type plants entered the reproductive growing stage 4-5 weeks after germination, *nas4x-2* plants remained in the vegetative growing stage up to 7 weeks. Wild type plants entered the senescence stadium usually in the age of 7-8 weeks, whereas *nas4x-2* mutants remained green for 12 weeks until they dried. Unlike wild type plants, *nas4x-2* mutants developed numerous small rosette leaves in the reproductive stage, which did not expand and remained small (Fig. 4.4.4).

4. Results

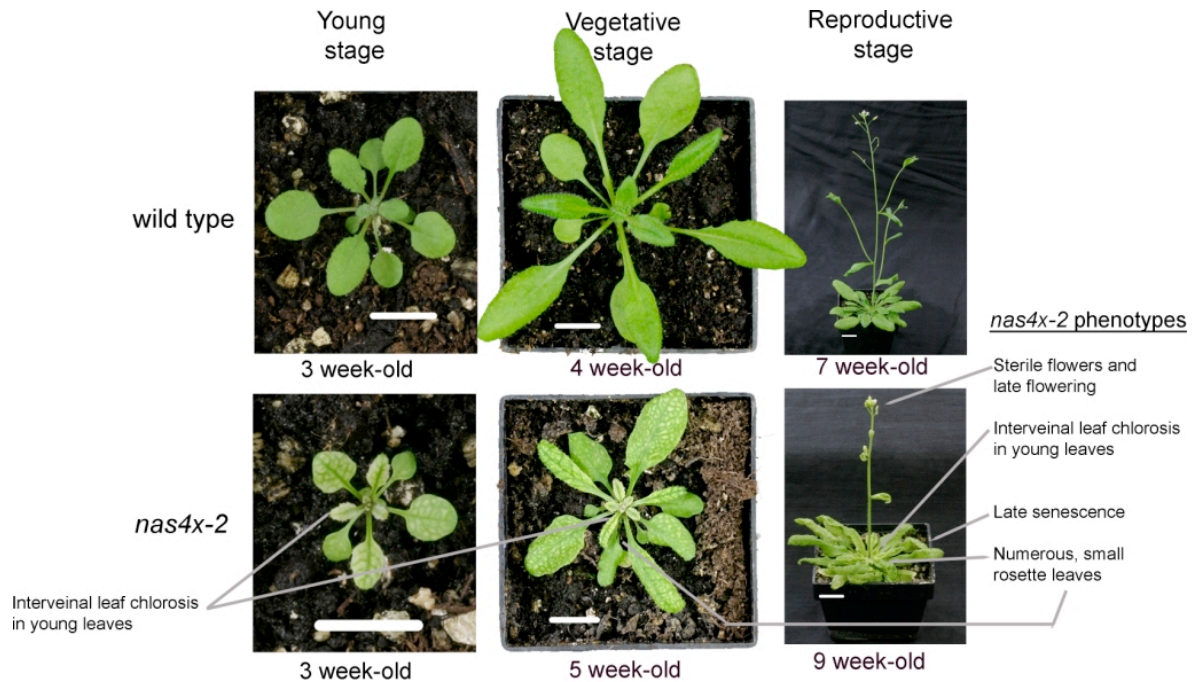


Fig. 4.4.4: Phenotypes of *nas4x-2* mutants compared to wild type plants

Plants were grown on soil under long-day conditions over a time course of nine weeks. *nas4x-2* plants show a reduced growth, are completely sterile and exhibit a characteristic interveinal leaf chlorosis in young leaves which is decreasing with age of the leaf. Bar = 1 cm

4.4.2.2 Investigation of the Fe and Cu root-to-leaf transport in *nas4x-2* plants

4.4.2.2.1 Metal determination of *nas4x-2* roots and leaves compared to wild type

In order to investigate how the full loss of NA influenced the root-to-leaf long-distance metal movement, we performed Fe and Cu measurements of roots and leaves of *nas4x-2* compared to wild type plants. From studies on *nas4x-1* plants we expected a slight increase of Fe contents in roots due to the upregulation of the Fe uptake machinery, which occurred in *nas4x-1* plants and might be even stronger in *nas4x-2* plants. For leaves, we expected due to the strong interveinal leaf chlorosis of *nas4x-2* a more intensive change in metal contents in leaves compared to leaves of *nas4x-1* plants. Moreover, the phenotypical analysis of *nas4x-2* showed that the interveinal leaf chlorosis depended on the age of the leaf. Thus, we decided to measure Fe and Cu contents of L2, L3 and L4 leaves from three different growth stages: young stage, vegetative stage and reproductive stage of the plant (Detailed description in Fig. 4.4.5). For root metal determination, wild type and *nas4x-2* plants were grown in quarter-strength Hoagland solution supplied with 10 μ M Fe for five weeks under long-day conditions. For leaf metal determination, *nas4x-2* and wild type plant were grown under long-day conditions on soil. Rosette leaves of wild type plants were harvested in the

4. Results

third week (young stage), fourth week (vegetative stage) and seventh week (reproductive stage) after germination, while rosette leaves of *nas4x-2* plants, that showed reduced growth and late flowering, were harvested in the third week (young stage), fifth (vegetative stage) and ninth week (reproductive stage) after germination (Fig.4.4.5).

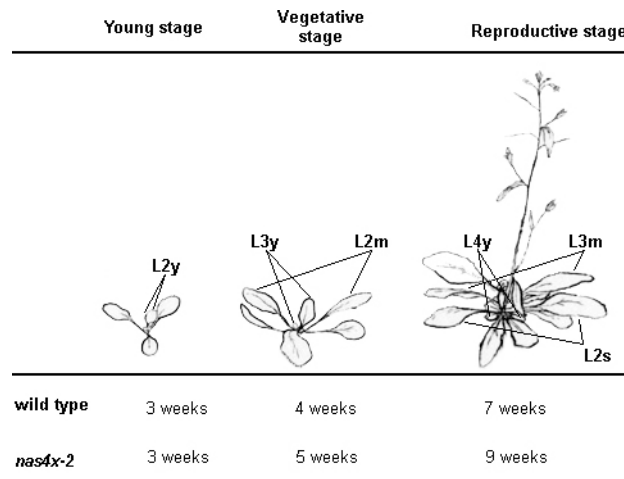


Fig. 4.4.5: Scheme indicating the time point wild type and *nas4x-2* plants reside in the different developmental stages. Leaves harvested from different developmental stages for molecular-physiological analysis are marked. L2 leaves can be young leaves in young stage (L2y), middle age leaves in the vegetative stage (L2m) and old leaves in the reproductive stage (L2s), which already start to senescent. L3 leaves can be young leaves in the vegetative stage (L3y) and middle age leaves (L3m) in the reproductive stage. L4y leaves are the youngest leaves in the reproductive stage. y = young; m = mature; s = senescent

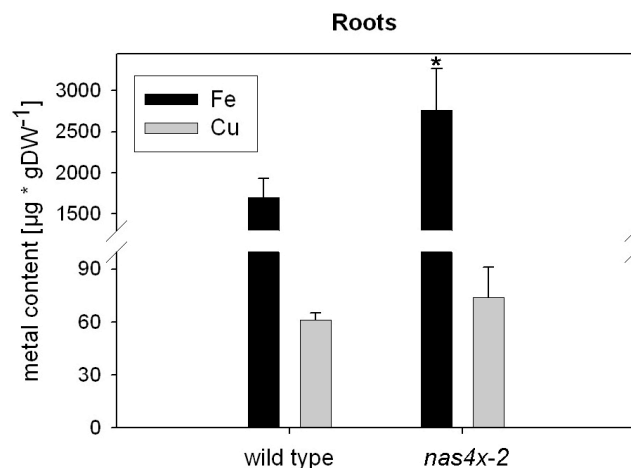


Fig. 4.4.6: Metal contents in roots of *nas4x-2* compared to wild type plants

Plants were grown in hydroponic solution supplied with 10 µM FeNa-EDTA under long-day conditions. Roots were harvested from five week-old plants during reproductive growth (n=4). * $P < 0.05$ using unpaired t-test

nas4x-2 roots showed a 1.6-fold increase of Fe content in roots compared to wild type roots and no change in Cu content compared to wild type which could be explained

4. Results

with the increased Fe uptake due the upregulation of *IRT1*, *FRO2* and *FIT* which has already been demonstrated for *nas4x-1* plants in previous study (Klatte, Schuler et al., 2009) and will be further investigated in *nas4x-2* plants in next sections.

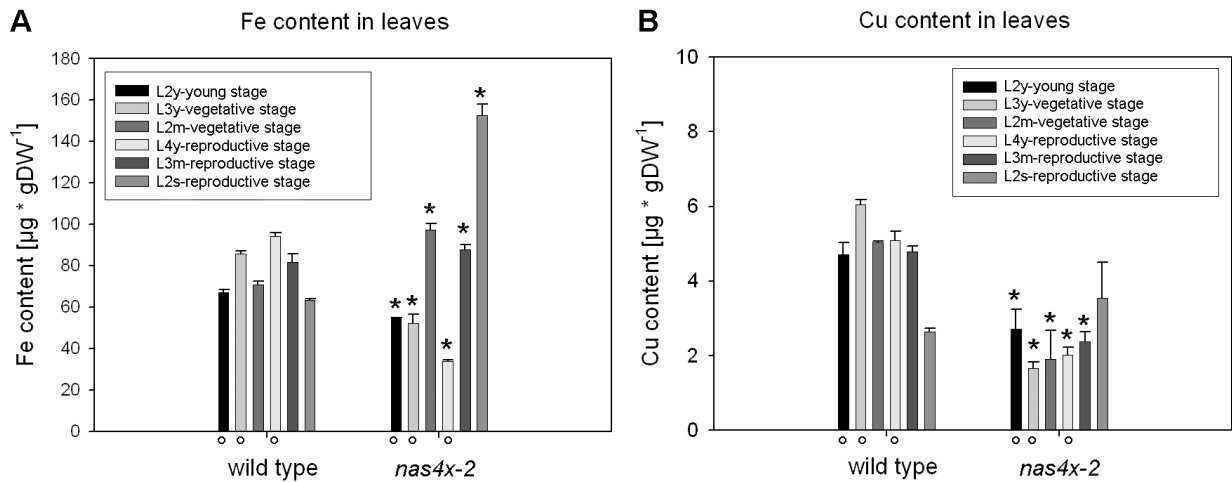


Fig. 4.4.7: Metal determination in rosette leaves of *nas4x-2* compared to wild type plants

Leaves were harvested from soil-grown plants of different growing stages (Fig. 4.4.5) (n=4). **A)** Fe contents of *nas4x-2* plants compared to wild type. **B)** Cu contents of *nas4x-2* plants compared to wild type. ° Expression in young leaves. * $P < 0.05$ using unpaired t-test

All leaf types of *nas4x-2* plants showed significant changes in Fe contents (Fig. 4.4.7A). Young L2, L3 and L4 leaves (L2y, L3y, L4y) showed a decrease of Fe content in *nas4x-2* plants compared to wild type and all mature leaves showed an increase in Fe contents. Young L2y leaves showed a 1.2-fold decrease, young L3y leaves of vegetative stage showed a 1.3-fold decrease and L4y leaves of reproductive stage showed the strongest decrease of 2.8-fold of Fe content. Middle age L2m leaves of vegetative stage showed an 1.6-fold increase and old L2s leaves showed the strongest increase of 2.4-fold. These results confirmed a correlation between leaf chlorosis and Fe contents, since young leaves with low Fe contents suffered from severe chlorosis, while mature leaves with increased Fe contents exhibited a weak interveinal chlorosis. These results hint to a role of NA in the root-to-leaf transport to young leaves, since only young leaves of *nas4x-2* plants were affected by a strong interveinal leaf chlorosis. Presumably mature leaves are supplied by xylem Fe-citrate, whereas young leaves might be supplied by phloem Fe-NA.

The effect of NA loss on Cu content was more severe compared to the Fe contents in *nas4x-2* mutants compared to wild type. In general, Cu content was decreased in all leaf types (Fig. 4.4.7B). Young L2y leaves showed a 1.7-fold decrease, young L3y leaves of the vegetative stage showed a 3.6-fold decrease and L4y leaves of reproductive stage

4. Results

showed a decrease of 2.5-fold of Cu content. Middle age L2m leaves of the vegetative stage showed a 2.6-fold decrease and old L2s leaves showed no significant change. These results indicated that NA is generally needed for the Cu root-to-leaf transport independent of the developmental stage of the plant suggesting that NA is involved in the phloem and xylem Cu transport.

4.4.2.2.2 Gene expression studies of Fe homeostasis genes in *nas4x-2* plants

chloronerva was shown to suffer from Fe deficiency, although leaves accumulate more Fe than wild type plants (Pich et al., 2004). Since we detected lower Fe levels in young leaves of *nas4x-2* plants, but higher Fe contents in mature leaves of *nas4x-2* plants we tested the overall influence of NA loss on internal Fe sensing by studying the expression levels of Fe acquisition genes *IRT1* (*Fe transporter*), *FRO2* (*Fe reductase*) (Eide et al., 1999; Robinson et al., 1999; Vert et al., 2002), which are up-regulated by Fe deficiency dependent on the transcription factor *FIT* (Colangelo and Guerinot, 2004; Jakoby et al., 2004; Yuan et al., 2005.). We compared the expression levels of *nas4x-2* plants to *nas4x-1* and wild type expression levels to test whether the induction was dependent on the internal NA level. Therefore, we grew wild type, *nas4x-1* and *nas4x-2* plants in quarter-strength hydroponic solution supplied with 10 μ M FeNaEDTA for five weeks, and measured transcript levels of *IRT1*, *FRO2* and *FIT* using RT-qPCR.

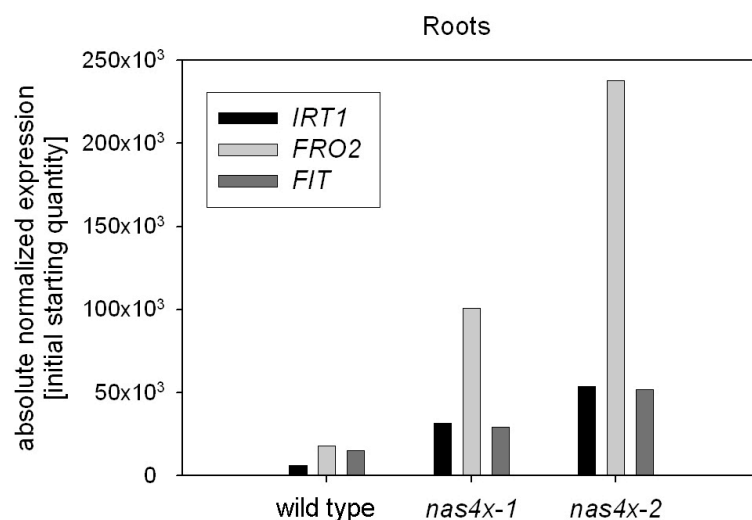


Fig.4.4.8: *IRT1*, *FRO2* and *FIT* gene expression levels in roots of *nas4x-2* compared to *nas4x-1* and wild type plants. Roots were harvested from five week-old wild type plants grown under long-day conditions in a quarter strength hydroponic solution supplied with 10 μ M FeNaEDTA.

Fe deficiency marker genes *IRT1*, *FRO2* and *FIT* were expressed at higher levels upon sufficient Fe supply conditions in *nas4x-1* and *nas4x-2* plants demonstrating that although older leaves of the mutants have more Fe, *nas4x-1* and *nas4x-2* plants sensed

4. Results

Fe deficiency and induced its Fe deficiency response system in the root. Moreover, the expression levels were higher in *nas4x-2* compared to *nas4x-1* mutants showing that the Fe deficiency response depends on the internal NA level of the plant. These results confirm that the mutant phenotype of *nas4x-1* and *nas4x-2* plants cannot be explained by the inability to induce Fe deficiency responses.

To further investigate the internal Fe status of *nas4x-2* rosette leaves, we measured the expression levels of the ferritin gene *FER1*, a marker gene for Fe excess and the associated oxidative stress (Petit et al., 2001; Ravet et al., 2009). We expected that the young chlorotic leaves of *nas4x-2* plants with low Fe levels might not show an induction of *FER1*, while mature, re-greened leaves with high Fe contents might show increased *FER1* transcript levels due to local Fe overload and oxidative stress.

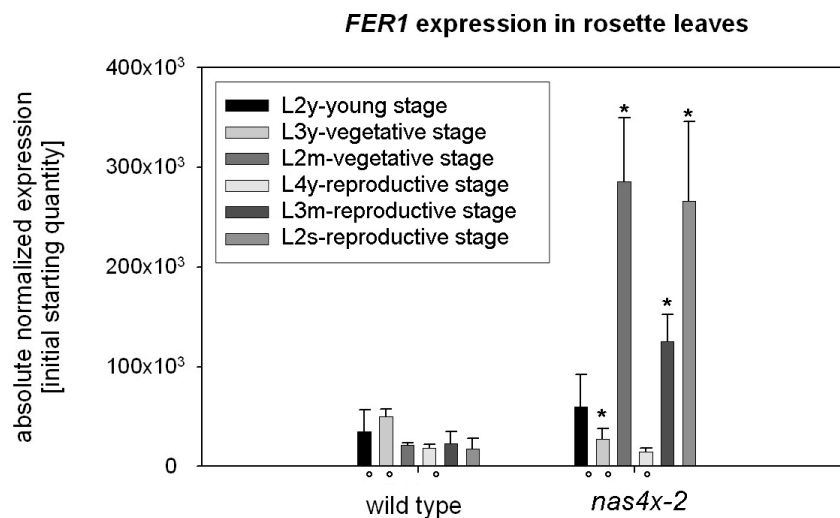


Fig.4.4.9: *FER1* gene expression levels of rosette leaves of different ages of *nas4x-2* compared to wild type plants using RT-qPCR (n=3). Plants were grown on soil under long-day conditions and different rosette leaves were harvested as described in Fig. 4.4.5 for the determination of gene expression levels. ° Expression in young leaves. * $P < 0.05$ using unpaired t-test

As expected, *FER1* was highly induced in older leaves and showed no change in younger leaves compared to wild type. It was even repressed in young L3y leaves of the vegetative stage (Fig. 4.4.9). This finding confirmed that young chlorotic leaves of *nas4x-2* suffer from Fe deficiency while mature and old leaves with an increased Fe content suffer from oxidative stress which assumed that the elimination of NA led to the accumulation of free Fe in leaves which in consequence induces oxidative stress. These results point to a role of NA in subcellular Fe distribution.

Next, we studied whether altered distribution of Fe might cause the phenotype of *nas4x-2* leaves. Therefore, we studied gene expression of the three *YSL* genes: *YSL1*, *YSL2*,

4. Results

YSL3 encoding potential transporters for NA-metal complexes (Curie et al., 2009). We also determined *OPT3* expression, since it might also be able to transport NA-metal complexes. We expected to get a hint about individual functions of the single *YSL* and *OPT3* genes. If they were differentially expressed in the *nas4x-2* mutant, this would support a role of YSLs and *OPT3* in unloading or loading of different NA-metal complexes from the vasculature, (Curie et al., 2009). Therefore, we grew wild type and *nas4x-2* plants on soil under long-day conditions and harvested rosette leaves of L2, L3 and L4 leaves from three different growth stages as described in Fig. 4.4.5 and we analyzed transcripts levels of *YSL1*, *YSL2*, *YSL3* and *OPT3* of all leaf types using RT-qPCR.

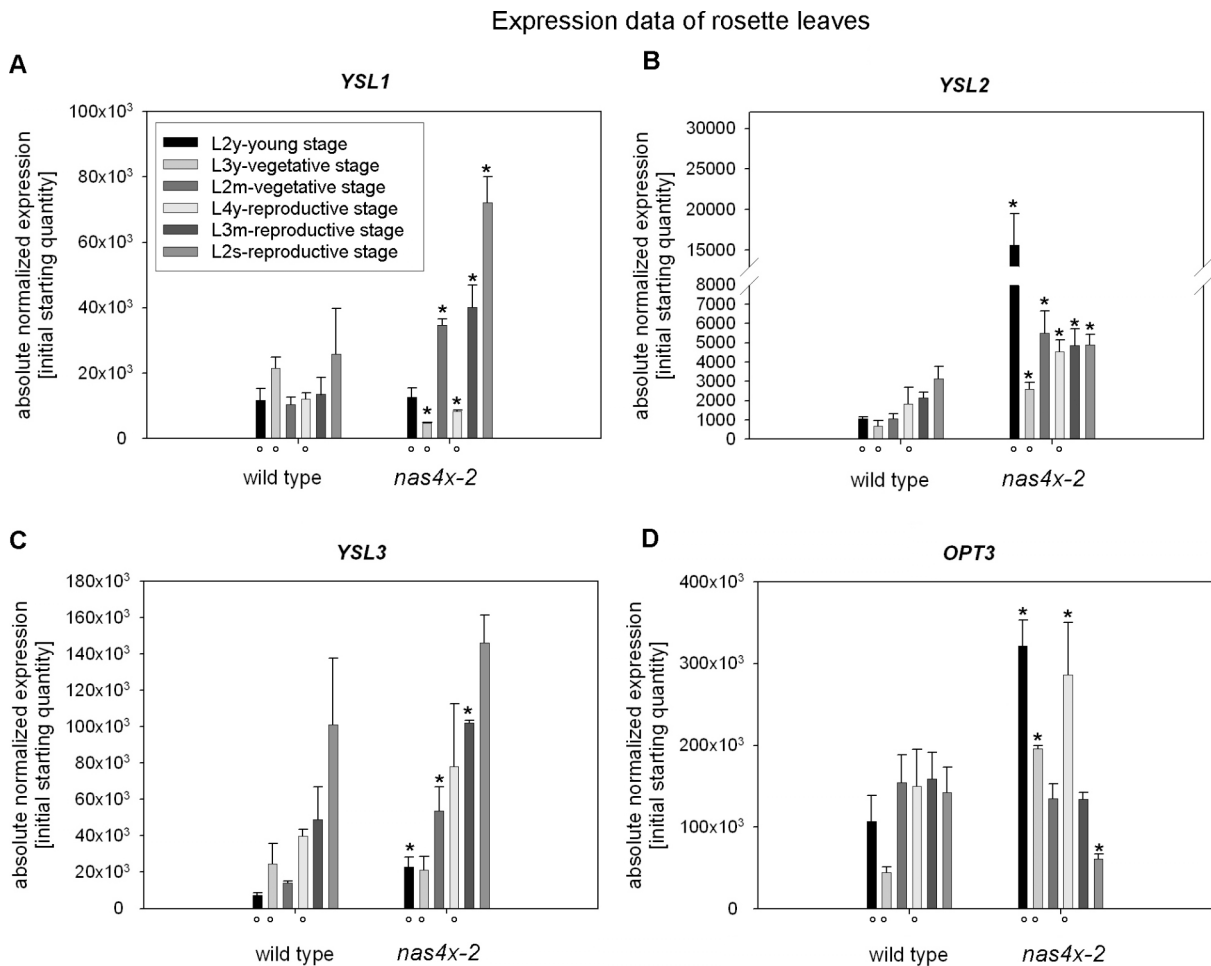


Fig. 4.4.10: Gene expression levels of rosette leaves of different ages of *nas4x-2* compared to wild type plants using qRT-PCR (n=3). Plants were grown on soil under long-day conditions. Different leaf types were harvested as described in Fig. 4.3.5. **A)** Quantitative gene expression of *YSL1*. **B)** Quantitative gene expression levels of *YSL2*. **C)** Quantitative gene expression levels of *YSL3*. **D)** Quantitative gene expression levels of *OPT3*.

° Expression in young leaves. * $P < 0.05$ using unpaired t-test

The *YSL* and *OPT3* genes showed different regulation pattern relative to wild type. We expected the repression of *YSL* genes in young leaves with low Fe contents and an

4. Results

induction in old leaves with high Fe contents in order to remove high levels of Fe of the xylem or phloem (DiDonato et al., 2004; le Jean et al., 2005; Schaaf et al., 2005; Waters et al., 2006). We found a general repression of *YSL1* in young leaves (L2y, L3y, L4y) and a general induction in mature leaves (L2m, L3m, L2s). L3y leaves showed a 4.4 repression, while L4y leaves showed a 1.4 repression, whereas L2y leaves showed no change compared to wild type. *YSL2* expression was induced in all leaf types in particular in L2y leaves of *nas4x-2* with a 14.9-fold induction compared to wild type L2y leaves. *YSL2* was 3.9-fold induced in L3y and 2.5-fold induced in L4y leaves. In mature leaves it was 5.2-fold induced in L2m leaves, 3.3-fold induced in L3m leaves and 1.6-fold induced in L2s leaves compared to wild type. *YSL3* was 3.3-fold induced in L2y leaves, 3.8-fold in L2m leaves and 2-fold induced in L3m leaves compared to wild type, while it was not differentially regulated in L3y, L4y and L2s leaves. *OPT3* showed a general induction in young leaves (L2y: 3-fold, L3y: 4.4-fold, L4y: 1.9-fold) and no differential regulation in mature leaves (L2m, L3m) and a 2.3-fold repression in senescent leaves (L2s). These findings suggest that *YSL* genes undertake distinct roles in Fe distribution. Since *YSL1* expression was repressed in young leaves and induced in older leaves, it is likely that its function first becomes important when the leaf is fully expanded, when the leaf Fe status changes from sink to source. *YSL1* might be responsible for a phloem to xylem switch of NA-Fe complexes in mature leaves for the long-distance transport to reproductive organs especially during senescence, which was predicted by (Chu et al. 2010; Waters et al. 2006). From these results, we can exclude that *YSL* expression is regulated by NA levels, since it might be possible that *YSLs* transport other substrates than NA-metal complexes. The expression patterns of *YSL2* and *YSL3* indicate that they might participate in xylem unloading or phloem loading of older leaves, but their induction in young leaves also suggests that they may function in phloem unloading in young leaves. In middle age leaves, which are not yet fully expanded *YSLs* could also participate in xylem unloading or metal exchange between phloem and xylem. Moreover, all *YSL* genes can be considered to play a role in the subcellular sequestration of Fe-NA complexes into the vacuole. Because older leaves of *nas4x-2* plants have higher Fe levels, this might be the explanation for an elevated expression of *YSL* genes. The induction of *OPT3* in young leaves suggests a role in phloem unloading of NA-Fe complexes in young leaves, but its repression in senescing leaves excludes its role in remobilization process of metals out of the leaves.

4. Results

4.4.2.3 Investigation of intercellular Fe transport in leaves of *nas4x-2* plants

The interveinal leaf chlorosis of *nas4x-2* only appeared in young leaves and decreased during leaf maturation which indicates that the elimination of NA led to a strong impairment of the transport from roots-to-young leaves, but not to a disruption of the long-distance transport from roots-to-older leaves. Metal measurements showed that older *nas4x-2* leaves had more Fe than wild type leaves, whereas young *nas4x-2* leaves had less Fe than wild type plants. The expression analyses showed further that the Fe excess and oxidative stress marker *FER1* was increased with the age of the leaf indicating that the loss of NA caused oxidative stress, which was likely caused by the accumulation of free Fe in a specific tissue of the leaf. We hypothesized that a large disorder of NA free plants might be the disruption of short-distance transport from the vasculature to the leaf mesophyll cells. To investigate this, we performed Perls stainings, of Fe deposits in plant cells (Rogers and Gueriot, 2002; Durrett et al., 2007; Roschttardt et al., 2009). Perls stain is a well suitable method to detect hyperaccumulated Fe(III) in tissues. However, under normal conditions the Fe concentration in most tissues is too low to detect it with the Perls stain method.

4.4.2.3.1 Fe localization in *nas4x-2* plant organs compared to wild type plants

In the first experiment we stained *nas4x-2* leaves in order to find an accumulation of Fe in specific parts of the leaf (Fig. 4.4.11B, C). We observed a blue staining in all leaf - types of three different developmental stages. The Fe accumulation was observed in young leaves (Fig. 4.4.11A) and the staining intensified with the age of the leaf. Interestingly, the blue stain in middle age leaves was concentrated at the distal part of the leaf, especially in the small distal branches of the vascular tissue, whereas the main vein of the leaf was not stained (Fig. 4.4.11B). Blue staining of older leaves was equally distributed throughout the leaf veins. This alteration in Fe accumulation in *nas4x-2* leaves points to switch from phloem-Fe to xylem-Fe supply during leaf expansion.

A deep blue staining could be observed in the hydathodes which are areas of secretory tissues in leaves that secrete water through pores in the epidermis or margin of leaves, typically at the tip of a marginal tooth or serration (Fig. 4.4.11B). Hydathodes probably evolved from modified stomata and are involved in guttation, where water is released from the top in order to transport the nutrients in the water from the roots to the leaves. Hydathodes are connected to the plant vascular system by a vascular bundle. Since the

4. Results

liquid which is extruded from the stems xylem, contains salts, sugars, and organic compounds dissolved in water, occasionally crystallizes upon evaporation, forming a white powdery substance on the leaf's edge (Neil Campbell, Biology). It is possible that through the elimination of NA, Fe is not unloaded from the xylem and finally ends up in hydathodes of *nas4x-2* leaves.

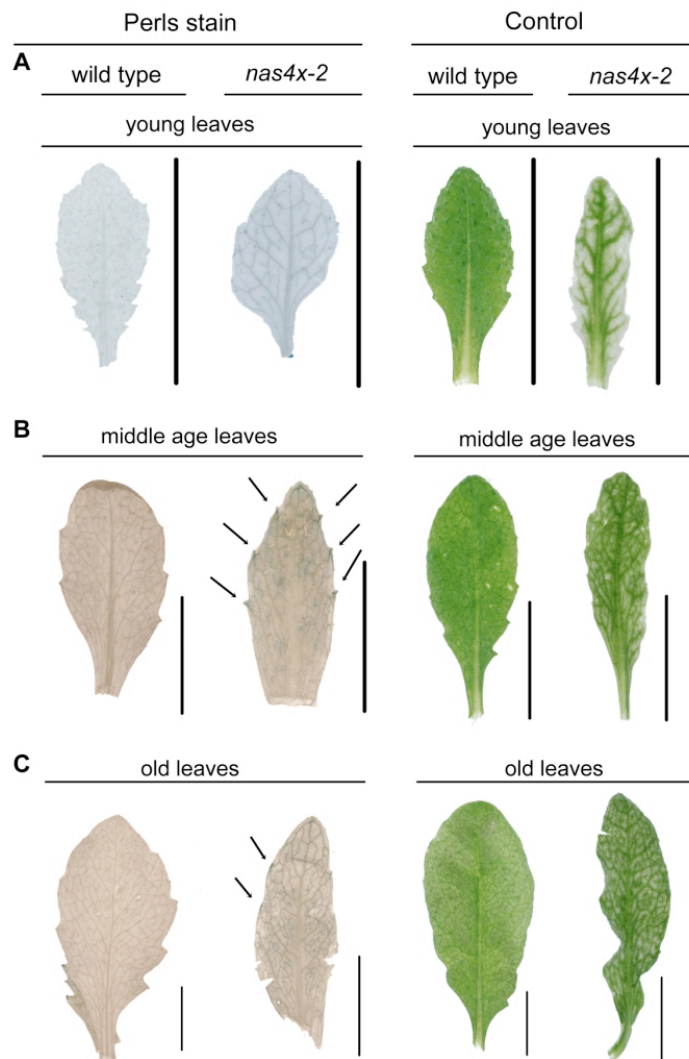


Fig. 4.4.11: Fe accumulation in leaves of different maturation stages

Wild type and *nas4x-2* plants were grown on soil under long-day conditions upon reproductive growing stage. (A) Young leaves, (B) middle age leaves and (C) senescing leaves were harvested and stained using the Perls stain method. Bar= 1 cm

An intensive blue stain was visible in the vasculature of mature and old leaves of *nas4x-2* plants, whereas in wild type plants no blue stain was detectable (Fig. 4.4.11 B, C). Even leaf veins of young *nas4x-2* leaves showed a slight blue staining in leaf veins. These findings indicate a high accumulation of Fe in the vasculature in *nas4x-2* leaves.

4. Results

Since young *nas4x-2* leaves have low Fe contents in contrast to old leaves, the Fe stain of veins in young leaves was very surprising. We conclude that a major defect of *nas4x-2* plants may thus be in the lateral movement of Fe in leaves.

4.4.2.3.2 Fe localization in sections of *nas4x-2* plant organs

To specifically localize Fe we produced 7 μm sections of stained *nas4x-2* leaves. Leaves harvested from young stage and old stage, were embedded in resin and dissected using a rotation microtome and analyzed under the microscope.

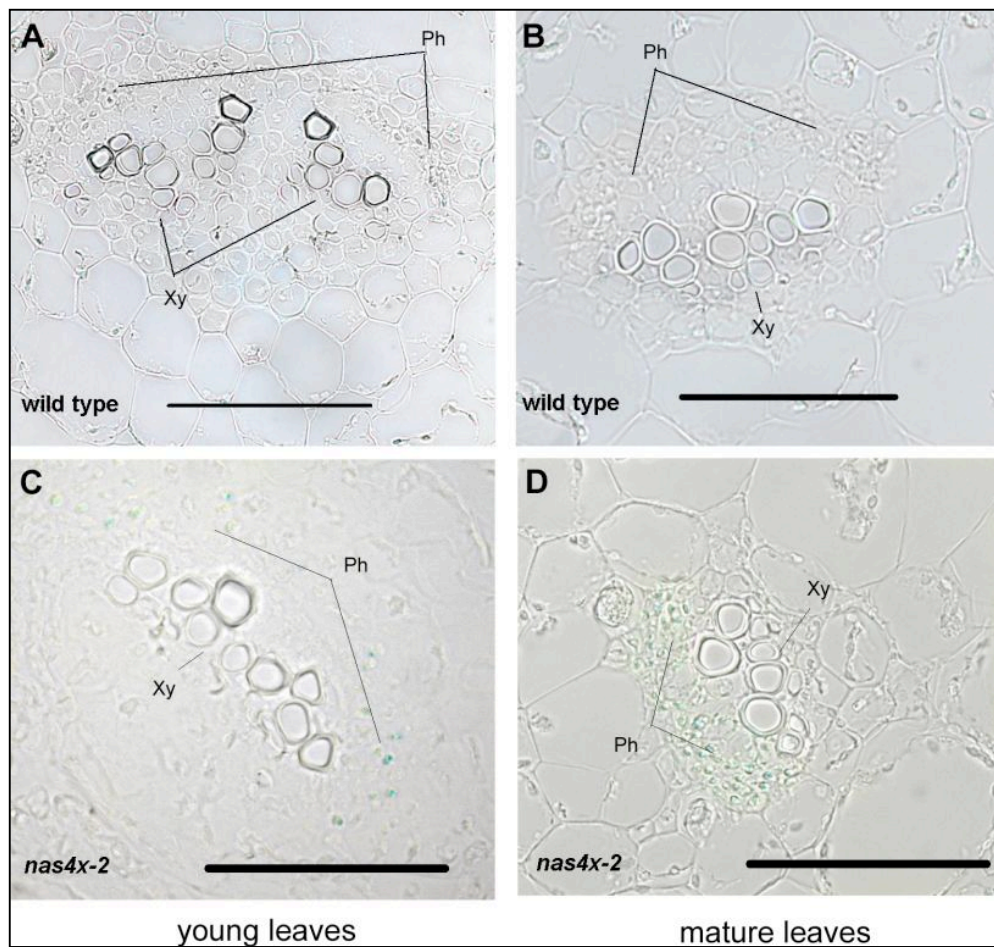


Fig. 4.4.12: Fe accumulation in sections of wild type and *nas4x-2* leaves

Wild type and *nas4x-2* plants were grown on soil under long-day conditions upon reproductive growing stage and were embedded in Technovit and dissected into 7 μm sections. Blue colour indicates Fe accumulation. Young leaves (A+C) and mature leaves (B+C) were harvested and stained using the Perls stain method. **A)** Section of a stained three week-old wild type leaf. **C)** Section of a stained three week-old *nas4x-2* leaf. **B)** Section of a stained seven week-old wild type leaf. **D)** Section of a stained nine week-old *nas4x-2* leaf. Xy= Xylem; Ph= Phloem; Bar= 0,05 mm

We were able to localize the blue staining in leaf sections of *nas4x-2* (Fig. 4.4.12). The blue Fe staining was localized to the phloem of young and mature leaves of *nas4x-2* plants suggesting that NA may be needed to unload phloem Fe. This finding was surprising since Fe was transported over the long-distance in the xylem, but a

4. Results

retranslocation to the phloem must have occurred. However, since Fe accumulation resided to the phloem in *nas4x-2* leaves, we can exclude that NA is needed for xylem unloading.

4.4.3 Investigation of the crosstalk of citrate and NA

4.4.3.1 Quantitative RT-PCR of the *FRD3* gene in *nas4x-2* plants and the *NAS* genes in *frd3* plants

The re-greening of *nas4x-2* leaves with age suggested that the loss of NA might be compensated by other chelator molecules, which might overtake the role of NA in long-distance transport. Rogers and Guerinot reported 2002 in their study of *frd3* mutants a 2.0-fold increase of NA level in the xylem of *frd3* mutants, which suggested that NA might also be able to compensate reduced citrate levels. Furthermore, we detected an increased gene expression level of the *FDR3* gene in *nas4x-1* roots compared to wild type in our microarray experiment (Table A2.1 and A2.4). The striking interveinal leaf chlorosis of *nas4x-2*, which is appearing in young leaves and is decreasing with age of the leaf hints to an at least partial compensation of NA by other metal chelators. Since citrate is supposed to be the main Fe transporter in the xylem (Rellán-Alvarez et al. 2010; von Wiren et al. 1999), we hypothesized that a total loss of citrate and NA would lead to a persisting strong leaf chlorosis of the interveinal leaf chlorosis. Therefore, we have chosen *FRD3* as candidate gene to investigate this. *FRD3* mediates the citrate efflux into the xylem (Durrett et al., 2007). Hence, *frd3* mutant plants show 40 % reduced citrate levels in the xylem (Durrett et al., 2007). Since we observed an induction of *FRD3* in *nas4x-1* mutants compared to wild type plants in the gene chip experiment, we verified *FRD3* expression in RT-qPCR in *nas4x-2* mutants. Vice versa, we also determined *NAS* gene expression in *frd3* mutants. Therefore, we grew wild type plants, *frd3* and *nas4x-2* mutants in quarter strength hydroponic solution supplied with 10 μ M FeNaEDTA for five weeks under long-day conditions and harvested roots and leaves separately to analyze transcript levels of *FRD3* and *NAS* expression in *frd3* and *nas4x-2* mutants.

Indeed, *FRD3* was 11.9-fold induced in *nas4x-2* roots (Fig. 4.4.13 A), while *NAS1* was 14.3-fold, *NAS2* was 51-fold and *NAS4* was 3.6-fold induced in *frd3* roots compared to wild type plants (Fig. 4.4.13B). We could not find any changes in gene expression levels in leaves of both mutants suggesting that NA synthesis and loading of citrate to the vasculature have to be in particular compensated in the root to ensure Fe or Cu long-

4. Results

distance transport. These findings suggest that citrate and NA indeed act partially redundant.

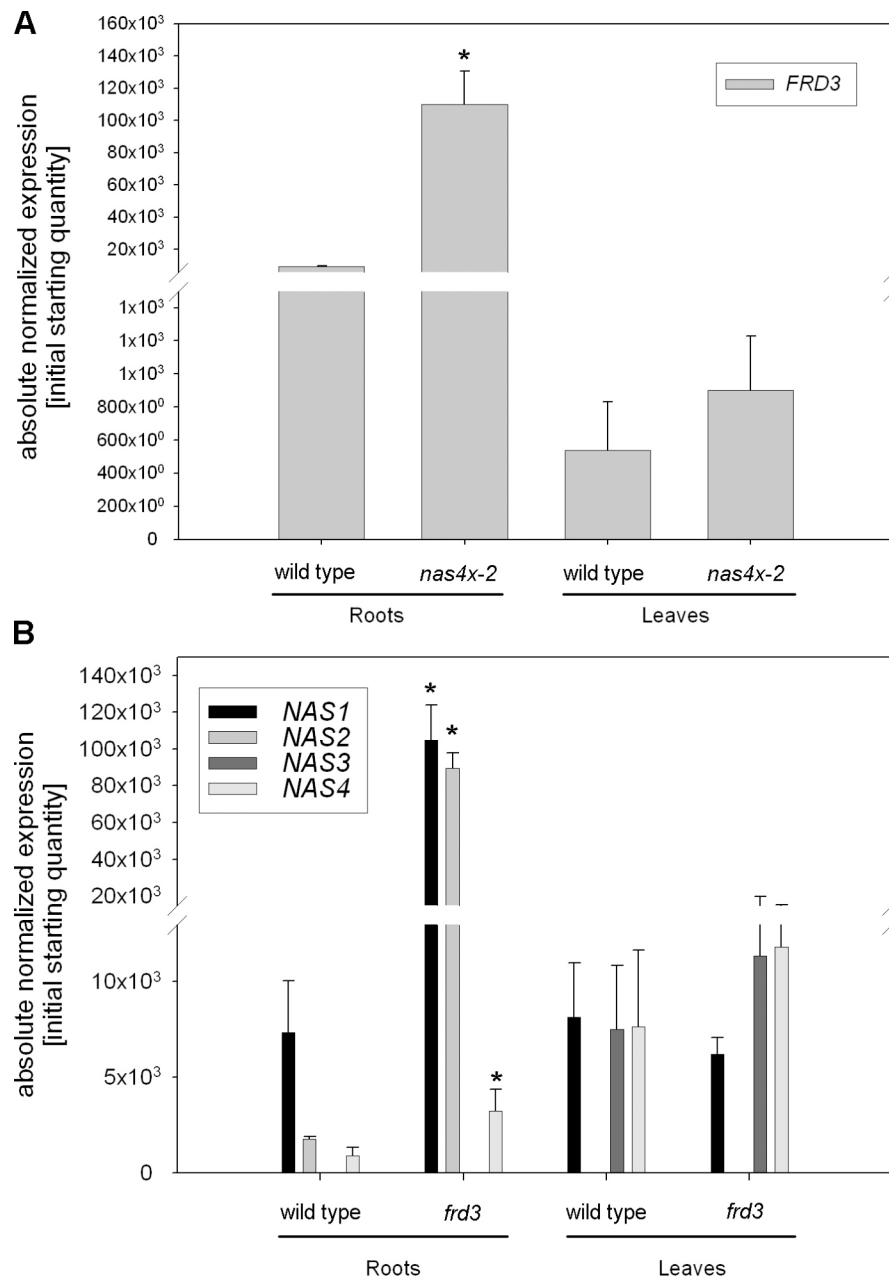


Fig. 4.4.13: Gene expression of roots and leaves of *frd3* and *nas4x-2* mutants compared to wild type plants Roots and leaves were harvested from five week-old wild type plants and seven week-old *frd3* and *nas4x-2* plants grown in a quarter strength hydroponic solution supplied with 10 μ M FeNaEDTA under long-day conditions. (n=3). **A**) Quantitative gene expression level of *FRD3* in *nas4x-2* mutant roots and leaves compared to wild type. **B**) Quantitative gene expression level of the four *NAS* genes in *frd3* mutant roots and leaves compared to wild type. * $P < 0.05$ using unpaired t-test

4.4.3.2 Generation of a quintuple mutant line

To further investigate the possible redundancy between citrate and NA, we generated a quintuple mutant mutated in the *FRD3* gene and the four *NAS* genes by crossing. The

4. Results

aim was the investigation of the consequences of loss of NA together with a strong reduction of citrate in the xylem in *frd3/nas4x-2* quintuple mutants. Because *nas4x-2* plants are completely sterile, we crossed a segregating *nas* quadruple mutant (*nas1^{-/-}2^{-/-}3^{-/-}4^{+/-}*) heterozygous for *NAS4* to the *frd3-1* mutant. *frd3* mutants accumulate high levels of Fe in the central cylinder, which can be easily stained with Perls stain (Green and Rogers., 2004). Since *frd3* mutants originated from a EMS induced point mutation and not from a T-DNA insertion, *frd3* mutants were selected by Fe stainings of the root. Homozygous *nas* mutations were selected via PCR genotyping. After selection we finally obtained in the F3 generation a homozygous quintuple mutant, termed *frd3/nas4x-2*, which are mutated in the *FRD3* gene and all four *NAS* genes. These mutants were maintained as segregating line (*frd3^{-/-}, nas1-1^{+/-}, nas2-2^{-/-}, nas3-1^{-/-}, nas4-1^{-/-}*).

4.4.3.3 Phenotypical analysis of 5x mutant in a time course experiment

First, we characterized the phenotype of the quintuple mutant, termed *frd3/nas4x-2* in a time course experiment and documented the phenotypes of *frd3/nas4x-2* mutants compared to *frd3*, *nas4x-2* mutants and wild type plants to study the effect on reduced citrate levels in the xylem together with a full loss of NA.

frd3/nas4x-2 mutants developed an interveinal leaf chlorosis, which was stronger than the chlorosis of *nas4x-2* plants (Fig.4.4.14). This chlorosis then intensified in all young leaves developed afterwards. In the reproductive stage young leaves turned almost white. During full expansion of leaves during growth, exclusively the leaf veins of *frd3/nas4x-2* mutants re-greened (Fig.4.4.14). This phenotype suggested that without NA and with less citrate in the xylem the long-distance Fe transport is disrupted. This also confirms that citrate is an important Fe chelator in the xylem. The phenotypes suggest that the loss of NA in *nas4x-2* plants could have been partially compensated by citrate. Surprisingly, *frd3* mutants showed a weaker growth than *frd3/nas4x-2* plants, which we further investigated.

4. Results

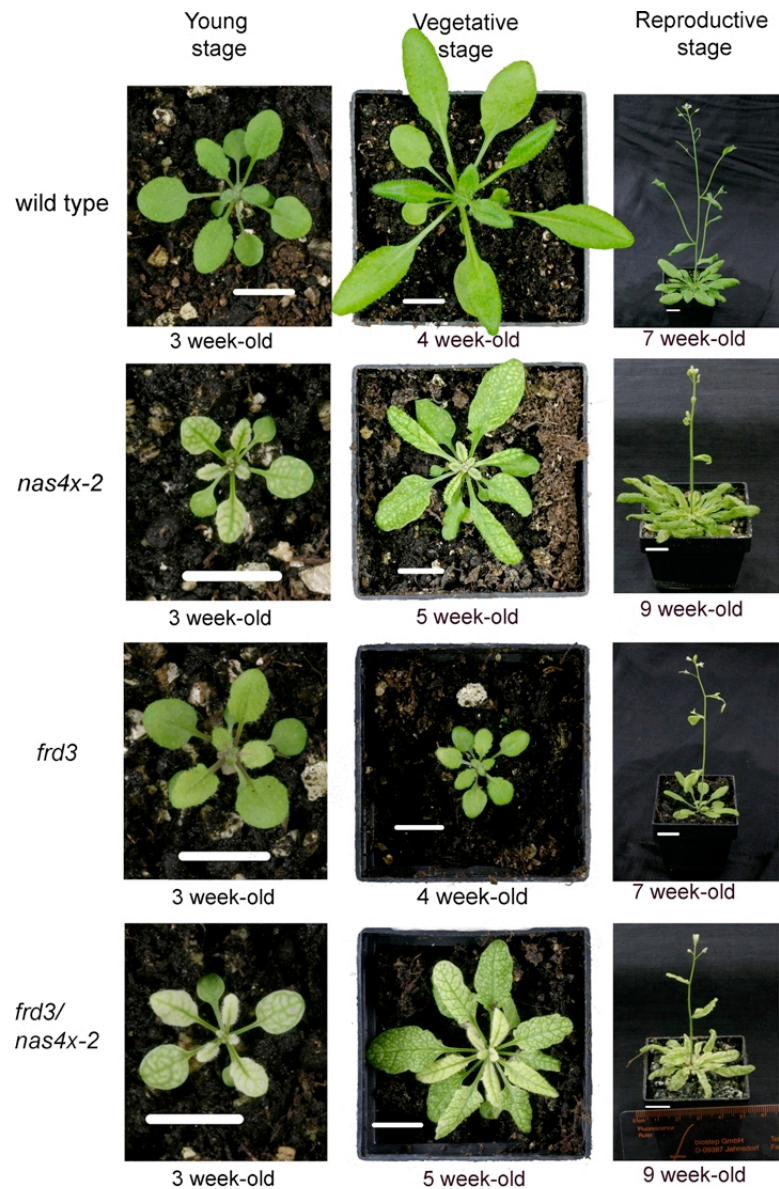


Fig. 4.4.14: Phenotypes of *frd3/nas4x-2* mutants compared to *frd3*, *nas4x-2* mutant and wild type plants

Plants were grown on soil under long-day conditions over a time course of nine weeks. *5x* = *frd3/nas4x-2* mutant; Bar = 1 cm

4.4.3.4 Metal measurement of *frd3/nas4x-2* mutants

Next, we analyzed the alteration of *frd3/nas4x-2* leaf Fe and Cu contents. Therefore, *frd3/nas4x-2*, *frd3*, *nas4x-2* and wild type plants were grown on soil. For metal determination different leaf types were harvested as described in Fig. 4.4.5 from seven week-old wild type and nine week-old *frd3/nas4x-2* and *nas4x-2* plants.

4. Results

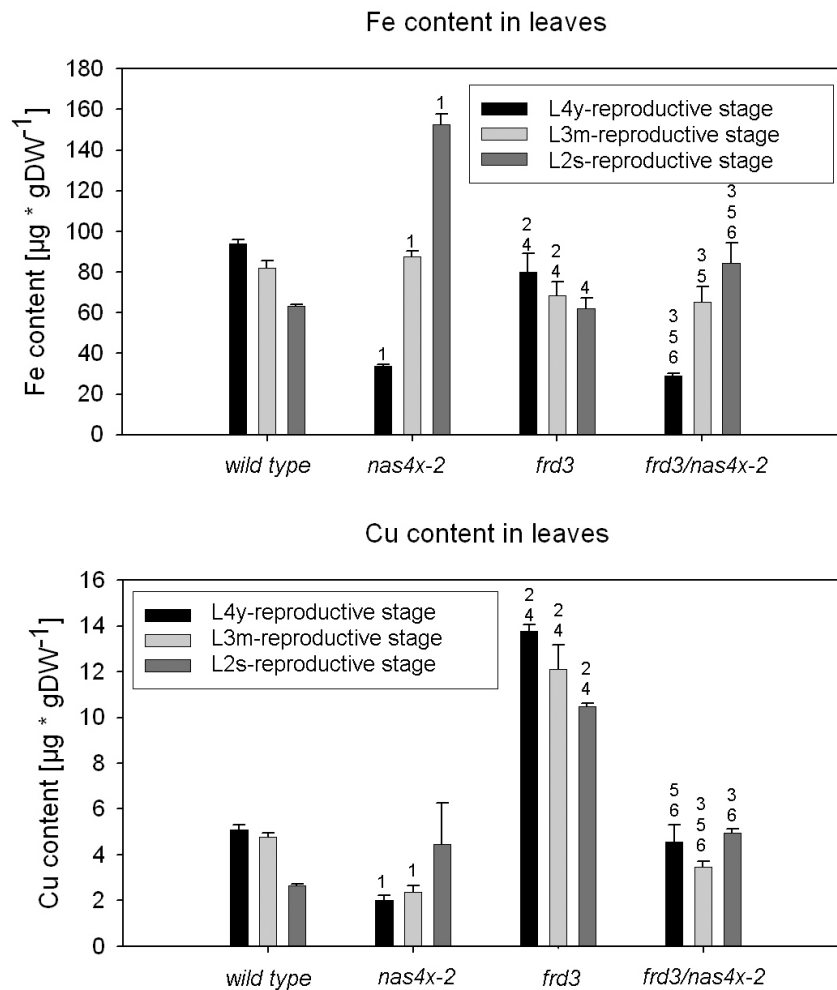


Fig.4.4.15: Metal determination in rosette leaves of *frd3/nas4x-2* mutants compared to *frd3*, *nas4x-2* and wild type plants

Leaves were harvested from soil grown plants of different growing stages (Fig. 4.4.5) under long-day conditions ($n=4$). **A)** Fe contents of *frd3/nas4x-2*, *frd3* and *nas4x-2* mutant compared to wild type. **B)** Cu contents of *frd3/nas4x-2*, *frd3* and *nas4x-2* mutant compared to wild type. Numbers 1-6 indicate a statistical significance of $P < 0.05$ of different comparisons using unpaired t-test: ¹WT/*nas4x-2*; ²WT/*frd3*; ³WT/*frd3/nas4x-2*; ⁴*nas4x-2*/*frd3/nas4x-2*; ⁵*nas4x-2*/*frd3/nas4x-2*; ⁶*frd3*/*frd3/nas4x-2*.

As expected *nas4x-2* mutants had reduced Fe contents in young leaves, slightly increased Fe contents in mature leaves and increased Fe contents in old leaves compared to wild type (Fig. 4.4.15A). As expected *frd3* mutants showed significantly reduced Fe levels in L4y and L2m leaves, while in L2s leaves there was no difference compared to wild type (Rogers and Guerinot, 2002). L4y leaves of the quintuple mutant showed reduced Fe contents compared to *frd3*, *nas4x-2* compared to wild type, slightly reduced Fe levels in L3m leaves compared to wild type and *nas4x-2* and higher Fe levels in L2s leaves compared and to *frd3* and to wild type, but a lower Fe content in L2s compared to *nas4x-2* plants. Through the reduction of citrate levels in the *frd3/nas4x-2* quintuple mutant, Fe contents, which were increased in mature *nas4x-2*

4. Results

leaves, approached to the wild type Fe content in older leaves *frd3/nas4x-2* (Fig. 4.4.15A). Young leaves of quintuple mutants had even less Fe than *nas4x-2* plants suggesting that citrate can act at least partially redundant with NA in very young leaves, but cannot fully replace its function. However, it was surprising that *frd3/nas4x-2* mutants had almost equal Fe contents than wild type plants (Fig. 4.4.15A), since we expected significantly lower Fe contents due to the additional reduction of citrate in quintuple mutants. This finding suggests further compensation of Fe transport by other chelator molecules.

As described in previous metal measurements, Cu contents of *nas4x-2* plants were reduced in L4y, L3y leaves, while no difference could be detected for L2s leaves compared to wild type (Fig. 4.3.15B). Interestingly, *frd3* mutants showed significantly higher Cu contents than wild type Cu contents in all leaf types. Cu contents of L4y leaves of the quintuple mutants were equal to the wild type Cu contents, while Cu contents turned into the middle of *nas4x-2* and *frd3* contents. L3m leaves were lower than wild type contents and higher than *nas4x-2* Cu contents. L2s leaves had higher Cu levels than wild type, lower Cu levels than *frd3* mutants and equal levels compared to *nas4x-2* mutants (Fig. 4.4.15B). It was shown that *frd3* mutants accumulate Mn in the shoot (Rogers and Guerinot, 2002), which might have toxic effects for the plant. It is possible that the increased uptake of Mn, Co and Cu in *frd3* mutants might be compensated by the additional loss of NA in *frd3/nas4x-2* mutants. In consequence, the plant has less Fe but a lower toxic metal stress in the shoot, which could be an explanation for the slight rescue effect in growth and biomass of *frd3/nas4x-2* mutants compared to *frd3* plants.

Next, we analyzed the root Fe and Cu content of *frd3/nas4x-2* mutants compared to *frd3*, *nas4x-2* and wild type plants.

4. Results

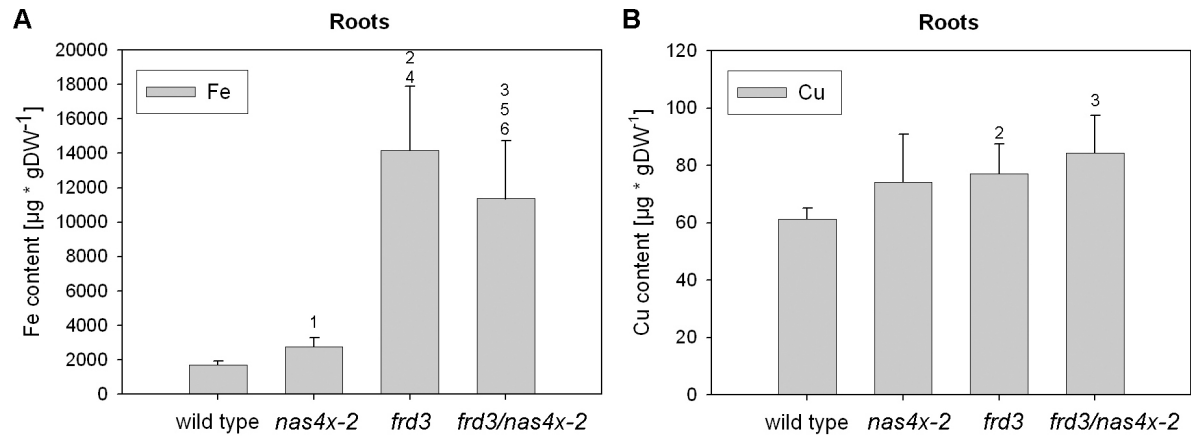


Fig. 4.4.16: Metal determination in roots of *frd3/nas4x-2* mutants compared to *frd3*, *nas4x-2* and wild type plants

Roots were harvested from plants in reproductive stage, grown in a quarter strength hydroponic solution supplied with $10\mu\text{M}$ FeNaEDTA under long-day conditions ($n=4$). **A**) Fe contents of *5x*, *frd3* and *nas4x-2* mutant compared to wild type. **B**) Cu contents of *5x*, *frd3* and *nas4x-2* mutant compared to wild type. Numbers 1-6 indicate a statistical significance of $P < 0.05$ of different comparisons using unpaired t-test: ¹WT/*nas4x-2*; ²WT/*frd3*; ³WT/*frd3/nas4x-2*; ⁴*nas4x-2/frd3*; ⁵*nas4x-2/5x*; ⁶*frd3/frd3/nas4x-2*.

As described in previous studies *frd3* mutants had significant higher root Fe contents than wild type plants (Rogers and Guerinot, 2002; Green and Rogers, 2004) (Fig. 4.4.16A). Also *frd3/nas4x-2* plants showed a significant increase in Fe content, which was slightly lower compared to *frd3* mutants. *nas4x-2* also showed slightly increased Fe levels compared to wild type. This increase of Fe in roots of all three mutants can be explained with the induced Fe uptake machinery in all mutants (FRO2, IRT1 and FIT) due to Fe deficiency sensed from leaves, which was also shown for the *frd3* mutant in (Rogers and Guerinot, 2002). The massive amount of Fe in *frd3* and *frd3/nas4x-2* plants can be explained with the combination of increased Fe uptake and decrease of Fe root-to-shoot transport due to the reduction of citrate in the xylem.

frd3 and the quintuple mutant showed slightly induced Cu contents in roots compared to wild type, but no difference when compared to the other mutants, which might also hint to a lowered Cu translocation to the shoot in the quintuple mutant (Fig. 4.4.16B).

4.4.3.5 Organic acid measurement in the xylem sap of *frd3/nas4x-2*, *nas4x-2*, *frd3* and wild type plants

To confirm whether *nas4x-2* plants indeed have increased citrate levels in xylem sap due to the increased *FRD3* levels, we measured the citrate content in the xylem sap collected from *frd3/nas4x-2*, *nas4x-2* and *frd3* mutant and wild type plants. Moreover, the *frd3/nas4x-2* mutant was found to contain similar Fe levels than *wild type mature leaves* (Fig 4.4.15A). This was surprising since citrate was expected to be an important

4. Results

factor in the compensation of the loss of NA, which was consistent with the severe chlorosis of *frd3/nas4x-2* mutants. We therefore presumed that additional Fe chelators might be present in xylem of *frd3/nas4x-2* mutants to compensate Fe transport. To determine organic acid concentration in the xylem sap of wild type, *nas4x-2*, *frd3* and *frd3/nas4x-2* mutants, plants were grown on soil until the reproductive growth stage for xylem sap collection. Xylem sap was finally collected from soil-grown seven week-old wild type and *frd3* plants and nine week-old *nas4x-2* and *frd3/nas4x-2* mutants. Citrate contents have been determined with a newly established liquid chromatography-electrospray ionization time-of-flight mass spectrometry method (HPLC-TOFMS), which enables the quantification of low molecular mass carboxylates in plant extracts (Rellan-Alvarez and Lopez-Gomollon, 2011). We also measured 2-oxoglutaric acid, malic acid and succinic acid to test if these organic acids might be able to compensate the loss of NA combined with reduced citrate levels in *frd3/nas4x-2* mutants.

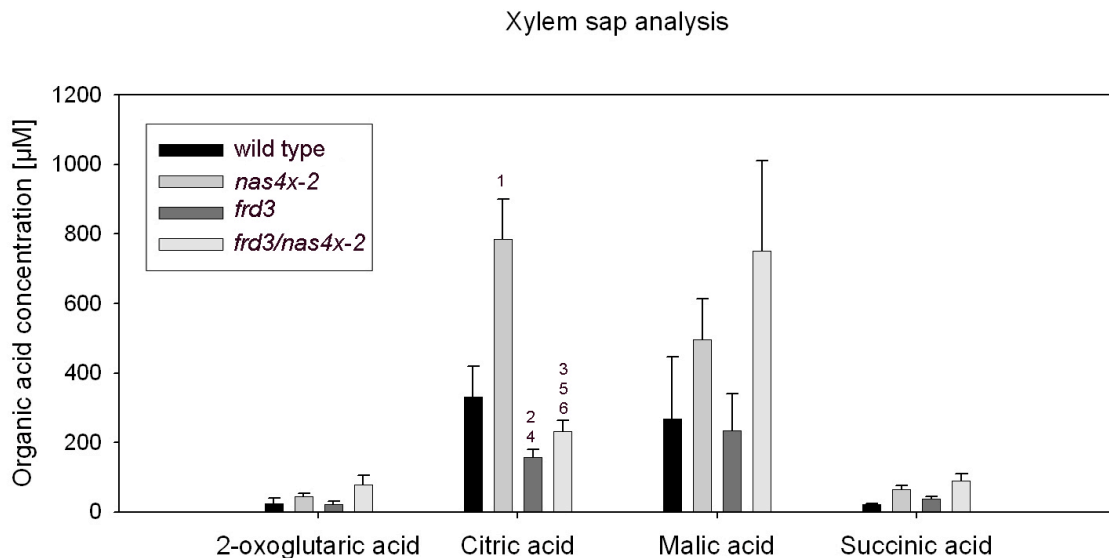


Fig. 4.4.17: Citrate contents of xylem sap of *frd3*, *nas4x-2* and *frd3* mutants compared to wild type plants

Xylem sap was collected from plants in reproductive stage, grown on soil under long-day conditions (n=5). Numbers 1-3 indicate a statistical significance of $P < 0.05$ of different comparisons using unpaired t-test: ¹WT/*nas4x-2*; ²WT/*frd3*; ³WT/*frd3/nas4x-2*.

Although measurements showed a large variability, *frd3* showed as expected a significant decrease of 32 % of citrate level compared to wild type. *nas4x-2* showed an increase of 74 % compared to wild type, which confirmed the compensatory increase of citrate in *nas4x-2* plants. The citrate level of *frd3/nas4x-2* mutants only decreased to a lower extent of only 21 % than *frd3* plants suggesting that the additional loss of NA led to an increased citrate efflux through other transporter, which might be localized to the

4. Results

pericycle. No difference could be determined for 2-oxoglutaric acid, malic acid and succinic acid indicating that these organic acids were not involved in the compensation of Fe transport in xylem of *frd3/nas4x-2* mutants.

4.4.4 Investigation of the influence of the loss of NA on reproduction

nas4x-2 plants are sterile suggesting an important role of NA in the fertilization process. *nas4x-2* flowers did not show any developmental defect like it was observed in *naat* transgenic tobacco lines, which showed strong morphological changes in flowers (Takahashi et al., 2003). The investigation of *nas4x-2* flowers showed that *nas4x-2* plants produce low amounts of pollen (Fig. 4.4.18).

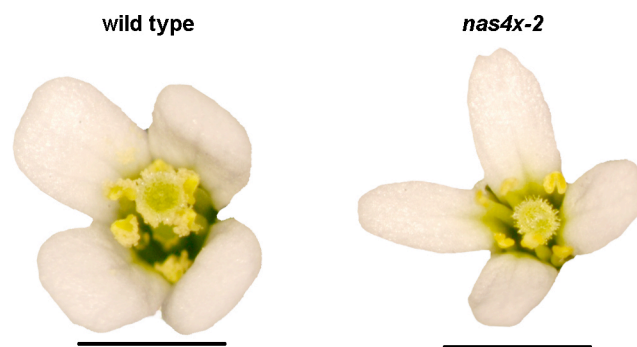


Fig. 4.3.18: Flower phenotypes of wild type and *nas4x-2* plants
nas4x-2 showed no developmental defects, but produce only few pollen.

4.4.4.1 Analysis of the long-distance metal transport of *nas4x-2* plants to flowers

First, we investigated whether the sterility in *nas4x-2* plants could be traced back to impaired Fe or Cu transport to the reproductive organs. Therefore, we determined the Fe and Cu contents of *nas4x-2* flowers compared to wild type. *nas4x-2* and wild type plants were grown on soil under long-day conditions and whole flowers were harvested from six week-old wild type plants and nine week-old *nas4x-2* plants for metal determination.

4. Results

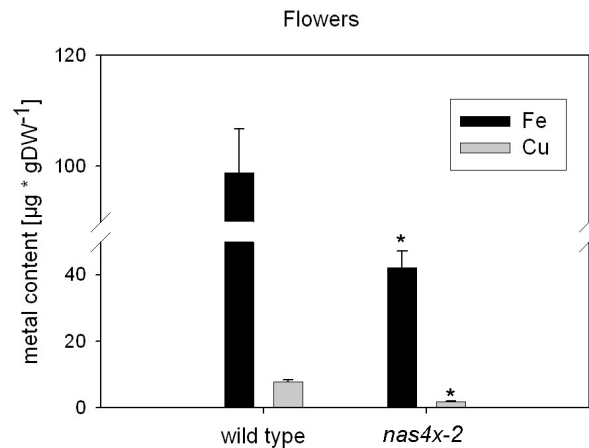


Fig. 4.4.19: Metal contents of wild type and *nas4x-2* flowers

Flowers were harvested from six week-old wild type plants and nine week-old *nas4x-2* plants grown on soil under long-day conditions (n=4). **A)** Fe contents of *nas4x-2* plants compared to wild type. **B)** Cu contents of *nas4x-2* plants compared to wild type. * $P < 0.05$ using unpaired t-test

Flowers of *nas4x-2* plants showed a significant 2.3-fold decrease of Fe and a 4.3-fold decrease of Cu compared to wild type plants which indicate that NA is needed either for the root-to-flower or the leaf-to-flower Fe and Cu translocation.

Next, we analyzed the expression of two marker genes for both Fe sufficiency and Fe deficiency in flowers of *nas4x-2* plants compared to wild type. The marker gene for Fe excess was again *FER1*. As Fe deficiency marker we used the Fe transporter *IRT1* whose expression was described before to localize to the anther filament and pollen grains (Vert et al., 2002). Since the expression of *IRT1* was reported to appear exclusively upon Fe deficiency (Vert et al., 2002) we assessed *IRT1* as physiological marker for Fe deficiency in flowers. To study the expression of both marker genes, we have grown wild type plants for six weeks and *nas4x-2* plants for nine weeks on soil under long-day conditions. Since we expected a difference in expression pattern before and during pollination we harvested floral buds (unpollinated) and open flowers (post-pollinated) separately and measured gene expression of *IRT1* and *FER1* using RT-qPCR.

4. Results

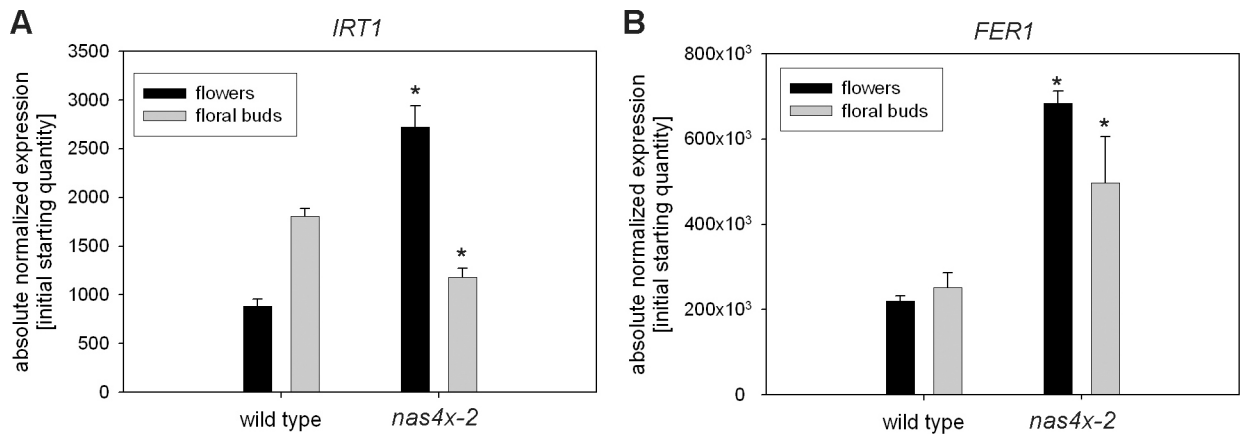


Fig. 4.4.20: Gene expression of floral buds and open flowers of *nas4x-2* compared to wild type plants Inflorescences were harvested from six week-old wild type plants and nine week-old *nas4x-2* plants grown on soil under long-day conditions (n=3). **A)** Quantitative gene expression level of *IRT1*. **B)** Quantitative gene expression level of *FER1*. * $P < 0.05$ using unpaired t-test

Interestingly, *IRT1* showed a repression in pollinated flowers of wild type plants while its expression increased in *nas4x-2* plants indicating that the Fe deficiency increases during pollination in *nas4x-2* plants (Fig. 4.4.20A). Contradictory, *nas4x-2* flowers showed also induction of *FER1* in floral buds and open flowers (Fig. 4.4.20B). These results show that despite of the reduced Fe content in *nas4x-2* flowers, which we demonstrated before (Fig. 4.4.19), flowers might suffer from oxidative stress caused by the loss of NA.

To further localize Fe deficiency and Fe excess coupled with an oxidative stress response within the flower, we analyzed gene expression of *IRT1* and *FER1* in floral organs: sepals, petals, carpels and stamina. We grew wild type plants for six weeks and *nas4x-2* plants for nine weeks on soil under long-day conditions and harvested the four floral organs for gene expression analyses (Fig. 4.3.21).

IRT1 transcripts were present in carpels and showed a 3-fold induction in carpels of *nas4x-2* plants compared to wild type indicating that *nas4x-2* carpels were not supplied adequately with Fe (Fig. 4.3.21). *FER1* expression was induced in sepals (5.9-fold) and carpels (2.5-fold) and was highly induced (7.4)-fold) in stamina of *nas4x-2* plants compared to wild type, which suggests an altered distribution of Fe in *nas4x-2* flowers compared to wild type flowers, whereas particularly stamina might suffer from oxidative stress (Fig. 4.3.21).

4. Results

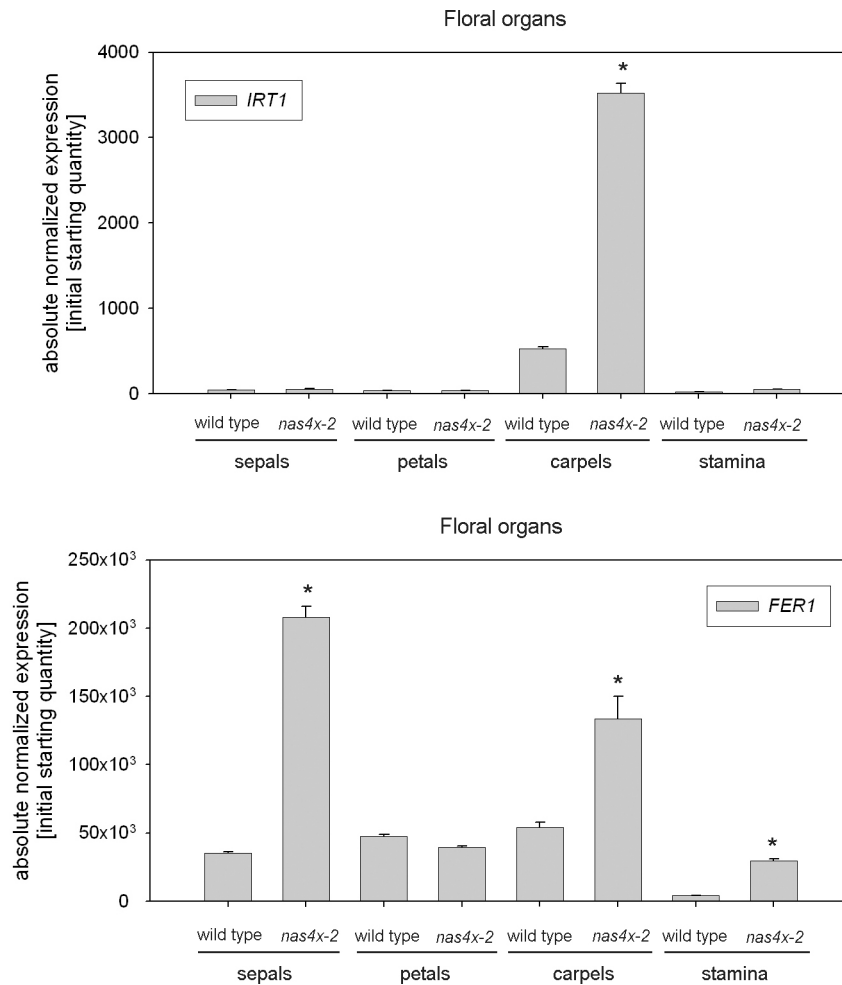


Fig. 4.3.21: Gene expression of floral organs: sepals, petals, carpels and stamina of *nas4x-2* compared wild type plants using RT-qPCR. Floral organs were harvested from six week-old wild type plants and nine week-old *nas4x-2* plants grown on soil under long-day conditions (n=2). **A)** Quantitative gene expression level of *IRT1*. **B)** Quantitative gene expression level of *FER1*. * $P < 0.05$ using unpaired t-test

To further test in which floral organs NA might be needed for the Fe or Cu transport and to test whether NA might be synthesized in flowers or synthesized in lower parts of the plants and transported upwards in a complex with metals, we analyzed gene expression levels of all four *NAS* genes of floral buds, open flowers and the four floral organs in wild type plants.

Only *NAS3* was expressed in flowers of wild type plants, and its expression increased during pollination suggesting a higher Fe or Cu demand during pollination (Fig. 4.4.22A). Within the flower *NAS* expression could be localized to the leaf-like floral organs sepals and petals suggesting a spatial separation of NA synthesis and place of activity. It might be possible that NA is synthesized in the vascular tissue of petals and

4. Results

in particular green sepals, which might have a special importance in the direct supply of carpels and stamina by remobilizing Fe to transport it to the reproductive floral organs.

Next, we analyzed gene expression levels of the three *YSL* genes in floral buds, open flowers and floral organs in *nas4x-2* plants compared to wild type since *YSL1* and *YSL3* are predicted to be important in metal unloading from vascular tissue to supply reproductive organs (Chu et al., 2010).

YSL2 showed a 19-fold induction in open flowers and a 11-fold induction in floral buds in *nas4x-2* plants compared to wild type (Fig. 4.4.22). *YSL3* indicated a 7.3-fold induction in open flowers and a 13.5-fold induction in floral buds of *nas4x-2* compared to wild type. *YSL1* was not significantly induced in floral buds and only 1.3-fold induced in open flowers. To localize the expression of the *YSLs* within the flower, we also analyzed the expression in floral organs. *YSL2* was induced in all floral organs, whereas *YSL3* was induced in petals and carpels but repressed in sepals and stamina. Changes in *YSL1* expression in *nas4x-2* compared to wild type could be neglected. *YSL2* was 10.2-fold induced and *YSL3* was 3.6-fold induced in petals, while *YSL2* (19.3-fold induction) and *YSL3* (44.4-fold induction) showed the highest induction in carpels. *YSL2* showed a 2.3-fold induction, whereas *YSL3* showed a 3.6-fold repression in stamina of *nas4x-2* plants compared to wild type. These results hint to a special importance of NA-dependent metal transport within these organs and confirm the specificity and spatially separated activity of the three different *YSL* genes. *YSL1* might be repressed in sepals and petals to guide up-coming Fe via the transpiration stream to the carpels and stamina, whose metal supply is most important for successful reproduction. *YSL2* and *YSL3* might be important for unloading of Fe from the vascular tissue while only *YSL2* seemed to mediate the Cu or Fe transport, respectively to stamina. Since *YSLs* are upregulated upon + Fe (DiDonato et al., 2004; Le Jean 2005; Schaaf et al., 2005; Waters et al., 2006). Since Fe might accumulate particularly in phloem of *nas4x-2* plants, which is supported by the high induction of *FER1* in carpels (4.4.21B), *YSL2* and *YSL3* are presumably responsible for phloem unloading of Fe in carpels of *nas4x-2* plants. However, it is also possible that *YSLs* are not only involved in Fe-NA transport but also in the Cu-NA transport within the flower, since Cu is particularly needed for pollen production (Azouaou and Souvire 1993; Sancenón et al. 2004).

4. Results

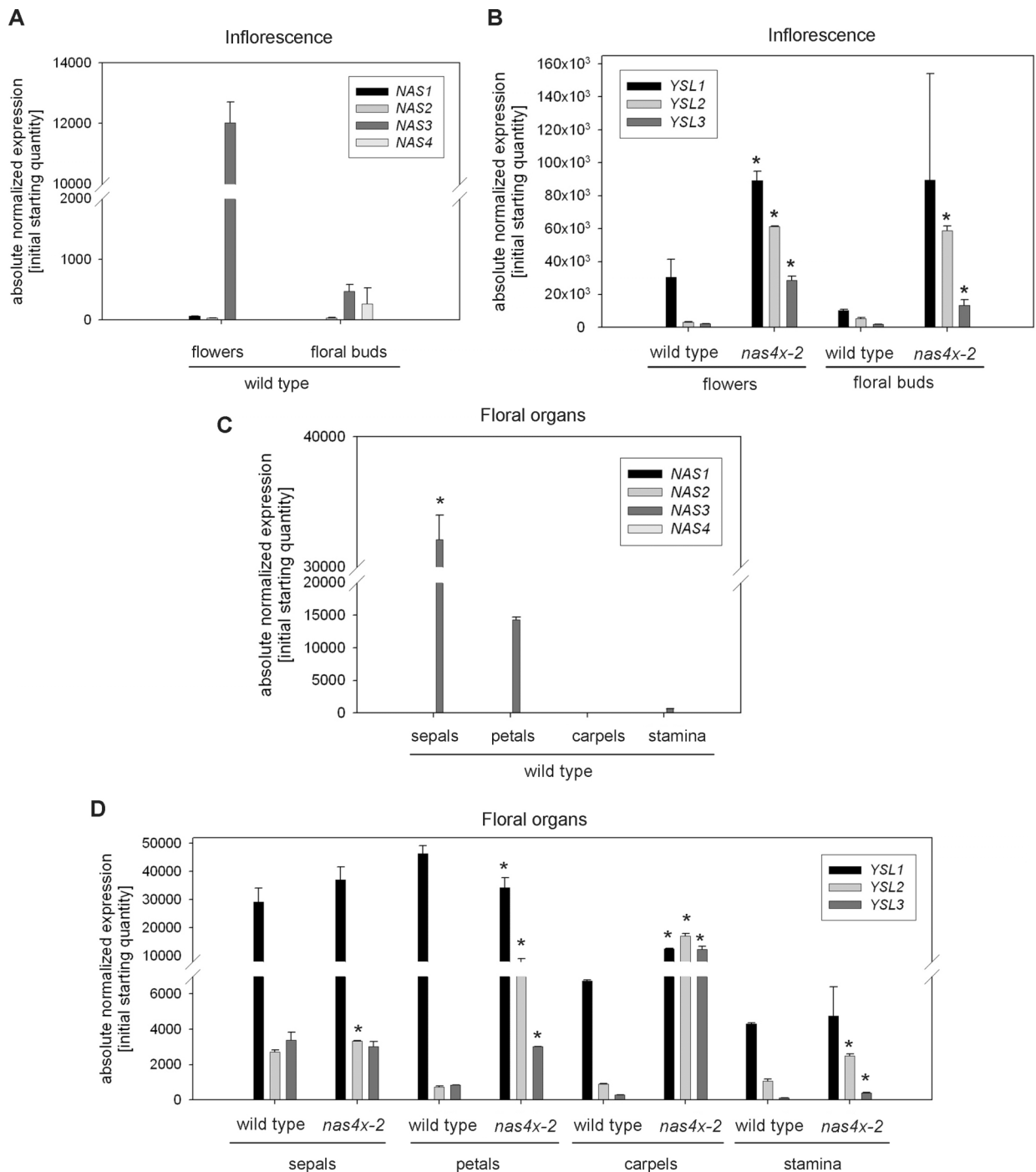


Fig. 4.4.22: Gene expression of floral buds, open flowers and floral organs: sepals, petals, carpels and stamina of *nas4x-2* compared wild type plants using RT-qPCR. Floral organs were harvested from six week-old wild type plants and nine week-old *nas4x-2* plants grown on soil under long-day conditions (Floral buds and flowers n=3; floral organs n=2). **A)** Quantitative gene expression levels of the four *NAS* genes in floral buds and open flowers. **B)** Quantitative gene expression level of *YSL1*, *YSL2* and *YSL3* in floral buds and open flowers. **C)** Quantitative gene expression levels of the four *NAS* genes in the four floral organs. **D)** Quantitative gene expression level of *YSL1*, *YSL2* and *YSL3* in the 4 floral organs. * $P < 0.05$ using unpaired t-test.

It remained unclear if the sterility of *nas4x-2* plants was due to a NA defect NA in the female reproductive tissues of the pistil or the loss in the male tissues of anthers that produce pollen. To further investigate this we performed reciprocal crosses with *nas4x-*

4. Results

2 and wild type plants (wild type x *nas4x-2*; *nas4x-2* x wild type). Crossings were repeated in both directions 20 times. No siliques developed, so that fertilization was not possible which suggests that NA has to be maternally and paternally supplied for successful reproduction.

To further test whether the pollen of *nas4x-2* was able to germinate on the *nas4x-2* and on wild type pistils after pollination, we performed an aniline blue stain on pollinated stigmas to assess the degree of pollen germination (Fig. 4.4.23). The cross of *nas4x-2* x *nas4x-2* with aberrant pollen gave no signal.

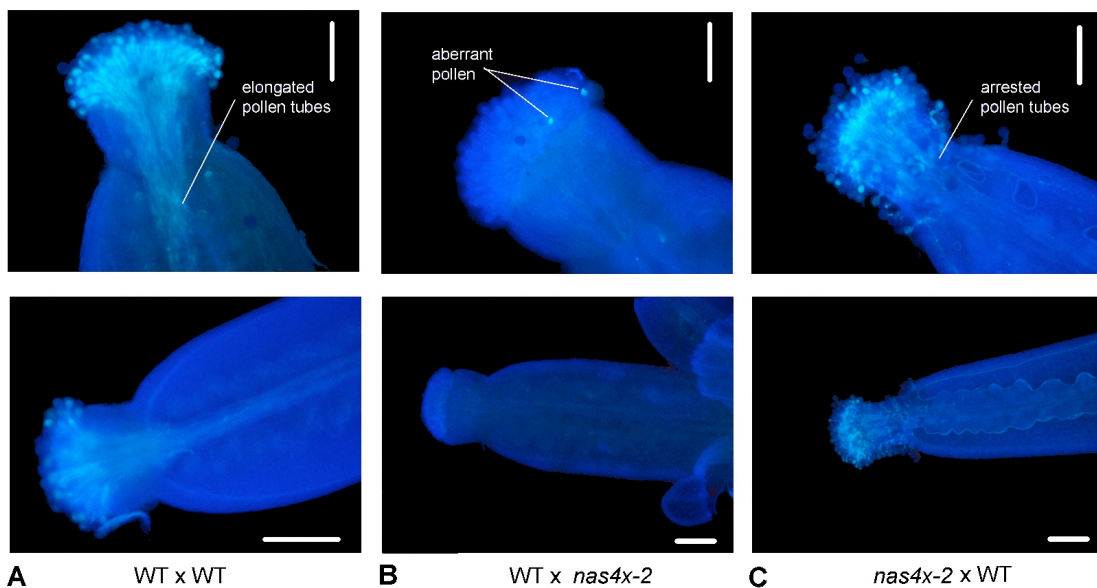


Fig. 4.4.23: Pollen germination was visualized under the UV light after aniline blue staining

A) As a control wild type pollen has been crossed to wild type plants (WT x WT). **B)** *nas4x-2* pollen were crossed to wild type plants (WT x *nas4x-2*) and **C)** wild type pollen were crossed to *nas4x-2* plants. Aniline blue germination assay has been performed 24 h after crossing. The crossings were repeated in three independent studies yielding to the same result. Bar= 500 μ m

In the wild type control (WT x WT) (Fig. 4.4.23A) pollen germination was visible as the simultaneous elongation of multiple pollen tubes through the pistil towards the ovule. The pollination of aberrant *nas4x-2* pollen on the wild type pistil (WT x *nas4x-2*) showed that only very few pollen grains were present which were not able to germinate (Fig. 4.4.23B). Interestingly, the pollination of *nas4x-2* pistils with wild type pollen (*nas4x-2* x WT) showed that wild type pollen germinated but then were arrested after about 20 μ m in the style tissue. The pollen tubes were not able to penetrate further through the pistil towards the ovules. Thus, we can conclude that NA has to be maternally provided to enable pollen tube penetration through the pistil. Furthermore, NA has to be paternally provided for proper pollen production and germination.

4. Results

4.4.4.2 Analysis of pistil tissues of *nas4x-2* and wild type plants

Previous findings of the pollen germination assay revealed that wild type pollen was arrested in a distinct area in the pistil of *nas4x-2* plants. We hypothesized that this area of the pistil has to be supplied by NA-Fe and the loss of NA might lead to a stop of pollen tube penetration. In order to investigate whether the Fe distribution was changed in this region of the pistil, we performed Perls stains of *nas4x-2* pistils compared to wild type plants. For Perls stain we dissected un-pollinated pistils from closed floral buds.

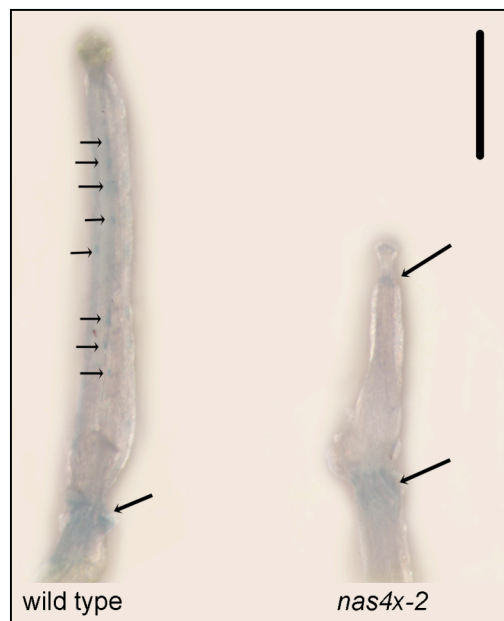


Fig. 4.4.24: Fe accumulation in pistils of un-pollinated wild type and *nas4x-2* plants

Plants were grown on soil under long-day conditions. Pistils were dissected from floral buds and stained using Perls stain method. Arrows point at the blue staining. Bar= 1mm

The more intensive blue staining of wild type pistils compared to *nas4x-2* confirmed a reduction of the overall Fe content in pistils of *nas4x-2* plants compared to wild type pistils. Moreover, it revealed that the Fe distribution in pistils was indeed altered in *nas4x-2* mutants compared to wild type plants. The Fe accumulation in wild type pistils was concentrated on small dots distributed over the whole pistil (Fig. 4.4.24). These areas presumably indicate the location of ovules, which probably have a high Fe demand after pollination. Furthermore, we indeed observed a blue staining below the stigma, exactly in the position where wild type pollen tube elongation was stopped in *nas4x-2* pistils. In both, wild type and *nas4x-2* Fe accumulated also in the stem below the pistil which could represent an area of active Fe transport into the pistil.

4. Results

Next, we concentrated on the examination of *nas4x-2* pistils in order to find an explanation for the elongation stop of pollen tubes in the specific region of *nas4x-2* pistils. We assumed that developmental changes occurred in *nas4x-2* pistils, which might have led to the abortion of pollen elongation. To test this idea, we analyzed cross-sections over the entire length of wild type and *nas4x-2* pistils.

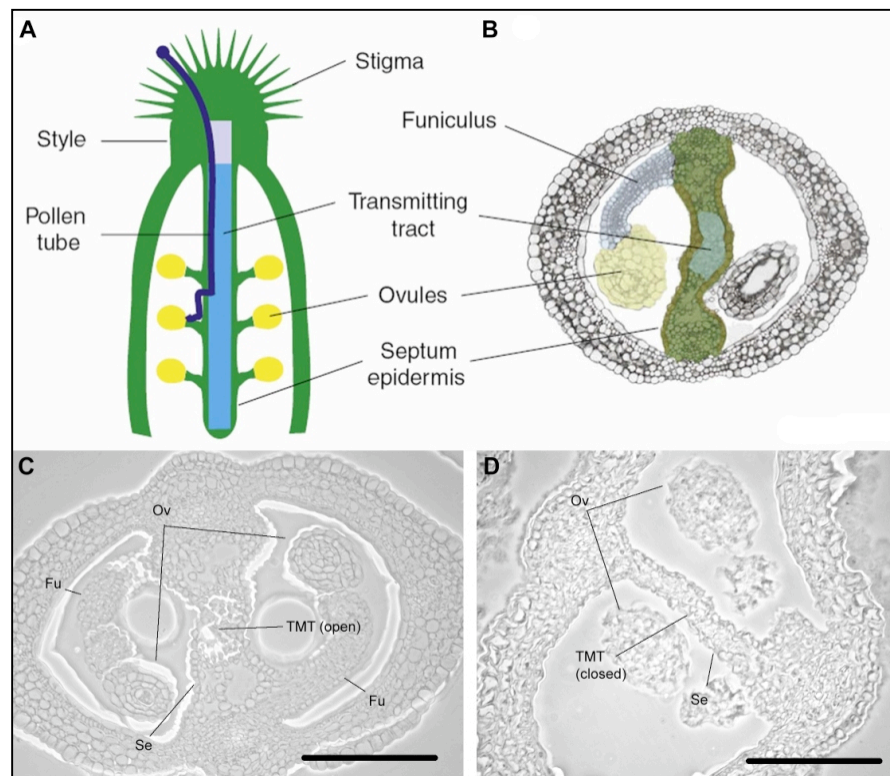


Fig. 4.4.25: Tissue specific differences in pistils of wild type and *nas4x-2* plants

Upper part of the figure explains the structure of the Arabidopsis pistil (Crawford and Yanofsky, 2008). **A)** Scheme of longitudinal section of the Arabidopsis pistil indicating the female reproductive tract. **B)** Cross-section of an Arabidopsis pistil indicating tissue of the reproductive tract and the ovule **C)** Cross-section of a wild type pistil, **D)** Cross-section of a *nas4x-2* pistil. Bar = 0.125 mm

The analysis revealed striking changes in sections of *nas4x-2* plants compared to wild type sections. The tissues, known collectively as the female reproductive tract, consist of stigma, style, transmitting tract and funiculus (Fig. 4.4.25A and B) within the carpel, were altered in *nas4x-2* mutants. The transmitting tract is involved in facilitating pollen tube movement and has been proposed to have multiple roles in guidance, nutrition, defense and adhesion (Lord et al., 2002). To facilitate the pollen growth through the style to the ovary chamber, cells of the transmitting tract induce developmentally regulated cell death which enables the pollen tube to migrate to the ovary (Brian C W Crawford and Martin F Yanofsky 2008). In our experiment, we could observe this degradation of the cells of the transmitting tract in sections of wild type carpels (Fig.

4. Results

4.4.25C), whereas in *nas4x-2* the transmitting tract remained closed (Fig. 4.4.25D). This finding could explain the abortion of pollen tube movement within the style of *nas4x-2* plants. It is likely that cells of the transmitting tract have to be supplied with NA-Fe complexes to be able to induce cell death.

5. Discussion

The small chelator molecule NA was just recently shown to have a great enhancing effect on bioavailability of Fe in Caco-2 cells (Zheng et al., 2010). Therefore NA is a novel and potent promoter of Fe bioavailability and may potentially be used as a biofortifying target compound in staples and in food fortificants to improve Fe utilization by resource-poor people in the developing world. This study contributes to a better understanding of NA function in metal homeostasis which forms the basis to achieve this long-term aim. This study shows that complete loss of NA resulted in a *chloronerva* phenotype, namely in severe chlorosis and sterility. Analysis of the NA-free Arabidopsis mutant *nas4x-2* revealed functions of NA in the long-distance transport of Fe to young leaves and in the long-distance movement of Cu to leaves and the inflorescence. Moreover, we discovered an important role of NA in the lateral removal of Fe from phloem in young growing tissues like young leaves and reproductive organs. Due to its ability to unload Fe from phloem, NA is furthermore involved in the remobilization of metals from senescing leaves for the long-distance translocation to the inflorescence. Furthermore, we demonstrated that citrate is able to partially compensate the loss of NA in leaves. The knock-down mutant *nas4x-1*, that had residual NA still allowed the plants to complete their life cycle and produce seeds. The obtained results with NA-reduced *nas4x-1* plants showed that NA is required for seed Fe loading.

5.1 Investigation of the NA-free mutant *nas4x-2* revealed distinct functions of NA in metal homeostasis

5.1.1 NA is needed for the phloem-dependent root-to-leaf Fe transport in young leaves, while its loss can be partially compensated by citrate

The full elimination of *NAS* gene activity finally resulted in a *chloronerva*-like phenotype of *nas4x-2* plants. To elucidate the role of NA in the long-distance circulation of metals we first asked why the strong interveinal leaf chlorosis in *nas4x-2* plants is only appearing in young leaves and decreases with age of the leaf. The metal measurements indicated that young leaves of *nas4x-2* plants had less Fe, while mature and old leaves had increased Fe contents. This clearly hints to different Fe translocation routes to young and to older leaves. A recent study of Tsukamoto et al. (2009) in barley

5. Discussion

provided evidence that young leaves receive Fe primarily from phloem, while older leaves receive Fe from xylem. Furthermore, the differentiation of xylem might be slower than that of phloem, which could explain that young leaves and apical meristems are mostly fed by the phloem and the provascular tissues (Curie et al., 2009). However, another explanation for the phloem-dependent Fe transport could be the insufficient transpiration of young leaves, although xylem is already fully developed. The interveinal leaf chlorosis in young leaves of *nas4x-2* therefore indicates that NA function is needed in the phloem-dependent long-distance transport from roots to young leaves. It is also possible that NA functions as ferry to load Fe to the iron transport proteins (ITP) which might then mediate the long-distance transport in the phloem (Krüger et al., 2002) (section 1.2.4.3.1). Nevertheless, NA is not needed for the long-distance transport to mature leaves, which is most probably xylem-dependent. This brought us to the question whether citrate indeed mediates xylem-dependent transport in Arabidopsis, which has been shown in tomato plants (Rellan-Alvarez et al., 2010). We hypothesized further that citrate can partially overtake the function of NA, since long-distance transport of *nas4x-2* mutants is impaired, but mature leaves have even elevated Fe levels compared to wild type. As model plant to investigate citrate-dependent xylem transport, we used *frd3* mutants, which show a 40 % reduced citrate content in the xylem (Rogers and Guerinot, 2002; Green and Rogers, 2004). FRD3 encodes for a transporter mediating the efflux of citrate into xylem (Durrett et al., 2007). Already in our microarray study of *nas4x-1* plants we found an induction of *FRD3* (Table A2.1; A2.4) in *nas4x-1* roots compared to wild type roots under Fe supply conditions. In RT-qPCR we confirmed an elevated *FRD3* expression in roots of *nas4x-2* plants (Fig. 4.4.13A) and vice versa an elevated *NAS1*, *NAS2* and *NAS4* expression in roots of *frd3* plants (Fig. 4.4.13B). We determined also that citrate levels in *nas4x-2* mutants were 74 % increased compared to wild type plants. In the study of Rogers and Guerinot (2002) the authors also claimed that *frd3* mutants contained increased NA levels. We concluded from these findings that the two long-distance transport mechanisms via citrate and NA might complement each other. To prove our hypothesis *in planta* we generated and analyzed the quintuple *frd3/nas4x-2* mutant. Due to reduced citrate levels and fully eliminated NA levels the *frd3/nas4x-2* mutant suffered from a more severe leaf chlorosis in young leaves intensifying in all younger leaves produced later on in the development (Fig. 4.4.14). Contrary to *nas4x-2* whose leaves fully re-greened with age, *frd3/nas4x-2* leaves exclusively showed a re-greening of their veins during their

5. Discussion

development, while young leaves produced later on in the development turned almost white. Furthermore, metal measurements of leaves showed that Fe accumulation like in *nas4x-2* leaves disappeared in mature leaves of *frd3/nas4x-2* mutants (Fig. 4.4.15A). However, due to the severe leaf chlorosis we were surprised that Fe levels of old leaves were similar to wild type Fe levels. Thus we assume that residual citrate levels are able to accomplish the Fe transport to mature leaves. Another explanation would be that other metal chelators might overtake the compensation of Fe transport in *frd3/nas4x-2* mutants which has to be further investigated.

Further effects could be observed in *frd3/nas4x-2* plants. We found that *frd3* single mutants accumulate Cu in leaves, while *nas4x-2* leaves have less Cu in leaves compared to wild type plants. This Cu accumulation also disappeared in leaves of *frd3/nas4x-2* mutants (Fig. 4.4.15B). Interestingly, *frd3/nas4x-2* mutants suffered from severe chlorosis, but their growth seemed to be less impaired than the growth of *frd3* single mutants (Fig. 4.4.14). This effect could be caused by increased compensatory NA in *frd3* mutants, which might lead to an enhanced root-to-shoot transport of Mn (Green and Rogers, 2004). Perhaps toxic amounts of Mn in the shoot of *frd3* mutants cause the impaired growth, which obviously disappears in *frd3/nas4x-2* mutants through the additional elimination of NA. We therefore conclude that the additional elimination of NA rescued the impaired growth of *frd3* mutation. These findings have to be confirmed with Mn determination in shoots of *frd3/nas4x-2* mutants compared to *frd3* and *nas4x-2* plants. Thus, the combination of these multiple mutations led to an enhancement of the phenotypes occurring in parental lines, but also to new phenotypical effects in *frd3/nas4x-2* mutants due to altered metal distribution throughout the plant.

All in all, NA is required for the long-distance Fe transport of Fe to young leaves, while its function can be partially compensated by citrate in the long-distance Fe transport. However, the impaired phloem translocation of Fe and Cu to reproductive organs cannot be compensated by citrate, since this effect causes the sterility of *nas4x-2* plants.

5.1.2 NA is required for phloem unloading in young leaves and for proper phloem loading in mature leaves

The increased Fe levels in mature leaves of *nas4x-2* could be explained with the enhanced Fe deficiency response in roots. Like in *chloronerva*, *nas4x-2* plants showed a constitutively induced Fe deficiency response (Fig. 4.4.8) leading to elevated Fe uptake

5. Discussion

and translocation to leaves. The question remained where exactly the Fe deficiency is sensed, which subsequently induces the Fe uptake system, since mature leaves even have higher Fe levels than wild type plants. It is possible that the Fe deficiency signal derives from chlorotic intercostal areas in leaf mesophyll cells. We therefore hypothesized that the short-distance intercellular Fe transport from the vascular tissue to the mesophyll cells might be disturbed in *nas4x-2* plants. Therefore we performed Fe stains of young, middle age and old leaves and found Fe unequivocally accumulated in phloem of all *nas4x-2* leaves types (Fig. 4.4.11). It was surprising that Fe already accumulated in young leaves which even showed significantly reduced Fe levels compared to wild type. In case young leaves are indeed provided with phloem-Fe, while mature leaves become supplied with xylem-Fe (Tsukamoto et al. 2009) we concluded from this finding that NA functions in phloem unloading of Fe in young leaves. But although older leaves become served with xylem-Fe we observed that Fe accumulation intensified with age of the leaf. Thus, NA might also function in the unloading of Fe from the phloem during remobilization process of metals which might enter xylem tissue for the long-distance transport to the inflorescence. This would also explain that Fe levels are highest in senescent leaves since Fe which should usually be mobilized to the inflorescence persists in older leaves. NA is presumably not needed for the switch from xylem to phloem. In an experiment with ^{59}Fe we applied the isotope on leaves of *nas4x-2* plants to investigate the recovery of the isotope to inflorescences of *nas4x-2* plants. Surprisingly, we detected the radioactivity all over the shoot after 2 h (data not shown). Considering the fact that Fe is also able to enter the xylem and reach the upper shoot parts directly over the apoplast by entering leaf cell walls, diffusion through plasmodesmata straight into the xylem stream (Rellan-Alvarez et al., 2010; Konrad Mengel, 7. Band), we could not prove whether Fe remobilization via phloem to reproductive organs is functioning in *nas4x-2* plants. It is also possible that citrate partially takes over the function of NA in the remobilization process. To address this question, remobilization studies with ^{59}Fe could be repeated with the quintuple *frd3/nas4x-2* mutants. Therefore, the question whether NA is needed for the remobilization of Fe out of leaves during flower development and senescence has to be further investigated. Surprisingly, recent publication reported an accumulation of Fe in the xylem of peach leaves (*Prunus persica*) in response to Fe deficiency (Abadía et al. 2011). The Fe accumulation in the leaf mid rib and veins was already earlier shown in Fe deficient peach (Jiménez et al. 2008) and tomato plants (Tomasi et al. 2009) and was

5. Discussion

called „the Fe-chlorosis paradox“. This phenomenon could not be explained yet. We could not detect Fe accumulation in wild type leaves and we also did not perform Perls stain of Fe deficient wild type leaves. It might be possible that Fe-deficient wild type plant concentrate essential micronutrients to the main veins of xylem upon stress conditions in order to maintain the most important processes like reproduction upon stress conditions. This might be comparable to the stress reaction in the human organism, which reacts with a detraction of the blood stream from the periphery and a concentration to the main veins in order to maintain brain and heart supply under stress conditions. It is possible that Fe deficient plants require NA to transport Fe from mesophyll cells to phloem and subsequently to xylem. This might also be an explanation for the Fe accumulation in phloem of *nas4x-2* leaves.

However, in the work of Abadia et al. (2011) the blue staining was enhanced using a not quantitative intensification method, since the accumulation was presumably too weak to detect it with the Perls stain method alone. It is also arguable whether Arabidopsis is comparable with a three leaf peach.

Due to significantly reduced Fe contents in flowers of *nas4x-2* plants, long-distance metal transport to the inflorescence must be impaired, although the long-distance transport to mature leaves was intact. We considered also the possibility that the reduced Fe content in flowers was due to reduced transpiration of *nas4x-2* plants compared to wild type plants. We hypothesized that the fertilization in the wild type situation might lead to a sink-to-source switch of leaves, so that fertilized flowers become the main sink, accompanied by an increased transport from roots to flowers via xylem. Thereby green and senescing leaves change from sink to source for micronutrients which might be transported via the phloem to the flowers. We therefore measured the transpiration rates of *nas4x-2* plants compared to wild type and another sterile mutant, named *agamous*, but we could not detect any difference between the sterile mutants and wild type (data not shown) indicating that the impaired Fe supply of flowers in *nas4x-2* plants was not due to reduced transpiration. Moreover, the analysis of xylem sap (Fig. 4.4.15) showed equal levels of succinic, malic and 2-oxoglutaric acid between which points to a normal transpiration rate of all tested mutants. We deduced from these results that transpiration rates were similar in the mutants compared to wild type plants, which means that NA must be required for proper Fe and Cu translocation to reproductive organs.

5. Discussion

Next, we investigated whether the short-distance of metal transport could be impaired in *nas4x-2* plants. Therefore, we analyzed the expression patterns of *YSL1*, *YSL2* and *YSL3*, which are supposed to mediate the lateral transport of metal-chelator complexes from and to the vascular tissue (Curie et al., 2009). In case YSL proteins are indeed competent in NA-metal transport, there are several possibilities for their functions: They could participate a) in the unloading of metals from the xylem sap through the uptake from phloem parenchyma cells, b) in the loading of phloem sieve tubes via uptake by phloem-associated cells, c) in the loading of phloem sieve tubes from leaf mesophyll cells or d) in the exchange of metals between xylem and phloem (Curie et al., 2009). We additionally assumed that the unloading of phloem sieve tubes to mesophyll cell in young leaves might function via YSL transporter. The subclass of *YSL1*, *YSL2* and *YSL3* genes is usually repressed about 2-fold by Fe deficiency and induced by Fe excess (Didonato et al. 2004; Le Jean et al., 2005; Schaaf et al., 2005; Waters et al., 2006) in order to block Fe exit in older plant parts and roots to enhance Fe transport to younger plant parts. Consistently to the general Fe accumulation in phloem of *nas4x-2* plants (Fig. 4.4.11) we detected a deregulation of the three YSL genes in *nas4x-2* compared to wild type. YSLs which act in the unloading of phloem Fe might sense Fe accumulation in the phloem of *nas4x-2* plants and were in consequence induced in young leaves of *nas4x-2* plants (Fig. 4.4.10; 5.1) like e.g. *YSL2*. Due to its expression pattern *OPT3* is also a putative candidate for the unloading of Fe-NA complexes from phloem in young leaves (Fig. 5.1). YSLs which act in the unloading of metals from the xylem sap might be induced in mature leaves like *YSL1* and *YSL3*, whereby NA is not involved. Due to the intensive Fe accumulation in the phloem of mature *nas4x-2* leaves, the loading of phloem sieve tubes from leaf mesophyll cells seems to be intact in mature *nas4x-2* leaves. Thus, YSLs involved in this process might be repressed or not differentially regulated in mature leaves of *nas4x-2* plants. *YSL1* and *YSL3* were just recently shown to be important in the remobilization of Fe out of senescing leaves in grafting studies of Chu et al. (2010). Consistent to this, we found an induction of *YSL1* and *YSL3* in older leaves of *nas4x-2* plants compared to wild type plants indicating that *YSL1* and *YSL3* might be involved in a possible switch from phloem to xylem for the uptransport to the inflorescence (Fig. 5.1). Moreover, expression data available from genevestigator indicate the highest *NAS3* expression in senescing leaves of wild type plants. These finding strongly suggests a role of NA in the remobilization of Fe from leaves to the developing flowers. Arrived in the inflorescence metals presumably again undergo a

5. Discussion

xylem-to-phloem switch in not-transpiring organs or tissues like anthers and seeds which are not directly connected with xylem (Fig. 5.1). YSL1 and YSL3 might be needed in the inflorescence to unload metal-NA complexes from phloem. We postulate that NA has, like YSL1 and YSL3, dual roles in reproduction (Chu et al., 2011): Its presence in leaves is required for normal fertility and presumably normal seed development due to its function in the remobilization of metals out of leaves, while its activity in the inflorescence itself is required for proper loading of metals into the developing pollen before pollination and proper loading into the ovaries and seeds after pollination (Fig. 5.1).

5.1.3 Successful reproduction requires NA for pollen production and cell death in female pistil tissue

Due to the sterility of *nas4x-2* plants we asked how the loss of NA affects the fertilization process in the male tissue of the anthers and the female tissue of the pistil. Besides general reduced Cu and Fe levels in *nas4x-2* plants we observed that pollen production was strongly impaired in *nas4x-2* plants and residual pollen failed to germinate (Fig. 4.3.18). A similar derogation could be found in *ysl1ysl3* double mutant and we additionally observed an altered *YSL1* and *YSL3* expression pattern in flowers of *nas4x-2* plant compared to wild type plants. This corroborates the necessity of NA for proper Cu-NA or Fe-NA to the anthers, where Fe and Cu are needed for pollen production (Azouaou and Souvre, 1993; Sancenon et al., 2004). In pollen germination assay we observed that wild type pollen arrested in the style of the *nas4x-2* pistil (Fig. 4.4.23).

We were also able to detect Fe accumulation exactly in the area of the *nas4x-2* styles where pollen arrested as well as at the base of the pistil (Fig. 4.4.24). To investigate whether the sterility was due to affected metal distribution in carpels we did expression studies of the carpel. Interestingly, *YSL2* and *YSL3* were highly induced (*YSL2*: 19.3-fold compared to wild type; *YSL3*: 44.4-fold compared to wild type) in carpels of *nas4x-2* compared to wild type plants suggesting that *YSL2* and *YSL3* are responsible for phloem unloading of Fe in carpels. This high induction further implicates that nutritional stream arriving in the flowers might be concentrated on the female reproductive tissue which would still enable cross-pollination, in case the plant is not able to produce its own pollen. This would also explain the Fe accumulation at the base of the pistil. Also *FER1* and *IRT1* were induced in carpels, which on one hand could

5. Discussion

indicate an impaired Fe distribution coupled with oxidative stress as well as a Fe deficiency situation in a certain tissue. In wild type plants *IRT1* expression only occurs under Fe deprived conditions in anthers (Vert et al., 2002). With the ectopic expression of *IRT1* in carpels, *nas4x-2* plants presumably try to compensate reduced Fe import into the carpel. On the other hand it is possible that the enhanced production of ferritin might execute a temporary sink effect on Fe, which might lead in consequence to a local Fe deficiency and to the induction of *IRT1*. This phenomenon has also been reported in the study of van Wuytswinkel et al. (1999). The authors observed an elevated Fe accumulation in leaves accompanied by a Fe deficiency response in transgenic tobacco lines overexpressing ferritin cDNA from soybean.

All, in all, the expression studies strongly hint to a particular requirement of NA in the carpels' metal supply. To further analyze the pistil tissue of *nas4x-2*, we produced cross sections of the *nas4x-2* pistil and compared it to wild type pistils. The analysis of cross-sections of *nas4x-2* and wild type pistils indeed showed a striking difference in the development of the female reproductive tract, since *nas4x-2* plants failed to form the transmitting tract (Fig. 4.4.25D). The style connects the stigma to the ovary chamber and can vary in length in different plant species (Fig. 4.4.25A+B). In lily, for example, the style is very long and has an open structure, whereas, in Arabidopsis, it is short and closed. In Arabidopsis, the transmitting tract begins within the style at the stigma-style boundary and extends to the base of the ovary (Crawford and Yanofsky, 2008). The transmitting tract is involved in facilitating pollen tube movement and has been proposed to have multiple roles in guidance, nutrition, defense and adhesion (Lord et al., 2002). Studies on tobacco (Wang et al., 1996) and Arabidopsis (Crawford et al., 2007) have shown that death and degeneration of these transmitting-tract cells is important for pollen tube movement. Interestingly, only one mutant is known so far, which is defective in the breakdown of cells in the transmitting tract, namely *ntt*. The *NO TRANSMITTING TRACT (NTT)* gene encoding for a zinc finger transcription factor is specifically expressed in the transmitting tract and has recently been shown to be required for the formation of the transmitting tract (Crawford et al., 2007). *ntt* mutants are defective in extracellular matrix ECM production and in developmentally regulated cell death that normally occurs to open the transmitting tract. EMC is a complex mixture of polysaccharides, glycoproteins and glycolipids, which is possibly providing nutrients for pollen tube growth. Interestingly, *ntt* mutants are like *nas4x-2* not able to form a transmitting tract through programmed cell death (PCD). However, *ntt* mutants

5. Discussion

produce 60 % less seeds compared to wild type, but are still fertile. Pollen tubes of *ntt* mutants only reach the apically localized ovaries, whereas the basal ovaries remain unfertilized. Conclusively, the generation of the transmitting tract induced by PCD seems not to be essential for successful fertilization (Crawford et al., 2007). But how can we explain the aborted pollen tube growth in the style of *nas4x-2* plant? It is possible that NA-dependent Fe delivery to this tissue has to be enhanced to induce PCD on one hand or there is a special need of metal-NA complexes for pollen tube growth. Since transmitting tract only facilitates and accelerates the pollen tube growth, but is not essential for it, it is more likely that NA-dependent Fe transport is important to supply pollen tube with nutrients, since pollen tubes are also able to grow *in vitro* on a matrix (Kim et al., 2006) and do not necessarily need the transmitting tract. The reason for the loss of transmitting tract formation in *nas4x-2* plants might be that distinct amounts of Fe are needed for the formation of ROS to induce PCD (Swidzinski et al., 2004; Carlini et al. 2006).

Yet, we could not prove, whether the reduced Fe supply in the female tissue of *nas4x-2* was due to defective phloem unloading like in leaves. We indeed managed in a preliminary experiment to detect a Fe accumulation located to the phloem within the *nas4x-2* pistil. But unfortunately we were not able repeat this result due to technical problems (not shown). Presumably this Fe accumulation exclusively concentrates on the phloem of the style tissue and is therefore difficult to find among numerous sections of the whole pistil.

Nevertheless, we suggest that the defect in pollen production and the arrest of pollen tube growth in the style were due to the impaired phloem unloading of metal-NA complexes in specific areas of the reproductive organs of *nas4x-2* plants.

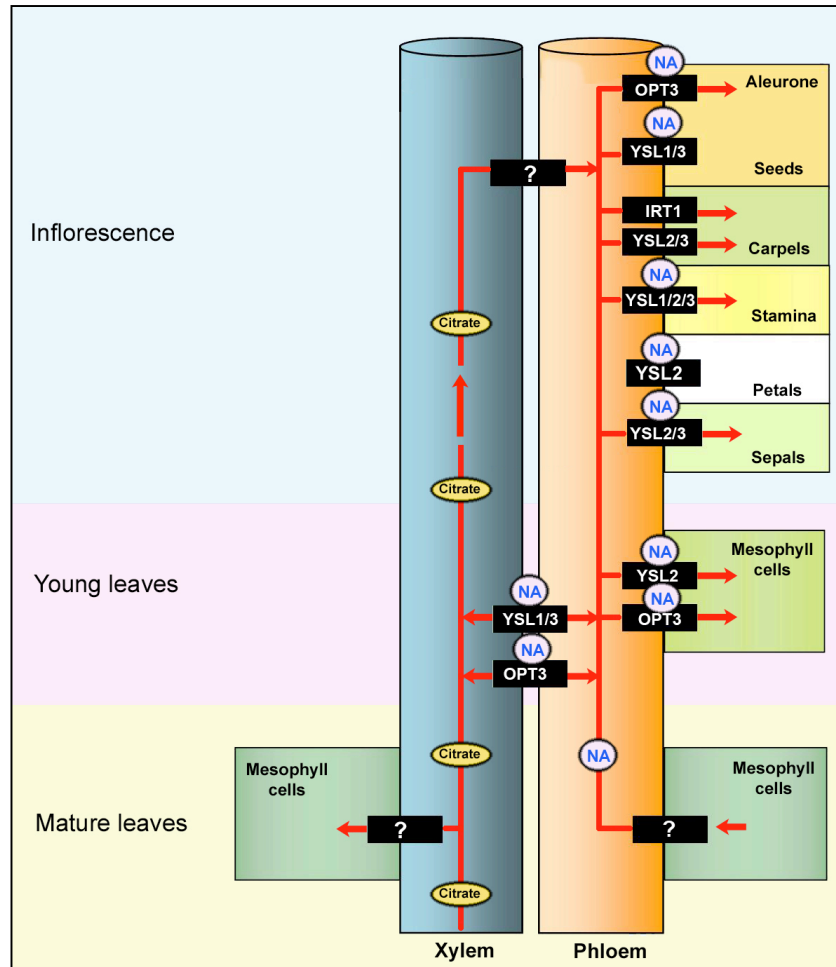


Fig.5.1: Scheme of hypothetical NA-dependent Fe transport

Fe (red stream) enters the xylem in the root pericycle and gets bind to citrate. Mature leaves are supplied with Fe via xylem in a NA-independent manner. Young growing leaves need a xylem-to-phloem exchange and are supplied by phloem-Fe, which is NA-dependent. The remobilization of Fe from mature leaves and the phloem-dependent transport to the inflorescence are NA-dependent. Fe can probably switch between phloem and xylem for the long-distance transport, but the import into stamena, carpels and seeds is presumably mediated by the phloem, which is NA-dependent, but can probably be compensated by other Fe transporters like IRT1, for example. Specific YSL and the OPT3 transporter, located in the different plant tissues surrounding the vasculature, were attributed to distinct phloem loading or unloading processes based on expression analysis.

5.1.4 NA has an essential function in root-to-shoot translocation of Cu

The results of Cu measurements of roots, all different leaf types and flowers clearly demonstrated that one of the main disorders of *nas4x-2* plants concerns the long-distance transport of Cu. Like *chloronerva* (Pich et al., 1994; Pich and Scholz, 1996), leaves of *nas4x-2* plants suffer from severe deficiency (Fig. 4.4.7). The induction of the copper transporter *COPT2* (Table A2.2) observed in the microarray experiment of the *nas4x-1* mutants, although they are not fully NA-depleted, is an additional indicator for reduced Cu long-distance transport. Also the induction of *ZIP4* encoding for a putative Cu transporter in roots of *nas4x-1* plants compared to wild type detected in the

5. Discussion

microarray study (Table A2.2) might be an additional indicator for an increased Cu uptake system in response to Cu deficiency in the shoot and due to reduced NA levels. ZIP4 is transcriptional upregulated by Cu and is able to transport Cu in yeast (Wintz et al. 2003). The strongest reduction rate of Cu contents compared to wild type plants could be observed in flowers of *nas4x-2* plants. These findings are consistent with the reduced Cu root-to shoot translocation rates in *chloronerva* (Pich and G Scholz 1996). Supported by the fact that Cu-NA complexes are completely stable at the pH of the phloem and the xylem sap (von Wiren et al., 1999 and Rellan-Alvarez et al., 2008) our results are largely in favour of a direct role of NA in the root-to shoot translocation of Cu via the xylem sap.

5.1.5 NA is needed for subcellular distribution of Fe

Studies on tomato plants utilizing Fe imaging techniques and immuno-histochemical localization of NA (Pich et al., 1997 and 2001), pointed to a role of NA in maintaining Fe in a soluble and available form under control conditions. NA is presumably also involved in the Fe detoxification mechanism by sequestering Fe into the vacuole. The study with anti-NA antibodies on the tomato cultivar Bonner Beste under control conditions showed that most of the labelling was cytosolic, whereas in Fe-overloaded plants a strong labelling of the vacuoles could be detected in electron dense protein-rich structures (Pich et al., 2001). This shift of NA from the cytosol to the vacuole upon Fe excess conditions indicates that NA may play an important role in the detoxification of excess Fe by chelation and sequestration into the vacuole.

The situation in older leaves of *nas4x-2* might mimic a Fe overload situation since the root uptake machinery is constantly on and Fe is constitutively loaded into the leaves via xylem. This could be the explanation for the strong increase of the Fe excess and oxidative stress marker *FER1* (Fig. 4.4.9), which was repressed in young leaves of *nas4x-2* and highly induced in old leaves. Other oxidative stress marker, like superoxid dismutases *CSD1*, *CSD2* and *CCS* (Table A.2.2; A2.5), have been detected in the genechip experiment of *nas4x-1* leaves. This may indicate that Fe presumably exists in an unbound form in the cytosol when NA is not present, which may cause oxidative stress.

5.2 Supportive analysis of *nas4x-1* mutants combined with previous findings demonstrate the requirement of NA for seed Fe loading

(Klatte, Schuler et al., 2009)

At the beginning of this work we concentrated on the analysis of the knock-down mutant *nas4x-1* that had residual NA. Remaining NA contents in *nas4x-1* still allowed the plants to complete their life cycle and produce seeds. Therefore, *nas4x-1* was useful to investigate NA function in the late reproductive stage. Previous results reported reduced Fe contents in seeds of *nas4x-1* plants and residual 60 % of wild type NA seed contents (Dissertation Marco Klatte, 2008). Due to the chlorosis which is primarily occurring in *nas4x-1* leaves in reproductive stage, we asked whether NA is still present in leaves of vegetative stage and primarily disappeared in reproductive stage. We found that rosette leaves of the reproductive stage did not have any NA, whereas during the vegetative stage *nas4x-1* leaves contained a residual NA content of 12 % relative to the wild type's NA content. We deduced from these findings that NA had disappeared from the rosette leaves after the turn to reproductive stage and was no longer replaced through synthesis or transport into the leaves which implicates that NA is essential for a normal Fe supply of seeds. The findings in *nas4x-1* plants are consistent with our results obtained with *nas4x-2* plants, indicating dual roles of NA in the plant: Its presence in leaves is required to mobilize leaf metals to the developing seed, while its activity in the inflorescence itself is required for proper loading of metals into the developing pollen before pollination and proper loading into the ovaries and seeds after pollination. The removal of NA out of leaves in reproductive stage of *nas4x-1* plants and the sterility of *nas4x-2* plants suggest a priority function of NA in the inflorescence, while its function in leaves might be partially compensated by citrate and other metal chelators.

The removal of NA in leaves of reproductive stage presumably led to a phloem accumulation of Fe in leaves as observed in the *nas4x-2* mutant. Thus, the interveinal leaf chlorosis primarily occurred in leaves of reproductive stage, when older leaves of reproductive stage start to accumulate Fe. The question remained why did the *nas4x-1* mutants increase Fe acquisition during the reproductive phase while Fe accumulated in leaves? Previous systemic signaling studies of a number of mutants had suggested that systemic Fe deficiency signals must exist that derive from leaves and that regulate Fe acquisition in the root (Enomoto et al. 2007; Grusak and Pezeshgi 1996; Wang et al.

5. Discussion

2007; Vert et al. 2002). As discussed above, *nas4x-2* leaves showed signs of Fe sufficiency but also of Fe deficiency. In both mutants we detected an elevated Fe acquisition response, which could be explained due to a Fe deficiency signal. Some cells or compartments of *nas4x-1* plants indeed suffered from Fe deficiency since the Fe acquisition system of *IRT1*, *FRO2* and *FIT* was induced during reproductive stage (Fig.4.4.8). However, *nas4x-1* plants had elevated Fe levels in leaves compared to wild type, which primary occurred during reproductive stage. But this Fe obviously did not reach leaf target mesophyll cell, which probably suffer from Fe deficiency and subsequently send Fe deficiency signals to the roots, which in consequence continuously take up Fe.

Expression data of the comparative microarray analysis of the *nas4x-1* transcriptome compared to wild type also indicated that *nas4x-1* plants might sense different Fe status in roots and leaves. We detected an induction of Fe deficiency marker genes like *IRT2* (G Vert, J F Briat, and C Curie 2001) (Table A.2.1; A2.2; A.2.4; A2.5) in the root as well as the induction of Fe excess or oxidative stress marker genes like *FER3* (Ravet et al., 2009) in leaves of *nas4x-1* plants. Furthermore, *NRAMP3* was induced, which is an indicator for increased Fe mobilization from intracellular Fe stores in the vacuole (Lanquar et al., 2005). The differential expression of these Fe homeostasis marker genes, together with the detection of altered Fe distribution in *nas4x-2* leaves, confirms that NA is required for proper Fe allocation in leaves. Another explanation for the induction of Fe acquisition in roots could be the high demand for Fe in the plants. Very interestingly *BHLH100*, *FRO3* and *IRT1* were shown to be induced in flowers and siliques in previous study (dissertation Marco Klatte, 2008) and *IRT1* was shown to be induced in flowers of *nas4x-2* plants (Fig. 4.4.20), showing that these organs not only had low Fe levels but also responded to that. It is possible that due to reduced NA-Fe transport in flowers and siliques, alternative routes for Fe uptake were switched on based on *FRO3/IRT1*. Perhaps these reproductive organs with their Fe deficiency were capable of producing a systemic signal that overruled the potential Fe sufficiency of leaves so that they acted as sink organs for Fe.

Conclusively, the investigations of *nas4x-1* knock-down mutants were advantageous in particular with respect to answering the question on the role of NA in Fe seed loading (published in Klatte, Schuler et al., 2009).

5.3 NAS4 has an individual function upon Fe deficiency

Gene expression studies of the collection of multiple *nas* mutants indicated that *NAS* genes act in a functionally redundant matter, since the enzyme product NA is a mobile compound in the plant. Despite the redundancy, individual *NAS* enzymes have gained specific properties, for example due to differential gene expression patterns such as in different tissues and by regulation through metal supply. While it was known that *NAS1* and *NAS4* are expressed in roots and leaves, *NAS3* is expressed in leaves and *NAS2* expression is restricted to roots, we could show that the only *NAS* gene expressed in the inflorescence was *NAS3*, while its expression could exclusively be detected in leaf-like parts of the flower like sepals and petals (Fig. 4.4.22) indicating that the inflorescence has its own NA production. Since *nas* triple mutants showed similar NA levels all *NAS* isoforms contribute to the synthesis of the same amount of NA in leaves (Fig. 4.3.1). Whether NA contents of other plant parts are also similar in the different triple *nas* mutants has to be further investigated. However, results of the effect of Fe deficiency on single and multiple *nas* mutants demonstrated an individual function of *NAS4*, since all mutants harboring a mutated *nas4-1* allele were more susceptible to Fe deficiency than others (Fig.4.3.3). Previous study already reported a particular importance of *NAS4* in Ni detoxification. Moreover, *NAS4* was induced in response to high levels of Cd in a microarray experiment (van de Mortel et al., 2006). These findings strongly suggest a particular function of the *NAS4* enzyme in providing tolerance to Ni and Cd and Fe deficiency.

5.4 Transcriptome analysis by GeneTrail revealed regulation of functional categories in response to alterations of iron homeostasis in *Arabidopsis thaliana* (Schuler et al., 2011)

In this work we mined comparative *Arabidopsis* transcriptome data and identified differentially regulated functional categories and pathways using the web-based tool GeneTrail. By performing Gene Set Enrichment Analysis (GSEA) of eight meaningful pairwise comparisons between leaf and root, *nas4x-1* mutant versus wild type samples, in response to + vs. – Fe, respectively, we were able to characterize phenotypes at cell biological level, at whole-organism physiological level and with respect to metal

5. Discussion

homeostasis. 258 differentially expressed genes were identified from the eight meaningful pairwise comparisons. By Over-Representation Analysis (ORA) of these pre-selected genes we could determine which plant physiological categories were mostly affected by Fe supply and *nas4x-1*. With our analysis we aimed to test the use of GeneTrail for plant specific analysis. Moreover, we present an outline that guides researchers through microarray analysis with the aim of identifying regulated functional categories of genes in plants.

5.4.1 Confirmation of molecular phenotypes by GSEA, and identification of differentially expressed categories

GSEA of general biochemical and cell biological categories demonstrated that roots and leaves of wild type plants had reacted with similar strength to – Fe. 26 and 31 categories in total were differentially regulated in wild type roots and leaves, respectively, between + and – Fe. This number of enriched categories was higher than that of any comparisons involving *nas4x-1* samples. Multiple reasons may have accounted for differential regulation of these categories. Regulation of the category might indicate an adaptation to Fe deficiency stress such as for example defense responses. Alternatively, the lack of Fe as a cofactor for specific enzyme activities may have led to deregulated gene expression of these enzymes due to feedback control, such as for example oxidoreductase activity, nitrate and amino acid metabolism. The lowered photosynthetic activity at – Fe may also have caused extensive metabolic changes for production of anaerobic energy as represented for example by carbohydrate and energy categories.

The lowest numbers of differentially regulated categories were detected between roots – Fe, *nas4x-1* vs. wild type, and leaves + Fe, *nas4x-1* vs. wild type. We conclude from these numbers of regulated categories that + Fe *nas4x-1* mutant root cells had approximated the cellular status present in – Fe wild type roots, while + Fe *nas4x-1* mutant leaf cells had reacted closest to those of + Fe wild type cells. These findings correlated well with our previous analysis of the *nas4x-1* mutant. Based on our previous investigation of Fe content, regulation of Fe deficiency genes, *YSL2* transporter and ferritin genes we had proposed that the lack of nicotianamine had caused increased Fe deficiency responses in the root, but Fe deficiency and sufficiency responses in the leaves (Klatte, Schuler et al., 2009). Although the comparison of the numbers of regulated cell biological categories was meaningful to us, the exact nature of these categories was not suitable for finding overlaps in regulatory patterns between different

5. Discussion

samples. Due to this lack of overlaps we were not able to represent the results in Venn diagrams. One possible explanation for this puzzling finding could be that the cell biological categories contained mostly rather few genes so that the diversity of categories was high. Perhaps if the high number of general categories derived from KEGG, GO, TRANSFAC and TRANSPATH was reassembled into areas each comprising several of the categories more overlap in regulatory patterns may become apparent, e.g. through assembly of individual pyrimidine, purine and nucleoside metabolism into a large nucleoside/nucleotide metabolism category, or of individual leucine, tyrosine, etc. categories into a large N metabolism category.

Interestingly, the above conclusion about the cell physiological status of mutant and wild type situations was not possible when analyzing MapMan plant physiological categories. In those cases, a low number of differentially expressed categories were found for the comparison of wild type, + vs. – Fe, whereas the highest number was revealed in the comparison of – Fe, *nas4x-1* vs. wild type. A reason could be that the enriched plant physiological MapMan categories had represented adaptations to + or - Fe, mutant or wild type at whole organ level rather than at cellular level, such as for example stress responses. On the other hand, the MapMan categories comprised plant-specific categories like plant hormone metabolism and regulation which could be made responsible for conferring adaptations at cellular level so that cellular differences became more or less apparent.

GSEA with a nearly complete metal homeostasis category showed that in all meaningful pairwise comparisons, between + and – Fe, wild type and *nas4x-1* samples, metal homeostasis was found affected. The metal homeostasis category contained many genes involved in metal transport or metal regulation assembled from studies reporting mainly their up-regulation in response to – Fe. From the observation that this category was found induced in wild type - vs. + Fe in roots and in leaves we can deduce that indeed the metal homeostasis category was an indicator for Fe deficiency responses. In all root comparisons of *nas4x-1* vs. wild type and of – Fe vs. + Fe this category was induced and hence the *nas4x-1* mutant status of roots can be considered Fe-deficient, in agreement with the above findings on cell biological categories and the previous findings reported (Klatte, Schuler et al., 2009). On the other hand, we have previously determined that *nas4x-1* leaf cells showed partially signs of Fe deficiency and partially of Fe sufficiency. This was reflected by the observation that in the comparisons of leaf samples the metal homeostasis category was found induced and repressed, respectively.

5. Discussion

Only from GSEA results of MapMan and the metal homeostasis categories we were able to construct meaningful Venn diagrams that revealed overlaps in regulatory patterns between the different samples. In roots and partially in leaves (under – Fe vs. + Fe) and at + Fe (*nas4x-1* vs. wild type) we found induction of the biotic stress category, indicative of an adaptation to avoid pathogen infection under – Fe. Carbohydrate metabolism was also affected in multiple pairwise comparisons indicative of altered sugar utilization due to reduced photosynthesis at - Fe. In leaves, photosystem regulation was apparent as major regulated category. Hence, the metal homeostasis, biotic stress, root carbohydrate and leaf photosystem categories were the main targets for regulated changes in response to – Fe and *nas4x-1*.

5.4.2 Identification of major regulated categories among differentially expressed genes using a combination of ORA and GSEA

The above discussed GSEA results might have masked regulated categories if they contained few differentially regulated genes but a high number of unregulated genes. To circumvent this potential obstacle we identified from our transcriptome data all genes that were differentially expressed in any of the meaningful pairwise comparisons and performed Over-Representation Analysis (ORA). None of the general cell biological categories was over-represented among these 258 genes. An explanation for this finding could be again that the categories from KEGG, GO, TRANSFAC and TRANSPATH were too low in size, unspecific and diverse for statistical analysis. On the other hand, ORA with MapMan categories identified several meaningful functional pathways differentially regulated in response to Fe supply and *nas4x-1*. In addition to metal homeostasis categories, this analysis revealed redox dismutase and catalase categories, a cell division and a GCN5-related N-acetyltransferase category. The reappearance of the metal homeostasis categories not only in GSEA but also in ORA shows again how significantly this pathway was affected in the transcriptome comparisons. As discussed above, an influence of – Fe and of *nas4x-1* on metal homeostasis was expected from previous analysis and represented here a positive control for proper functioning of the GeneTrail tool. Redox dismutase and catalase genes were differentially regulated presumably because these enzymes often use Fe as cofactor. Low enzyme activity at – Fe may have resulted in differential expression as the result of a feedback control. Alternatively, upon – Fe new enzyme isoforms with different metal requirements might have been produced. It is also reasonable to argue that decreased Fe toxicity upon – Fe

5. Discussion

might have been the cause for the differential regulation of these genes. The differentially regulated cell division category may have reflected an adaptation of root growth behaviour. Finally, the GCN5-related N-acetyltransferase category represented specifically genes involved in histone acetylation, a process associated generally with gene activation. This study and others have shown that – Fe conditions caused an up-regulation of genes and proteins that was more important than a down-regulation (Dinnyen et al., 2008; Brumbarova et al., 2008; Yang et al., 2010). It is therefore plausible that genes and enzymes involved in histone acetylation were activated to render more chromosomal areas accessible to the transcription machineries.

All together, GeneTrail was found highly suitable to reveal functional categories among comparative transcriptome data. We could use the quantitative and qualitative aspects provided by GSEA to interpret molecular-physiological phenotypes. A combination of the GeneTrail analysis methods, GSEA and ORA, together with other analysis tools, like the NIA array tool, was successfully applied for data mining. The main strength of GeneTrail was that it offered answers to individual biological questions with its feature of incorporation of individually defined categories (such as MapMan and metal homeostasis). Hence, GeneTrail can be applied to analyze novel physiological treatments or unknown mutations to identify functional pathways that are affected.

6. Conclusion and Perspectives

This work strongly supports a general role of NA in phloem unloading of Fe in developing tissues like young leaves, the pistil tissue, anthers and seeds. With further Fe stains and cross-sections of the *nas4x-2* style it has to be further investigated whether Fe indeed accumulates in the phloem of the style tissue. Fe staining could also be deduced with *nas4x-1* seeds in order to confirm that seed Fe is also localized to the phloem due to reduced NA levels in the *nas4x-1* mutant. Moreover, we assume that NA has an essential function in phloem-to-xylem exchange of Fe in older leaves for the further long-distance transport to the inflorescence. Whether NA is further bound to Fe or whether NA loads Fe to ITP in phloem in the long-distance transport from leaves to flowers by keeping it soluble remains elusive. Concerning NA-dependent Cu transport we can conclude that NA has an essential role in both xylem and phloem transport, since leaves and inflorescence of *nas4x-2* contain drastically reduced Cu levels (Fig. 4.4.7), while Cu contents in *nas4x-2* roots were elevated (Fig. 4.4.7A). In cooperation with Dr. Javier Abadias group, we are trying to detect Fe-chelator complexes effectively present in the xylem sap of *nas4x-2*, *frd3* and *frd3/nas4x-2* plants in comparison to wild type plants with an integrated mass spectrometry approach based on exact molecular mass, isotopic signature, Fe determination and retention time, termed HPLC-ESI-TOFMS. Our cooperation partners just recently accomplished to detect tri-Fe(III) and tri-citrate complexes in the xylem sap of tomato (Rellan-Alvarez et al., 2010) which provided the first evidence of the presence of Fe-citrate complexes in xylem sap with this study. With these technical prerequisites we expect to find Cu-NA in xylem sap of wild type plants and also Fe-NA complexes in *frd3* mutants. Which chelator is able to overtake the function of NA and citrate in *frd3/nas4x-2* mutants will provide new information about other chelators involved in xylem Fe and Cu transport.

Another very interesting phenomenon is the inability of *nas4x-2* plants to form the female transmitting tract. Rescue experiment could help to reveal whether pollen elongation can be rescued by the application of FeNa-EDTA and NA on *nas4x-2* pistils. Pollen germination assays and sections of the Fe-treated pistils should answer this question. To measure the differential expression of genes like *NTT* (Crawford et al., 2007), *AUXIN RESPONSIVE FACTOR (ARF6)* (Nagpal et al. 2005), *ARF8* (Vivian-Smith et al. 2001) or *FRUIT WITHOUT FERTILIZATION (FWF)* (Goetz et al. 2006; Goetz et al. 2007) in the pistil of *nas4x-2* plants compared to wild type plants, which are

6. Conclusion and Perspectives

involved in the formation of the transmitting tract, will provide interesting hints to the understanding of the connection between Fe supply and the formation of the transmitting tract. To get a general overview which genes are deregulated in carpels of *nas4x-2* plants, there is also the possibility to perform a microarray experiment with pistils of *nas4x-2* plants compared to wild type.

The investigation of NAS3 and NAS4 fusion proteins will give further hints to the sub-cellular localization of NAS proteins. With the newly generated transgenic plants it will be possible to quantify protein levels of NAS3 and NAS4 throughout the plant in response to altered nutritional status, which will provide valuable hints to the role of NA in the intracellular transport. Preliminary protein quantification indicated (Fig. 4.3.6) that protein levels of NAS4 are not noticeably altered in response to Fe deficiency compared to Fe supply condition. It is likely that plants not necessarily react with an increased NA synthesis, more with an increased transport of NA to Fe deficient plant parts, which could also be explained with the fact that only *NAS2* in roots and *NAS4* in leaves are induced upon Fe deficiency, whereas *NAS3* is even repressed upon Fe deficiency in leaves (Klatte et al., 2009). It would be further interesting to investigate NAS3 protein presence in inflorescence over a time course experiment in order to analyze whether NAS3 activity increases after pollination and whether it can be located to seeds.

With transgenic lines it will be at last possible to investigate NAS regulation on protein level. The transcription factor POPEYE (PYE), involved in maintaining iron homeostasis has recently been discovered and was shown to bind directly to the promoter region of *NAS4* and seems to positively regulate *NAS* gene expression (TA Long et al. 2010). Therefore PYE represents a putative candidate in the regulation of the *NAS4* gene. Since not much is known about the regulation of the *NAS* genes it would be interesting to transform *pye* mutants with the NAS4-GFP or NAS4-GUS constructs in order to analyze whether NAS4 is exclusively regulated by the transcription factor PYE.

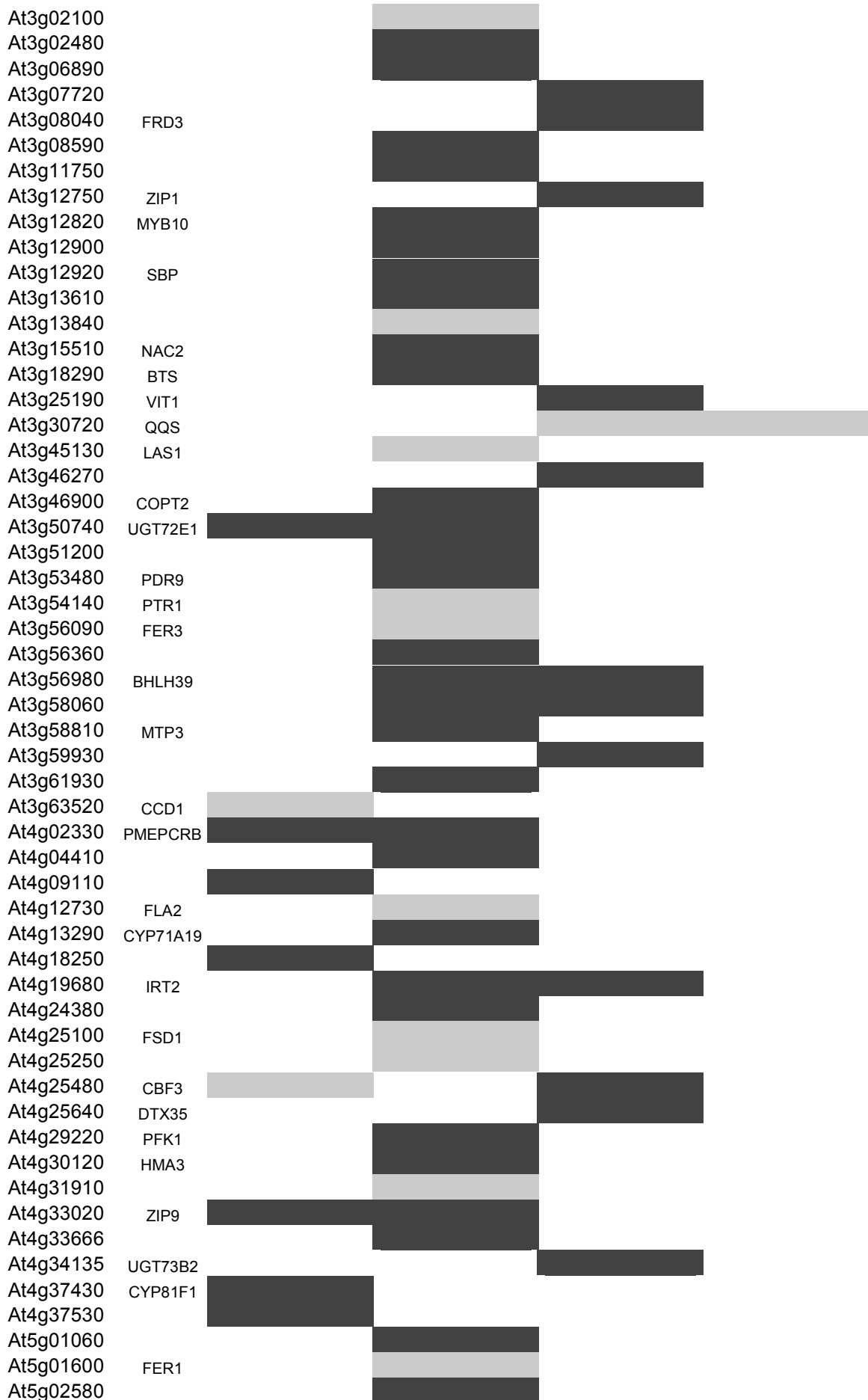
Transgenic lines become especially important by following the aim to increase bioavailability of Fe in seeds. With the investigation of transgenic NAS3 and NAS4 plants in the background of *nas4x-2* plants, it is possible to determine seed NA as well as seed Fe contents in order to find those NAS genes whose activity resulted in the highest NA content in seeds which might also correlate with the Fe contents in seeds. Thus, those NAS genes can be used as targets for biofortification approaches.

Appendix

Table A 2.1: Expression patterns of 125 differentially regulated root genes selected in four pair-wise comparisons. Statistical significance was verified by t-test ($P < 0.05$). The shading illustrates whether genes are upregulated (dark grey), downregulated (light grey) or not regulated (white) in the respective pair-wise comparison. Statistical values are provided in Table A2.3

AGI code	Gene name	Pair-wise comparisons			
		WT -Fe vs +Fe	<i>nas4x-1</i> -Fe vs +Fe	+Fe <i>nas4x-1</i> vs WT	-Fe <i>nas4x-1</i> vs WT
At1g09560	GLP5		Dark grey		
At1g10970	ZIP4			Dark grey	
At1g11920		Dark grey			
At1g17960					Light grey
At1g18910			Dark grey		
At1g18970	GLP4			Dark grey	
At1g20380				Dark grey	
At1g21230	WAK5	Dark grey			
At1g21360	GLP2			Dark grey	
At1g28480		Dark grey			
At1g33890		Dark grey			
At1g36640		Dark grey			
At1g47400			Dark grey	Dark grey	
At1g49820	MTK			Dark grey	
At1g51620		Dark grey			
At1g52820			Light grey		
At1g54010				Dark grey	
At1g56160	MYB72		Dark grey		
At1g64640	ENODL8		Light grey		
At1g68650			Light grey		
At1g71870			Light grey		
At1g73120				Dark grey	
At1g74760			Dark grey		
At1g74770			Dark grey		
At1g76690	OPR2	Dark grey			
At1g80360				Dark grey	
At2g03760	SOT12		Dark grey		
At2g05830				Dark grey	
At2g19410		Dark grey			
At2g20800			Dark grey		Dark grey
At2g21640			Dark grey		Dark grey
At2g23150	NRAMP3			Dark grey	
At2g25510		Dark grey			
At2g27550				Light grey	
At2g28160				Dark grey	
At2g28400		Dark grey			
At2g28820			Dark grey		
At2g40300	FER4	Light grey	Light grey		
At2g41100	TCH3		Dark grey		
At2g41380			Light grey	Dark grey	
At2g41660			Dark grey		
At2g42250			Light grey		
At2g46740		Dark grey			

Appendix



Appendix

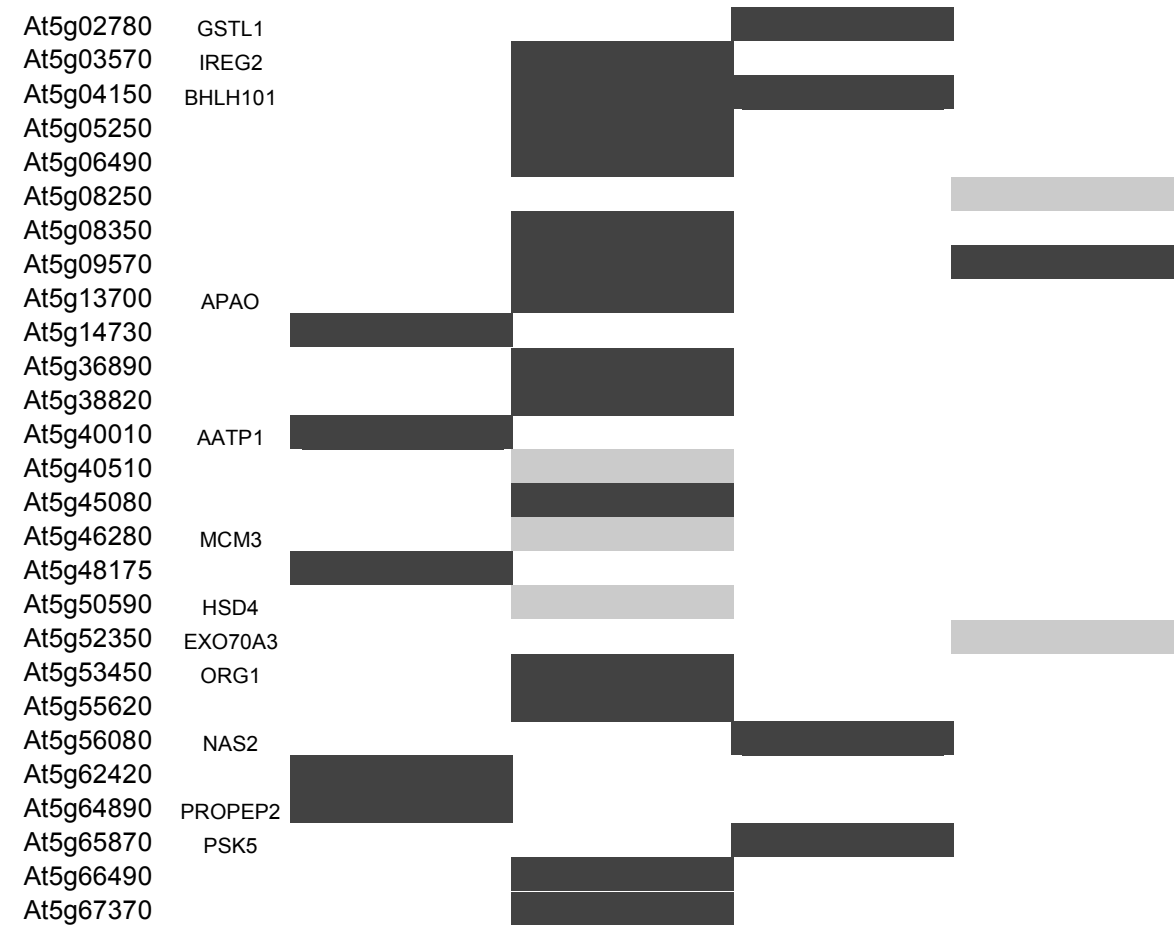
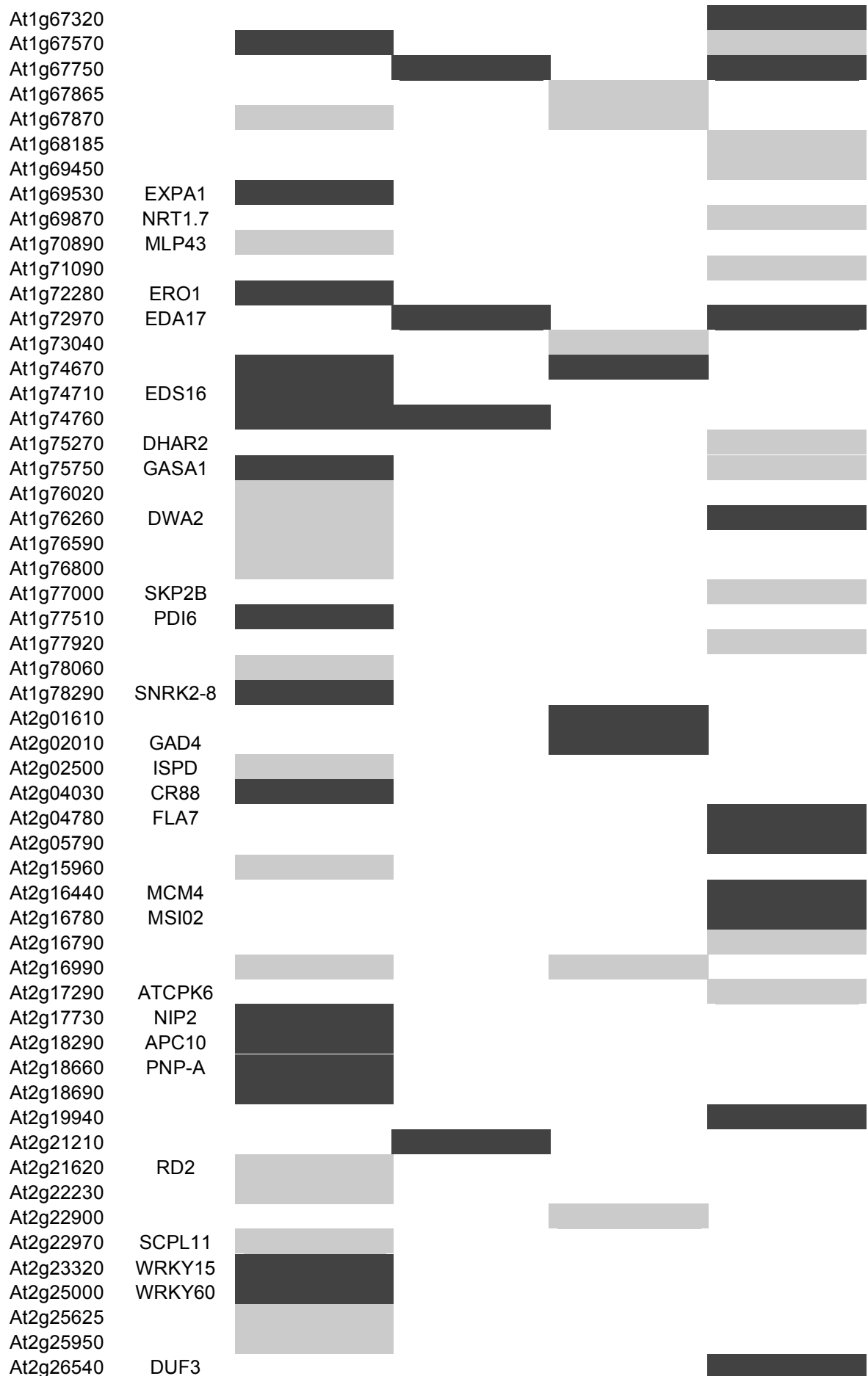


Table A2.2: Expression patterns of 337 differentially regulated leaf genes selected in the four pair-wise comparisons. Statistical significance was verified by t-test ($P < 0.05$). The shading illustrates whether genes are upregulated (dark grey), downregulated (light grey) or not regulated (white) in the respective pair-wise comparison. Statistical values are provided in Table A2.4

AGI code	Gene name	Pair-wise comparisons			
		WT -Fe vs +Fe	<i>nas4x-1</i> -Fe vs +Fe	+Fe <i>nas4x-1</i> vs WT	-Fe <i>nas4x-1</i> vs WT
At1g01010	NAC001	Dark			Light
At1g01390				Light	
At1g04110	SDD1				Dark
At1g04870	PRMT10	Dark			
At1g04980	PDI10	Dark			
At1g05340		Dark			
At1g07450			Dark		
At1g07500		Dark			
At1g08650	PPCK1	Dark			
At1g08830	CSD1		Dark		
At1g09080	BIP3	Dark			
At1g09200					Dark
At1g09795	PRT2	Light			
At1g09815		Dark			Light

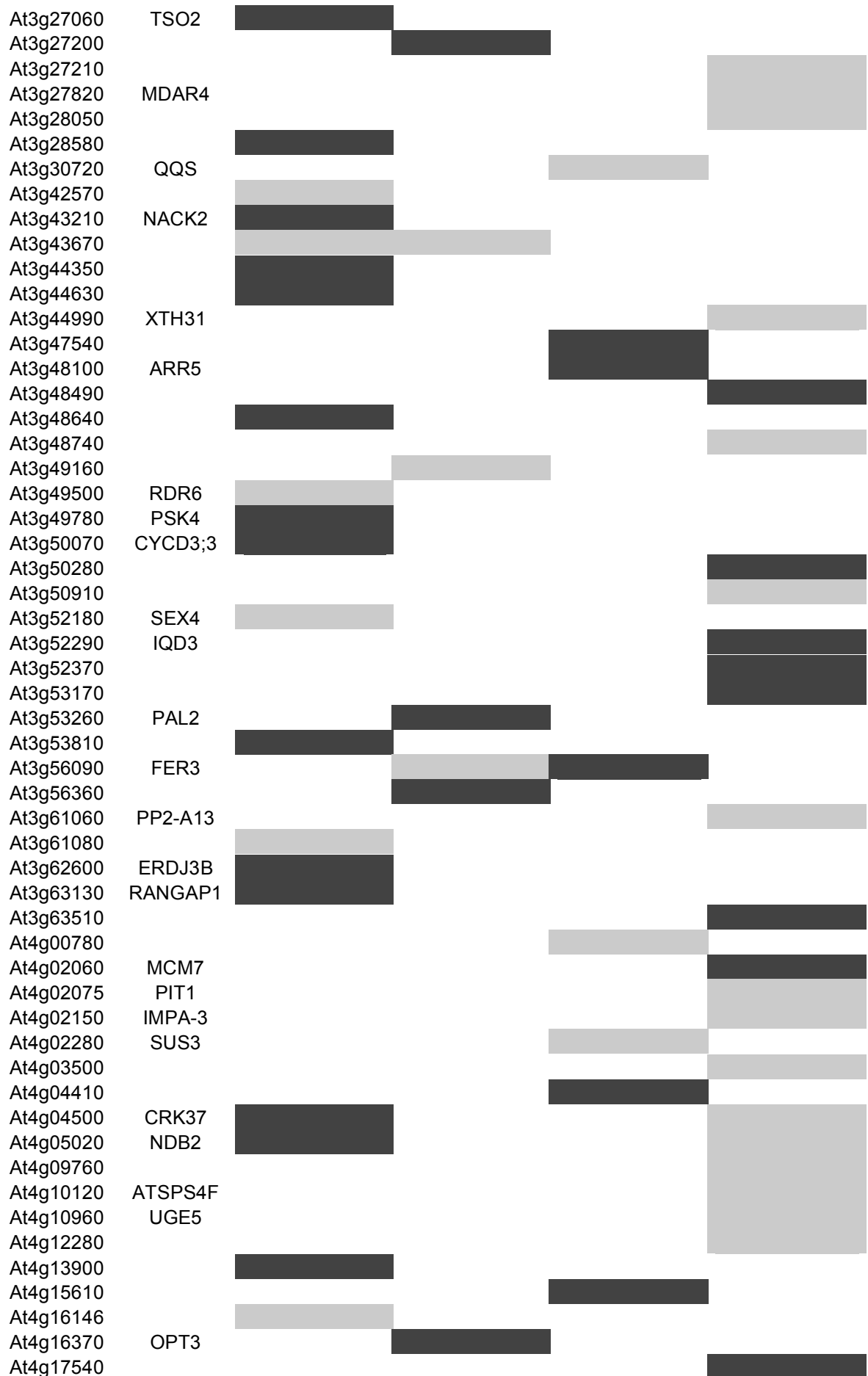
Appendix



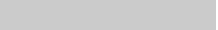
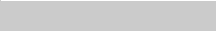
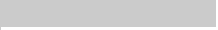
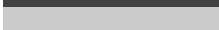
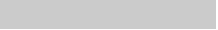
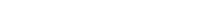
Appendix

At2g27360				
At2g28190	CSD2			
At2g28350	ARF10			
At2g29550	TUB7			
At2g30350				
At2g30750	CYP71A12			
At2g34490	CYP710A2			
At2g35170				
At2g35190	NPSN11			
At2g37790				
At2g38080	IRX12			
At2g38210	PDX1L4			
At2g39920				
At2g40010				
At2g40300	FER4			
At2g40610	EXP8			
At2g42740	RPL16A			
At2g42790	CSY3			
At2g43360	BIO2			
At2g45470	AGP8			
At2g46530	ARF11			
At3g01670				
At3g01830				
At3g02630				
At3g03000				
At3g04110	GLR1			
At3g07270				
At3g07520	GLR1.4			
At3g07800				
At3g09520	EXO70H4			
At3g10840				
At3g10940				
At3g11710				
At3g12710				
At3g13062				
At3g13950				
At3g14060				
At3g14220				
At3g14280				
At3g14595				
At3g16310				
At3g16670				
At3g17770				
At3g20570	ENODL9			
At3g20670	HTA13			
At3g20790				
At3g21600				
At3g22460	OASA2			
At3g22910				
At3g23295				
At3g23810	SAHH2			
At3g24090				
At3g25010	RLP41			
At3g25710	BHLH32			
At3g26590				

Appendix



Appendix

At4g18270	TRANS11			
At4g19390				
At4g21830	MSRB7			
At4g23600	CORI3			
At4g23670				
At4g23750	CRF2			
At4g23885				
At4g23920	UGE2			
At4g24450	GWD3			
At4g24610				
At4g25450	NAP8			
At4g25460				
At4g25480	CBF3			
At4g26150	CGA1			
At4g27435				
At4g28390	AAC3			
At4g28780				
At4g29360				
At4g29520				
At4g30020				
At4g30290	XTH19			
At4g31700	RPS6			
At4g32710				
At4g32940				
At4g33040				
At4g33960				
At4g37290				
At4g37590	NPY5			
At4g38530	PLC1			
At4g38560				
At4g38580	FP6			
At4g39460	SAM1C1			
At5g01015				
At5g01600	FER1			
At5g02220				
At5g02220				
At5g02490				
At5g02890				
At5g03170	FLA11			
At5g04360	LDA			
At5g04900	NOL			
At5g07030				
At5g07920	DGK1			
At5g08410	FTRA2			
At5g08415				
At5g09220	AAP2			
At5g09300				
At5g09995				
At5g13100				
At5g13140				
At5g13930	CHS			
At5g15490				
At5g15860	PCME			
At5g16200				
At5g17650				

Appendix

At5g20160		██████████		
At5g20220			██████████	
At5g21170	AKINBETA1			██████████
At5g22880	H2B			██████████
At5g23020	IMS2			██████████
At5g24110	WRKY30	██████████		
At5g24800	BZIP9			██████████
At5g28540	BIP1	██████████		
At5g28910			██████████	
At5g35740				██████████
At5g37010		██████████		
At5g39320				██████████
At5g40300				██████████
At5g40780	LHT1			██████████
At5g41600	BTI3	██████████		
At5g42830		██████████		
At5g43750	NDH18			██████████
At5g44110	POP1			██████████
At5g45380	DUR3			██████████
At5g46050	PTR3	██████████		
At5g46690	bHLH071	██████████		
At5g46800	BOU		██████████	
At5g48570	FKBP65			██████████
At5g49520	WRKY48		██████████	██████████
At5g49650	XK-2	██████████		
At5g50200	NRT3.1_	██████████		
At5g50460		██████████		
At5g50780				██████████
At5g52970				██████████
At5g53350	CLPX			██████████
At5g53420			██████████	
At5g53450	ORG1		██████████	
At5g53550	YSL3	██████████		
At5g54250	CNGC4			██████████
At5g55050				██████████
At5g56080	NAS2		██████████	
At5g57800	CER3	██████████		
At5g58120		██████████		
At5g58570				██████████
At5g59050				██████████
At5g59350				██████████
At5g59690				██████████
At5g61170		██████████		
At5g61790	CNX1	██████████		
At5g62350		██████████		
At5g62690	TUB2	██████████		
At5g65010	ASN2		██████████	
At5g66140	PAD2	██████████		

Appendix

Table A 2.3: Enriched MapMan categories testing the 462 NIA pre-selected genes compared to all the genes present on the ATH1 gene chip in the ORA

Enriched categories	Associated genes
metalhandling.binding,chelationandstorage	NAS3, ATCCS, ATFER4, ATFER3, CCH, ATFER1, NAS1, NAS2
redox.dismutasesandcatalases	ATCCS, CSD2, FSD1
redox.dismutasesandcatalases	WRKY60 WRKY46 WRKY47 WRKY53 WRKY48
transport.metal	NRAMP3, MTPA2, IRT2, ZIP5, HMA5, YSL1
cell.division	AT1G49910 AT1G69400 CDKB1;2 APC8 ATSMC3
misc.gcN5-related N-acetyltransferase	AT2G32020 AT2G32030 AT2G39030
notassigned.noontology	AT3G07720 AT5G52670 AT1G09450 CENP-C COR414-TM1ZW9 AT1G76260 ATNUDT6 ATEXO70H4 AT3G14100 ATNUDX13 AT4G36700

The table illustrates these genes among the 462 NIA preselected genes, which are associated with enriched categories.

Appendix

Table A2.4: Selection of all differentially expressed genes in the four pair-wise comparisons in roots

WT Ro - vs WT Ro +								
ATH1 Probe Set Identifier	AGI Code	Raw Signal Average Col Ro-	Raw Signal Average Col Ro+	SLR Average	Fold change	Change direction	T-Test p-value	Annotation
254660_at	At4g18250	60,77	32,02	0,99	1,90	Up	0,039	receptor serine/threonine kinase, putative
259875_s_at	At1g76690	157,07	70,8	1,02	2,22	Up	0,047	ATOPR2_OPR2__12-oxophytodienoate reductase 2
260123_at	At1g33890	52,83	37,27	0,6	1,42	Up	0,035	Avirulence induced gene (AIG1) family protein
256499_at	At1g36640	165,57	75,8	1,25	2,18	Up	0,003	unknown protein
255524_at	At4g02330	107,33	53,8	1,36	1,99	Up	0,044	ATPMEPCRB__Plant invertase/pectin methylesterase inhibitor superfamily
246584_at	At5g14730	51,73	25,79	1,31	2,01	Up	0,045	unknown protein
252183_at	At3g50740	665,5	273,64	1,76	2,43	Up	0,026	UGT72E1__UDP-glucosyl transferase 72E1
266711_at	At2g46740	177,07	102	0,84	1,74	Up	0,013	D-arabinono-1,4-lactone oxidase family protein
247205_at	At5g64890	86,33	34,52	1,55	2,50	Up	0,033	PROPEP2__elicitor peptide 2 precursor
265611_at	At2g25510	86,4	40,78	1,06	2,12	Up	0,032	unknown protein
249438_at	At5g40010	99,8	38,82	1,57	2,57	Up	0,037	AATP1__AAA-ATPase 1
253099_s_at	At4g37530	484,4	314,48	0,81	1,54	Up	0,018	Peroxidase superfamily protein
248717_at	At5g48175	58,9	34,49	1,11	1,71	Up	0,046	unknown protein
253413_at	At4g33020	35,07	22,08	1,12	1,59	Up	0,015	ATZIP9_ZIP9__ZIP metal ion transporter family

Appendix

253101_at	At4g37430	97,33	41,47	1,47	2,35	Up	0,025	CYP81F1_CYP91A2__cytochrome P450, family 91, subfamily A, polypeptide 2
259558_at	At1g21230	48,9	29,94	0,94	1,63	Up	0,047	WAK5__wall associated kinase 5
261443_at	At1g28480	32,73	17,63	1,31	1,86	Up	0,027	GRX480_roxy19__Thioredoxin superfamily protein
255075_at	At4g09110	119	55,62	1,11	2,14	Up	0,002	RING/U-box superfamily protein
265276_at	At2g28400	53,13	32,76	0,89	1,62	Up	0,034	Protein of unknown function, DUF584
251146_at	At3g63520	78,67	108,62	-0,57	0,72	Down	0,041	ATCCD1_ATNCED1_CCD1_NCED1__carotenoid cleavage dioxygenase 1
263831_at	At2g40300	31,6	65,22	-1,26	0,48	Down	0,028	ATFER4_FER4__ferritin 4

nas4x-1 Ro - vs *nas4x-1* Ro +

ATH1 Probe Set Identifier	AGI Code	Raw Signal Average 4x Ro -	Raw Signal Average 4x Ro +	SLR Average	Fold change	Change direction	T-Test p-value	Annotation
257062_at	At3g18290	198,67	124,37	0,62	1,60	Up	0,009	BTS_EMB2454__zinc finger protein-related
253709_at	At4g29220	342,2	209,1	0,69	1,64	Up	0,007	PFK1__phosphofructokinase 1
247072_at	At5g66490	385,37	234,57	0,75	1,64	Up	0,034	unknown protein
246034_at	At5g08350	296,8	185,1	0,79	1,60	Up	0,037	GRAM domain-containing protein / ABA-responsive protein-related
245113_at	At2g41660	209,13	131,87	0,83	1,59	Up	0,024	MIZ1__Protein of unknown function, DUF617
258679_at	At3g08590	426,03	253	0,85	1,68	Up	0,025	Phosphoglycerate mutase, 2,3-bisphosphoglycerate-independent
259472_at	At1g18910	391,83	201,17	0,89	1,95	Up	0,013	zinc ion binding;zinc ion binding
257858_at	At3g12920	622,3	320,5	0,92	1,94	Up	0,023	SBP (S-ribonuclease binding protein) family protein
264506_at	At1g09560	2550,17	1212,43	0,96	2,10	Up	0,007	GLP5__germin-like protein 5
250952_at	At5g03570	1039,03	511,2	0,98	2,03	Up	0,007	ATIREG2_FPN2_IREG2__iron regulated 2

Appendix

250246_at	At5g13700	38,57	18,87	0,99	2,04	Up	0,001	APAO_ATPAO1_PAO1__polyamine oxidase 1
248979_at	At5g45080	661,03	321,3	0,99	2,06	Up	0,014	AtPP2-A6_PP2-A6__phloem protein 2-A6
256647_at	At3g13610	3484,63	1801,4	0,99	1,93	Up	0,035	2-oxoglutarate (2OG) and Fe(II)-dependent oxygenase superfamily protein
250730_at	At5g06490	34,87	17,1	1,01	2,04	Up	0,022	RING/U-box superfamily protein
254158_at	At4g24380	69,07	33,63	1,03	2,05	Up	0,024	CONTAINS InterPro DOMAIN/s: Serine hydrolase (InterPro:IPR005645)
254767_s_at	At4g13290	310,37	124,07	1,04	2,50	Up	0,029	CYP71A19__cytochrome P450, family 71, subfamily A, polypeptide 19
267083_at	At2g41100	585,03	302,6	1,05	1,93	Up	0,015	ATCAL4_TCH3__Calcium-binding EF hand family protein
245692_at	At5g04150	210,8	97,13	1,1	2,17	Up	0,01	BHLH101__basic helix-loop-helix (bHLH) DNA-binding superfamily protein
251704_at	At3g56360	949,93	416,47	1,11	2,28	Up	0,011	unknown protein
258551_at	At3g06890	148,63	64,03	1,21	2,32	Up	0	unknown protein
251125_at	At5g01060	58,73	26,1	1,23	2,25	Up	0,008	Protein kinase protein with tetratricopeptide repeat domain
251942_at	At3g53480	1180,57	527,8	1,31	2,24	Up	0,029	ABCG37_ATPDR9_PDR9_PIS1__pleiotropic drug resistance 9
258385_at	At3g15510	93	34,13	1,32	2,72	Up	0,023	ANAC056_ATNAC2_NAC2_NARS1__NAC domain containing protein 2
251012_at	At5g02580	171	71,9	1,35	2,38	Up	0,006	Plant protein 1589 of unknown function
	At1g74760	794,43	309,1	1,39	2,57	Up	0,001	
253658_at	At4g30120	110,43	41,2	1,4	2,68	Up	0,001	ATHMA3_HMA3__heavy metal atpase 3
264042_at	At2g03760	34,37	14,57	1,4	2,36	Up	0,005	AtSOT1_AtSOT12_ATST1_RAR047_SOT12_ST_ST1__sulphotransferase 12
251545_at	At3g58810	872,33	331,27	1,44	2,63	Up	0,013	ATMTP3_ATMTPA2_MTP3_MTPA2__metal tolerance protein A2
248270_at	At5g53450	395,9	144,53	1,46	2,74	Up	0,009	ORG1__OBP3-responsive gene 1
251677_at	At3g56980	513,87	185,53	1,46	2,77	Up	0,011	BHLH039_ORG3__basic helix-loop-helix (bHLH) DNA-binding superfamily protein

Appendix

253413_at	At4g33020	82,87	30,27	1,51	2,74	Up	0,047	ATZIP9_ZIP9__ZIP metal ion transporter family
262217_at	At1g74770	169,2	55,03	1,58	3,07	Up	0,004	zinc ion binding
252502_at	At3g46900	234,73	93,13	1,58	2,52	Up	0,016	COPT2__copper transporter 2
255524_at	At4g02330	237,5	76,83	1,6	3,09	Up	0,013	ATPMEPCRB__Plant invertase/pectin methylesterase inhibitor superfamily
250828_at	At5g05250	180,77	45,8	1,67	3,95	Up	0,035	unknown protein
251620_at	At3g58060	146,33	50,93	1,71	2,87	Up	0,036	Cation efflux family protein
257689_at	At3g12820	132,03	39,1	1,79	3,38	Up	0,018	AtMYB10_MYB10__myb domain protein 10
249535_at	At5g38820	281,53	72,33	1,8	3,89	Up	0,009	Transmembrane amino acid transporter family protein
252183_at	At3g50740	1160,57	338,63	1,85	3,43	Up	0,009	UGT72E1__UDP-glucosyl transferase 72E1
	At2g28820	22,53	6,13	1,85	3,68	Up	0,041	
261684_at	At1g47400	198,33	55,93	2,02	3,55	Up	0,009	unknown protein
246998_at	At5g67370	69,93	15,93	2,16	4,39	Up	0,002	Protein of unknown function (DUF1230)
254534_at	At4g19680	259,43	57,07	2,2	4,55	Up	0,02	ATIRT2_IRT2__iron regulated transporter 2
253305_at	At4g33666	89,67	16,17	2,34	5,55	Up	0,036	unknown protein
249636_at	At5g36890	811,97	167,53	2,39	4,85	Up	0,02	BGLU42__beta glucosidase 42
258498_at	At3g02480	27,47	5,17	2,57	5,31	Up	0,045	Late embryogenesis abundant protein (LEA) family protein
251293_at	At3g61930	664,5	107,1	2,58	6,20	Up	0,017	unknown protein
262091_at	At1g56160	197,23	28,4	2,66	6,94	Up	0,036	ATMYB72_MYB72__myb domain protein 72
257135_at	At3g12900	1522,03	212,8	2,84	7,15	Up	0,007	2-oxoglutarate (2OG) and Fe(II)-dependent oxygenase superfamily protein
250515_at	At5g09570	103,53	14,33	3	7,22	Up	0,006	Cox19-like CHCH family protein

Appendix

248028_at	At5g55620	129	12,4	3,43	10,40	Up	0,005	unknown protein
263515_at	At2g21640	92,23	8,7	3,45	10,60	Up	0,017	Encodes a protein of unknown function that is a marker for oxidative stress response.
248891_at	At5g46280	42,87	61,4	-0,52	0,70	Down	0,002	MCM3 homolog (emb CAA03887.1)
254785_at	At4g12730	302,63	444,73	-0,53	0,68	Down	0,006	FLA2__FASCICLIN-like arabinogalactan 2
261514_at	At1g71870	76,07	107,53	-0,59	0,71	Down	0,022	MATE efflux family protein
253483_at	At4g31910	316,13	468,93	-0,6	0,67	Down	0,04	HXXXD-type acyl-transferase family protein
251882_at	At3g54140	122,77	199	-0,67	0,62	Down	0,005	ATPTR1_PTR1__peptide transporter 1
261975_at	At1g64640	75,2	136,1	-0,73	0,55	Down	0,008	AtENODL8_ENODL8__early nodulin-like protein 8
262277_at	At1g68650	59,7	97,33	-0,79	0,61	Down	0,007	Uncharacterized protein family (UPF0016)
249358_at	At5g40510	269,6	525,13	-0,86	0,51	Down	0,005	Sucrase/ferredoxin-like family protein
251735_at	At3g56090	114,33	232,3	-0,96	0,49	Down	0,036	ATFER3_FER3__ferritin 3
263831_at	At2g40300	20,93	42,33	-1,04	0,49	Down	0,031	ATFER4_FER4__ferritin 4
252611_at	At3g45130	21,23	62,07	-1,43	0,34	Down	0	LAS1__lanosterol synthase 1
251109_at	At5g01600	420,23	1093,87	-1,46	0,38	Down	0,026	ATFER1_FER1__ferretin 1
254056_at	At4g25250	37,2	120,97	-1,71	0,31	Down	0,025	Plant invertase/pectin methylesterase inhibitor superfamily protein
257605_at	At3g13840	13,83	49,93	-1,71	0,28	Down	0,016	GRAS family transcription factor
248519_at	At5g50590	122,93	567,5	-2,44	0,22	Down	0,026	AtHSD4_HSD4__hydroxysteroid dehydrogenase 4
267626_at	At2g42250	52,43	264,5	-2,68	0,20	Down	0,039	CYP712A1__cytochrome P450, family 712, subfamily A, polypeptide 1
260150_at	At1g52820	68,43	395,97	-2,72	0,17	Down	0,031	2-oxoglutarate (2OG) and Fe(II)-dependent oxygenase superfamily protein
254098_at	At4g25100	1,6	35,97	-4,53	0,04	Down	0,03	ATFSD1_FSD1__Fe superoxide dismutase 1

Appendix

nas4x-1 Ro + vs WT Ro +

ATH1 Probe Set Identifier	AGI Code	Raw Signal Average 4x Ro +	Raw Signal Average WT Ro +	SLR Average	Fold change	Change direction	T-Test p-value	Annotation
263153_s_at	At1g54010	761,1	496,2	0,62	1,53	Up	0,037	myrosinase-associated protein
254077_at	At4g25640	81,13	44,9	0,75	1,81	Up	0,022	ATDTX35_DTX35_FFT__detoxifying efflux carrier 35
259819_at	At1g49820	473,83	282,3	0,78	1,68	Up	0,023	ATMTK_MTK__S-methyl-5-thioribose kinase
259481_at	At1g18970	276,2	159,83	0,81	1,73	Up	0,03	GLP4__germin-like protein 4
260328_at	At1g80360	408,9	231,93	0,82	1,76	Up	0,002	Pyridoxal phosphate (PLP)-dependent transferases superfamily protein
	At2g28160	309,77	147,6	0,92	2,10	Up	0,011	
257715_at	At3g12750	105,13	51,6	1,1	2,04	Up	0,035	ZIP1__zinc transporter 1 precursor
266033_at	At2g05830	401,3	186,2	1,13	2,16	Up	0,003	NagB/RpiA/CoA transferase-like superfamily protein
252510_at	At3g46270	290,2	124,2	1,27	2,34	Up	0,004	receptor protein kinase-related
247109_at	At5g65870	34,67	14,57	1,43	2,38	Up	0,007	ATPSK5_PSK5_PSK5__phytosulfokine 5 precursor
253268_s_at	At4g34135	88,47	31,7	1,52	2,79	Up	0,008	UGT73B2__UDP-glucosyltransferase 73B2
248048_at	At5g56080	162,97	51,2	1,63	3,18	Up	0,048	ATNAS2_NAS2__nicotianamine synthase 2
260462_at	At1g10970	84,93	31,77	1,7	2,67	Up	0,008	ATZIP4_ZIP4__zinc transporter 4 precursor
251620_at	At3g58060	50,93	11,73	1,74	4,34	Up	0,001	Cation efflux family protein
258646_at	At3g08040	338,43	101,93	1,86	3,32	Up	0,021	ATFRD3_FRD3_MAN1__MATE efflux family protein
260926_at	At1g21360	114,37	25,97	1,87	4,40	Up	0	GLTP2__glycolipid transfer protein 2
257823_at	At3g25190	981,67	295,07	2,06	3,33	Up	0,025	Vacuolar iron transporter (VIT) family protein

Appendix

267266_at	At2g23150	359,3	90,97	2,08	3,95	Up	0,003	ATNRAMP3_NRAMP3__natural resistance-associated macrophage protein 3
255940_at	At1g20380	185,33	41,93	2,13	4,42	Up	0,027	Prolyl oligopeptidase family protein
250983_at	At5g02780	215,37	49,37	2,21	4,36	Up	0,001	GSTL1__glutathione transferase lambda 1
251677_at	At3g56980	185,53	40,3	2,21	4,60	Up	0,004	BHLH039_ORG3__basic helix-loop-helix (bHLH) DNA-binding superfamily protein
266368_at	At2g41380	26,6	5,93	2,28	4,49	Up	0,001	S-adenosyl-L-methionine-dependent methyltransferases superfamily protein
259228_at	At3g07720	1817	427,83	2,29	4,25	Up	0,002	Galactose oxidase/kelch repeat superfamily protein
254534_at	At4g19680	57,07	8,5	2,47	6,71	Up	0,01	ATIRT2_IRT2__iron regulated transporter 2
261684_at	At1g47400	55,93	10,53	2,77	5,31	Up	0,04	unknown protein
262373_at	At1g73120	667,77	81,9	3,08	8,15	Up	0,001	unknown protein
251438_s_at	At3g59930	1252,23	174,9	3,1	7,16	Up	0,025	Encodes a defensin-like (DEFL) family protein.
245692_at	At5g04150	97,13	9,6	3,58	10,12	Up	0	BHLH101__basic helix-loop-helix (bHLH) DNA-binding superfamily protein
266209_at	At2g27550	33,53	62,77	-0,95	0,53	Down	0,027	ATC__centroradialis
254066_at	At4g25480	14,93	32,77	-1,18	0,46	Down	0,024	ATCBF3_CBF3_DREB1A__dehydration response element B1A
256940_at	At3g30720	39	931,17	-4,51	0,04	Down	0,021	QQS__qua-quine starch

nas4x-1 Ro - vs WT Ro -

ATH1 Probe Set Identifier	AGI Code	Raw Signal Average 4x Ro -	Raw Signal Average WT Ro -	SLR Average	Fold change	Change direction	T-Test p-value	Annotation
263515_at	At2g21640	92,23	19,5	2,17	4,73	Up	0,013	unknown protein
250515_at	At5g09570	103,53	13,97	2,83	7,41	Up	0,01	Cox19-like CHCH family protein
255893_at	At1g17960	34,2	55,17	-0,68	0,62	Down	0,015	Threonyl-tRNA synthetase

Appendix

248356_at	At5g52350	56,43	98,17	-0,7	0,57	Down	0,027	ATEXO70A3_EXO70A3__excyst subunit exo70 family protein A3
256940_at	At3g30720	21,47	710,73	-4,94	0,03	Down	0,015	QQS__qua-quine starch

Table A2.5: Selection of all differentially expressed genes in 4 pair-wise comparisons in leaves

WT Le - vs WT Le +								
ATH1 Probe Set Identifier	AGI Code	Raw Signal Average Col Le -	Raw Signal Average Col Le +	"SLR Average"	Fold change	Change direction	T-Test p-value	Annotation
260852_at	At1g21900	205,03	140,37	0,51	1,46	Up	0,006	emp24/gp25L/p24 family/GOLD family protein
259489_at	At1g15790	50,5	33	0,51	1,53	Up	0,004	unknown protein
259069_at	At3g11710	345,03	244,97	0,52	1,41	Up	0,031	ATKRS-1__lysyl-tRNA synthetase 1
260896_at	At1g29310	96,43	66,37	0,54	1,45	Up	0,021	SecY protein transport family protein
246070_at	At5g20160	389,5	275,27	0,55	1,41	Up	0,021	Ribosomal protein L7Ae/L30e/S12e/Gadd45 family protein
253487_at	At4g31700	425,7	291,3	0,55	1,46	Up	0,038	RPS6_RPS6A__ribosomal protein S6
247566_at	At5g61170	500,8	313,8	0,58	1,60	Up	0,02	Ribosomal protein S19e family protein
258834_at	At3g07270	169,37	111,57	0,58	1,52	Up	0,004	GTP cyclohydrolase I
256543_at	At1g42480	133,7	82,07	0,59	1,63	Up	0,001	unknown protein
258617_at	At3g03000	39,63	22,6	0,63	1,75	Up	0,026	EF hand calcium-binding protein family
265336_at	At2g18290	190,67	121,63	0,63	1,57	Up	0,041	APC10__anaphase promoting complex 10
264588_at	At2g17730	75,77	49,93	0,65	1,52	Up	0,007	NIP2__NEP-interacting protein 2
256216_at	At1g56340	407,27	247,6	0,66	1,64	Up	0,014	AtCRT1a_CRT1_CRT1a__calreticulin 1a
247080_at	At5g66140	432,47	276,73	0,66	1,56	Up	0,014	PAD2__proteasome alpha subunit D2
247442_s_at	At5g62690	773,17	443,7	0,69	1,74	Up	0,03	TUB2__tubulin beta chain 2
247884_at	At5g57800	316,5	186,63	0,7	1,70	Up	0,048	CER3_FLP1_WAX2_YRE__Fatty acid hydroxylase superfamily
263483_at	At2g04030	266,33	159,8	0,7	1,67	Up	0,011	AtHsp90.5_CR88_EMB1956_Hsp88.1_HSP90.5__Chaperone protein htpG family protein

Appendix

252189_at	At3g50070	32,73	16,4	0,7	2,00	Up	0,001	CYCD3;3__CYCLIN D3;3
252648_at	At3g44630	285,47	167,57	0,71	1,70	Up	0,03	Disease resistance protein (TIR-NBS-LRR class) family
264442_at	At1g27480	211,47	126,87	0,71	1,67	Up	0,041	alpha/beta-Hydrolases superfamily protein
256666_at	At3g20670	164	99,2	0,71	1,65	Up	0,006	HTA13__histone H2A 13
248512_at	At5g50460	579,1	327,83	0,75	1,77	Up	0,02	secE/sec61-gamma protein transport protein
262082_s_at	At1g56120	255,47	163,73	0,77	1,56	Up	0,02	Leucine-rich repeat transmembrane protein kinase
251910_at	At3g53810	51,23	27,63	0,79	1,85	Up	0	Concanavalin A-like lectin protein kinase family protein
259378_at	At3g16310	95,67	55,2	0,8	1,73	Up	0,047	mitotic phosphoprotein N' end (MPPN) family protein
255259_at	At4g05020	227,77	120,87	0,84	1,88	Up	0,014	NDB2__NAD(P)H dehydrogenase B2
259626_at	At1g42990	406,93	216,1	0,86	1,88	Up	0,032	ATBZIP60_BZIP60__basic region/leucine zipper motif 60
264783_at	At1g08650	142,63	81,97	0,87	1,74	Up	0,03	ATPPCK1_PPCK1__phosphoenolpyruvate carboxylase kinase 1
260481_at	At1g10960	1272,87	693,8	0,87	1,83	Up	0	ATFD1_FD1__ferredoxin 1
265646_at	At2g27360	85,53	44,1	0,87	1,94	Up	0,003	GDSL-like Lipase/Acylhydrolase superfamily protein
254190_at	At4g23885	61,13	30,43	0,88	2,01	Up	0,01	unknown protein
261130_at	At1g04870	163,6	92,13	0,89	1,78	Up	0,04	ATPRMT10_PRMT10__protein arginine methyltransferase 10
262947_at	At1g75750	626,03	331,13	0,9	1,89	Up	0,049	GASA1__GAST1 protein homolog 1
261205_at	At1g12790	44,73	22,77	0,9	1,96	Up	0,036	CONTAINS InterPro DOMAIN/s: RuvA domain 2-like (InterPro:IPR010994)
257314_at	At3g26590	103,53	48,97	0,91	2,11	Up	0,044	MATE efflux family protein
245051_at	At2g23320	112,83	67,1	0,91	1,68	Up	0,001	WRKY15__WRKY DNA-binding protein 15
261979_at	At1g37130	2118,47	1096,07	0,93	1,93	Up	0,044	ATNR2_B29_CHL3_NIA2_NIA2-1_NR_NR2__nitrate reductase 2
251182_at	At3g62600	518,53	255,2	0,94	2,03	Up	0,045	ATERDJ3B_ERDJ3B__DNAJ heat shock family protein
252234_at	At3g49780	106,37	44,6	0,94	2,38	Up	0,042	ATPSK3 (FORMER SYMBOL)_ATPSK4_PSK4__phytosulfokine 4 precursor
260196_at	At1g67570	49,8	24,67	0,98	2,02	Up	0,031	Protein of unknown function (DUF3537)
251152_at	At3g63130	73,13	27,83	1	2,63	Up	0,042	ATRANGAP1_RANGAP1__RAN GTPase activating protein 1
264674_at	At1g09815	337,7	165,77	1	2,04	Up	0,049	POLD4__polymerase delta 4
267138_s_at	At2g38210	886,8	402,53	1,06	2,20	Up	0,049	PDX1L4__putative PDX1-like protein 4
266518_at	At2g35170	45,8	22,17	1,06	2,07	Up	0,028	Histone H3 K4-specific methyltransferase SET7/9 family protein

Appendix

261585_at	At1g01010	33,63	14,13	1,06	2,38	Up	0,048	ANAC001_NAC001__NAC domain containing protein 1
255822_at	At2g40610	395,4	192,57	1,07	2,05	Up	0,024	ATEXP8_ATEXPA8_ATHEXP ALPHA 1.11_EXP8_EXPA8__expansin A8
264580_at	At1g05340	34,67	14,2	1,07	2,44	Up	0,046	unknown protein
259852_at	At1g72280	38,7	18,53	1,07	2,09	Up	0,038	AERO1_ERO1__endoplasmic reticulum oxidoreductins 1
247494_at	At5g61790	559,83	276,57	1,07	2,02	Up	0,046	ATCNX1_CNX1__calnexin 1
262731_at	At1g16420	14,93	6,4	1,1	2,33	Up	0,022	ATMC8_MC8__metacaspase 8
245956_s_at	At5g28540	1452,87	680,2	1,12	2,14	Up	0,043	BIP1__heat shock protein 70 (Hsp 70) family protein
259065_at	At3g07520	77,5	35,6	1,13	2,18	Up	0,049	ATGLR1.4_GLR1.4__glutamate receptor 1.4
246524_at	At5g15860	67	29,37	1,19	2,28	Up	0,007	ATPCME_PCME__prenylcysteine methylesterase
261914_at	At1g65870	33,33	12,67	1,22	2,63	Up	0,009	Disease resistance-responsive (dirigent-like protein) family protein
261557_at	At1g63640	56,8	26,37	1,22	2,15	Up	0,049	P-loop nucleoside triphosphate hydrolases superfamily protein with CH (Calponin Homology) domain
261485_at	At1g14360	146,63	64,53	1,22	2,27	Up	0,012	ATUTR3_UTR3__UDP-galactose transporter 3
264774_at	At1g22890	233,17	94,73	1,25	2,46	Up	0,024	unknown protein
253776_at	At4g28390	179,07	71,63	1,27	2,50	Up	0,03	AAC3_ATAAC3__ADP/ATP carrier 3
254016_at	At4g26150	35,37	13,87	1,27	2,55	Up	0,006	CGA1_GATA22__cytokinin-responsive gata factor 1
256911_at	At3g24090	48,2	21,8	1,27	2,21	Up	0,009	glutamine-fructose-6-phosphate transaminase (isomerizing)s;sugar binding;transaminases
259757_at	At1g77510	412,5	156,67	1,3	2,63	Up	0,04	ATPDI6_ATPDIL1-2_PDI6_PDIL1-2__PDI-like 1-2
260221_at	At1g74670	1304,4	548,8	1,31	2,38	Up	0,006	Gibberellin-regulated family protein
258209_at	At3g14060	26	10,63	1,32	2,45	Up	0,02	unknown protein
249644_at	At5g37010	39,4	15,7	1,34	2,51	Up	0,019	unknown protein
266295_at	At2g29550	176	70,5	1,35	2,50	Up	0,039	TUB7__tubulin beta-7 chain
254741_s_at	At4g13900	121,13	47,23	1,35	2,56	Up	0,03	unknown protein
263536_at	At2g25000	65,53	21,13	1,38	3,10	Up	0,033	ATWRKY60_WRKY60__WRKY DNA-binding protein 60
259511_at	At1g12520	701,07	253,37	1,41	2,77	Up	0,007	ATCCS_CCS__copper chaperone for SOD1
259629_at	At1g56510	230,2	91,83	1,44	2,51	Up	0,037	ADR2_WRR4__Disease resistance protein (TIR-NBS-LRR class)
267349_at	At2g40010	33,9	8	1,48	4,24	Up	0,046	Ribosomal protein L10 family protein
261000_at	At1g26540	15,87	3,63	1,52	4,37	Up	0,001	Agenet domain-containing protein

Appendix

256299_at	At1g69530	1167,6	454,8	1,56	2,57	Up	0,038	AT-EXP1_ATEXP1_ATEXPA1_ATHEXP ALPHA 1.2_EXP1_EXPA1__expansin A1
261167_at	At1g04980	84,9	23,73	1,57	3,58	Up	0,009	ATPDI10_ATPDIL2-2_PDI10_PDIL2-2__PDI-like 2-2
252736_at	At3g43210	37,27	12,9	1,58	2,89	Up	0,037	ATNACK2_NACK2_TES__ATP binding microtubule motor family protein
260774_at	At1g78290	196,07	72,47	1,59	2,71	Up	0,005	SNRK2-8_SNRK2.8_SRK2C__Protein kinase superfamily protein
253687_at	At4g29520	97,67	33,83	1,66	2,89	Up	0,028	LOCATED IN: endoplasmic reticulum, plasma membrane
248932_at	At5g46050	65,57	19,23	1,66	3,41	Up	0,047	ATPTR3_PTR3__peptide transporter 3
254235_at	At4g23750	41,53	13,57	1,68	3,06	Up	0,045	CRF2_TMO3__cytokinin response factor 2
247848_at	At5g58120	97,2	25,47	1,71	3,82	Up	0	Disease resistance protein (TIR-NBS-LRR class) family
258203_at	At3g13950	88,27	25,03	1,73	3,53	Up	0,002	unknown protein
248551_at	At5g50200	176,13	57,03	1,74	3,09	Up	0,013	ATNRT3.1_NRT3.1_WR3__nitrate transmembrane transporters
253044_at	At4g37290	17,3	5,47	1,83	3,16	Up	0,015	unknown protein
265161_at	At1g30900	169,53	62,43	1,88	2,72	Up	0,021	BP80-3;3_VSR3;3_VSR6__VACUOLAR SORTING RECEPTOR 6
256833_at	At3g22910	27,53	9,5	1,91	2,90	Up	0,039	ATPase E1-E2 type family protein / haloacid dehalogenase-like hydrolase family protein
264635_at	At1g65500	131,63	34,53	1,99	3,81	Up	0,003	unknown protein
250994_at	At5g02490	143,1	38,5	2	3,72	Up	0,049	Heat shock protein 70 (Hsp 70) family protein
262177_at	At1g74710	297,8	65,47	2,14	4,55	Up	0,035	ATICS1_EDS16_ICs1_SID2__ADC synthase superfamily protein
257100_at	At3g25010	106,87	27,47	2,17	3,89	Up	0,017	AtRLP41_RLP41__receptor like protein 41
261005_at	At1g26420	12,33	2,93	2,23	4,21	Up	0,007	FAD-binding Berberine family protein
261021_at	At1g26380	19,67	3,13	2,24	6,28	Up	0,006	FAD-binding Berberine family protein
261065_at	At1g07500	71,33	16,37	2,36	4,36	Up	0,038	unknown protein
252977_at	At4g38560	57	15,17	2,38	3,76	Up	0,023	Arabidopsis phospholipase-like protein (PEARLI 4) family
259507_at	At1g43910	77,07	13,7	2,39	5,63	Up	0,008	P-loop containing nucleoside triphosphate hydrolases superfamily protein
254385_s_at	At4g21830	78,2	15,03	2,43	5,20	Up	0,019	ATMSRB7_MSRB7__methionine sulfoxide reductase B7
258752_at	At3g09520	18	3,23	2,44	5,57	Up	0,006	ATEXO70H4_EXO70H4__exocyst subunit exo70 family protein H4
259224_at	At3g07800	676,33	129,87	2,45	5,21	Up	0,046	Thymidine kinase
252345_at	At3g48640	75,97	16,43	2,5	4,62	Up	0,01	unknown protein
266489_at	At2g35190	116,2	21,23	2,51	5,47	Up	0,032	ATNPSN11_NPSN11_NSPN11__novel plant snare 11

Appendix

258947_at	At3g01830	82,3	13,67	2,6	6,02	Up	0,001	Calcium-binding EF-hand family protein
249188_at	At5g42830	41,63	8,33	2,62	5,00	Up	0,009	HXXXD-type acyl-transferase family protein
266017_at	At2g18690	457,6	82,53	2,77	5,54	Up	0,001	unknown protein
262218_at	At1g74760	84,67	9,23	2,95	9,17	Up	0,048	unknown protein
255341_at	At4g04500	104,6	13,1	2,96	7,98	Up	0,016	CRK37__cysteine-rich RLK (RECEPTOR-like protein kinase) 37
246405_at	At1g57630	151,07	17,1	3	8,83	Up	0,031	Toll-Interleukin-Resistance (TIR) domain family protein
249770_at	At5g24110	19,73	1,77	3,07	11,15	Up	0,003	ATWRKY30_WRKY30__WRKY DNA-binding protein 30
264648_at	At1g09080	77,77	11,1	3,36	7,01	Up	0,011	BIP3__Heat shock protein 70 (Hsp 70) family protein
267565_at	At2g30750	12,3	1,4	3,45	8,79	Up	0,042	CYP71A12__cytochrome P450, family 71, subfamily A, polypeptide 12
255912_at	At1g66960	32,87	3,13	3,46	10,50	Up	0,035	Terpenoid cyclases family protein
252681_at	At3g44350	42,43	2,77	3,61	15,32	Up	0,012	anac061_NAC061__NAC domain containing protein 61
266070_at	At2g18660	770,23	75,43	3,62	10,21	Up	0,041	PNP-A__plant natriuretic peptide A
257809_at	At3g27060	1612,97	109,33	3,71	14,75	Up	0,031	ATTSO2_TSO2__Ferritin/ribonucleotide reductase-like family protein
256989_at	At3g28580	14,4	1,57	3,85	9,17	Up	0,021	P-loop containing nucleoside triphosphate hydrolases superfamily protein
251035_at	At5g02220	37,93	0,7	4,77	54,19	Up	0,018	Pollen Ole e 1 allergen and extensin family protein
265913_at	At2g25625	11	102,2	-4,08	0,11	Down	0,011	unknown protein;
251109_at	At5g01600	256,3	2173,83	-3,43	0,12	Down	0,001	ATFER1_FER1__ferretin 1
252698_at	At3g43670	44,93	186,57	-2,37	0,24	Down	0,03	Copper amine oxidase family protein
263831_at	At2g40300	51,33	205,1	-2,36	0,25	Down	0,003	ATFER4_FER4__ferritin 4
259871_at	At1g76800	44,43	145,3	-1,78	0,31	Down	0,023	Vacuolar iron transporter (VIT) family protein
254232_at	At4g23600	857,4	2508,73	-1,65	0,34	Down	0,05	CORI3_JR2__Tyrosine transaminase family protein
267361_at	At2g39920	190,73	538,27	-1,57	0,35	Down	0,016	HAD superfamily, subfamily IIIB acid phosphatase
255866_at	At2g30350	22,43	65,97	-1,5	0,34	Down	0,017	Excinuclease ABC, C subunit, N-terminal
261774_at	At1g76260	18,7	51,37	-1,33	0,36	Down	0,002	DWA2__DWD (DDB1-binding WD40 protein) hypersensitive to ABA 2
246495_at	At5g16200	20,3	40,03	-1,32	0,51	Down	0,009	50S ribosomal protein-related
261203_at	At1g12845	109,43	260,87	-1,27	0,42	Down	0,047	unknown protein
263574_at	At2g16990	131,13	288,2	-1,18	0,45	Down	0,006	Major facilitator superfamily protein
253002_at	At4g38530	26,1	48,9	-1,12	0,53	Down	0,034	ATPLC1_PLC1__phospholipase C1

Appendix

267220_at	At2g02500	105,1	214,77	-1,09	0,49	Down	0,046	ATMEPCT_ISPD_MCT__Nucleotide-diphospho-sugar transferases superfamily protein
257890_s_at	At3g42570	93,43	186,23	-1,07	0,50	Down	0,019	peroxidase family protein
256676_at	At3g52180	606,93	1229,07	-1,06	0,49	Down	0,031	ATPTPKIS1_ATSEX4_DSP4_SEX4__dual specificity protein phosphatase (DsPTP1) family protein
252956_at	At4g38580	247,17	487,23	-1,06	0,51	Down	0,034	ATFP6_FP6_HIPP26__farnesylated protein 6
248839_at	At5g46690	28,47	56,37	-1,04	0,51	Down	0,022	bHLH071__beta HLH protein 71
246007_at	At5g08410	491,1	910,83	-0,99	0,54	Down	0,02	FTRA2__ferredoxin/thioredoxin reductase subunit A (variable subunit) 2
250812_at	At5g04900	109,7	216,8	-0,98	0,51	Down	0,013	NOL__NYC1-like
265454_at	At2g46530	39,63	76,8	-0,97	0,52	Down	0,007	ARF11__auxin response factor 11
262700_at	At1g76020	175,93	351,13	-0,95	0,50	Down	0,004	Thioredoxin superfamily protein
260548_at	At2g43360	77,97	139,2	-0,95	0,56	Down	0,033	BIO2_BIOB__Radical SAM superfamily protein
245884_at	At5g09300	14,9	32,9	-0,94	0,45	Down	0,006	Thiamin diphosphate-binding fold (THDP-binding) superfamily protein
251353_at	At3g61080	181,63	332,1	-0,93	0,55	Down	0,011	Protein kinase superfamily protein
245319_at	At4g16146	406,8	743,13	-0,92	0,55	Down	0,041	cAMP-regulated phosphoprotein 19-related protein
258485_at	At3g02630	205,7	372,3	-0,89	0,55	Down	0,042	Plant stearyl-acyl-carrier-protein desaturase family protein
246005_at	At5g08415	68,8	114,07	-0,87	0,60	Down	0,015	Radical SAM superfamily protein
254662_at	At4g18270	122,33	229,6	-0,87	0,53	Down	0,045	ATTRANS11_TRANS11__translocase 11
263517_at	At2g21620	766,07	1328,1	-0,87	0,58	Down	0,035	RD2__Adenine nucleotide alpha hydrolases-like superfamily protein
260986_at	At1g53580	241,33	527,97	-0,87	0,46	Down	0,006	ETHE1_GLX2-3_GLY3__glyoxalase II 3
249267_at	At5g41600	322,67	605,77	-0,84	0,53	Down	0	BTI3_RTNLB4__VIRB2-interacting protein 3
247450_at	At5g62350	1478,57	2686,23	-0,83	0,55	Down	0,018	Plant invertase/pectin methylesterase inhibitor superfamily protein
252261_at	At3g49500	43,63	72,27	-0,81	0,60	Down	0,021	RDR6_SDE1_SGS2__RNA-dependent RNA polymerase 6
265481_at	At2g15960	695,03	1167,7	-0,78	0,60	Down	0,007	unknown protein
253650_at	At4g30020	172,47	297,8	-0,76	0,58	Down	0,004	PA-domain containing subtilase family protein
267264_at	At2g22970	79,63	124,27	-0,74	0,64	Down	0,004	SCPL11__serine carboxypeptidase-like 11
256441_at	At3g10940	317,53	582,27	-0,73	0,55	Down	0,003	dual specificity protein phosphatase (DsPTP1) family protein
245712_at	At5g04360	138,53	237,83	-0,72	0,58	Down	0,046	ATLDA_ATPU1_LDA_PU1__limit dextrinase
262181_at	At1g78060	81,33	132,97	-0,72	0,61	Down	0,012	Glycosyl hydrolase family protein

Appendix

259977_at	At1g76590	174,1	299,37	-0,7	0,58	Down	0,013	PLATZ transcription factor family protein
248276_at	At5g53550	79,13	139,57	-0,69	0,57	Down	0,011	ATYSL3_YSL3__YELLOW STRIPE like 3
260007_at	At1g67870	1616,03	2549,57	-0,68	0,63	Down	0,041	glycine-rich protein
263432_at	At2g22230	82	145,7	-0,68	0,56	Down	0,016	Thioesterase superfamily protein
266848_at	At2g25950	122,4	191,67	-0,68	0,64	Down	0,024	Protein of unknown function (DUF1000)
256209_at	At1g50940	119,1	185,83	-0,64	0,64	Down	0,014	ETFALPHA__electron transfer flavoprotein alpha
264673_at	At1g09795	192,33	319,73	-0,61	0,60	Down	0,009	ATATP-PRT2_ATP-PRT2_HISN1B__ATP phosphoribosyl transferase 2
262304_at	At1g70890	534,67	789,37	-0,59	0,68	Down	0,011	MLP43__MLP-like protein 43
248591_at	At5g49650	174,4	255,87	-0,56	0,68	Down	0,005	XK-2_XK2__xylulose kinase-2

nas4x-1 Le - vs *nas4x-1* Le +

ATH1 Probe Set Identifier	AGI Code	Raw Signal Average 4x Le -	Raw Signal Average 4x Le +	SLR Average	Fold change	Change direction	T-Test p-value	Annotation
257093_at	At3g20570	200,4	127,3	0,62	1,57	Up	0,031	AtENODL9_ENODL9__early nodulin-like protein 9
246268_at	At1g31800	371,43	223,53	0,67	1,66	Up	0,039	CYP97A3_LUT5__cytochrome P450, family 97, subfamily A, polypeptide 3
262645_at	At1g62750	1649,3	916,53	0,67	1,80	Up	0,004	ATSCO1_ATSCO1/CPEF-G_SCO1__Translation elongation factor EFG/EF2 protein
257533_at	At3g10840	167,77	88,6	0,78	1,89	Up	0,028	alpha/beta-Hydrolases superfamily protein
260112_at	At1g63310	61,33	37,43	0,79	1,64	Up	0,042	unknown protein
246069_at	At5g20220	97,8	55,37	0,79	1,77	Up	0,025	zinc knuckle (CCHC-type) family protein
253062_at	At4g37590	64,53	36,73	0,82	1,76	Up	0,049	NPY5__Phototropic-responsive NPH3 family protein
260481_at	At1g10960	1738,43	975,43	0,85	1,78	Up	0,018	ATFD1_FD1__ferredoxin 1
259166_at	At3g01670	193,33	99,5	0,86	1,94	Up	0,01	unknown protein
248838_at	At5g46800	749,4	387,43	0,92	1,93	Up	0,027	BOU__Mitochondrial substrate carrier family protein
264014_at	At2g21210	410,77	220,47	0,95	1,86	Up	0,023	SAUR-like auxin-responsive protein family
262526_at	At1g17050	188,6	83,37	1,04	2,26	Up	0,018	SPS2__solaneyl diphosphate synthase 2
257642_at	At3g25710	44,7	20,13	1,04	2,22	Up	0,002	ATAIG1_BHLH32_TMO5__basic helix-loop-helix 32
245981_at	At5g13100	169,13	78,7	1,07	2,15	Up	0,003	unknown protein

Appendix

251984_at	At3g53260	518,73	197,33	1,11	2,63	Up	0,002	ATPAL2_PAL2__phenylalanine ammonia-lyase 2
245196_at	At1g67750	192,8	84,1	1,14	2,29	Up	0,037	Pectate lyase family protein
263973_at	At2g42740	96,8	46,5	1,14	2,08	Up	0,046	RPL16A__ribosomal protein large subunit 16A
247218_at	At5g65010	433,4	197,1	1,17	2,20	Up	0,012	ASN2__asparagine synthetase 2
257151_at	At3g27200	94	40,1	1,27	2,34	Up	0,012	Cupredoxin superfamily protein
262376_at	At1g72970	183,37	78,17	1,32	2,35	Up	0,015	EDA17_HTH__Glucose-methanol-choline (GMC) oxidoreductase family protein
250661_at	At5g07030	200,77	61,03	1,36	3,29	Up	0,002	Eukaryotic aspartyl protease family protein
264809_at	At1g08830	2564,97	935,2	1,39	2,74	Up	0,04	CSD1__copper/zinc superoxide dismutase 1
261068_at	At1g07450	23,77	9,47	1,43	2,51	Up	0,036	NAD(P)-binding Rossmann-fold superfamily protein
261914_at	At1g65870	47,8	19,8	1,43	2,41	Up	0,036	Disease resistance-responsive (dirigent-like protein) family protein
257866_at	At3g17770	179,3	64,57	1,47	2,78	Up	0,002	Dihydroxyacetone kinase
264931_at	At1g60590	137,9	33,63	2,03	4,10	Up	0,006	Pectin lyase-like superfamily protein
266165_at	At2g28190	3261,7	803,13	2,15	4,06	Up	0,001	CSD2_CZSOD2__copper/zinc superoxide dismutase 2
259511_at	At1g12520	676,73	156,77	2,17	4,32	Up	0,001	ATCCS_CCS__copper chaperone for SOD1
258419_at	At3g16670	646,17	145,13	2,3	4,45	Up	0,027	Pollen Ole e 1 allergen and extensin family protein
245296_at	At4g16370	892,63	130,8	2,63	6,82	Up	0,047	ATOPT3_OPT3_OPT3__oligopeptide transporter
248270_at	At5g53450	1871,3	210,57	3,07	8,89	Up	0,037	ORG1__OBP3-responsive gene 1
251704_at	At3g56360	1512,67	132,07	3,21	11,45	Up	0,047	unknown protein
262218_at	At1g74760	58,87	6,33	3,61	9,30	Up	0,022	unknown protein
251109_at	At5g01600	186,63	4363,63	-4,64	0,04	Down	0,026	ferritin 1 precursor ;supported by full-length cDNA: Ceres:1100.
252698_at	At3g43670	19,93	246,43	-3,59	0,08	Down	0,002	Copper amine oxidase family protein
263831_at	At2g40300	38,67	378,47	-3,58	0,10	Down	0,019	ATFER4_FER4__ferritin 4
252300_at	At3g49160	8,3	115,2	-3,5	0,07	Down	0,023	pyruvate kinase family protein
251735_at	At3g56090	92	868,43	-3,5	0,11	Down	0,013	ATFER3_FER3__ferritin 3

nas4x-1 Le + vs WT Le +

ATH1 Probe Set Identifier	AGI Code	Raw Signal Average 4x Le +	Raw Signal Average WT Le +	SLR Average	Fold change	Change direction	T-Test p-value	Annotation
---------------------------	----------	----------------------------	----------------------------	-------------	-------------	------------------	----------------	------------

Appendix

257701_at	At3g12710	62,47	31,33	0,8	1,99	Up	0,001	DNA glycosylase superfamily protein
260221_at	At1g74670	1085,53	548,8	1,04	1,98	Up	0,032	Gibberellin-regulated family protein
252421_at	At3g47540	121,3	49,33	1,04	2,46	Up	0,019	Chitinase family protein
266352_at	At2g01610	40,77	15,87	1,14	2,57	Up	0,042	Plant invertase/pectin methylesterase inhibitor superfamily protein
252374_at	At3g48100	71,6	26,4	1,2	2,71	Up	0,034	ARR5_ATRR2_IBC6_RR5__response regulator 5
245317_at	At4g15610	40,9	17,43	1,37	2,35	Up	0,007	Uncharacterised protein family (UPF0497)
248611_at	At5g49520	31,5	8,87	1,37	3,55	Up	0,018	ATWRKY48_WRKY48__WRKY DNA-binding protein 48
255822_at	At2g40610	495,43	192,57	1,5	2,57	Up	0,035	ATEXP8_ATEXPA8_ATHEXP ALPHA 1.11_EXP8_EXPA8__expansin A8
256526_at	At1g66090	52,5	18,9	1,53	2,78	Up	0,017	Disease resistance protein (TIR-NBS class)
255333_at	At4g04410	40,3	9,7	1,92	4,15	Up	0,036	unknown protein
251735_at	At3g56090	868,43	249,13	1,93	3,49	Up	0,015	ATFER3_FER3__ferritin 3
265221_s_at	At2g02010	31,8	6	2,38	5,30	Up	0,037	GAD4__glutamate decarboxylase 4
253608_at	At4g30290	27	2,77	3,76	9,75	Up	0,032	ATXTH19_XTH19__xyloglucan endotransglucosylase/hydrolase 19
248048_at	At5g56080	99,17	6,6	4,15	15,03	Up	0	ATNAS2_NAS2__nicotianamine synthase 2
261594_at	At1g33240	187,37	118,83	0,52	1,58	Up	0,008	AT-GTL1_AT-GTL2_GTL1__GT-2-like 1
258288_at	At3g23295	22,27	12,9	0,87	1,73	Up	0,022	unknown protein
254225_at	At4g23670	1528,83	2262,63	-0,58	0,68	Down	0,003	Polyketide cyclase/dehydrase and lipid transport superfamily protein
260086_at	At1g63240	61,63	92	-0,63	0,67	Down	0,001	unknown protein
253382_at	At4g33040	109,8	174,6	-0,69	0,63	Down	0	Thioredoxin superfamily protein
248271_at	At5g53420	317,63	515,13	-0,74	0,62	Down	0,038	CCT motif family protein
255626_at	At4g00780	924,2	1570,17	-0,75	0,59	Down	0,006	TRAF-like family protein
266802_at	At2g22900	66,67	108,17	-0,77	0,62	Down	0,042	Galactosyl transferase GMA12/MNN10 family protein
264899_at	At1g23130	1824,03	3295,97	-0,82	0,55	Down	0,028	Polyketide cyclase/dehydrase and lipid transport superfamily protein
262811_at	At1g11700	108,67	203,23	-0,83	0,53	Down	0,018	Protein of unknown function, DUF584
254580_at	At4g19390	137,1	272,23	-0,89	0,50	Down	0,006	Uncharacterised protein family (UPF0114)
259765_at	At1g64370	1177,1	2287,3	-0,9	0,51	Down	0,023	unknown protein
255521_at	At4g02280	17,7	28,67	-0,96	0,62	Down	0,015	ATSUS3_SUS3__sucrose synthase 3
261046_at	At1g01390	15,4	36,63	-0,97	0,42	Down	0,02	UDP-Glycosyltransferase superfamily protein

Appendix

265272_at	At2g28350	24,63	65,97	-0,97	0,37	Down	0,046	ARF10__auxin response factor 10
260007_at	At1g67870	1342,4	2549,57	-0,99	0,53	Down	0,048	glycine-rich protein
262357_at	At1g73040	70,93	131,43	-1,06	0,54	Down	0,047	Mannose-binding lectin superfamily protein
254066_at	At4g25480	237,23	507,13	-1,07	0,47	Down	0,007	ATCBF3_CBF3_DREB1A__dehydration response element B1A
263574_at	At2g16990	152,77	288,2	-1,09	0,53	Down	0,04	Major facilitator superfamily protein
260012_at	At1g67865	1280,63	2957,83	-1,15	0,43	Down	0,044	unknown protein
266996_at	At2g34490	33,87	74,47	-1,17	0,45	Down	0,006	CYP710A2__cytochrome P450, family 710, subfamily A, polypeptide 2
254153_at	At4g24450	84,67	232,13	-1,54	0,36	Down	0,004	ATGWD2_GWD3_PWD__phosphoglucan, water dikinase
246716_s_at	At5g28910	7,37	23,93	-1,57	0,31	Down	0,024	unknown protein
250207_at	At5g13930	269,3	675,63	-1,62	0,40	Down	0,033	ATCHS_CHS_TT4__Chalcone and stilbene synthase family protein
256940_at	At3g30720	179,9	1098,23	-2,51	0,16	Down	0,019	QQS__qua-quine starch
259632_at	At1g56430	10,1	56,73	-2,9	0,18	Down	0,025	ATNAS4_NAS4__nicotianamine synthase 4

nas4x-1 Le - vs WT Le -

ATH1 Probe Set Identifier	AGI Code	Raw Signal Average 4x Le -	Raw Signal Average WT Le -	SLR Average	Fold change	Change direction	T-Test p-value	Annotation
259577_at	At1g35340	361,27	235,13	0,6	1,54	Up	0,008	Annotation (Lookup from 2009-07-29)
260704_at	At1g32470	1945,77	1242,43	0,63	1,57	Up	0,02	ATP-dependent protease La (LON) domain protein
249063_at	At5g44110	65,1	43,23	0,64	1,51	Up	0,03	Single hybrid motif superfamily protein
265377_at	At2g05790	460,23	298,1	0,67	1,54	Up	0,019	ATNAP2_ATPOP1_POP1__P-loop containing nucleoside triphosphate hydrolases superfamily protein
256671_at	At3g52290	94,63	58,6	0,67	1,61	Up	0,041	O-Glycosyl hydrolases family 17 protein
257072_at	At3g14220	219,33	140,03	0,67	1,57	Up	0,007	IQD3__IQ-domain 3
245042_at	At2g26540	206,87	136,93	0,72	1,51	Up	0,005	GDSL-like Lipase/Acylhydrolase superfamily protein
246511_at	At5g15490	151,97	98,37	0,77	1,54	Up	0,024	ATDUF3_ATUROS_DUF3_HEMD_UROS__uroporphyrinogen-III synthase family protein
266704_at	At2g19940	204,07	116,2	0,8	1,76	Up	0,009	UDP-glucose 6-dehydrogenase family protein
249916_at	At5g22880	104,07	63,3	0,8	1,64	Up	0,012	oxidoreductases, acting on the aldehyde or oxo group of donors, NAD or NADP as acceptor;copper ion binding
253877_at	At4g27435	53,63	33,07	0,81	1,62	Up	0,007	H2B_HTB2__histone B2

Appendix

246028_at	At5g21170	155,43	92,63	0,82	1,68	Up	0,009	Protein of unknown function (DUF1218)
249120_at	At5g43750	644,23	379,93	0,84	1,70	Up	0,018	AKINBETA1__5'-AMP-activated protein kinase beta-2 subunit protein
250512_at	At5g09995	79,1	45,83	0,85	1,73	Up	0,036	NDH18__NAD(P)H dehydrogenase 18
253729_at	At4g29360	24,4	13	0,87	1,88	Up	0,029	unknown protein
257983_at	At3g20790	247,27	138,97	0,9	1,78	Up	0,002	O-Glycosyl hydrolases family 17 protein
250933_at	At5g03170	62	37	0,91	1,68	Up	0,05	NAD(P)-binding Rossmann-fold superfamily protein
261306_at	At1g48610	53,67	31,17	0,91	1,72	Up	0,023	ATFLA11_FLA11__FASCICLIN-like arabinogalactan-protein 11
251972_at	At3g53170	35,03	18,2	0,92	1,92	Up	0,034	AT hook motif-containing protein
246962_s_at	At5g24800	194,2	103,93	0,93	1,87	Up	0,034	Tetratricopeptide repeat (TPR)-like superfamily protein
266087_at	At2g37790	131,2	61,93	0,95	2,12	Up	0,019	ATBZIP9_BZIP9_BZO2H2__basic leucine zipper 9
248287_at	At5g52970	438,53	231,33	0,95	1,90	Up	0,012	NAD(P)-linked oxidoreductase superfamily protein
267094_at	At2g38080	78,07	38,5	0,96	2,03	Up	0,021	thylakoid lumen 15.0 kDa protein
247692_s_at	At5g59690	676,63	345	0,98	1,96	Up	0,009	ATLMCO4_IRX12_LAC4_LMCO4__Laccase/Diphenol oxidase family protein
262796_at	At1g20850	261,4	136,47	0,98	1,92	Up	0,008	Histone superfamily protein
256673_at	At3g52370	51,93	25,97	1,01	2,00	Up	0,017	XCP2__xylem cysteine peptidase 2
263689_at	At1g26820	59,67	29,03	1,04	2,06	Up	0,032	FLA15__FASCICLIN-like arabinogalactan protein 15 precursor
245426_at	At4g17540	49,3	25,03	1,05	1,97	Up	0,011	RNS3__ribonuclease 3
249469_at	At5g39320	81,63	40,33	1,05	2,02	Up	0,025	unknown protein
253397_at	At4g32710	28,27	12,8	1,08	2,21	Up	0,002	UDP-glucose 6-dehydrogenase family protein
245196_at	At1g67750	192,8	96,43	1,09	2,00	Up	0,049	Protein kinase superfamily protein
251395_at	At2g45470	451,1	217,6	1,09	2,07	Up	0,016	Pectate lyase family protein
245980_at	At5g13140	145,17	64,47	1,1	2,25	Up	0,003	AGP8_FLA8__FASCICLIN-like arabinogalactan protein 8
245981_at	At5g13100	169,13	79,17	1,1	2,14	Up	0,008	Pollen Ole e 1 allergen and extensin family protein
257173_at	At3g23810	1061,3	438,43	1,15	2,42	Up	0,009	unknown protein
264969_at	At1g67320	45,13	19,03	1,15	2,37	Up	0,023	ATSAHH2_SAHH2__S-adenosyl-l-homocysteine (SAH) hydrolase 2
258170_at	At3g21600	52,93	21,57	1,16	2,45	Up	0,043	DNA primase, large subunit family
249718_at	At5g35740	53,73	19,43	1,18	2,77	Up	0,049	Senescence/dehydration-associated protein-related
251119_at	At3g63510	73,07	30,7	1,18	2,38	Up	0,024	Carbohydrate-binding X8 domain superfamily protein

Appendix

252878_at	At4g39460	283,47	125,07	1,22	2,27	Up	0,008	FMN-linked oxidoreductases superfamily protein
265383_at	At2g16780	24,83	11,5	1,26	2,16	Up	0,012	SAMC1_SAMT1__S-adenosylmethionine carrier 1
250968_at	At5g02890	113,57	49,63	1,26	2,29	Up	0,006	MSI02_MSI2_NFC02_NFC2__Transducin family protein / WD-40 repeat family protein
252361_at	At3g48490	26,5	9,77	1,28	2,71	Up	0,018	HXXXD-type acyl-transferase family protein
252200_at	At3g50280	29,27	11,67	1,28	2,51	Up	0,048	unknown protein
263628_at	At2g04780	174	76,23	1,31	2,28	Up	0,024	HXXXD-type acyl-transferase family protein
251142_at	At5g01015	148,23	69,07	1,34	2,15	Up	0,007	FLA7__FASCICLIN-like arabinogalactan 7
264262_at	At1g09200	288,1	100,8	1,36	2,86	Up	0,016	unknown protein
263612_at	At2g16440	41,1	14,83	1,38	2,77	Up	0,009	Histone superfamily protein
261774_at	At1g76260	50,4	18,7	1,4	2,70	Up	0,003	MCM4__Minichromosome maintenance (MCM2/3/5) family protein
250661_at	At5g07030	200,77	75,63	1,45	2,65	Up	0,005	DWA2__DWD (DDB1-binding WD40 protein) hypersensitive to ABA 2
262376_at	At1g72970	183,37	66,37	1,55	2,76	Up	0,018	Eukaryotic aspartyl protease family protein
253736_at	At4g28780	100,03	36,37	1,63	2,75	Up	0,017	EDA17_HTH__Glucose-methanol-choline (GMC) oxidoreductase family protein
264931_at	At1g60590	137,9	47,3	1,65	2,92	Up	0,013	GDSL-like Lipase/Acylhydrolase superfamily protein
255513_at	At4g02060	52,73	12,6	1,82	4,18	Up	0,036	Pectin lyase-like superfamily protein
264319_at	At1g04110	35,03	8,63	1,9	4,06	Up	0,034	MCM7_PRL__Minichromosome maintenance (MCM2/3/5) family protein
256527_at	At1g66100	1840,73	490,9	2,32	3,75	Up	0,04	SDD1__Subtilase family protein
258419_at	At3g16670	646,17	111,57	2,59	5,79	Up	0,034	Plant thionin
251035_at	At5g02220	4,67	37,93	-2,84	0,12	Down	0,011	Pollen Ole e 1 allergen and extensin family protein
249867_at	At5g23020	17,5	107,57	-2,54	0,16	Down	0,032	unknown protein
257154_at	At3g27210	34,57	113,33	-1,86	0,31	Down	0,031	IMS2_MAM-L_MAM3__2-isopropylmalate synthase 2
254833_s_at	At4g12280	53,97	182,83	-1,82	0,30	Down	0,031	unknown protein
245891_at	At5g09220	201,2	587,27	-1,58	0,34	Down	0,008	copper amine oxidase family protein
262137_at	At1g77920	67,8	206,23	-1,56	0,33	Down	0,003	AAP2__amino acid permease 2
251356_at	At3g61060	79,53	189,9	-1,53	0,42	Down	0,032	bZIP transcription factor family protein
258362_at	At3g14280	14,83	45,6	-1,45	0,33	Down	0,027	AtPP2-A13_PP2-A13__phloem protein 2-A13
247800_at	At5g58570	60,53	149,6	-1,44	0,40	Down	0,037	unknown protein

Appendix

253358_at	At4g32940	762,2	2014,8	-1,42	0,38	Down	0,005	unknown protein
252327_at	At3g48740	413,03	1021,23	-1,41	0,40	Down	0,027	GAMMA-VPE_GAMMAVPE__gamma vacuolar processing enzyme
255511_at	At4g02075	14,2	42,47	-1,4	0,33	Down	0,014	Nodulin MtN3 family protein
248118_at	At5g55050	33	83,57	-1,4	0,39	Down	0,029	PIT1__RING/FYVE/PHD zinc finger superfamily protein
261585_at	At1g01010	13,03	33,63	-1,39	0,39	Down	0,034	GDSL-like Lipase/Acylhydrolase superfamily protein
246440_at	At5g17650	54,47	128,6	-1,35	0,42	Down	0,028	ANAC001_NAC001__NAC domain containing protein 1
255377_at	At4g03500	10,33	34,27	-1,32	0,30	Down	0,001	glycine/proline-rich protein
253317_at	At4g33960	30,27	73,73	-1,25	0,41	Down	0,002	Ankyrin repeat family protein
249346_at	At5g40780	317	755,03	-1,25	0,42	Down	0,033	unknown protein
261046_at	At1g01390	16,77	41,87	-1,21	0,40	Down	0,027	LHT1__lysine histidine transporter 1
266518_at	At2g35170	19,13	45,8	-1,15	0,42	Down	0,019	UDP-Glycosyltransferase superfamily protein
254140_at	At4g24610	31,07	79,07	-1,15	0,39	Down	0,047	Histone H3 K4-specific methyltransferase SET7/9 family protein
262947_at	At1g75750	279,67	626,03	-1,11	0,45	Down	0,023	unknown protein
255016_at	At4g10120	202,17	427,67	-1,11	0,47	Down	0,021	GASA1__GAST1 protein homolog 1
256930_at	At3g22460	35,7	84,7	-1,09	0,42	Down	0,016	ATSPS4F__Sucrose-phosphate synthase family protein
264674_at	At1g09815	154,53	337,7	-1,09	0,46	Down	0,034	OASA2__O-acetylserine (thiol) lyase (OAS-TL) isoform A2
265382_at	At2g16790	11,73	27,63	-1,02	0,42	Down	0,018	POLD4__polymerase delta 4
260196_at	At1g67570	26,7	49,8	-1,02	0,54	Down	0,031	P-loop containing nucleoside triphosphate hydrolases superfamily protein
247751_at	At5g59050	37,4	77,9	-1,02	0,48	Down	0,015	Protein of unknown function (DUF3537)
248970_at	At5g45380	87,8	185,23	-0,99	0,47	Down	0,008	unknown protein
263986_at	At2g42790	237,3	481,83	-0,95	0,49	Down	0,008	ATDUR3_DUR3__solute:sodium symporters;urea transmembrane transporters
255341_at	At4g04500	48,5	104,6	-0,95	0,46	Down	0,028	CSY3__citrate synthase 3
264635_at	At1g65500	71,2	131,63	-0,95	0,54	Down	0,028	CRK37__cysteine-rich RLK (RECEPTOR-like protein kinase) 37
245776_at	At1g30260	159,63	308,03	-0,95	0,52	Down	0,018	unknown protein
259661_at	At1g55265	67	124,7	-0,93	0,54	Down	0,006	unknown protein
254998_at	At4g09760	291,97	537	-0,93	0,54	Down	0,022	Protein of unknown function, DUF538
265119_at	At1g62570	39,83	69,93	-0,93	0,57	Down	0,044	Protein kinase superfamily protein

Appendix

260410_at	At1g69870	225,67	471,53	-0,92	0,48	Down	0,039	FMO GS-OX4__flavin-monooxygenase glucosinolate S-oxygenase 4
256294_at	At1g69450	98	188,4	-0,89	0,52	Down	0,019	NRT1.7__nitrate transporter 1.7
252607_at	At3g44990	73,83	142,83	-0,88	0,52	Down	0,013	Early-responsive to dehydration stress protein (ERD4)
262607_at	At1g13990	250,13	474,57	-0,87	0,53	Down	0,022	ATXTR8_XTH31_XTR8__xyloglucan endo-transglycosylase-related 8
247716_at	At5g59350	86,13	147,33	-0,87	0,58	Down	0,045	unknown protein
258566_at	At3g04110	61,13	123,2	-0,85	0,50	Down	0,009	unknown protein
255507_at	At4g02150	79,7	141,43	-0,85	0,56	Down	0,04	ATGLR1.1_GLR1_GLR1.1__glutamate receptor 1.1
258092_at	At3g14595	445,77	786,03	-0,82	0,57	Down	0,029	ATIMPALPHA3_IMPA-3_MOS6__ARM repeat superfamily protein
248153_at	At5g54250	47,9	81,33	-0,78	0,59	Down	0,009	Ribosomal protein L18ae family
260443_at	At1g68185	45,6	78,33	-0,77	0,58	Down	0,048	ATCNGC4_CNGC4_DND2_HLM1__cyclic nucleotide-gated cation channel 4
254952_at	At4g10960	63,67	115,57	-0,75	0,55	Down	0,001	Ubiquitin-like superfamily protein
248495_at	At5g50780	20,73	36,33	-0,75	0,57	Down	0,008	UGE5__UDP-D-glucose/UDP-D-galactose 4-epimerase 5
264772_at	At1g22930	200,63	321,3	-0,74	0,62	Down	0,017	Histidine kinase-, DNA gyrase B-, and HSP90-like ATPase family protein
256453_at	At1g75270	73,73	136,47	-0,72	0,54	Down	0,01	T-complex protein 11
248657_at	At5g48570	41,63	70,6	-0,72	0,59	Down	0,03	DHAR2__dehydroascorbate reductase 2
254188_at	At4g23920	60,63	95,57	-0,71	0,63	Down	0,014	ATFKBP65_FKBP65_ROF2__FKBP-type peptidyl-prolyl cis-trans isomerase family protein
257227_at	At3g27820	442,13	770,37	-0,69	0,57	Down	0,019	ATUGE2_UGE2__UDP-D-glucose/UDP-D-galactose 4-epimerase 2
262867_at	At1g64960	41,4	69,03	-0,69	0,60	Down	0,048	ATMDAR4_MDAR4__monodehydroascorbate reductase 4
261141_at	At1g19740	325,97	533,03	-0,69	0,61	Down	0,04	ARM repeat superfamily protein
262496_at	At1g21790	87,3	139,83	-0,68	0,62	Down	0,031	ATP-dependent protease La (LON) domain protein
264851_at	At2g17290	67,97	107,63	-0,67	0,63	Down	0,043	TRAM, LAG1 and CLN8 (TLC) lipid-sensing domain containing protein
250556_at	At5g07920	57,77	111,47	-0,65	0,52	Down	0,003	ATCDPK3_ATCPK6_CPK6__Calcium-dependent protein kinase family protein
254068_at	At4g25450	155,27	249,87	-0,63	0,62	Down	0,033	ATDGK1_DGK1__diacylglycerol kinase1
257860_at	At3g13062	183,1	319,53	-0,62	0,57	Down	0,02	ATNAP8_NAP8__non-intrinsic ABC protein 8
255259_at	At4g05020	148,17	227,77	-0,61	0,65	Down	0,015	Polyketide cyclase/dehydrase and lipid transport superfamily protein
252134_at	At3g50910	86,8	130,43	-0,61	0,67	Down	0,042	NDB2__NAD(P)H dehydrogenase B2
264957_at	At1g77000	93,57	131,97	-0,59	0,71	Down	0,018	unknown protein

Appendix

248255_at	At5g53350	458,67	716,03	-0,59	0,64	Down	0,008	ATSKP2;2_SKP2B__RNI-like superfamily protein
259754_at	At1g71090	195,63	325,87	-0,56	0,60	Down	0,006	CLPX__CLP protease regulatory subunit X
257299_at	At3g28050	198,83	300,33	-0,53	0,66	Down	0,043	Auxin efflux carrier family protein
249400_at	At5g40300	101,37	167,57	-0,52	0,60	Down	0,024	nodulin MtN21 /EamA-like transporter family protein
254067_at	At4g25460	70,93	111,73	-0,51	0,63	Down	0,039	Uncharacterised protein family (UPF0497)

Appendix

Table A 2.6: List of enriched GO categories among the 125 differentially expressed root genes selected by ORA. Up indicates an over-representation of the gene of a specific category compared to the entire genome, down indicates an under-representation of the genes of a specific functional category. Sub-categories were assigned to six biological processes.

Enriched sub-category	Category identifier	Number of assigned genes	Category <i>P</i> -value	Regulation direction
Stress response				
response to stress	GO:0006950	59	5,40	up
response to endoplasmic reticulum stress	GO:0034976	3	0.0130285	up
anthocyanin biosynthetic process	GO:0009718	3	0.0243753	up
response to abiotic stimulus	GO:0009628	31	0.029189	up
regulation of anthocyanin biosynthetic process	GO:0031540	2	0.043968	up
cellular response to stress	GO:0033554	12	0.0456656	up
Metal homeostasis				
response to iron ion	GO:0010039	5	5,40	up
di-, tri-valent inorganic cation homeostasis	GO:0055066	7	0.0014695	up
response to inorganic substance	GO:0010035	20	0.00161192	up
ferric iron binding	GO:0008199	3	0.00186431	up
cellular di-, tri-valent inorganic cation homeostasis	GO:0030005	6	0.00251839	up
zinc ion binding	GO:0008270	4	0.00695462	down
cellular iron ion homeostasis	GO:0006879	3	0.0118087	up
response to metal ion	GO:0010038	15	0.0124338	up
iron ion homeostasis	GO:0055072	3	0.0148829	up
iron ion transport	GO:0006826	3	0.0181105	up
di-, tri-valent inorganic cation transport	GO:0015674	4	0.0361504	up
metal ion homeostasis	GO:0055065	4	0.043968	up
Oxidative stress				
response to reactive oxygen species	GO:0000302	8	0.00097568	up
catalytic activity	GO:0003824	147	0.00265569	up
response to oxidative stress	GO:0006979	14	0.00265569	up
superoxide dismutase activity	GO:0004784	3	0.0071467	up
oxidoreductase activity, acting on superoxide radicals as acceptor	GO:0016721	3	0.0071467	up
oxidoreductase activity	GO:0016491	36	0.00894733	up
cellular response to reactive oxygen species	GO:0034614	3	0.0243753	up
cellular response to oxidative stress	GO:0034599	3	0.029189	up

Appendix

Enriched sub-category	Category identifier	Number of assigned genes	Category <i>P</i>-value	Regulation direction
Small organic acid metabolism				
radical SAM enzyme activity	GO:0070283	3	0.0014695	up
organic acid metabolic process	GO:0006082	24	0.00296259	up
carboxylic acid metabolic process	GO:0019752	24	0.00296259	up
oxoacid metabolic process	GO:0043436	24	0.00296259	up
small molecule metabolic process	GO:0044281	37	0.0120423	up
peptide transporter activity	GO:0015197	3	0.0396078	up
oligopeptide transporter activity	GO:0015198	3	0.0396078	up
small molecule biosynthetic process	GO:0044283	20	0.041828	up
amine metabolic process	GO:0009308	13	0.0419101	up
organic acid biosynthetic process	GO:0016053	12	0.0419101	up
carboxylic acid biosynthetic process	GO:0046394	12	0.0419101	up
monocarboxylic acid metabolic process	GO:0032787	12	0.0496013	up
NA biosynthesis				
nicotianamine synthase activity	GO:0030410	2	0.0282811	up
nicotianamine metabolic process	GO:0030417	2	0.0282811	up
nicotianamine biosynthetic process	GO:0030418	2	0.0282811	up
DNA modification				
DNA-dependent DNA replication	GO:0006261	5	0.0130285	up
DNA replication	GO:0006260	7	0.0131401	up
DNA conformation change	GO:0071103	6	0.0266157	up
Others				
response to stimulus	GO:0050896	87	5,40	up
cell	GO:0005623	238	0.00015478	up
cell part	GO:0044464	238	0.00015478	up
cell wall	GO:0005618	22	0.0014695	up
cellular ketone metabolic process	GO:0042180	26	0.0014695	up
cation homeostasis	GO:0055080	8	0.0014695	up

Appendix

external encapsulating structure	GO:0030312	22	0.0015162	up
response to chemical stimulus	GO:0042221	49	0.00186431	up
ion homeostasis	GO:0050801	8	0.00223776	up
cellular cation homeostasis	GO:0030003	7	0.00251068	up
cellular ion homeostasis	GO:0006873	7	0.00350783	up
cellular chemical homeostasis	GO:0055082	7	0.00368611	up
chemical homeostasis	GO:0048878	8	0.00695462	up
vacuole	GO:0005773	20	0.0071467	up
endoplasmic reticulum lumen	GO:0005788	3	0.0071467	up
cytoplasm	GO:0005737	115	0.008115	up
defense response	GO:0006952	23	0.00894473	up
sulfurtransferase activity	GO:0016783	3	0.00894733	up
cytoplasmic part	GO:0044444	106	0.0131265	up
cofactor binding	GO:0048037	11	0.0135957	up
cellular process	GO:0009987	155	0.0148829	up
intracellular part	GO:0044424	145	0.0148829	up
FAD binding	GO:0050660	6	0.0243753	up
response to biotic stimulus	GO:0009607	19	0.0250222	up
membrane-bounded organelle	GO:0043227	125	0.029189	up
intracellular membrane-bounded organelle	GO:0043231	125	0.029189	up
subsynaptic reticulum	GO:0071212	5	0.029189	up
starch metabolic process	GO:0005982	4	0.0309575	up
sulfur compound biosynthetic process	GO:0044272	6	0.0312366	up
lipoic acid metabolic process	GO:0000273	2	0.0361504	up
intracellular	GO:0005622	146	0.0372427	up
cellular homeostasis	GO:0019725	8	0.0372427	up
coenzyme biosynthetic process	GO:0009108	5	0.0396078	up
homeostatic process	GO:0042592	9	0.0473612	up
response to bacterium	GO:0009617	10	0.04801	up
protein folding	GO:0006457	9	0.0496013	up
coenzyme binding	GO:0050662	8	0.0496013	up

Table A 2.7: List of enriched GO categories among the 337 differentially expressed leaf genes selected by ORA. Up indicates an over-representation of a gene of a specific category compared to the entire genome, down indicates an under-representation of the gene of a specific functional category. Sub-categories were assigned to six biological processes.

Enriched sub-category	Category identifier	Number of assigned genes	Category <i>P</i> -value	Regulation direction
Stress response				
response to stress	GO:0006950	59	5.40	up
response to endoplasmic reticulum stress	GO:0034976	3	0.0130285	up
anthocyanin biosynthetic process	GO:0009718	3	0.0243753	up
response to abiotic stimulus	GO:0009628	31	0.029189	up
regulation of anthocyanin biosynthetic process	GO:0031540	2	0.043968	up
cellular response to stress	GO:0033554	12	0.0456656	up
Enriched sub-category	Category identifier	Number of assigned genes	Category <i>P</i> -value	Regulation direction

Appendix

Metal homeostasis				
response to iron ion	GO:0010039	5	5,40	up
di-, tri-valent inorganic cation homeostasis	GO:0055066	7	0.0014695	up
response to inorganic substance	GO:0010035	20	0.00161192	up
ferric iron binding	GO:0008199	3	0.00186431	up
cellular di-, tri-valent inorganic cation homeostasis	GO:0030005	6	0.00251839	up
di-, tri-valent inorganic cation transport	GO:0015674	4	0.0361504	up
oligopeptide transporter activity	GO:0015198	3	0.0396078	up
zinc ion binding	GO:0008270	4	0.00695462	down
cellular iron ion homeostasis	GO:0006879	3	0.0118087	up
response to metal ion	GO:0010038	15	0.0124338	up
iron ion homeostasis	GO:0055072	3	0.0148829	up
iron ion transport	GO:0006826	3	0.0181105	up
metal ion homeostasis	GO:0055065	4	0.043968	up
Enriched sub-category	Category identifier	Number of assigned genes	Category P-value	Regulation direction
Oxidative stress				
response to reactive oxygen species	GO:0000302	8	0.00097568	up
catalytic activity	GO:0003824	147	0.00265569	up
response to oxidative stress	GO:0006979	14	0.00265569	up
superoxide dismutase activity	GO:0004784	3	0.0071467	up
oxidoreductase activity, acting on superoxide radicals as acceptor	GO:0016721	3	0.0071467	up
oxidoreductase activity	GO:0016491	36	0.00894733	up
cellular response to reactive oxygen species	GO:0034614	3	0.0243753	up
cellular response to oxidative stress	GO:0034599	3	0.029189	up
Enriched sub-category	Category identifier	Number of assigned genes	Category P-value	Regulation direction
Small organic acid metabolism				
radical SAM enzyme activity	GO:0070283	3	0.0014695	up
organic acid metabolic process	GO:0006082	24	0.00296259	up
carboxylic acid metabolic process	GO:0019752	24	0.00296259	up
oxoacid metabolic process	GO:0043436	24	0.00296259	up
small molecule metabolic process	GO:0044281	37	0.0120423	up
peptide transporter activity	GO:0015197	3	0.0396078	up
small molecule biosynthetic process	GO:0044283	20	0.041828	up
amine metabolic process	GO:0009308	13	0.0419101	up
organic acid biosynthetic process	GO:0016053	12	0.0419101	up
carboxylic acid biosynthetic process	GO:0046394	12	0.0419101	up
monocarboxylic acid metabolic process	GO:0032787	12	0.0496013	up
Enriched sub-category	Category identifier	Number of assigned genes	Category P-value	Regulation direction
NA biosynthesis				
nicotianamine synthase activity	GO:0030410	2	0.0282811	up
nicotianamine metabolic process	GO:0030417	2	0.0282811	up
nicotianamine biosynthetic process	GO:0030418	2	0.0282811	up

Appendix

Enriched sub-category	Category identifier	Number of assigned genes	Category P-value	Regulation direction
DNA modification				
DNA-dependent DNA replication	GO:0006261	5	0.0130285	up
DNA replication	GO:0006260	7	0.0131401	up
DNA conformation change	GO:0071103	6	0.0266157	up
Enriched sub-category	Category identifier	Number of assigned genes	Category P-value	Regulation direction
Others				
response to stimulus	GO:0050896	87	5,40	up
cell	GO:0005623	238	0.00015478	up
cell part	GO:0044464	238	0.00015478	up
cell wall	GO:0005618	22	0.0014695	up
cellular ketone metabolic process	GO:0042180	26	0.0014695	up
cation homeostasis	GO:0055080	8	0.0014695	up
external encapsulating structure	GO:0030312	22	0.0015162	up
response to chemical stimulus	GO:0042221	49	0.00186431	up
ion homeostasis	GO:0050801	8	0.00223776	up
cellular cation homeostasis	GO:0030003	7	0.00251068	up
cellular ion homeostasis	GO:0006873	7	0.00350783	up
cellular chemical homeostasis	GO:0055082	7	0.00368611	up
chemical homeostasis	GO:0048878	8	0.00695462	up
vacuole	GO:0005773	20	0.0071467	up
endoplasmic reticulum lumen	GO:0005788	3	0.0071467	up
cytoplasm	GO:0005737	115	0.008115	up
defense response	GO:0006952	23	0.00894473	up
sulfurtransferase activity	GO:0016783	3	0.00894733	up
heterocycle biosynthetic process	GO:0018130	8	0.0130285	up
cytoplasmic part	GO:0044444	106	0.0131265	up
cofactor binding	GO:0048037	11	0.0135957	up
cellular process	GO:0009987	155	0.0148829	up
intracellular part	GO:0044424	145	0.0148829	up
lipoate metabolic process	GO:0009106	2	0.0200588	up
lipoate biosynthetic process	GO:0009107	2	0.0200588	up
FAD binding	GO:0050660	6	0.0243753	up
response to biotic stimulus	GO:0009607	19	0.0250222	up
lipoic acid biosynthetic process	GO:0009105	2	0.0282811	up
starch metabolic process	GO:0005982	4	0.0309575	up
sulfur compound biosynthetic process	GO:0044272	6	0.0312366	up
lipoic acid metabolic process	GO:0000273	2	0.0361504	up
intracellular	GO:0005622	146	0.0372427	up
cellular homeostasis	GO:0019725	8	0.0372427	up
coenzyme biosynthetic process	GO:0009108	5	0.0396078	up
homeostatic process	GO:0042592	9	0.0473612	up
response to bacterium	GO:0009617	10	0.04801	up
protein folding	GO:0006457	9	0.0496013	up
coenzyme binding	GO:0050662	8	0.0496013	up

References

- Abadía J, S Vázquez, R Rellán-Álvarez, H El-Jendoubi, A Abadía, A Alvarez-Fernández, and A F López-Millán. 2011. Towards a knowledge-based correction of iron chlorosis. *Plant Physiology and Biochemistry* 49, no. 5: 482-471.
- Abdel-Ghany, S E, Salah E, and M Pilon. 2008. MicroRNA-mediated systemic down-regulation of copper protein expression in response to low copper availability in Arabidopsis. *The Journal of biological Chemistry* 283, no. 23: 15932-45.
- Alonso, J M, A Stepanova, T J Leisse, C J Kim, H Chen, P Shinn, K Stevenson, et al. 2003. Genome-wide insertional mutagenesis of Arabidopsis thaliana. *Science*, 301, no. 5630: 653-657
- Alscher, R. G. 2002. Role of superoxide dismutases (SODs) in controlling oxidative stress in plants. *Journal of Experimental Botany* 53, no. 372: 1331-1341.
- Anderegg, G, and H Ripperger. 1989. Correlation between Metal Complex Formation and Biological Activity of Nicotianamine Analogues. *Journal of the Chemical Society, Chemical Communications* 10, no. 3: 647-650.
- Andres-Colas, N, V Sancenon, S Rodriguez-Navarro, S Mayo, D J Thiele, J R Ecker, S Puig, and L Penarrubia. 2006. The Arabidopsis heavy metal P-type ATPase HMA5 interacts with metallochaperones and functions in copper detoxification of roots. *Plant J* 45, no. 2: 225-236.
- Azouaou, Z, and A Souvre. 1993. Effects of copper deficiency on pollen fertility and nucleic acids in the durum wheat anther. *Sexual Plant Reproduction* 6, no. 3: 199-204-204.
- Backes, C, A Keller, J Kuentzer, B Kneissl, N Comtesse, Y A Elnakady, R Muller, E Meese, and H P Lenhof. 2007. GeneTrail--advanced gene set enrichment analysis. *Nucleic Acids Res* 35, no. Web Server issue: W186-92.
- Balk, J, and S Lobréaux. 2005. Biogenesis of iron-sulfur proteins in plants. *Trends in plant science* 10, no. 7: 324-31.
- Bashir, K, H Inoue, Seiji Nagasaka, Michiko Takahashi, Hiromi Nakanishi, Satoshi Mori, and Naoko K Nishizawa. 2006. Cloning and characterization of deoxymugineic acid synthase genes from graminaceous plants. *Journal of Biological Chemistry* 281, no. 43: 32395-32402.
- Bauer, P, Z Berczky, T Brumbarova, M Klatter, and H Y Wang. 2004. Molecular regulation of iron uptake in the dicot species *Lycopersicon esculentum* and Arabidopsis thaliana. *Soil Science and Plant Nutrition* 50, no. 7: 997-1001.
- Beard, J L, J W Burton, E C Theil. 1996. Purified Ferritin and Soybean Meal Can be Sources of Iron for Treating Iron Deficiency in Rats. *The Journal of Nutrition*, no. 126: 154-160

References

- Becher, M, I N Talke, L Krall, and U Krämer. 2004. Cross-species microarray transcript profiling reveals high constitutive expression of metal homeostasis genes in shoots of the zinc hyperaccumulator *Arabidopsis halleri*. *Plant Journal* 37, no. 2: 251-268.
- Bechthold, N. 1994. *Arabidopsis protocols*.
- Becker, R, E Fritz, and R Manteuffel. 1995. Subcellular Localization and Characterization of Excessive Iron in the Nicotianamine-less Tomato Mutant chloronerva. *Plant Physiology* 108, no. 1: 269-275.
- Bell, W D, L Bogorad, and W J McIlrath. 1958. Response of the Yellow-Stripe Maize Mutant *ysl* to Ferrous and Ferric Iron. *Botanical Gazette* 120, no. 1: 36-39.
- Bencze, K Z, Kalyan C Kondapalli, J D Cook, S McMahon, C Millán-Pacheco, N Pastor, and T L Stemmler. 2006. The structure and function of frataxin. *Critical reviews in biochemistry and molecular biology* 41, no. 5: 269-91.
- Benes, I, K Schreiber, H Ripperger, and A Kircheiss. 1983. Metal complex formation of nicotianamine, a possible phytosiderophore. *Experientia* 39: 261-262.
- Bennett, M. D. 2003. Comparisons with *Caenorhabditis* (100 Mb) and *Drosophila* (175 Mb) Using Flow Cytometry Show Genome Size in *Arabidopsis* to be 157 Mb and thus 25 % Larger than the *Arabidopsis* Genome Initiative Estimate of 125 Mb. *Annals of Botany* 91, no. 5: 547-557.
- Bohn, L, A S Meyer, and S K Rasmussen. 2008. Phytate: impact on environment and human nutrition. A challenge for molecular breeding. *Journal of Zhejiang University. Science. B* 9, no. 3: 165-91.
- Bolstad, B M, R A Irizarry, M Astrand, and T P Speed. 2003. A comparison of normalization methods for high density oligonucleotide array data based on variance and bias. *Bioinformatics* 19, no. 2: 185-193.
- Bradford, M. 1976. A rapid and sensitive method for the quantitation of microgram quantities of protein utilizing the principle of protein-dye binding. *Analytical Biochemistry* 72, no.
- Briat, J F, and M Lebrun. 1999. Plant responses to metal toxicity. *Comptes Rendus de l'Academie des Sciences. Serie III* 322, no. 1: 43-54.
- Briat, J F, S Lobreaux, N Grignon, and G Vansuyt. 1999. Regulation of plant ferritin synthesis: how and why. *Cellular and Molecular Life Sciences* 56, no. 1-2: 155-166.
- Briat, J. F. 1996. Roles of ferritin in plants. *Journal of Plant Nutrition* 19, no. 8:157-162
- Briat, J.F., and S. Lobreaux. 1997. Iron transport and storage in plants. *Trends in Plant Science* 2, no. 5: 187-193.

References

- Buchanan-Wollaston, V, and C Ainsworth. 1997. *Leaf senescence in Brassica napus: cloning of senescence related genes by subtractive hybridisation*. *Plant Molecular Biology*. Vol. 33. Springer Netherlands.
- Buděšínský, M, H Budzikiewicz, Ž Procházka, H Ripperger, A Römer, G Scholz, and K Schreiber. 1980. Nicotianamine, a possible phytosiderophore of general occurrence. *Phytochemistry* 19, no. 11: 2295-2297.
- Busch, A, B Rimbauld, B Naumann, S Rensch, and M Hippler. 2008. Ferritin is required for rapid remodeling of the photosynthetic apparatus and minimizes photo-oxidative stress in response to iron availability in *Chlamydomonas reinhardtii*. *The Plant journal: for cell and molecular biology* 55, no. 2: 201-11.
- Busi, M V, M V Maliandi, H Valdez, M Clemente, E J Zabaleta, A Araya, and D F Gomez-Casati. 2006. Deficiency of *Arabidopsis thaliana* frataxin alters activity of mitochondrial Fe-S proteins and induces oxidative stress. *The Plant journal: for cell and molecular biology* 48, no. 6: 873-82.
- Busi, V, E J Zabaleta, A Araya, and D F Gomez-Casati. 2004. Functional and molecular characterization of the frataxin homolog from *Arabidopsis thaliana*. *FEBS letters* 576, no. 1-2: 141-4.
- Böhme, H, and G Scholz. 1960. Versuche zur Normalisierung des Phänotyps der Mutante chloronerva von *Lycopersicon esculentum*. *Kulturpflanze* 8, no. 1: 93-109.
- Callahan, D L, S D Kolev, R A J O'Hair, D E Salt, and A J M Baker. 2007. Relationships of nicotianamine and other amino acids with nickel, zinc and iron in *Thlaspi* hyperaccumulators. *New Phytologist* 176, no. 4: 836-848.
- Carlini, R G, E Alonzo, E Bellorin-Font, and J R Weisinger. 2006. Apoptotic stress pathway activation mediated by iron on endothelial cells in vitro. *Nephrology, dialysis, transplantation: official publication of the European Dialysis and Transplant Association - European Renal Association* 21, no. 11: 3055-61.
- Carrondo, M Arménia. 2003. Ferritins, iron uptake and storage from the bacterioferritin viewpoint. *The EMBO journal* 22, no. 9: 1959-68.
- Cheng, L, F Wang, H Shou, F Huang, L Zheng, F He, J Li, et al. 2007. Mutation in Nicotianamine Aminotransferase Stimulated the Fe(II) Acquisition System and Led to Iron Accumulation in Rice. *Plant Physiology* 145: 1647-1657.
- Cherian, G, and H Chan. 1993. Biological functions of metallothioneins—a review: 1993-1993.
- Chu, H-H, J Chiecko, T Punshon, A Lanzirrotti, B Lahner, D E Salt, and E L Walker. 2010. Successful reproduction requires the function of *Arabidopsis* Yellow Stripe-Like1 and Yellow Stripe-Like3 metal-nicotianamine transporters in both vegetative and reproductive structures. *Plant physiology* 154, no. 1: 197-210.

References

- Clausen, C, I Ilkavets, R Thomson, K Philippar, A Vojta, T Mohlmann, E Neuhaus, H Fulgosi, and J Soll. 2004. Intracellular localization of VDAC proteins in plants. *Planta* 220, no. 1: 30-37.
- Clemens, S, Michael G Palmgren, and U Krämer. 2002. A long way ahead: understanding and engineering plant metal accumulation. *Trends in Plant Science* 7, no. 7: 309-315.
- Clough, S J, and A F Bent. 1998. Floral dip: a simplified method for *Agrobacterium*-mediated transformation of *Arabidopsis thaliana*. *The Plant Journal* 16, no. 6: 735-743.
- Cobbett, C S. 2000. Update on Heavy Metal Stress Phytochelatins and Their Roles in Heavy Metal Detoxification. *Society* 123, no.3: 825-832.
- Cobbett, C, and P Goldsbrough. 2002a. Phytochelatins and metallothioneins: roles in heavy metal detoxification and homeostasis. *Annual review of plant biology*, no. 53: 159-82.
- Cohu, C M., and M Pilon. 2007. Regulation of superoxide dismutase expression by copper availability. *Physiologia Plantarum* 129, no. 4: 747-755.
- Colangelo, E P, and M L Guerinot. 2004. The essential basic helix-loop-helix protein FIT1 is required for the iron deficiency response. *Plant Cell* 16, no. 12: 3400-3412.
- Colangelo, E P, and M L Guerinot. 2006. Put the metal to the petal: metal uptake and transport throughout plants. *Current opinion in plant biology* 9, no. 3: 322-30.
- Connolly, E L, N H Campbell, N Grotz, C L Prichard, and M L Guerinot. 2003. Overexpression of the FRO2 ferric chelate reductase confers tolerance to growth on low iron and uncovers posttranscriptional control. *Plant Physiology* 133, no. 3: 1102-1110.
- Cordano, A. 1998. Clinical manifestations of nutritional copper deficiency in infants and children. *Am J Clin Nutr* 67, no. 5: 1012S-1016.
- Crawford, B C W, G Ditta, and M F Yanofsky. 2007. The NTT gene is required for transmitting-tract development in carpels of *Arabidopsis thaliana*. *Current Biology: CB* 17, no. 13: 1101-8.
- Crawford, B C W, and M F Yanofsky. 2008. The formation and function of the female reproductive tract in flowering plants. *Current Biology: CB* 18, no. 20: R972-8.
- Curie, C, G Cassin, D Couch, F Divol, K Higuchi, M Le Jean, J Misson, A Schikora, P Czernic, and S Mari. 2009. Metal movement within the plant: contribution of nicotianamine and yellow stripe 1-like transporters. *Ann Bot* 103, no. 1: 1-11.
- Curie, C, Z Panaviene, C Loulergue, S L Dellaporta, J F Briat, and E L Walker. 2001. Maize yellow stripe1 encodes a membrane protein directly involved in Fe(III) uptake. *Nature* 409, no. 6818: 346-349.

References

- Curie, C, and J-F Briat. 2003. Iron transport and signaling in plants. *Annual Review of Plant Biology*, no. 54: 183-206.
- Curtis, M D, and U Grossniklaus. 2003. A gateway cloning vector set for high-throughput functional analysis of genes in planta. *Plant Physiol* 133, no. 2: 462-469.
- Delhaize, E, and P R Ryan. 1995. Aluminum Toxicity and Tolerance in Plants. *Plant Physiology* 107, no. 2: 315-321.
- Deák, M, G V Horváth, S Davletova, K Török, L Sass, I Vass, B Barna, Z Király, and D Dudits. 1999. Plants ectopically expressing the iron-binding protein, ferritin, are tolerant to oxidative damage and pathogens. *Nature biotechnology* 17, no. 2 : 192-196.
- DiDonato, Jr J, L A Roberts, T Sanderson, R B Eisley, and E L Walker. 2004. Arabidopsis Yellow Stripe-Like2 (YSL2): a metal-regulated gene encoding a plasma membrane transporter of nicotianamine-metal complexes. *Plant Journal* 39, no. 3: 403-414.
- Dietz, K-J, M. Baier, and U Kramer. 1999. Free radicals and reactive oxygen species as mediators of heavy metal toxicity in plants. In *Heavy Metal Stress in Plants: from Molecules to Ecosystems* (Prasad, M.N.V. and Hagemeyer, J., eds). *Ecosystems, Springer Verlag*: pp. 73–97.
- Dinneny, J R, Terri A Long, J Y Wang, J W Jung, D Mace, S Pointer, C Barron, S M Brady, J Schiefelbein, and P N Benfey. 2008. Cell identity mediates the response of Arabidopsis roots to abiotic stress. *Science New York*, no.6: 127-35.
- Douchkov, D, C Gryczka, U W Stephan, R Hell, and H Bäumlein. 2005. Ectopic expression of nicotianamine synthase genes results in improved iron accumulation and increased nickel tolerance in transgenic tobacco. *Plant, Cell and Environment* 28: 365-374.
- Douchkov, D, R Hell, U W Stephan, and H Bäumlein. 2001. Increased iron efficiency in transgenic plants due to ectopic expression of nicotianamine synthase. *Plant Nutrition*
- Drakakaki, G, P Christou, and E Stöger. 2000. Constitutive expression of soybean ferritin cDNA in transgenic wheat and rice results in increased iron levels in vegetative tissues but not in seeds. *Transgenic Research* 9, no. 6: 445-452.
- Durrett, T P, W Gassmann, and E E Rogers. 2007. The FRD3-mediated Efflux of Citrate into the Root Vasculature Is Necessary for Efficient Iron Translocation. *Plant Physiology*.
- Duy, D, J Soll, and K Philippar. 2007. Solute channels of the outer membrane: from bacteria to chloroplasts. *Biol Chem* 388, no. 9: 879-889.

References

- Duy, D, R Stübe, G Wanner, and K Philippar. 2011. The Chloroplast Permease PIC1 Regulates Plant Growth and Development by Directing Homeostasis and Transport of Iron. *Plant physiology* 155, no. 4: 1709-22.
- Duy, D, G Wanner, A R Meda, N von Wiren, J Soll, and K Philippar. 2007. PIC1, an Ancient Permease in Arabidopsis Chloroplasts, Mediates Iron Transport. *Plant Cell*. 9, no. 6: 445-452.
- Edgar, R, M Domrachev, and A E Lash. 2002. Gene Expression Omnibus: NCBI gene expression and hybridization array data repository. *Nucleic Acids Res* 30, no. 1: 207-210.
- Eide, D, M Broderius, J Fett, and M L Guerinot. 1996. A novel iron-regulated metal transporter from plants identified by functional expression in yeast. *Proceedings of the National Academy of Sciences of the United States of America* 93, no. 11: 5624-5628.
- Enomoto, Y, H Hodoshima, H Shimada, K Shoji, T Yoshihara, and F Goto. 2007. Long-distance signals positively regulate the expression of iron uptake genes in tobacco roots. *Planta* 227, no. 1: 444-452.
- Fenton, H J H. 1894. Oxidation of tartaric acid in presence of iron. *Journal of the Chemical Society, Transactions* 65: 899-910.
- Fischer, Pw, A Giroux, and Mr L'Abbe. 1984. Effect of zinc supplementation on copper status in adult man. *Am J Clin Nutr* 40, no. 4: 743-746.
- Garnett, T P, and R D Graham. 2005. Distribution and remobilization of iron and copper in wheat. *Annals of botany* 95, no. 5: 817-26.
- Goetz, M, L C Hooper, S D Johnson, J C M Rodrigues, A Vivian-Smith, and A M Koltunow. 2007. Expression of aberrant forms of AUXIN RESPONSE FACTOR8 stimulates parthenocarpy in Arabidopsis and tomato. *Plant physiology* 145, no. 2 (October): 351-61
- Goetz, M, A Vivian-Smith, S D Johnson, and A M Koltunow. 2006. AUXIN RESPONSE FACTOR8 is a negative regulator of fruit initiation in Arabidopsis. *The Plant cell* 18, no. 8: 1873-86.
- Goto, F, T Yoshihara, N Shigemoto, S Toki, and F Takaiwa. 1999a. Iron fortification of rice seed by the soybean ferritin gene. *Nature Biotechnology* 17, no. 3: 282-286.
- Green, L S, and E E Rogers. 2004. FRD3 Controls Iron Localization in Arabidopsis. *Plant Physiology*, no.136: 2523-2531.
- Grusak, M A. 1994. Iron Transport to Developing Ovules of *Pisum sativum* (I. Seed Import Characteristics and Phloem Iron-Loading Capacity of Source Regions). *Plant Physiology* 104, no. 2: 649-655.

References

- Grusak, M A, and S Pezeshgi. 1996. Shoot-to-Root Signal Transmission Regulates Root Fe(III) Reductase Activity in the *dgl* Mutant of Pea. *Plant Physiology* 110, no. 1: 329-334.
- Guerinot, M L, and Y Yi. 1994. Iron: Nutritious, Noxious, and Not Readily Available. *Plant Physiology* 104, no. 3: 815-820.
- Haag-Kerwer, A, H Schafer, S Heiss, C Walter, and T Rausch. 1999. Cadmium exposure in *Brassica juncea* causes a decline in transpiration rate and leaf expansion without effect on photosynthesis. *J. Exp. Bot.* 50, no. 341:123-139
- Haydon, M J, and C S Cobbett. 2007. Transporters of ligands for essential metal ions in plants. *New Phytologist* 174, no. 3: 499-506.
- Heazlewood, J L, J S Tonti-Filippini, A M Gout, D A Day, J Whelan, and A Harvey Millar. 2004. Experimental analysis of the *Arabidopsis* mitochondrial proteome highlights signaling and regulatory components, provides assessment of targeting prediction programs, and indicates plant-specific mitochondrial proteins. *The Plant cell* 16, no. 1: 241-56.
- Hell, R, and U W Stephan. 2003. Iron uptake, trafficking and homeostasis in plants. *Planta* no. 3: 633-640
- Henriques, R, J Jasik, M Klein, E Martinoia, U Feller, J Schell, M S Pais, and C Koncz. 2002. Knock-out of *Arabidopsis* metal transporter gene *IRT1* results in iron deficiency accompanied by cell differentiation defects. *Plant Molecular Biology* 50, no. 4-5: 587-597.
- Herbik, A, A Giritch, C Horstmann, R Becker, H J Balzer, H Bäumlein, and U W Stephan. 1996. Iron and copper nutrition-dependent changes in protein expression in a tomato wild type and the nicotianamine-free mutant *chloronerva*. *Plant Physiology* 111, no. 2: 533-540.
- Higuchi, K, N-K Nishizawa, H Yamaguchi, V Römheld, H Marschner, and S Mori. 1995. Response of nicotianamine synthase activity to Fe-deficiency in tobacco plants as compared with barley. *Journal of Experimental Botany* 46, no. 8: 1061-1063.
- Himmelblau, E, and R M Amasino. 2000. Delivering copper within plant cells. *Current Opinion in Plant Biology* 3, no. 3: 205-210.
- Hintze, K J, and E C Theil. 2006. Cellular regulation and molecular interactions of the ferritins. *Cellular and molecular life sciences: CMLS* 63, no. 5: 591-600.
- Howden, R. 1995. Cadmium-sensitive, *cad1* mutants of *Arabidopsis thaliana* are phytochelatin deficient. *PLANT PHYSIOLOGY* 107, no. 4: 1059-1066.
- Hurrell, F. 2002. Fortification: Overcoming Technical and Practical Barriers. *J. Nutr.* 132, no. 4: 806S-812.

References

- Jakoby, M, H-Y Wang, W Reidt, B Weisshaar, and P Bauer. 2004. FRU (BHLH029) is required for induction of iron mobilization genes in *Arabidopsis thaliana*. *FEBS Letters* 577, no. 3: 528-534.
- Jeong, J, C Cohu, L Kerkeb, M Pilon, E L Connolly, and M L Guerinot. 2008. Chloroplast Fe(III) chelate reductase activity is essential for seedling viability under iron limiting conditions. *Proceedings of the National Academy of Sciences of the United States of America* 105, no. 30: 10619-24.
- Jiménez, S., F. Morales, A. Abadía, J. Abadía, M. A. Moreno, and Y. Gogorcena. 2008. Elemental 2-D mapping and changes in leaf iron and chlorophyll in response to iron re-supply in iron-deficient GF 677 peach-almond hybrid. *Plant and Soil* 315, no. 1-2: 93-106.
- Kaegi, H, R, Jeremis, and A Schaeffer. 1988. Biochemistry of metallothionein. *Biochemistry* 27, no. 23: 8509-8515.
- Kehr, J, and M Rep. 2007. Protein extraction from xylem and phloem sap. *Methods in molecular biology (Clifton, N.J.)* 355: 27-35.
- Keller, A, C Backes, M Al-Awadhi, A Gerasch, J Kuntzer, O Kohlbacher, M Kaufmann, and H P Lenhof. 2008. GeneTrailExpress: a web-based pipeline for the statistical evaluation of microarray experiments. *BMC Bioinformatics* 9: 552.
- Keller, A, C Backes, and H P Lenhof. 2007. Computation of significance scores of unweighted Gene Set Enrichment Analyses. *BMC Bioinformatics* 8: 290.
- Kim, S, and M L Guerinot. 2007. Mining iron: iron uptake and transport in plants. *FEBS Letters* 581, no. 12: 2273-2280.
- Kim, S A, T Punshon, A Lanzirrotti, L Li, J M Alonso, J R Ecker, J Kaplan, and M L Guerinot. 2006. Localization of iron in *Arabidopsis* seed requires the vacuolar membrane transporter VIT1. *Science* 314, no. 5803: 1295-1308
- Kim, S, M Takahashi, K Higuchi, K Tsunoda, H Nakanishi, E Yoshimura, S Mori, and N K Nishizawa. 2005. Increased nicotianamine biosynthesis confers enhanced tolerance of high levels of metals, in particular nickel, to plants. *Plant and Cell Physiology* 46, no. 11: 1809-1818.
- Kim, S T, K Zhang, J Dong, E M Lord. 2006. Exogenous free ubiquitin enhances lily pollen tube adhesion to an in vitro stylar matrix and may facilitate endocytosis of SCA. *Plant Physiology*: 142, no. 4: 1397-411
- Kispal, G, P Csere, B Guiard, and R Lill. 1997. The ABC transporter Atm1p is required for mitochondrial iron homeostasis. *FEBS letters* 418, no. 3: 346-50.
- Klaassen, C D, J Liu, and S Choudhuri. 1999. Metallothionein: an intracellular protein to protect against cadmium toxicity. *Annual review of pharmacology and toxicology* 39: 267-94.

References

- Klatte, M, M Schuler, M Wirtz, C Fink-Straube, R Hell, and P Bauer. 2009. The analysis of Arabidopsis nicotianamine synthase mutants reveals functions for nicotianamine in seed iron loading and iron deficiency responses. *Plant Physiol* 150, no. 1: 257-271.
- Klatte, Marco, and Petra Bauer. 2008. Accurate real-time reverse transcription quantitative PCR. In , ed. T Pfannschmidt, 479. *Humana Press*.
- Kobayashi, Y, K Kuroda, K Kimura, J L Southron-Francis, A Furuzawa, S Iuchi, M Kobayashi, G J Taylor, and H Koyama. 2008. Amino acid polymorphisms in strictly conserved domains of a P-type ATPase HMA5 are involved in the mechanism of copper tolerance variation in Arabidopsis. *Plant Physiol* 148, no. 2: 969-80.
- Koike, S, H Inoue, D Mizuno, M Takahashi, H Nakanishi, S Mori, and N K Nishizawa. 2004. OsYSL2 is a rice metal-nicotianamine transporter that is regulated by iron and expressed in the phloem. *Plant Journal* 39, no. 3: 415-424.
- Koncz, C, N Martini, R Mayerhofer, Z Koncz-Kalman, H Körber, G P Redei, and J Schell. 1989. High-frequency T-DNA-mediated gene tagging in plants. *Proceedings of the National Academy of Sciences of the United States of America* 86, no. 21: 8467-71.
- Korshunova, Y O, D Eide, W G Clark, M L Guerinot, and H B Pakrasi. 1999. The IRT1 protein from Arabidopsis thaliana is a metal transporter with a broad substrate range. *Plant Mol Biol* 40, no. 1: 37-44.
- Krämer, U, I J Pickering, R C Prince, I Raskin, and D E Salt. 2000. Subcellular localization and speciation of nickel in hyperaccumulator and non-accumulator Thlaspi species. *Plant Physiol* 122, no. 4: 1343-1353.
- Krämer, Ute. 2010. Metal hyperaccumulation in plants. *Annual review of plant Biology*, no. 61: 517-34.
- Krüger, C, O Berkowitz, U W Stephan, and R Hell. 2002. A metal-binding member of the late embryogenesis abundant protein family transports iron in the phloem of Ricinus communis L. *Journal of Biological Chemistry* 277, no. 28: 25062-25069.
- Kuepper, H, A Mijovilovich, W Meyer-Klaucke, and P M H Kroneck. 2004. Tissue- and age-dependent differences in the complexation of cadmium and zinc in the cadmium/zinc hyperaccumulator Thlaspi caerulescens (Ganges ecotype) revealed by x-ray absorption spectroscopy. *Plant Physiology* 134, no. 2: 748-757.
- Kushnir, S, E Babiychuk, S Storozhenko, M W Davey, J Papenbrock, R De Rycke, G Engler, et al. 2001. A mutation of the mitochondrial ABC transporter Sta1 leads to dwarfism and chlorosis in the Arabidopsis mutant starik. *The Plant cell* 13, no. 1: 89-100.
- Lane, B, R Kajioka, and T Kennedy. 1987. The wheat-germ Ec protein is a zinc-containing metallothionein. *Biochemistry and Cell Biology* 65, no. 11: 1001-1005.

References

- Lanquar, V, F Lelievre, S Bolte, C Hames, C Alcon, D Neumann, G Vansuyt, et al. 2005. Mobilization of vacuolar iron by AtNRAMP3 and AtNRAMP4 is essential for seed germination on low iron. *EMBO J* 24, no. 23: 4041-4051.
- Le Jean, M, A Schikora, S Mari, J-F Briat, and Catherine Curie. 2005. A loss-of-function mutation in AtYSL1 reveals its role in iron and nicotianamine seed loading. *Plant Journal* 44, no. 5: 769-782.
- Lee, S, U S Jeon, S Jin Lee, Y-K Kim, D Pergament Persson, S Husted, J K Schjørring, et al. 2009. Iron fortification of rice seeds through activation of the nicotianamine synthase gene. *Proceedings of the National Academy of Sciences of the United States of America* 106, no. 51: 22014-9.
- Levi, S, B Corsi, M Bosisio, R Invernizzi, A Volz, D Sanford, P Arosio, and J Drysdale. 2001. A human mitochondrial ferritin encoded by an intronless gene. *The Journal of biological chemistry* 276, no. 27: 24437-40.
- Li, Y, M G Rosso, N Strizhov, P Viehoveer, and B Weisshaar. 2003. GABI-Kat SimpleSearch: a flanking sequence tag (FST) database for the identification of T-DNA insertion mutants in *Arabidopsis thaliana*. *Bioinformatics* 19, no. 11: 1441-1442.
- Ling, H Q, G Koch, H Bäumlein, and M W Ganal. 1999. Map-based cloning of chloronerva, a gene involved in iron uptake of higher plants encoding nicotianamine synthase. *Proceedings of the National Academy of Sciences of the United States of America* 96, no. 12: 7098-7103.
- Lobreaux, S, and J F Briat. 1991. Ferritin accumulation and degradation in different organs of pea (*Pisum sativum*) during development. *The Biochemical journal*, no. 274: 601-6.
- Long, J C, Frederik Sommer, M D Allen, S-F Lu, and S S Merchant. 2008. FER1 and FER2 encoding two ferritin complexes in *Chlamydomonas reinhardtii* chloroplasts are regulated by iron. *Genetics* 179, no. 1: 137-47.
- Long, T A, H Tsukagoshi, W Busch, B Lahner, D E Salt, and N Benfey. 2010. The bHLH Transcription Factor POPEYE Regulates Response to Iron Deficiency in *Arabidopsis* Roots. *The Plant cell* 22, no. 7: 2219-2236.
- Lord, E M, S D Russell. 2002. The mechanism of pollination and fertilization in plants. *Annual Review of Cell and Dev Biol*: no.18: 81-105
- Sanders, L C, and E M Lord. 1989. Directed movement of latex particles in the gynoeceia of three species of flowering plants, *Science* 243, no.3:1606–1608
- Lott, J. 1995. Greenwood, JS and Batten. GD (1995) Mechanisms and regulation of mineral nutrient storage during seed development. *Seed Development and Germination*. New York: 367-375.

References

- Lucca, P, R Hurrell, and I Potrykus. 2001. Approaches to improving the bioavailability and level of iron in rice seeds. *Journal of the Science of Food and Agriculture* 81, no. 9: 828-834.
- Lucca, P, R Hurrell, I Potrykus 2002. Fighting Iron Deficiency Anemia with Iron-Rich Rice. *J. Am. Coll. Nutr.* 21, no. 90003: 184S-190.
- Lönnerdal, Bo. 2009. Soybean ferritin: implications for iron status of vegetarians. *The American journal of clinical nutrition* 89, no. 5: 1680S-1685S.
- Danks, D M.1988. Copper deficiency in humans. *Annu. Rev. Nutr.* 8:235-257
- Ma, J F, D Ueno, F-J Zhao, and S P McGrath. 2005. Subcellular localisation of Cd and Zn in the leaves of a Cd-hyperaccumulating ecotype of *Thlaspi caerulescens*. *Planta* 220, no. 5: 731-736.
- Marentes, E, and M A Grusak. 1998. Iron transport and storage within the seed coat and embryo of developing seeds of pea (*Pisum sativum* L.). *Seed Science Research* 8, no. 03: 367-375.
- Mari, S, D Gendre, K Pianelli, L Ouerdane, R Lobinski, J-F Briat, M Lebrun, and P Czernic. 2006. Root-to-shoot long-distance circulation of nicotianamine and nicotianamine-nickel chelates in the metal hyperaccumulator *Thlaspi caerulescens*. *Journal of experimental botany* 57, no. 15: 4111-22.
- Marschner, H. 1995. Mineral nutrition of higher plants. *2nd ed. Academic Press*, no.11:147–148
- Masuda, T, F Goto, and T Yoshihara. 2001. A novel plant ferritin subunit from soybean that is related to a mechanism in iron release. *The Journal of biological chemistry* 276, no. 22
- Maxfield, A B, D N Heaton, and D R Winge. 2004. Cox17 is functional when tethered to the mitochondrial inner membrane. *The Journal of biological chemistry* 279, no. 7: 5072-80.
- Mendoza-Cózatl, D G, E Butko, F Springer, J W Torpey, E A Komives, J Kehr, and J I Schroeder. 2008. Identification of high levels of phytochelatins, glutathione and cadmium in the phloem sap of *Brassica napus*. A role for thiol-peptides in the long-distance transport of cadmium and the effect of cadmium on iron translocation. *The Plant journal: for cell and molecular biology* 54, no. 2: 249-59.
- Missirlis, F, S Holmberg, T Georgieva, B C Dunkov, T A Rouault, and J H Law. 2006. Characterization of mitochondrial ferritin in *Drosophila*. *Proceedings of the National Academy of Sciences of the United States of America* 103, no. 15: 5893-8.
- Moreno, I, L Norambuena, D Maturana, M Toro, C Vergara, A Orellana, A Zurita-Silva, and V R Ordenes. 2008. AtHMA1 is a thapsigargin-sensitive Ca²⁺/heavy metal pump. *The Journal of biological chemistry* 283, no. 15: 9633-41.

References

- Mori, S. 1999. Iron acquisition by plants. *Current Opinion in Plant Biology* 2, no. 3: 250-253.
- Morrissey, J, I R Baxter, J Lee, L Li, B Lahner, N Grotz, J Kaplan, D E Salt, and M L Guerinot. 2009. The ferroportin metal efflux proteins function in iron and cobalt homeostasis in Arabidopsis. *Plant Cell* 21, no. 10: 3326-3338.
- Morrissey, J, and M L Guerinot. 2009. Iron uptake and transport in plants: the good, the bad, and the ionome. *Chem Rev* 109, no. 10: 4553-4567.
- Mukherjee, I, N H Campbell, J S Ash, and E L Connolly. 2006. Expression profiling of the Arabidopsis ferric chelate reductase (FRO) gene family reveals differential regulation by iron and copper. *Planta* 223, no. 6: 1178-1190.
- Murphy, A. 1997. Purification and immunological identification of metallothioneins 1 and 2 from Arabidopsis thaliana. *PLANT PHYSIOLOGY* 113, no. 4 (April): 1293-1301.
- Murray-Kolb, L E, F Takaiwa, F Goto, T Yoshihara, E C Theil, and J L Beard. 2002. Transgenic rice is a source of iron for iron-depleted rats.
- Murray-Kolb, L E, R Welch, EC Theil, and J L Beard. 2003. Women with low iron stores absorb iron from soybeans. *Am J Clin Nutr* 77, no. 1: 180-184.
- Myouga, F, C Hosoda, T Umezawa, H Iizumi, T Kuromori, R Motohashi, Y Shono, N Nagata, M Ikeuchi, and K Shinozaki. 2008. A heterocomplex of iron superoxide dismutases defends chloroplast nucleoids against oxidative stress and is essential for chloroplast development in Arabidopsis. *The Plant cell* 20, no. 11: 3148-62.
- Nagasaka, Seiji, M Takahashi, R Nakanishi-Itai, K Bashir, H Nakanishi, S Mori, and N K Nishizawa. 2009. Time course analysis of gene expression over 24 hours in Fe-deficient barley roots. *Plant molecular biology* 69, no. 5: 621-31.
- Nagpal, P, C M Ellis, H Weber, S E Ploense, L S Barkawi, T J Guilfoyle, G Hagen, et al. 2005. Auxin response factors ARF6 and ARF8 promote jasmonic acid production and flower maturation. *Development (Cambridge, England)* 132, no. 18: 4107-18.
- Nakanishi, H, H Yamaguchi, T Sasakuma, N K Nishizawa, and S Mori. 2000. Two dioxygenase genes, Ids3 and Ids2, from Hordeum vulgare are involved in the biosynthesis of mugineic acid family phytosiderophores. *Plant Molecular Biology* 44, no. 2: 199-207.
- Naveh, Y, A Hazani, and M Berant. 1981. Copper Deficiency with Cow's Milk Diet. *Pediatrics* 68, no. 3: 397-400.
- Neumann, G, C Haake, and V Römheld. 1999. Improved HPLC method for determination of phytosiderophores in root washings and tissue extracts. *Journal of Plant Nutrition* 22, no. 9: 1389-1402.

References

- Noma, M, M Noguchi, and E Tamaki. 1971. A new amino acid, nicotianamine, from tobacco leaves. *Tetrahedron Letters* 12, no. 22: 2017-2020.
- Obayashi, T, S Hayashi, M Saeki, H Ohta, and K Kinoshita. 2009. ATTED-II provides coexpressed gene networks for Arabidopsis. *Nucleic Acids Res* 37, no. Database issue: D987-91.
- Obayashi, T, K Kinoshita, K Nakai, M Shibaoka, S Hayashi, M Saeki, D Shibata, K Saito, and H Ohta. 2007. ATTED-II: a database of co-expressed genes and cis elements for identifying co-regulated gene groups in Arabidopsis. *Nucleic Acids Res* 35, no. Database issue: D863-9.
- Ouerdane, L, S Mari, P Czernic, M Lebrun, and R Lobinski. 2006. Speciation of non-covalent nickel species in plant tissue extracts by electrospray Q-TOFMS/MS after their isolation by 2D size exclusion-hydrophilic interaction LC (SEC-HILIC) monitored by ICP-MS. *Journal of Analytical Atomic Spectrometry* 21, no. 7: 676.
- Palmgren, M G. 2001. PLANT PLASMA MEMBRANE H⁺ATPases: Powerhouses for Nutrient Uptake. *Annual Review of Plant Physiology and Plant Molecular Biology* 52: 817-845.
- Palmiter, R. D. 1998. The elusive function of metallothioneins. *Proceedings of the National Academy of Sciences* 95, no. 15: 8428-8430.
- Petit, J M, O van Wuytswinkel, J F Briat, and S Lobreaux. 2001. Characterization of an iron-dependent regulatory sequence involved in the transcriptional control of AtFer1 and ZmFer1 plant ferritin genes by iron. *Journal of Biological Chemistry* 276, no. 8: 5584-5590.
- Pianelli, K, S Mari, L Marques, M Lebrun, and P Czernic. 2005. Nicotianamine over-accumulation confers resistance to nickel in Arabidopsis thaliana. *Transgenic Research* 14, no. 5: 739-748.
- Pich, A, R Manteuffel, S Hillmer, G Scholz, and W Schmidt. 2001. Fe homeostasis in plant cells: Does nicotianamine play multiple roles in the regulation of cytoplasmic Fe concentration? *Planta* 213, no. 6: 967-976.
- Pich, A, and G Scholz. 1991. Nicotianamine and the Distribution of Iron into Apoplast and Symplast of Tomato (*Lycopersicon esculentum* Mill.): II. Uptake of iron by protoplasts from the variety Bonner Beste and its nicotianamine-less mutant chloronerva and the compartmentalization of. *Journal of Experimental Botany* 42, no. 12: 1517-1523.
- Pich, A, and G Scholz. 1996. Translocation of copper and other micronutrients in tomato plants (*Lycopersicon esculentum* Mill.): nicotianamine-stimulated copper transport in the xylem. *Journal of Experimental Botany* 47, no. 294: 41-47.
- Pich, A, G Scholz, and U W Stephan. 1994. Iron-dependent changes of heavy-metals, nicotianamine, and citrate in different plant organs and in the xylem exudate of 2

References

- tomato genotypes - Nicotianamine as possible copper translocator. *Plant and Soil* 165, no. 2: 189-196.
- Pilon, M, S E Abdel-Ghany, C M Cohu, K A Gogolin, and H Ye. 2006: Copper cofactor delivery in plant cells. *Current Opinion in Plant Biology* 9, no. 3: 256-263.
- Puig, S, N Andres-Colass, A Garcia-Molina, and L Penarrubia. 2007. Copper and iron homeostasis in Arabidopsis: responses to metal deficiencies, interactions and biotechnological applications. *Plant Cell and Environment* 30, no. 3: 271-290.
- Punshon, T, M L Guerinot, and A Lanzirotti. 2009. Using synchrotron X-ray fluorescence microprobes in the study of metal homeostasis in plants. *Annals of botany* 103, no. 5: 665-72.
- Qu, Le Qing, T Yoshihara, A Ooyama, F Goto, and F Takaiwa. 2005. Iron accumulation does not parallel the high expression level of ferritin in transgenic rice seeds. *Planta* 222, no. 2: 225-33.
- Raboy, V. 2007. The ABCs of low-phytate crops. *Nature biotechnology* 25, no. 8: 874-5.
- Rauser, W E. 1995. Phytochelatins and related peptides. Structure, biosynthesis, and function. *Plant physiology* 109, no. 4: 1141-9.
- Rauser, WE. 1999. Structure and function of metal chelators produced by plants. *Cell Biochemistry and Biophysics* 31, no. 1: 19-48.
- Ravet, K, B Touraine, J Boucherez, J F Briat, F Gaymard, and F Cellier. 2009. Ferritins control interaction between iron homeostasis and oxidative stress in Arabidopsis. *Plant J* 57, no. 3: 400-412.
- Ravet, K, B Touraine, J Boucherez, J-F Briat, F Gaymard, and F Cellier. 2009. Ferritins control interaction between iron homeostasis and oxidative stress in Arabidopsis. *The Plant J: for cell and molecular biology* 57, no. 3: 400-12.
- Ray J Rose. 2007. Plant mitochondria. Ed. *Encyclopedia of Life Sciences*. Chichester, UK: John Wiley & Sons, Ltd, May.
- Rellán-Alvarez, R, J Giner-Martínez-Sierra, J Orduna, I Orera, J A Rodríguez-Castrillón, José I García-Alonso, J Abadía, and A Alvarez-Fernández. 2010. Identification of a Tri-Iron(III), Tri-Citrate Complex in the Xylem Sap of Iron-Deficient Tomato Resupplied with Iron: New Insights into Plant Iron Long-Distance Transport. *Plant & cell physiology* 51, no. 1: 91-102.
- Rellán-Álvarez, R., J. Abadia, and A. Álvarez-Fernández. 2008. Formation of metal-nicotianamine complexes as affected by pH, ligand exchange with citrate and metal exchange. A study by electrospray ionization time-of-flight mass spectrometry. *Rapid Communications in Mass Spectrometry* 22, no. 10: 1553–1562.

References

- Rengel, Z, and P Marschner. 2005. Nutrient availability and management in the rhizosphere: exploiting genotypic differences. *The New phytologist* 168, no. 2: 305-12.
- Rhee, S Y, W Beavis, T Z Berardini, G Chen, D Dixon, A Doyle, M Garcia-Hernandez, et al. 2003. The Arabidopsis Information Resource (TAIR): a model organism database providing a centralized, curated gateway to Arabidopsis biology, research materials and community. *Nucleic Acids Research* 31, no. 1: 224-228.
- Roberts, L A, Abbey J Pierson, Z Panaviene, and E L Walker. 2004. Yellow stripe1. Expanded roles for the maize iron-phytosiderophore transporter. *Plant Physiology* 135, no. 1: 112-120.
- Robinson, N J, C M Procter, E L Connolly, and M L Guerinot. 1999. A ferric-chelate reductase for iron uptake from soils. *Nature* 397, no. 6721: 694-697.
- Robinson, N J, A M Tommey, C Kuske, and P J Jackson. 1993. Plant metallothioneins. *The Biochemical journal*, no. 295: 1-10.
- Rodríguez, F. I. 1999. A Copper Cofactor for the Ethylene Receptor ETR1 from Arabidopsis. *Science* 283, no. 5404: 996-998.
- Roemheld, V, and H Marschner. 1986. Evidence for a Specific Uptake System for Iron Phytosiderophores in Roots of Grasses. *Plant Physiology* 80, no. 1: 175-180.
- Rogers, E E, and M L Guerinot. 2002. FRD3, a member of the multidrug and toxin efflux family, controls iron deficiency responses in Arabidopsis. *Plant Cell* 14, no. 8: 1787-1799.
- Roschttardt, H, G Conéjéro, C Curie, and S Mari. 2009. Identification of the endodermal vacuole as the iron storage compartment in the Arabidopsis embryo. *Plant physiology* 151, no. 3: 1329-38.
- Saier, M. H. 2000. A Functional-Phylogenetic Classification System for Transmembrane Solute Transporters. *Microbiology and Molecular Biology Reviews* 64, no. 2: 354-411.
- Salt, D. E., and W. E. Rauser. 1995. MgATP-Dependent Transport of Phytochelatins Across the Tonoplast of Oat Roots. *Plant Physiology* 107, no. 4: 1293-1301.
- Salt, D E., Roger C. Prince, A J. M. Baker, I Raskin, and I J. Pickering. 1999. Zinc Ligands in the Metal Hyperaccumulator *Thlaspi caerulescens* As Determined Using X-ray Absorption Spectroscopy. *Environmental Science & Technology* 33, no. 5: 713-717.
- Sambrook, J, E F Fritsch, and T Maniatis. 1989. Molecular Cloning: A Laboratory Manual. 2nd ed. New York: Cold Spring Harbor Laboratory Press.

References

- Sancenón, V, S Puig, I Mateu-Andrés, E Dorcey, D J Thiele, and L Peñarrubia. 2004. The Arabidopsis copper transporter COPT1 functions in root elongation and pollen development. *The Journal of biological chemistry* 279, no. 15: 15348-55.
- Santambrogio, P, G Biasiotto, F Sanvito, S Olivieri, P Arosio, and S Levi. 2007. Mitochondrial ferritin expression in adult mouse tissues. *The journal of histochemistry and cytochemistry: official journal of the Histochemistry Society* 55, no. 11:1129-37.
- Santi, S, and W Schmidt. 2009. Dissecting iron deficiency-induced proton extrusion in Arabidopsis roots. *The New phytologist* 183, no. 4:1072-84.
- Sarret, G, P Saumitou-Laprade, V Bert, O Proux, J-L Hazemann, A Traverse, M A Marcus, and A Manceau. 2002. Forms of zinc accumulated in the hyperaccumulator Arabidopsis halleri. *Plant physiology* 130, no. 4:1815-26.
- Schaaf, G, A Honsbein, A R Meda, S Kirchner, D Wipf, and N von Wiren. 2006. AtIREG2 encodes a tonoplast transport protein involved in iron-dependent nickel detoxification in Arabidopsis thaliana roots. *Journal of Biological Chemistry* 281, no. 35: 25532-25540.
- Schaaf, G, U Ludewig, B E Erenoglu, S Mori, T Kitahara, and N von Wiren. 2004. ZmYS1 functions as a proton-coupled symporter for phyto siderophore- and nicotianamine-chelated metals. *Journal of Biological Chemistry* 279, no. 10: 9091-9096.
- Schaaf, G, A Schikora, J Haeberle, G Vert, U Ludewig, J-F Briat, C Curie, and N von Wiren. 2005. A Putative Function for the Arabidopsis Fe-Phytosiderophore Transporter Homolog AtYSL2 in Fe and Zn Homeostasis. *Plant and Cell Physiology* 46, no. 5: 762-774.
- Schmidke, I, C Krüger, R Frömmichen, G Scholz, and U W Stephan. 1999. Phloem loading and transport characteristics of iron in interaction with plant-endogenous ligands in castor bean seedlings. *Physiologia Plantarum* 106, no. 1: 82-89.
- Schmidt, W., and C. Fühner. 1998. Sensitivity to and requirement for iron in Plantago species. *New Phytologist* 138, no. 4: 639-651.
- Scholz, G, and A Rudolph. 1968. A biochemical mutant of Lycopersicon esculentum Mill. Isolation and properties of the ninhydrinpositive "normalizing factor". *Phytochemistry* 7, no. 10: 1759-1764.
- Scholz, G, and H Böhme. 1961. Versuche zur Normalisierung des Phänotyps der Mutante chloronerva von Lycopersicon esculentum Mill. *Kulturpflanze* 9, no. 1: 181-191.
- Seigneurin-Berny, Daphné, A Gravot, P Auroy, C Mazard, A Kraut, G Finazzi, D Grunwald, et al. 2006. HMA1, a new Cu-ATPase of the chloroplast envelope, is essential for growth under adverse light conditions. *The Journal of biological chemistry* 281, no. 5: 2882-92.

References

- Sessions, A, E Burke, G Presting, G Aux, J McElver, D Patton, B Dietrich, et al. 2002. A high-throughput Arabidopsis reverse genetics system. *Plant Cell* 14, no. 12: 2985-2994.
- Sharov, A A, D B Dudekula, and M S Ko. 2005. A web-based tool for principal component and significance analysis of microarray data. *Bioinformatics* 21, no. 10: 2548-2549.
- Sherlock, G, T Hernandez-Boussard, A Kasarskis, G Binkley, J C Matese, S S Dwight, M Kaloper, et al. 2001. The Stanford Microarray Database. *Nucleic Acids Res* 29, no. 1: 152-155.
- Shikanai, T. 2003. PAA1, a P-Type ATPase of Arabidopsis, Functions in Copper Transport in Chloroplasts. *The Plant Cell Online* 15, no. 6: 1333-1346.
- Shojima, S, N-K Nishizawa, S Fushiya, S Nozoe, T Irifune, and S Mori. 1990. Biosynthesis of Phytosiderophores: In Vitro Biosynthesis of 2'-Deoxymugineic Acid from l-Methionine and Nicotianamine. *Plant Physiology* 93, no. 4: 1497-1503.
- Snowden, R. E. D., and B. D. Wheeler. 1995. Chemical Changes in Selected Wetland Plant Species with Increasing Fe Supply, with Specific Reference to Root Precipitates and Fe Tolerance. *New Phytologist*, no.131: 503-520
- Stacey, M G, H Osawa, A Patel, W Gassmann, and G Stacey. 2006. Expression analyses of Arabidopsis oligopeptide transporters during seed germination, vegetative growth and reproduction. *Planta* 223, no. 2: 291-305.
- Stacey, M G, A Patel, W E McClain, M Mathieu, M Remley, E E Rogers, W Gassmann, Dale G Blevins, and G Stacey. 2008. The Arabidopsis AtOPT3 protein functions in metal homeostasis and movement of iron to developing seeds. *Plant physiology* 146, no. 2: 589-601.
- Stacey, M. G. 2002. AtOPT3, a Member of the Oligopeptide Transporter Family, Is Essential for Embryo Development in Arabidopsis. *The Plant Cell Online* 14, no. 11: 2799-2811.
- Stephan, U W, I Schmidke, V W Stephan, and G Scholz. 1996. The nicotianamine molecule is made-to-measure for complexation of metal micronutrients. *BioMetals* 9: 84-90.
- Stephan, U W, and G Scholz. 1993. What 's New in Plant Physiology Nicotianamine: mediator of transport of iron and heavy metals in the phloem? *Physiologia Plantarum*, no. 1946: 522-529.
- Stevenson-Paulik, J, R J Bastidas, St Chiou, R A Frye, and J D York. 2005. Generation of phytate-free seeds in Arabidopsis through disruption of inositol polyphosphate kinases. *Proceedings of the National Academy of Sciences of the United States of America* 102, no. 35: 12612-7.

References

- Strozycki, P M., A Skapska, K Szczesniak, E Sobieszczuk, J-F Briat, and A B. Legocki. 2003. Differential expression and evolutionary analysis of the three ferritin genes in the legume plant *Lupinus luteus*. *Physiologia Plantarum* 118, no. 3: 380-389.
- Surguladze, N, S Patton, A Cozzi, M G Fried, and J R Connor. 2005. Characterization of nuclear ferritin and mechanism of translocation. *The Biochemical journal* 388, no. Pt 3: 731-40.
- Suzuki K, H Nakanishi, NK Nishizawa, S Mori. 2001. Analysis of upstream region of nicotianamine synthase gene from *Arabidopsis thaliana*: presence of putative ERE-like sequence. *Biosci Biotechnol Biochem*, no.65: no.12:2794-7
- Swidzinski, J A, C J Leaver, and L J Sweetlove. 2004. A proteomic analysis of plant programmed cell death. *Phytochemistry* 65, no. 12: 1829-38.
- Takahashi, M, H Nakanishi, S Kawasaki, N K Nishizawa, and S Mori. 2001. Enhanced tolerance of rice to low iron availability in alkaline soils using barley nicotianamine aminotransferase genes. *Nature Biotechnology* 19, no. 5: 466-469.
- Takahashi, M, Y Terada, I Nakai, H Nakanishi, E Yoshimura, S Mori, and N K Nishizawa. 2003. Role of Nicotianamine in the Intracellular Delivery of Metals and Plant Reproductive Development. *Plant Cell* 15, no. 6: 1263-1280.
- Talke, I., M. Hanikenne, and U. Krämer. 2006. Zinc-dependent global transcriptional control, transcriptional deregulation, and higher gene copy number for genes in metal homeostasis of the hyperaccumulator *Arabidopsis halleri*. *Plant Physiology* 142, no. 1: 148-167.
- Teng, Y-S, Y-S Su, L-J Chen, Y J Lee, I Hwang, and H-M Li. 2006. Tic21 is an essential translocon component for protein translocation across the chloroplast inner envelope membrane. *The Plant cell* 18, no. 9: 2247-57.
- Terry, N, and J Abadia. 1986. Function of iron in chloroplasts. *Journal of Plant Nutrition* 9, no. 3: 609-646.
- Theil, E C. 2004. Iron, ferritin, and nutrition. *Annual review of nutrition* 24: 327-43.
- Thimm, O, O Blasing, Y Gibon, A Nagel, S Meyer, P Kruger, J Selbig, L A Muller, S Y Rhee, and M Stitt. 2004. MAPMAN: a user-driven tool to display genomics data sets onto diagrams of metabolic pathways and other biological processes. *Plant J* 37, no. 6: 914-939.
- Thomine, S, F Lelievre, E Debarbieux, J I Schroeder, and H Barbier-Brygoo. 2003. AtNRAMP3, a multispecific vacuolar metal transporter involved in plant responses to iron deficiency. *Plant Journal* 34, no. 5: 685-695.
- Tomasi, N, C Rizzardo, R Monte, S Gottardi, N Jelali, R Terzano, B Vekemans, et al. 2009. Micro-analytical, physiological and molecular aspects of Fe acquisition in leaves of Fe-deficient tomato plants re-supplied with natural Fe-complexes in nutrient solution. *Plant and Soil* 325, no. 1-2: 25-38.

References

- Toufighi, K, S M Brady, R Austin, E Ly, and N J Provart. 2005. The Botany Array Resource: e-Northerns, Expression Angling, and promoter analyses. *Plant J* 43, no. 1: 153-163.
- Uauy, C, A Distelfeld, T Fahima, A Blechl, and J Dubcovsky. 2006. A NAC Gene regulating senescence improves grain protein, zinc, and iron content in wheat. *Science (New York, N.Y.)* 314, no. 5803: 1298-301.
- Urbano, G, M López-Jurado, P Aranda, C Vidal-Valverde, E Tenorio, and J Porres. 2000. The role of phytic acid in legumes: antinutrient or beneficial function? *Journal of Physiology and Biochemistry* 56, no. 3: 283-94.
- Vacchina, V, S Mari, P Czernic, L Marques, K Pianelli, D Schaumlöffel, M Lebrun, and R Lobinski. 2003. Speciation of nickel in a hyperaccumulating plant by high-performance liquid chromatography-inductively coupled plasma mass spectrometry and electrospray MS/MS assisted by cloning using yeast complementation. *Analytical Chemistry* 75, no. 11: 2740-2745.
- Valko, M, H Morris, and M T D Cronin. 2005. Metals, toxicity and oxidative stress. *Current Medicinal Chemistry* 12, no. 10: 1161-1208.
- van de Mortel, J E, L A Villanueva, H Schat, J Kwekkeboom, S Coughlan, P D Moerland, E Ver Loren van Themaat, M Koornneef, and M G M Aarts. 2006. Large expression differences in genes for iron and zinc homeostasis, stress response, and lignin biosynthesis distinguish roots of *Arabidopsis thaliana* and the related metal hyperaccumulator *Thlaspi caerulescens*. *Plant physiology* 142, no. 3: 1127-47.
- van Wuytswinkel, O, G Vansuyt, N Grignon, P Fourcroy, and J F Briat. 1999. Iron homeostasis alteration in transgenic tobacco overexpressing ferritin. *The Plant Journal for Cell and Molecular Biology* 17, no. 1: 93-7.
- Vansuyt, G. 2000. Soil-dependent variability of leaf iron accumulation in transgenic tobacco overexpressing ferritin. *Plant Physiology and Biochemistry* 38, no. 6: 499-506.
- Varotto, C, D Maiwald, P Pesaresi, P Jahns, F Salamini, and D Leister. 2002. The metal ion transporter IRT1 is necessary for iron homeostasis and efficient photosynthesis in *Arabidopsis thaliana*. *Plant Journal* 31, no. 5: 589-599.
- Vazzola, V, A Losa, C Soave, and I Murgia. 2007. Knockout of frataxin gene causes embryo lethality in *Arabidopsis*. *FEBS letters* 581, no. 4: 667-72.
- Verbruggen, N, C Hermans, and H Schat. 2009. Molecular mechanisms of metal hyperaccumulation in plants. *The New phytologist* 181, no. 4: 759-76.
- Vert, G, J F Briat, and C Curie. 2001. *Arabidopsis* IRT2 gene encodes a root-periphery iron transporter. *Plant J* 26, no. 2: 181-189.

References

- Vert, G, N Grotz, F Dedaldechamp, F Gaymard, M L Guerinot, J F Briat, and C Curie. 2002. IRT1, an Arabidopsis transporter essential for iron uptake from the soil and for plant growth. *Plant Cell* 14, no. 6: 1223-1233.
- Vivian-Smith, A, M Luo, A Chaudhury, and A Koltunow. 2001. Fruit development is actively restricted in the absence of fertilization in Arabidopsis. *Development* 128, no. 12: 2321-2331.
- van der Zaal, B J, L Neuteboom, J Pinas, A Chardonens, H Schat, J A C Verkleij, and P.J.J. Hooykaas. 1999. Overexpression of a Novel Arabidopsis Gene Related to Putative Zinc-Transporter Genes from Animals Can Lead to Enhanced Zinc Resistance and Accumulation. *Plant Physiol* 119, no. 3: 1047-1056.
- von Wiren, N, S Klair, S Bansal, J F Briat, H Khodr, T Shioiri, R A Leigh, and R C Hider. 1999. Nicotianamine chelates both Fe III and Fe II. Implications for metal transport in plants. *Plant Physiol* 119, no. 3: 1107-1114.
- von Wiren, N, S. Mori, H. Marschner, and V. Romheld. 1994. Iron Inefficiency in Maize Mutant ys1 (*Zea mays* L. cv Yellow-Stripe) Is Caused by a Defect in Uptake of Iron Phytosiderophores. *Plant Physiol* 106, no. 1: 71-77.
- Wang, H, H M Wu, and A Y Cheung. 1996. Pollination induces mRNA poly(A) tail-shortening and cell deterioration in flower transmitting tissue. *The Plant Journal* 9, no. 5: 715-727.
- Wang, H-Y, M Klatter, M Jakoby, H Bäumlein, B Weisshaar, and P Bauer. 2007. Iron deficiency-mediated stress regulation of four subgroup Ib BHLH genes in Arabidopsis thaliana. *Planta* 226, no. 4: 897-908.
- Waters, B M, H-H Chu, R J Didonato, L A Roberts, R B Eisley, B Lahner, D E Salt, and E L Walker. 2006. Mutations in Arabidopsis yellow stripe-like1 and yellow stripe-like3 reveal their roles in metal ion homeostasis and loading of metal ions in seeds. *Plant Physiol* 141, no. 4: 1446-1458.
- Weber, G., N. von Wiren, and H. Hayen. 2006. Analysis of iron(II)/iron(III) phytosiderophore complexes by nano-electrospray ionization Fourier transform ion cyclotron resonance mass spectrometry. *Rapid Communications in Mass Spectrometry* 20, no. 6: 973-980.
- Weber, M, E Harada, C Vess, E Roepenack-Lahaye, and S Clemens. 2004. Comparative microarray analysis of Arabidopsis thaliana and Arabidopsis halleri roots identifies nicotianamine synthase, a ZIP transporter and other genes as potential metal hyperaccumulation factors. *Plant J* 37, no. 2: 269-281.
- Winter, D, B Vinegar, H Nahal, R Ammar, G V Wilson, and N J Provart. 2007. An "electronic fluorescent pictograph" browser for exploring and analyzing large-scale biological data sets. *PLoS ONE* 2, no. 1: e718.
- Wintz, H, T Fox, Y-Y Wu, V Feng, W Chen, H-S Chang, T Zhu, and C Vulpe. 2003. Expression profiles of Arabidopsis thaliana in mineral deficiencies reveal novel

References

- transporters involved in metal homeostasis. *Journal of Biological Chemistry* 278, no. 48: 47644-47653.
- Yamasaki, H, S E Abdel-Ghany, C M Cohu, Y Kobayashi, T Shikanai, and M Pilon. 2007. Regulation of copper homeostasis by micro-RNA in Arabidopsis. *Journal of Biological Chemistry* 282, no. 22: 16369-16378.
- Yamasaki, H, M Hayashi, M Fukazawa, Y Kobayashi, and T Shikanai. 2009. SQUAMOSA Promoter Binding Protein-Like7 Is a Central Regulator for Copper Homeostasis in Arabidopsis. *The Plant Cell* 21, no. 1: 347-61.
- Yen, M.-R., Y.-H. Tseng, and M. H. Saier. 2001. Maize Yellow Stripe1, an iron-phytosiderophore uptake transporter, is a member of the oligopeptide transporter (OPT) family. *Microbiology* 147, no. 11: 2881-2883.
- Yokosho, K, N Yamaji, D Ueno, N Mitani, and J Feng Ma. 2009. OsFRDL1 is a citrate transporter required for efficient translocation of iron in rice. *Plant physiology* 149, no. 1: 297-305.
- Young, Jm, Ld Kuykendall, E Martinez-Romero, A Kerr, and H Sawada. 2001. A revision of Rhizobium Frank 1889, with an emended description of the genus, and the inclusion of all species of Agrobacterium Conn 1942 and Allorhizobium undicola de Lajudie et al. 1998 as new combinations: Rhizobium radiobacter, R. rhizogenes, R. rubi. *Int J Syst Evol Microbiol* 51, no. 1: 89-103.
- Yuan, D. S. 1995. The Menkes/Wilson Disease Gene Homologue in Yeast Provides Copper to a Ceruloplasmin-Like Oxidase Required for Iron Uptake. *Proceedings of the National Academy of Sciences* 92, no. 7: 2632-2636.
- Yuan, Y X, J Zhang, D W Wang, and H Q Ling. 2005. AtbHLH29 of Arabidopsis thaliana is a functional ortholog of tomato FER involved in controlling iron acquisition in strategy I plants. *Cell Research* 15, no. 8: 613-621.
- Zancani, M, C Peresson, A Biroccio, G Federici, A Urbani, I Murgia, C Soave, F Micali, A Vianello, and F Macri. 2004. Evidence for the presence of ferritin in plant mitochondria. *European journal of biochemistry / FEBS* 271, no. 18: 3657-64.
- Zheng, L, Z Cheng, C Ai, X Jiang, X Bei, Y Zheng, R P Glahn, et al. 2010. Nicotianamine, a novel enhancer of rice iron bioavailability to humans. Ed. Edward Newbigin *PLoS one* 5, no. 4: e10190.
- Zimmermann, P, M Hirsch-Hoffmann, L Hennig, and W Gruissem. 2004. GENEVESTIGATOR. Arabidopsis microarray database and analysis toolbox. *Plant Physiol* 136, no. 1: 2621-2632.

Danksagung

Oft gelten Danksagungen in Dissertationen der reinen Pflichterfüllung der Autoren gegenüber Arbeitskollegen und Verwandten. An dieser Stelle kommt sie tatsächlich von Herzen und ich nutze die Gelegenheit um allen meinen Dank auszusprechen die zum Überstehen einer nervlich anspruchsvollen Zeit beigetragen haben. Natürlich möchte ich zuerst meiner Doktormutter Prof. Dr. Petra Bauer danken. Ich weiß es wirklich zu schätzen, dass du mich so gefördert, unterstützt und für die Wissenschaft motiviert hast. Danke. Ich danke besonders Tzvetina und Rumen für die große Hilfsbereitschaft in allen wissenschaftlichen Fragen. Ich weiß, dass ihr oft eure Freizeit für mich geopfert habt. Danke, Angelika, für deine Hilfe im Labor und die unzerstörbare gute Laune. Vielen Dank, Moni, für die administrativen Künste, die in unserem Fall oft sehr wichtig waren. Danke Christine, ohne dein Geschick und deine Geduld hätte ich ein paar gute Ergebnisse weniger. Cham and Siva, thanks for the beautiful clash of cultures, I enjoyed it and I will definitely miss you. Johnny und Felix, das alles hat uns wirklich zusammengeschweißt. Ich weiß nicht, ob ich jemals wieder solche guten Freunde auf meinem Arbeitsplatz haben werde.

Ich danke natürlich auch von ganzem Herzen meiner Familie für den Rückhalt, den ich mein ganzes Leben lang genießen durfte und natürlich auch hier und da für die finanzielle Unterstützung. Meine besten Freunde sollten an dieser Stelle natürlich auch nicht leer ausgehen: Danke für die Akzeptanz einer Gelegenheitsfreundschaft, für den Spass und die Ablenkung (das gilt besonders für meine zwei Lieblings-WGs und meinen lieben Freund Kabani).

Da die Danksagung einer Dissertation natürlich keine Liebeserklärungen enthalten sollte, danke ich dir, Boris, ein andermal.

Curriculum vitae

Personal information

Name	Mara Lilien Schuler
Date and place of birth	02.01.1981 in Saarbrücken
Nationality	German
Family status	Unmarried

Academic profile

Education

Current position 01/2008 - today	PhD student Saarland University, Germany Department of Molecular Plant Biology Supervisor: Prof. Dr. Petra Bauer Thesis title: The role of nicotianamine in reproduction and iron homeostasis in <i>Arabidopsis thaliana</i>
-------------------------------------	---

Diploma

2007	Saarland University, Germany Supervisor: Prof. Dr. Petra Bauer Thesis title: Characterisation of <i>Arabidopsis thaliana</i> NAS gene family in the network of metal homeostasis Defended: October 2007, with score 1.3 (in a five scale awarding system, wherein the highest grade is 1.0 and the lowest positive grade 4.0)
------	---

Higher Education

2000 - 2007	Study of Biology at the Saarland University Graduation: Diploma Speciality: Human- and Molecular Biology Specialization: Molecular Plant biology
-------------	--

Publication list

Marco Klatte*, **Mara Schuler***, Markus Witz, Claudia Fink-Straube, Rüdiger Hell and Petra Bauer, 2009. The analysis of Arabidopsis nicotianamine synthase mutants reveals functions for nicotianamine in seed iron loading and iron deficiency responses. *Plant Physiology*, 150: 257-271

* These authors contributed equally to this article

Mara Schuler, Christina Backes, Andreas Keller, Katrin Phillipar and Petra Bauer, 2011. Transcriptome analysis by GeneTrail revealed regulation of functional categories in response to alterations of iron homeostasis in *Arabidopsis thaliana*. *BMC Plant Biology*, 18; 11:87

Mara Schuler and Petra Bauer 2011. Nicotianamine functions in the phloem unloading of Fe in young growing tissues and reproductive organs of *Arabidopsis thaliana*. (*Manuscript in preparation*)

Mara Schuler and Petra Bauer 2011. Heavy metals need assistance: The contribution of nicotianamine to metal circulation throughout the plant and the Arabidopsis *NAS* gene family. (*submitted*)

Personal Presentations at international Meetings

22th Meeting „Molecular Biology of Plants“, Feb. 2008, Dabringhausen, Germany. **Mara Schuler**, Marco Klatte, Markus Wirtz, Claudia Fink-Straube, Katrin Philippar, Rüdiger Hell, Petra Bauer. The role of Arabidopsis thaliana *NAS* genes in the network of iron deficiency responses (*Poster*)

Summer School in “Mineral nutrition in photosynthetic organisms, molecular, physiological and ecological aspects”. June 2009, Maratea, Italy. Mara Schuler, Marco Klatte, Markus Wirtz, R. Hell, Petra Bauer. The role of Arabidopsis thaliana *NAS* genes in reproduction and iron homeostasis (*oral presentation and Poster*)

15th International Symposium on Iron Nutrition and Interactions in Plants, June 2010, Budapest, Hungary. **Mara Schuler** and Petra Bauer. The interaction of *NAS* genes and *FRD3* in the long-distance transport of iron in Arabidopsis thaliana (*oral presentation*)